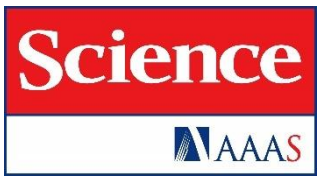

Supplementary Materials for

Asymmetric nucleophilic fluorination under hydrogen bonding phase-transfer catalysis

Gabriele Pupo,[†] Francesco Ibba,[†] David M. H. Ascough,[†] Anna Chiara Vicini, Paolo Ricci, Kirsten E. Christensen, Lukas Pfeifer, John Richard Morphy, John M. Brown, Robert S. Paton, Véronique Gouverneur[*]

[†] These authors have contributed equally to this work.

[*]To whom correspondence should be addressed: veronique.gouverneur@chem.ox.ac.uk

This PDF file includes:

Other Supplementary Materials for this manuscript includes the following:

Coordinates and MD Input Files (computational analysis)

General Information

Unless otherwise stated, all reagents were purchased from commercial suppliers (Sigma-Aldrich, Alfa Aesar, Fluorochem and Apollo Scientific) and used without further purification. Unless otherwise stated, solvents were used without prior drying/degassing. Reactions requiring anhydrous conditions are clearly stated and were conducted after flame-drying of the appropriate reaction vessel (round-bottom two-neck flasks or Schlenk) and under an inert atmosphere of nitrogen. Dry solvents were purchased from commercial suppliers or dried on a column of alumina. Reactions were monitored by thin layer chromatography (TLC) on silica gel pre-coated aluminium sheets (Merck Kieselgel 60 F_{254} plates). Visualization was accomplished by irradiation with UV light at 254 nm, and/or phosphomolybdic acid (PMA) stain, and/or Cerium Ammonium Molybdate (CAM) stain, and/or permanganate stain. Column chromatography was performed on Merck silica gel (60, particle size 0.040-0.063 mm). Optical rotations were measured on an Autopol L 2000 (Schmidt-Haensh) at 589 nm, 25 °C. Data are reported as: $[\alpha]_D^t$, concentration (c in g/100 mL), and solvent. The absolute configuration was determined by X-ray analysis. Low temperature single crystal X-ray diffraction data were collected using a (Rigaku) Oxford Diffraction SuperNova A diffractometer. Full crystallographic data (in CIF format) is available as ESI and has been deposited with the Cambridge Crystallographic Data Centre (CCDC 1812187-88). All NMR spectra were recorded on Bruker AVIIIHD 400, AVIIIHD 500 or AVII 500. ^{1}H and ^{13}C NMR spectral data are reported as chemical shifts (δ) in parts per million (ppm) relative to the solvent peak using the Bruker internal referencing procedure (edlock). ^{19}F NMR spectra are referenced relative to $CFCl_3$. Data are reported as follows: chemical shift, multiplicity (s = singlet, d = doublet, t = triplet, q = quartet, pent = pentet, sept = septet, br = broad, m = multiplet), coupling constants (Hz) and integration. NMR spectra were processed with MestReNova 11.0 or Topspin 3.5 or 4.0. UV-Vis spectra were recorded using a PG instruments T60 UV/Vis spectrophomtometer. High resolution mass spectra were determined on a Thermo Exactive mass spectrometer using electrospray ionization (ESI) or atmospheric pressure chemical ionization (APCI) or on an Agilent 7200 Q-TOF spectrometer equipped with a direct insertion probe supplied by Scientific Instrument Manufacturer (SIM) GmbH using electron ionization (EI – 20eV). The episulfonium precursors (bromo sulfides) were found to be unstable under a variety of MS ionization methods (CI, EI, ESI) and therefore no HRMS could be obtained for them; this is clearly stated in the single experiment. Infrared spectra were recorded as the neat compound or in solution using a Bruker tensor 27 FT-IR spectrometer. Absorptions are reported in wavenumber (cm^{-1}). Melting points of solids were measured on a Griffin apparatus and are uncorrected. All enantiomeric ratios were determined on spectroscopically pure compounds (after chromatographic purification) by HPLC analysis on a Shimadzu *i*-Prominence LC-2030 (PDA detector) employing a chiral stationary phase column and an eluent mixture specified in the individual experiment (HPLC traces analysis), by comparing the samples with the appropriate racemic mixtures.

Catalysts Synthesis and Characterization

ACHIRAL CATALYSTS

The following achiral catalysts were prepared according to literature procedures and their analytical data was in agreement with the literature values: catalyst **2a** and **2d** (*34*), **2c** (*35*), and **2f** (*36*). Catalysts **2e** and catalyst **2b** were unknown; their synthesis and characterization are therefore described herein.

1,3-bis(3,5-bis(trifluoromethyl)phenyl)-1-methylurea (2b)

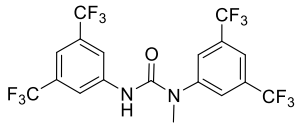

2b

In a flame-dried Schlenk under inert atmosphere, *N*-methyl-3,5-bis(trifluoromethyl)aniline (*37*) (0.411 mmol, 100 mg, 1 equiv.) was dissolved in dry CH_2Cl_2 (0.4 M). 3,5-bis(trifluoromethyl)phenyl isocyanate (0.411 mmol, 71 μL, 1 equiv.) was added dropwise and the solution was stirred overnight. After dilution with hexane (1 mL), the crude was filtered and the white solid was washed (2 x 5mL) with a hexane:CH_2Cl_2 mixture (8:2) to yield the desired compound as a white solid (68% yield, 140 mg). **^{1}H NMR** (400 MHz, $CDCl_3$) δ = 7.89 (s, 1H), 7.82 (s br, 4H), 7.56 (s, 1H), 6.43 (s, 1H), 3.45 (s, 3H), **^{19}F NMR** (376 MHz, $CDCl_3$) δ = –62.9 (s, 6F), –63.0 (s, 6F), **^{13}C NMR** (126 MHz, $CDCl_3$) δ = 153.0, 144.1, 139.5, 134.0 (q, $J_{C–F}$ = 34.2 Hz), 132.4 (q, $J_{C–F}$ = 34.2 Hz), 127.3 (d, $J_{C–F}$ = 3.0 Hz), 123.0 (q, $J_{C–F}$ = 273.5 Hz), 122.5 (q, $J_{C–F}$ = 274.5 Hz), 121.5 (m), 119.5 (d, $J_{C–F}$ = 3.4 Hz), 117.1 (q, $J_{C–F}$ = 3.7 Hz), 37.8; **IR** (thin layer film) ν = 3333, 3129, 1658, 1550, 1372, 1124, 1108, 937, 911, 887, 844, 757, 727, 701, 682, 657, 617 cm^{-1}; **MP** 166–167 °C; **HRMS** (APCIpos) m/z calculated for $C_{18}H_{11}ON_2F_{12}$ $(M+H)^+$ 499.06743, found 499.06623.

1-(3,5-bis(trifluoromethyl)phenyl)-3-(4-methoxyphenyl)urea (2e)

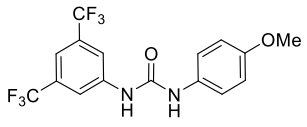

2e

Same protocol used for the synthesis of **2b**, by employing 4-methoxyaniline as starting material. **^{1}H NMR** (500 MHz, $CDCl_3$) δ = 9.31 (s br, 1H), 8.78 (s br, 1H), 8.13 (s, 2H), 7.61 (s, 1H), 7.38 (d, J = 9.0 Hz, 2H), 6.89 (d, J = 9.0 Hz, 2H), 3.73 (s, 3H), **^{19}F NMR** (470 MHz, $CDCl_3$) δ = –61.7 (s, 6F), **^{13}C NMR** (126 MHz, $CDCl_3$) δ = 155.5, 153.0, 142.6, 131.1 (q, $J_{C–F}$ = 32.7 Hz), 123.8 (q, $J_{C–F}$ = 272.2 Hz), 121.4, 118.3 (d, $J_{C–F}$ = 3.9 Hz), 114.5 (m), 114.4, 55.7; **IR** (thin layer film) ν = 3342, 3123, 1702, 1654, 1573, 1527, 1513, 1473, 1443, 1385, 1300, 1273, 1249, 1228, 1170, 1129, 1054, 1030, 951, 909, 884, 790, 704, 680, 621 cm^{-1}; **MP** 178–179 °C; **HRMS** (ESIpos) m/z calculated for $C_{16}H_{13}O_2N_2F_6$ $(M+H)^+$ 379.08757, found 379.08754.

ENANTIOPURE CHIRAL CATALYSTS

The following chiral catalysts were prepared according to literature procedures and their analytical data was in agreement with the literature values: catalyst **4a–b** (*38*), **4c** (*39*), and **4d** (*38*). Catalysts **4e–h** were unknown; their synthesis and characterization is therefore described herein.

Bis-aniline derivatives

Unless indicated otherwise, alkylated bis-anilines were prepared according to the general procedure described herein. Bis-methylated bis-aniline **5e** ((*S*)-N^2,$N^{2'}$-dimethyl-[1,1'-binaphthalene]-2,2'-diamine) is commercially available (Sigma-Aldrich) and/or was prepared according to literature procedures (*40*). *N*-methyl-3,5-bis(trifluoromethyl)aniline (*34*) was prepared according to published protocols (*37*).

*General procedure for the synthesis of N-alkylated 1,1'-binaphthyl-2,2'-diamines (**5b–c**)*: A round-bottom flask was charged with *N*,*N*'-([1,1'-binaphthalene]-2,2'-diyl)bis(2,2,2-trifluoroacetamide) **5a** (1 equiv.), K_2CO_3 (2 equiv.) and the appropriate alkyl iodide (1.05 equiv.) in acetone (0.25 M). After stirring at reflux for 18–36 h, the solvent was removed under reduced pressure and the crude mixture was redissolved in a 4:1 EtOH:H_2O mixture (0.25 M). 10 equiv. of KOH were added and the reaction was stirred at 70 °C for 12 h. The mixture was then cooled to rt and EtOAc was added. The phases were separated and the aqueous phase extracted three times with EtOAc. The combined organic phases were then washed with brine. After anhydrification with $MgSO_4$ and filtration, the solvents were evaporated under reduced pressure and the crude product was purified by FCC (hexane:CH_2Cl_2 or hexane:Et_2O as eluent) to afford the desired products as white solids.

(*S*)-*N*,*N*'-([1,1'-binaphthalene]-2,2'-diyl)bis(2,2,2-trifluoroacetamide) (5a)

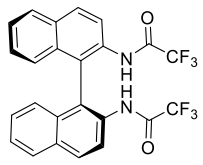

5a

A flame-dried two-neck round-bottom flask equipped with a magnetic stirrer was charged with (*S*)-1,1′-binaphthyl-2,2′-diamine (2.0 g, 7 mmol, 1 equiv.) under a flow of nitrogen. 14 mL of CH_2Cl_2 (0.5 M) were added followed by a dropwise addition of trifluoroacetic anhydride (5.8mL, 42 mmol, 6 equiv.) at 0 °C. The solution was allowed to warm to rt and stirred for 20 min. The volatiles were then carefully evaporated to afford the desired product without any further purification. White solid, 3.30 g, 99% yield. **^{1}H NMR** (500 MHz, $CDCl_3$) δ = 8.21 (d, J = 9.0 Hz, 2H), 8.17 (d, J = 9.0 Hz, 2H), 8.03 (d, J = 8.2 Hz, 2H), 7.73 (s br, 2H), 7.59 (t, J = 7.6 Hz, 2H), 7.41 (t, J = 7.6 Hz, 2H), 7.16 (d, J = 8.5 Hz, 2H), **^{19}F NMR** (470 MHz, $CDCl_3$) δ = –76.3 (s, 6F), **^{13}C NMR** (126 MHz, $CDCl_3$) δ = 155.6 (q, $J_{C–F}$ = 37.9 Hz), 132.3, 131.8, 131.7, 130.9, 128.7, 128.2, 127.0, 124.7, 123.9, 121.8, 114.3 (q, $J_{C–F}$ = 289.1 Hz); **IR** (thin layer film) ν = 3259, 1705, 1530, 1509, 1337, 1266, 1236, 1191, 1161, 933, 910, 864, 812, 765, 741, 717, 649 cm^{-1}; **MP** 179–180 °C;

HRMS (ESIpos) m/z calculated for $C_{24}H_{15}O_2N_2F_6$ $(M+H)^+$ 477.1032, found 477.1033; **$[\alpha]_D^{25\,°C}$** –100.1 ° (c = 0.5, $CHCl_3$).

(*S*)-N^2-methyl-[1,1'-binaphthalene]-2,2'-diamine (5b)

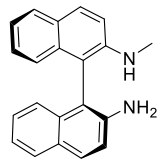

5b

N-methylated aniline **5b** was synthesized according to the general procedure by employing 2.0 g (4.20 mmol) of protected bis-aniline **5a** and 274 µL (4.41 mmol) of iodomethane and stirring for 18h. **Purification** FCC, eluent = hexane:Et_2O (90:10 to 80:20 gradient), white solid, 1.0 g, 80% yield. **^{1}H NMR** (400 MHz, $CDCl_3$) δ = 7.84 (d, *J* = 8.9 Hz, 1H), 7.77–7.70 (m, 3H), 7.22–7.04 (m, 6H), 6.99–6.91 (m, 2H), 3.65 (s, 2H), 2.77 (s, 3H), 1.48 (s br, 1H), **^{13}C NMR** (126 MHz, $CDCl_3$) δ = 144.9, 142.8, 133.9, 133.4, 129.8, 129.6, 128.5, 128.2, 128.1, 127.8, 126.9, 126.8, 124.0, 123.7, 122.5, 122.1, 118.4, 113.6, 112.5, 112.3, 31.4; **IR** (thin layer film) ν = 3349, 2813, 1616, 1594, 1508, 1494, 1470, 1420, 1381, 1337, 1300, 1280, 1247, 1212, 1168, 1153, 1022, 951, 912, 811, 773, 748 cm^{-1}; **MP** 177–178 °C; **HRMS** (ESIpos) m/z calculated for $C_{21}H_{19}N_2$ $(M+H)^+$ 299.1542, found 299.1538; **$[\alpha]_D^{25\,°C}$** –144.8 ° (c = 1.0, $CHCl_3$).

(*S*)-N^2-ethyl-[1,1'-binaphthalene]-2,2'-diamine (5c)

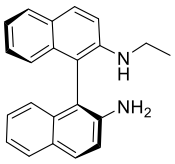

5c

N-ethylated aniline **5c** was synthesized according to the general procedure by employing 700 mg (1.47 mmol) of protected bis-aniline **5a** and 124 µL (1.54 mmol) of iodoethane and stirring for 36h. **Purification** FCC, eluent = hexane:CH_2Cl_2 (70:30 to 50:50 gradient), white solid, 330 mg, 72% yield. **^{1}H NMR** (400 MHz, $CDCl_3$) δ = 7.79 (d, *J* = 9.1 Hz, 1H), 7.67–7.74 (m, 3H), 7.20–7.03 (m, 6H), 6.98–6.94 (m, 1H), 6.93–6.80 (m, 1H), 6.56 (s br, 3H), 3.16 (q, *J* = 7.1 Hz, 2H), 0.95 (t, *J* = 7.1 Hz, 3H), **^{13}C NMR** (126 MHz, $CDCl_3$) δ = 144.4, 143.0, 134.0, 133.6, 129.6, 129.5, 128.5, 128.2, 128.1, 127.7, 126.8, 126.7, 124.0, 123.8, 122.4, 121.9, 118.3, 114.3, 112.5, 112.4, 38.7, 15.2; **IR** (thin layer film) ν = 3435, 3370, 3348, 2964, 1614, 1596, 1567, 1508, 1494, 1470, 1427, 1378, 1349, 1334, 1304, 1280, 1259, 1246, 1213, 1166, 1144, 1066, 1023, 964, 928, 860, 821, 810, 773, 755, 748, 683 cm^{-1}; **MP** 159–160 °C; **HRMS** (ESIpos) m/z calculated for $C_{22}H_{21}N_2$ $(M+H)^+$ 313.1699, found 313.1699; **$[\alpha]_D^{25\,°C}$** –170.4 ° (c = 1.0, $CHCl_3$).

(*S*)-N^2-isopropyl-[1,1'-binaphthalene]-2,2'-diamine

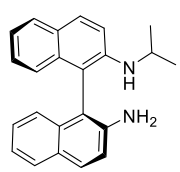

5d

N-isopropylated aniline **5d** was synthesized according to a slightly modified protocol from a previously published one (*41*). In a round-bottom flask equipped with a magnetic stirrer, acetone (361 µL, 4.92 mmol, 1.4 equiv.) was dissolved in THF (0.25M, 14 mL) and a 20% aqueous solution of H_2SO_4 (7 mL, 2 mL/mmol$_{substrate}$) was added. After stirring for 30 min, (*S*)-1,1′-binaphthyl-2,2′-diamine (1.0 g, 3.52 mmol, 1 equiv.) was added. After 5 min of

stirring, the solution was cooled to 0 °C and $NaBH_4$ (1.3 g, 70.0 mmol, 10 equiv.) was carefully added in portions. The mixture was stirred for 1 h at rt, then quenched with 1 M KOH and diluted with EtOAc. The phases were separated and the aqueous phase extracted three times with EtOAc. The combined organic phases were then washed with brine. After anhydrification with $MgSO_4$ and filtration, the solvents were evaporated under reduced pressure and the crude product was purified by FCC (hexane:EtOAc = 95:5 to 90:10 gradient) to afford the desired product as a white solid, 660 mg, 57% yield. **^{1}H NMR** (500 MHz, DMSO-d_6) δ = 7.90 (d, *J* = 9.0 Hz, 1H), 7.75–782 (m, 3H), 7.34 (d, *J* = 9.0 Hz, 1H), 7.24 (d, *J* = 8.8 Hz, 1H), 7.17–7.07 (m, 4H), 6.76 (dd, *J* = 8.2, 0.8 Hz, 1H), 6.73 (dd, *J* = 8.1, 0.8 Hz , 1H), 4.67 (s, 2H), 3.84–3.75 (m, 1H), 3.40 (s, 1H), 1.01 (d, *J* = 6.3 Hz, 3H), 0.91 (d, *J* = 6.3 Hz, 3H), **^{13}C NMR** (126 MHz, DMSO-d_6) δ = 144.8, 144.2, 134.1, 133.8, 129.5, 129.4, 128.6, 128.5, 127.7, 127.7, 126.7, 123.9, 123.4, 121.9, 121.7, 118.9, 115.9, 113.2, 109.8, 44.4, 23.6, 23.5; **IR** (thin layer film) ν = 3462, 3368, 2969, 1611, 1591, 1508, 1490, 1461, 1424, 1382, 1349, 1316, 1287, 1245, 1212, 1168, 1145, 1123, 1029, 958, 909, 821, 809, 772, 747, 687, 621 cm^{-1}; **MP** 165–166 °C; **HRMS** (APCIpos) m/z calculated for $C_{23}H_{23}N_2$ $(M+H)^+$ 327.1855, found 327.1847; **$[\alpha]_D^{25\,°C}$** –170.6 ° (c = 1.0, $CHCl_3$).

Chiral ureas catalysts

Catalyst **4a–b** (*38*), **4c** (*39*), and **4d** (*39*) were known and prepared according to literature procedures. The starting material (*S*)-BINAM mono-urea (1-(2'-amino-[1,1'-binaphthalen]-2-yl)-3-(3,5-bis(trifluoromethyl)phenyl)urea) for the synthesis of **4i** has also been reported previously (*40*).

General procedure for the synthesis of urea catalysts: In a flame-dried Schlenk under inert atmosphere, the appropriate bis-aniline (1 equiv.) was dissolved in dry CH_2Cl_2 (0.4 M) and 3,5-bis(trifluoromethyl)phenyl isocyanate (2 equiv.) was added dropwise. The mixture was stirred overnight at rt (**4e**) or for 36 h at reflux (**4f–m**). After removal of the solvent under reduced pressure, the crude mixture was directly purified by FCC (hexane:Et_2O or hexane:EtOAc mixtures) to afford the desired products as white solids. After FCC, the eluent was removed under reduced pressure and the solid catalyst was dried under vacuum at 60 °C overnight.

(*S*)-1,1'-(3,3'-bis(3,5-bis(trifluoromethyl)phenyl)-5,5',6,6',7,7',8,8'-octahydro-[1,1'-binaphthalene]-2,2'-diyl)bis(3-(3,5-bis(trifluoromethyl)phenyl)urea (4e)

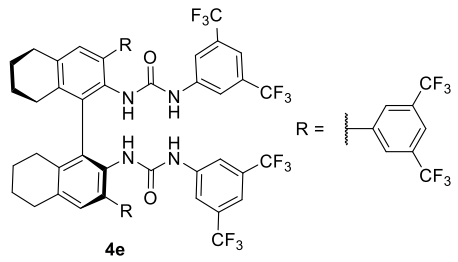

Catalyst **4e** was prepared according to the general procedure by employing (*S*)-3,3'-[3,5-$(CF_3)_2C_6H_3$]-1,1′-binaphthyl-2,2′-diamine (*38*) (0.22 mmol, 160 mg, 1 equiv.) as starting material. **Purification** FCC, eluent = hexane:EtOAc (98:2 to 90:10 gradient), white solid, 246 mg, 90% yield. **^{1}H NMR** (500 MHz, $CDCl_3$) δ = 7.86 (s, 4H), 7.77 (s, 2H), 7.52 (s, 4H), 7.49 (s, 2H), 7.21 (s, 2H), 6.55 (s br, 2H), 6.46 (s, 2H), 2.96–2.80 (m, 4H), 2.26–2.37 (m, 2H), 2.25–2.16 (m, 2H), 1.85–1.66 (m, 8H), **^{19}F NMR** (470 MHz, $CDCl_3$) δ = –63.1 (s, 12F), –63.3 (s, 12F), **^{13}C NMR** (126 MHz, $CDCl_3$) δ = 153.5, 141.6, 139.1, 138.6, 137.1, 135.7, 132.3 (q, $J_{C–F}$ = 33.8 Hz), 131.6 (q, $J_{C–F}$ = 33.8 Hz), 130.8, 129.1, 128.8, 123.2 (q, $J_{C–F}$ = 272.5 Hz), 122.9 (q, $J_{C–F}$ = 272.9 Hz), 121.0, 119.2, 117.0, 29.7, 27.6, 22.8, 22.5; **IR** (thin layer film) ν = 2963, 1655, 1621, 1569, 1472, 1384, 1275, 1172, 1126, 942, 899, 882, 845, 703, 681 cm^{-1}; **MP** 161–162 °C; **HRMS** (APCIpos) m/z calculated for $C_{54}H_{35}O_2N_4F_{24}$ $(M+H)^+$ 1227.2376, found 1227.2356; **$[\alpha]_D^{25\,°C}$** +219.2 ° (c = 0.4, $CHCl_3$).

(*S*)-3-(3,5-bis(trifluoromethyl)phenyl)-1-(2'-(3-(3,5-bis(trifluoromethyl)phenyl)ureido)-[1,1'-binaphthalen]-2-yl)-1-methylurea (4f)

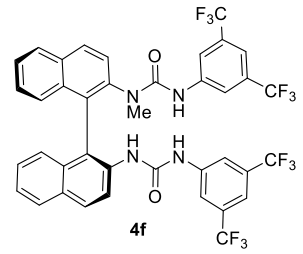

Catalyst **4f** was prepared according to the general procedure by employing (*S*)-*N*-methylated bis-aniline **5b** (0.33 mmol, 100 mg, 1 equiv.) as starting material. **Purification** FCC, eluent = hexane:Et_2O (80:20 to 60:40 gradient), white solid, 180.1 mg, 68% yield. **^{1}H NMR** (400 MHz, $CDCl_3$) δ = 8.50 (d, J = 8.7 Hz, 1H), 8.13 (d, J = 8.7 Hz, 1H), 7.91 (t, J = 9.2 Hz, 2H), 7.91 (d, J = 8.1 Hz, 1H), 7.80 (s, 2H), 7.64 (s, 2H), 7.60–7.37 (m, 6H), 7.32–7.22 (m, 2H), 7.12 (s br, 1H), 7.10 (d, J = 8.5 Hz, 1H), 6.93 (d, J = 8.5 Hz, 1H), 6.80 (s br, 1H), 2.89 (s, 3H), **^{19}F NMR** (376 MHz, $CDCl_3$) δ = –63.2 (s, 6F), –63.3 (s, 6F), **^{13}C NMR** (101 MHz, $CDCl_3$) [overlapping signals] δ = 156.0, 151.7, 139.9, 139.9, 139.2, 135.4, 133.5, 133.2, 133.0, 132.3 (q, $J_{C–F}$ = 32.9 Hz), 132.0 (q, $J_{C–F}$ = 32.9 Hz), 131.1, 131.0, 130.2, 129.8, 128.5, 128.3, 127.6, 127.3, 127.2, 126.5, 126.3, 125.0, 124.7, 123.1 (q, $J_{C–F}$ = 272.9 Hz), 122.8 (q, $J_{C–F}$ = 272.9 Hz), 120.1, 119.8, 118.11, 117.4, 115.9 (m), 37.1; **IR** (thin layer film) ν = 3326, 3064, 1654, 1621, 1600, 1538, 1505, 1473, 1443, 1386, 1358, 1340, 1317, 1276, 1173, 1127, 1058, 1001, 949, 881, 844, 823, 776, 750, 725, 700, 682 cm^{-1}; **MP** 156–157 °C; **HRMS** (APCIpos) m/z calculated for $C_{39}H_{25}O_2N_4F_{12}$ $(M+H)^+$ 809.1773, found 809.1780; **$[\alpha]_D^{25\,°C}$** –81.5 ° (c = 1.0, $CHCl_3$).

(*S*)-3-(3,5-bis(trifluoromethyl)phenyl)-1-(2'-(3-(3,5-bis(trifluoromethyl)phenyl)ureido)-[1,1'-binaphthalen]-2-yl)-1-ethylurea (4g)

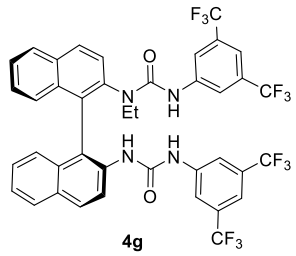

4g

Catalyst **4g** was prepared according to the general procedure by employing (*S*)-*N*-ethylated bis-aniline **5c** (0.48 mmol, 150 mg, 1 equiv.) as starting material. **Purification** FCC, eluent$_{\text{first column}}$ = pentane:CH_2Cl_2 (80:20 to 0:100 gradient), eluent$_{\text{second column}}$ = pentane:EtOAc (95:5 to 80:20 gradient), white solid, 257.0 mg, 65% yield. **^{1}H NMR** (400 MHz, $CDCl_3$) δ = 8.49 (d, J = 7.9 Hz, 1H), 8.13 (d, J = 8.7 Hz, 1H), 8.02–7.96 (m, 2H), 7.92 (d, J = 8.3 Hz, 1H), 7.83 (s br, 2H), 7.63 (s, 2H), 7.55–7.96 (m, 4H), 7.43–7.36 (m, 2H), 7.30–7.22 (m, 2H), 7.14 (s br, 1H), 7.08 (d, J = 8.3 Hz, 1H), 6.90 (d, J = 8.7 Hz, 2H), 3.30–3.18 (m, 1H), 3.18–3.03 (s br, 1H), 1.00 (d, J = 7.2 Hz, 3H), **^{19}F NMR** (376 MHz, $CDCl_3$) δ = –63.2 (s, 6F), –63.3 (s, 6F), **^{13}C NMR** (101 MHz, $CDCl_3$) [overlapping signals] δ = 155.7, 151.7, 139.8, 139.3, 138.7, 135.4, 133.6, 133.2, 130.0, 132.4 (q, $J_{C–F}$ = 33.2 Hz), 132.0 (q, $J_{C–F}$ = 33.6 Hz), 131.4, 130.7, 130.2, 129.8, 128.6, 128.2, 127.7, 127.6, 127.3, 127.2, 126.6, 124.9, 124.7, 123.0 (q, $J_{C–F}$ = 272.2 Hz), 122.9 (q, $J_{C–F}$ = 272.0 Hz), 122.3, 120.1 119.9, 118.1, 117.4, 115.8 (m), 44.5, 13.2; **IR** (thin layer film) ν = 3338, 3064, 1644, 1600, 1505, 1473, 1440, 1385, 1371, 1340, 1275, 1174, 1125, 1060, 1033, 1015, 1000, 968, 948, 880, 845, 823, 810, 787, 774, 749, 724, 700, 681 cm^{-1}; **MP** 141–142 °C; **HRMS** (APCIpos) m/z calculated for $C_{40}H_{27}O_2N_4F_{12}$ $(M+H)^+$ 823.1937, found 823.1916; **$[\alpha]_D^{25\,°C}$** –81.5 ° (c = 1.0, $CHCl_3$).

(*S*)-3-(3,5-bis(trifluoromethyl)phenyl)-1-(2'-(3-(3,5-bis(trifluoromethyl)phenyl)ureido)-[1,1'-binaphthalen]-2-yl)-1-isopropylurea (4h)

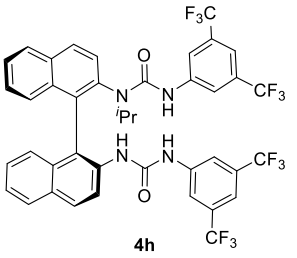

4h

Catalyst **4h** was prepared according to the general procedure by employing *N*-isopropylated bis-aniline (*S*)-**5d** (3.22 mmol, 1.0 g, 1 equiv.) as starting material. **Purification:** FCC, eluent = hexane:Et_2O (90:10 to 80:20 gradient), white solid, 2.451 g, 91% yield. **^{1}H-NMR** (500 MHz, $CDCl_3$) δ = 8.53 (d, J = 8.9 Hz, 1H), 8.15 (d, J = 8.9 Hz, 1H), 8.01 (d, J = 9.1 Hz, 1H), 7.99 (d, J = 8.1 Hz, 1H), 7.92 (d, J = 8.1 Hz, 1H), 7.80 (s, 2H), 7.60 (s, 2H), 7.56–7.48 (m, 4H), 7.42–7.38 (m, 2H), 7.32–7.28 (m, 1H), 7.26–7.21 (m, 1H), 7.17 (d, J = 8.4 Hz, 1H), 7.12 (s, 1H), 6.89 (d, J = 8.4 Hz, 1H), 6.79 (s br, 1H), 3.65 (sept, J = 7.0 Hz, 1H), 1.04 (d, J = 7.0 Hz, 3H), 0.67 (s br, 3H), **^{19}F NMR** (470 MHz, $CDCl_3$) [overlapping signals] δ = –63.2 (s, 12F), **^{13}C NMR** (126 MHz, $CDCl_3$) [overlapping signals] δ = 155.9, 151.8, 139.9, 139.8, 139.3, 135.6, 133.7, 133.2, 133.1, 132.3 (q, $J_{C–F}$ = 33.5 Hz), 131.9 (q, $J_{C–F}$ = 33.5 Hz), 131.8, 130.7, 130.3, 129.9, 128.5, 128.2, 127.9, 127.5, 127.3, 127.2, 127.1, 126.9, 125.2, 124.6, 123.1 (q, $J_{C–F}$ = 273.0 Hz), 122.9 (q, $J_{C–F}$ = 273.0 Hz), 120.2, 119.9, 118.1, 117.4, 115.8, 53.2, 20.9, 20.6, **IR** (thin

layer film) ν = 3328, 3064, 2929, 1687, 1637, 1621, 1602, 1540, 1506, 1473, 1439, 1385, 1338, 1276, 1175, 1127, 1060, 1035, 948, 930, 882, 843, 820, 785, 775, 749, 725, 700, 683, 634 cm^{-1}; **MP** 139–140 °C; **HRMS** (APCIpos) m/z calculated for $C_{41}H_{29}O_2N_4F_{12}$ $(M+H)^+$ 837.2093, found 837.2077; **$[\alpha]_D^{25\,°C}$** –49.9 ° (c = 1.0, $CHCl_3$).

The opposite enantiomer (*R*)-**4h** **$[\alpha]_D^{25\,°C}$** +50.2 ° (c = 1.0, $CHCl_3$) was prepared following the same protocol starting from 650 mg (1.99 mmol) of (*R*)-**5d** (1.440 g, 86% yield).

TBAF·4h complex was synthesized according to literature procedure (*24*): **4h** (100 mg, 0.12 mmol, 1 equiv.) and TBAF·$3H_2O$ (31 mg, 0.12 mmol, 1 equiv.) were refluxed in hexane (0.04 M, 3 mL) for 2 h. The resulting suspension was filtered and the solid dried *in vacuo* affording the desired complex. X-ray quality crystals were obtained by recrystallization layering hexane into a saturated solution of **TBAF·4h** in Et_2O.

Single Crystal Data for **TBAF·4h**: $C_{57}H_{64}F_{13}N_5O_2$, Mr =1098.14. 150 K – orthorhombic, P21 21 21, a = 10.22990(10) Å, b = 21.55920(10) Å, c = 25.00480(10) Å, V = 5514.77(6) Å, Data/restraints/parameters – 11531/456/751, Flack = 0.000(16) for 5144 Friedel pairs and Hooft = -0.007(16) for 5049 Friedel pairs, P2(correct) > 99.9999%, P3(correct) > 99.9999%, Rint = 0.046, Final R1 = 0.0511, wR2 = 0.1451 (I>2σ(I)).

(*S*)-1-(3,5-bis(trifluoromethyl)phenyl)-3-(2'-(3-(3,5-bis(trifluoromethyl)phenyl)ureido)-[1,1'-binaphthalen]-2-yl)-1-methylurea (4i)

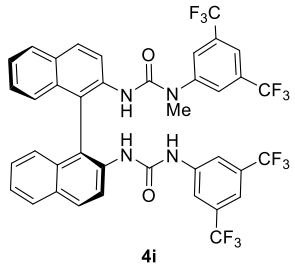

4i

In a flame-dried Schlenk under a flow of nitrogen, triphosgene (40.0 mg, 0.135 mmol, 0.5 equiv) was dissolved in DCE (1 mL). A 0.2 M solution of *N*-methyl-3,5-bis(trifluoromethyl)aniline (*34*) (72 mg, 0.3 mmol, 1.1 equiv.) in DCE (1.7 mL) was slowly added at 0 °C. Dry NEt_3 (150 µL, 1.08 mmol, 4 equiv.) was then added dropwise at the same temperature. After stirring for 2 h at rt, (*S*)-BINAM mono-urea (1-(2'-amino-[1,1'-binaphthalen]-2-yl)-3-(3,5-bis(trifluoromethyl)phenyl)urea) (39) (145 mg, 0.27 mmol, 1 equiv.) was added in one portion as a solid. The reaction was then refluxed (83 °C) for 24 h until full consumption of the starting material. The mixture was then cooled to rt and quenched with water. The phases were separated and the aqueous phase extracted three times with CH_2Cl_2. The combined organic phases were then washed with brine. After anhydrification with $MgSO_4$ and filtration, the solvents were evaporated under reduced pressure and the crude product was purified by FCC (first column, pentane:Et_2O = 100:0 to 80:20 gradient followed by a second column, pentane:CH_2Cl_2 = 70:30) to afford the desired product as a white solid (75 mg, 34% yield, unoptimized). **^{1}H NMR** (500 MHz, $CDCl_3$) δ = 8.53 (d, *J* = 9.1 Hz, 1H), 8.16 (d, *J* = 8.9 Hz, 1H), 7.98 (d, *J* = 8.9 Hz, 1H),

7.96–7.91 (m, 2H), 7.83–7.80 (m, 2H), 7.75 (s, 2H), 7.53 (s br, 1H), 7.48–7.44 (m, 1H), 7.42 (s br, 1H), 7.36–7.27 (m, 4H), 7.16–7.08 (m, 2H), 6.80–6.75 (2H), 5.70 (s, 1H), 3.10 (s, 3H), **^{19}F NMR** (470 MHz, $CDCl_3$) δ = –62.9 (s, 6F), –63.0 (s, 6F), **^{13}C NMR** (126 MHz, $CDCl_3$) [overlapping signals] δ = 155.6, 152.1, 143.3, 140.0, 135.3, 134.8, 133.2 (q, $J_{C–F}$ = 34.3 Hz), 132.8, 132.2 (q, $J_{C–F}$ = 33.4 Hz), 132.1, 131.7, 130.2, 130.1, 129.9, 128.5, 128.4, 127.7, 127.4, 127.3, 127.2, 126.3, 125.7, 125.0, 124.1 (overlapping signals), 123.9, 123.3 (q, $J_{C–F}$ = 273.6 Hz), 122.4 (q, $J_{C–F}$ = 273.0 Hz), 121.5 (m), 120.8, 120.1, 118.5, 118.1 (m), 115.9, 37.4; **IR** (thin layer film) ν = 3326, 3062, 2987, 1693, 1660, 1620, 1598, 1575, 1522, 1501, 1474, 1429, 1383, 1324, 1275, 1174, 1129, 1057, 1027, 1011, 950, 900, 882, 847, 819, 774, 746, 724, 703, 681, 620 cm^{-1}; **MP** 134–135 °C; **HRMS** (APCIpos) m/z calculated for $C_{39}H_{25}O_2N_4F_{12}Na$ $(M+H)^+$ 809.1780, found 809.1762; **$[\alpha]_D^{25\,°C}$** –58.1 ° (c = 0.3, $CHCl_3$).

(*S*)-1,1'-([1,1'-binaphthalene]-2,2'-diyl)bis(3-(3,5-bis(trifluoromethyl)phenyl)-1-methylurea) (4j)

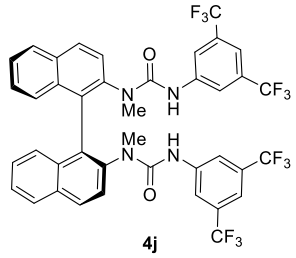

4j

Catalyst **4j** was prepared according to the general procedure by employing (*S*)-N^2,$N^{2'}$-dimethyl-[1,1'-binaphthalene]-2,2'-diamine **5e** (*37*) (75 mg, 0.24 mmol, 1 equiv.) as starting material. **Purification** FCC, eluent = pentane:Et_2O (100:0 to 80:20 gradient), white solid, 172 mg, 87% yield. Spectroscopic analysis of this compound is highly challenging due to the presence of multiple interconverting rotamers and aggregates. ^{1}H NMR spectra were dependant on sample concentration and only showed non-assignable very broad signals even at high temperatures (up to 90 °C). ^{1}H NMR and ^{19}F NMR could be recorded in a diluted solution of DMSO-d_6 (2 mg/mL) at 120 °C (1 main species observed). Due to instrument limitations at these high temperatures, ^{13}C-NMR could not be acquired. **^{1}H NMR** (500 MHz, DMSO-d_6, 120 °C) δ = 7.92 (d, *J* = 9.0 Hz, 2H), 7.80–7.77 (m, 2H), 7.30 (d, *J* = 9.0, 2H), 7.17–7.07 (m, 8H), 7.00 (s br, 2H), 6.79 (d, *J* = 8.4 Hz, 2H), 5.74 (s br, 2H), 2.79 (s, 3H), 2.78 (s, 3H) **^{19}F NMR** (470 MHz, DMSO-d_6, 120 °C) δ = –62.1 (s, 12F); **IR** (thin layer film) ν = 3422, 1665, 1619, 1595, 1536, 1472, 1440, 1387, 1347, 1312, 1276, 1169, 1127, 1001, 937, 880, 844, 821, 753, 733, 700, 682, 647, 615 cm^{-1}; **MP** 155–156 °C; **HRMS** (ESIpos) m/z calculated for $C_{40}H_{27}O_2N_4F_{12}$ $(M+H)^+$ 823.1915, found 823.1937; **$[\alpha]_D^{25\,°C}$** –288.7 ° (c = 1.0, $CHCl_3$).

(*S*)-1,1'-([1,1'-binaphthalene]-2,2'-diyl)bis(3-(3,5-bis(trifluoromethyl)phenyl)-3-methylurea) (4k)

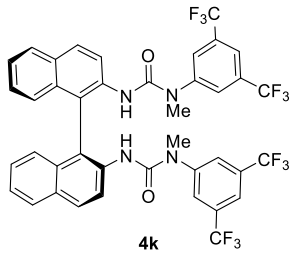

4k

In a flame-dried Schlenk under a flow of nitrogen, triphosgene (103.5 mg, 0.35 mmol, 0.7 equiv) was dissolved in 0.5 mL of CH_2Cl_2. A 0.5 M solution of *N*-methyl-3,5-bis(trifluoromethyl)aniline (*34*) (243 mg, 1 mmol, 2 equiv.) in CH_2Cl_2 (2 mL) was slowly added at 0 °C. Dry NEt_3 (278 μL, 2 mmol, 4 equiv.) was then added dropwise at the same temperature. After stirring for 2 h at rt, (*S*)-1,1′-binaphthyl-2,2′-diamine (142 mg, 0.5 mmol, 1 equiv.) was added in one portion as a solid. The reaction was then refluxed for 36 h until full consumption of the starting material. The mixture was then cooled to rt and quenched with water. The phases were separated and the aqueous phase extracted three times with CH_2Cl_2. The combined organic phases were then washed with brine. After anhydrification with $MgSO_4$ and filtration, the solvents were evaporated under reduced pressure and the crude product was purified by FCC (hexane:Et_2O,100:0 to 80:20 gradient) to afford the desired product as a white solid (218 mg, 53% yield). **^{1}H NMR** (500 MHz, $CDCl_3$) δ = 8.23 (d, J = 9.0 Hz, 2H), 7.83 (d, J = 8.1 Hz, 2H), 7.74 (d, J = 8.1 Hz, 2H), 7.51 (s, 2H), 7.34–7.30 (m, 6H), 7.16–7.12 (m, 2H), 6.83 (d, J = 8.4 Hz, 2H), 5.66 (s, 2H), 3.06 (s, 6H), **^{19}F NMR** (470 MHz, $CDCl_3$) δ = –62.7 (s, 12F), **^{13}C NMR** (126 MHz, $CDCl_3$) [overlapping signals] δ = 153.6, 143.5, 135.3, 132.8 (q, $J_{C–F}$ = 34.1 Hz), 131.5, 130.2, 129.6, 128.1, 127.3, 127.3 (overlapped), 125.1, 124.0, 122.5 (q, $J_{C–F}$ = 273.6 Hz), 121.0, 120.9 (sept, $J_{C–F}$ = 3.5 Hz), 119.1, 37.0; **IR** (thin layer film) ν = 3395, 1690, 1620, 1597, 1499, 1469, 1431, 1383, 1313, 1275, 1254, 1176, 1135, 1105, 1026, 1008, 965, 900, 847, 818, 774, 746, 705, 692, 682 cm^{-1}; **MP** 152–153 °C; **HRMS** (APCIpos) m/z calculated for $C_{40}H_{27}O_2N_4F_{12}$ $(M+H)^+$ 823.1915, found 823.1936; **$[\alpha]_D^{25\,°C}$** –121.8 ° (c = 1.0, $CHCl_3$).

Optimization of Reaction Conditions – Preliminary Screening

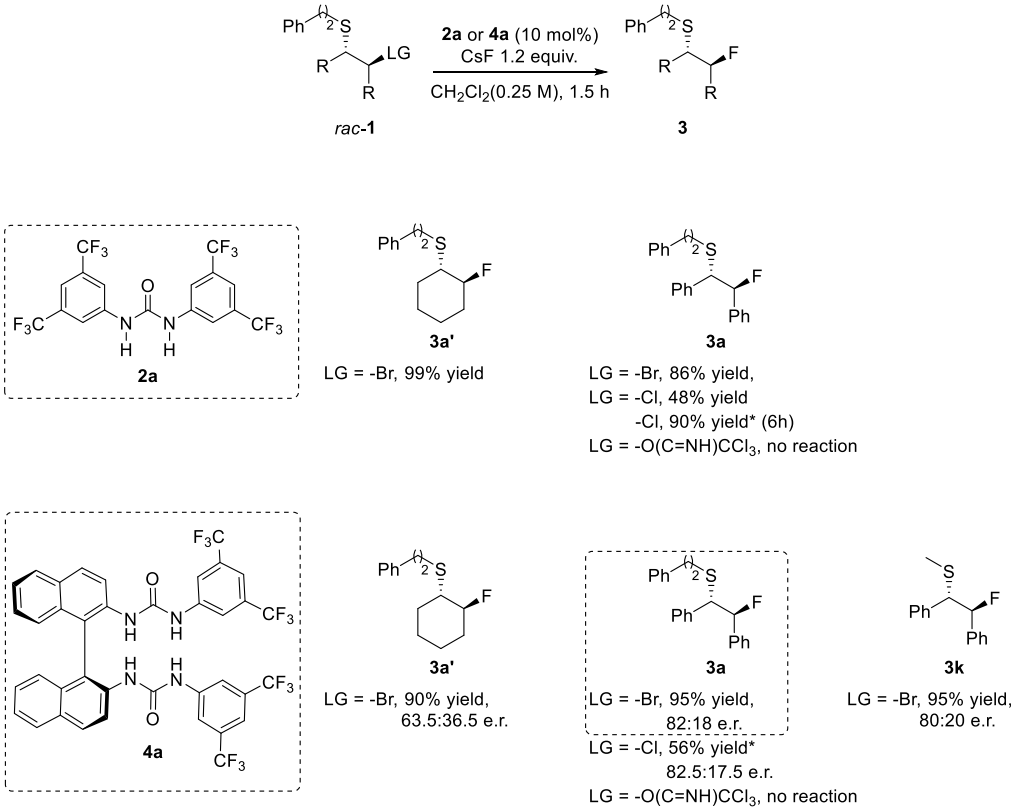

Figure S1. – *Preliminary screening*

Optimization of Reaction Conditions - Non-asymmetric Catalytic System

Table S1. – *Full screening*

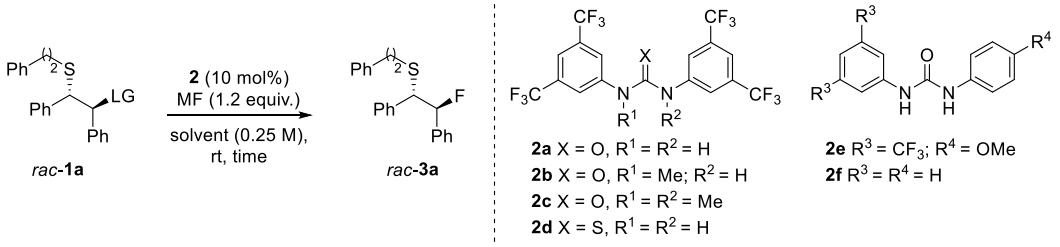

Entry	Solvent	LG	F^- source*	Catalyst	Cat. loading (mol %)	Time (h)	Yield (%)†
1	CH_2Cl_2	Br	CsF	**2a**	10	1.5	80
2	CH_2Cl_2	Br	CsF	--	--	1.5	no reaction
3	PhMe	Br	CsF	**2a**	10	1.5	33
4	PhMe	Br	CsF	--	--	1.5	< 5
5	CH_3CN	Br	CsF	**2a**	10	1.5	72
6	CH_3CN	Br	CsF	--	--	1.5	< 5
7	DMF	Br	CsF	**2a**	10	1.5	10
8	DMF	Br	CsF	--	--	1.5	9
9‡	MeOH	Br	CsF	**2a**	10	1.5	10
10‡	MeOH	Br	CsF	--	--	1.5	10
11	CH_2Cl_2	Br	CsF	**2b**	10	1.5	no reaction
12	CH_2Cl_2	Br	CsF	**2c**	10	1.5	no reaction
13	CH_2Cl_2	Br	CsF	**2d**	10	1.5	no reaction
14	CH_2Cl_2	Br	CsF	**2e**	10	1.5	20
15	CH_2Cl_2	Br	CsF	**2f**	10	1.5	5
16	CH_2Cl_2	Br	CsF	**2a**	5	24	64
17	CH_2Cl_2	Br	CsF	**2a**	0.5	24	6
18§	CH_2Cl_2	Br	KF	**2a**	10	24	55
19	CH_2Cl_2	Cl	CsF	**2a**	10	1.5	48
20‖	CH_2Cl_2	Cl	CsF	**2a**	10	6	90
21‖, ¶	CH_2Cl_2	$O(C{=}NH)CCl_3$	CsF	**2a**	10	1.5	no reaction

General conditions: Substrate (0.05 mmol), stirring at 1200 rpm, * CsF and KF used without any prior drying and used as provided by the supplier (Sigma-Aldrich, CsF 99.9% trace metal basis), † Determined by ^{19}F NMR using 4-fluoroanisole as internal standard, ‡ The major product detected by ^1H NMR was the methyl ether derived from MeOH attack of the episulfonium ion, § KF also afforded *rac*-**3a** despite longer reaction times; no reaction was observed with NaF and LiF, ‖ 3 equivalents of CsF were employed, ¶ 78% yield in the presence of 1 equiv. of a sulfonic acid (*p*-TSA).

Optimization of Reaction Conditions – Asymmetric Catalytic System

Table S2. – *Solvent, concentration, temperature and nucleophile equivalents screening (catalyst **4a**)*

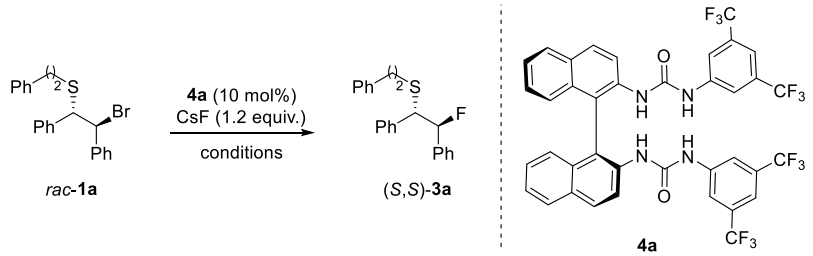

Entry	Solvent	CsF (equiv.)	Temp. (°C)	M	Time (h)	Yield (%)*	e.r.†
1	CH_2Cl_2	1.2	rt	0.25	1.5	95 (75)‡	82:18
2§	CH_2Cl_2	1.2	rt	0.25	1.5	99	82:18
3	CH_2Cl_2	1.2	rt	0.5	1.5	90	82:18
4	CH_2Cl_2	1.2	rt	0.1	1.5	62	82:18
5	1,2-DCE	1.2	rt	0.25	1.5	38	82:18
6	$CHCl_3$	1.2	rt	0.25	1.5	36	81.5:18.5
7	Et_2O or EtOAc	1.2	rt	0.25	1.5	<5	nd
8	Nitromethane	1.2	rt	0.25	1.5	40	74:26
9	PhF	1.2	rt	0.25	1.5	33	83:17
10	$PhCF_3$	1.2	rt	0.25	1.5	38	86:14
11	Benzene	1.2	rt	0.25	1.5	10	nd
12	1,3-DFB‖	1.2	rt	0.25	1.5	29	86:14
13	1,4-DFB	1.2	rt	0.25	1.5	12	nd
14	1,2-DFB	1.2	rt	0.25	1.5	8	85:15
15	1,2-DFB	1.2	rt	0.25	1.5	99	86:14
16	1,2-DFB	1.2	rt	0.25	0.5	60	86:14
17	1,2-DFB	2	rt	0.25	0.5	99	86:14
18	1,2-DFB	3	rt	0.25	0.5	99	86:14
19	1,2-DFB	1.2	–10	0.25	24	95	89.5:10.5
20	1,2-DFB:CH_2Cl_2 (3:1)	1.2	–30	0.25	24	31	89.5:10.5
21	CH_2Cl_2	1.2	–50	0.25	36	traces	89:11

General conditions: Substrate (0.05 mmol), catalyst (10 mol%) and flame-dried CsF (1.2 equiv.) in 200 µL of solvent stirred at 1200 rpm for the indicated time at the indicated temperature * Determined by ^{19}F NMR using 4-fluoroanisole as internal standard, † e.r. was determined by HPLC analysis using a chiral stationary phase; reference racemic mixtures for HPLC analysis were obtained by stirring the corresponding bromide starting material with 1.2 equiv of AgF in CH_2Cl_2 for 1h. ‡ In parenthesis, isolated yield on a 0.25 mmol scale § CsF used without any prior drying, as provided by the supplier (Sigma-Aldrich, CsF 99.9% trace metal basis), ‖ DFB = difluorobenzene.

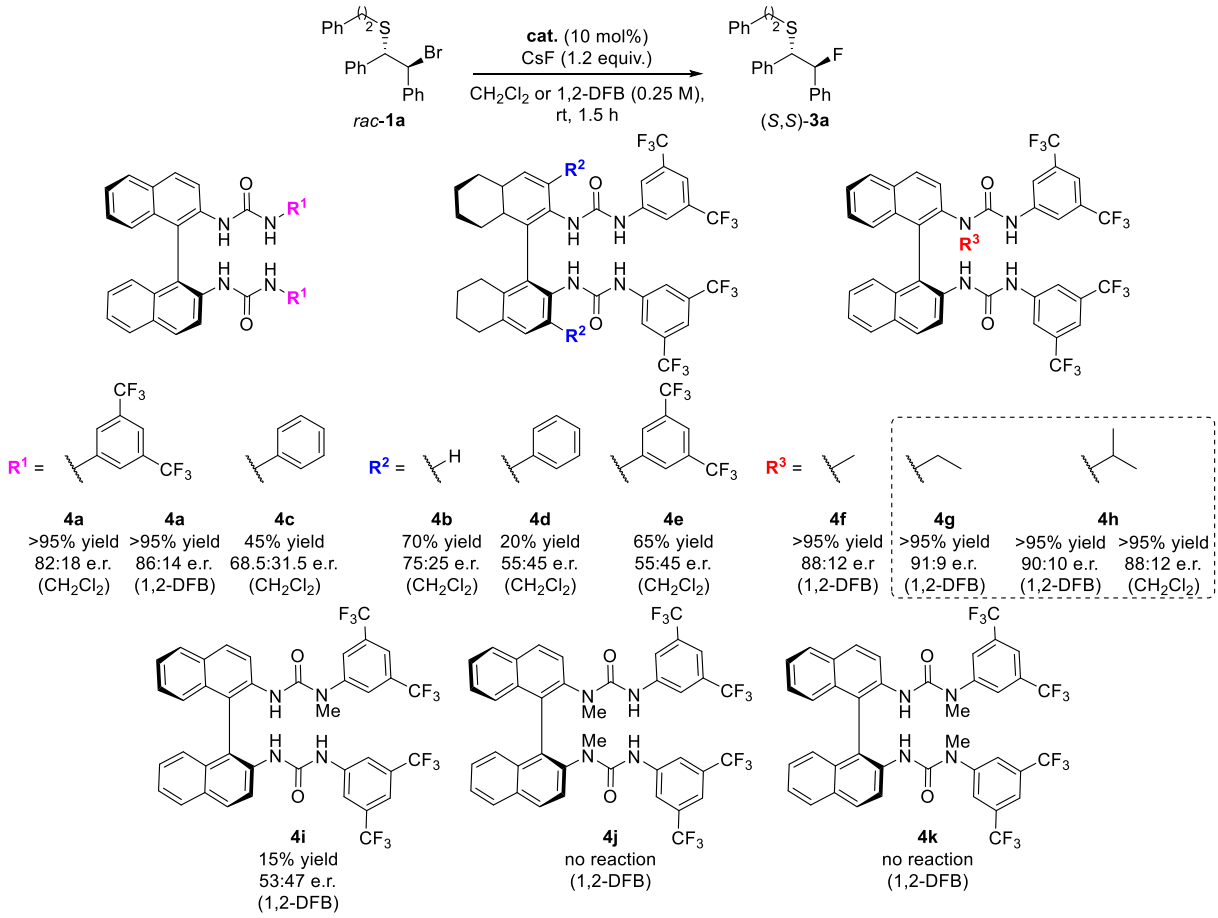

Figure S2. – *Catalyst screening and final optimization*

Table S3. – *Final optimization*

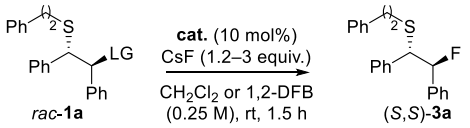

Entry	Catalyst	LG	CsF (equiv.)	Solvent	Temp. (°C)	Time (h)	Yield (%) *	e.r.†
1	**4g**	Br	1.2	1,2-DFB	rt	1.5	>95	91:9
2	**4g**	Br	2	1,2-DFB	–30	72	>95	94:6
3	**4h**	Br	1.2	1,2-DFB	rt	1.5	>95	90:10
4	**4h**	Br	1.2	CH_2Cl_2	rt	1.5	>95	88:12
5	**4h**	Cl	3	CH_2Cl_2	rt	6	90	88:12
7	**4h**	Br	2	1,2-DFB	–30	72	90 (83)‡	95.5:4.5

General conditions: Substrate (0.05 mmol), catalyst (10 mol%) and CsF (1.2–3 equiv.) in 200 µL of 1,2-difluorobenzene stirred at 1200 rpm for the indicated time at the indicated temperature. * Determined by ^{19}F NMR using 4-fluoroanisole as internal standard, † e.r. was determined by HPLC analysis using a chiral stationary phase, ‡ In parenthesis, the isolated yield on a 0.2 mmol scale is shown.

Urea vs. Thiourea Catalytic Performance

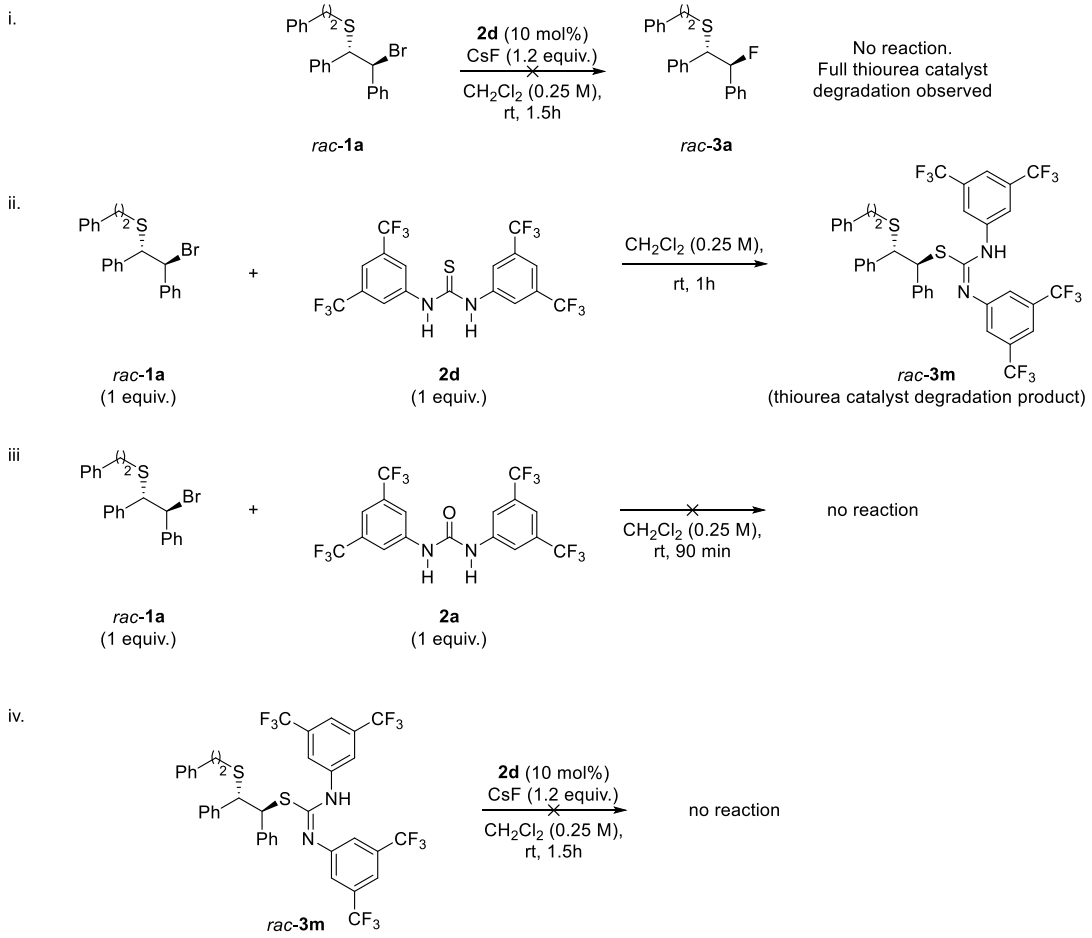

Figure S3. – *Thiourea vs. urea catalyst degradation experiments.*

While theoretical calculations predict thioureas to be suitable phase-transfer catalysts for fluoride anions (see page S54), these catalysts only afforded traces of the desired product **3a**. This is likely due to competitive formation of a covalent adduct (**3m**) between the substrate and the thiourea. Compound **3m** is stable and did not undergo fluorination if subjected to the reaction conditions, thus excluding the possibility of its involvement as an intermediate. Urea **2a**, less nucleophilic (*O vs. S*) than its thiourea counterpart (**2d**), did not react with *rac*-**1a** and was a suitable catalyst for fluorination.

General Procedure for the Asymmetric Nucleophilic Fluorination of Episulfonium Ions

For reaction optimization: In a screw-cap vial equipped with a magnetic stirring bar were sequentially added the appropriate substrate **1** (0.05 mmol, 1 equiv.), the catalyst (10 mol%), flame-dried CsF (1.2–3 equiv.) and 1,2-difluorobenzene (0.25 M, pre-cooled at the same temperature as the reaction). The vial was sealed and the reaction mixture was stirred at 1200 rpm at the appropriate temperature for 1.5–72 h. The crude mixture was then filtered through a small plug of silica (and eluted with cold CH_2Cl_2), evaporated to dryness, dissolved in $CDCl_3$ and analysed by ^{1}H and ^{19}F NMR (4-fluoroanisole as internal standard).

For the substrate scope and the gram-scale reaction: In a screw-cap vial equipped with a magnetic stirring bar were sequentially added the appropriate substrate **1** (1 equiv.), the catalyst (10 mol%), CsF (2 equiv.)[*] and 1,2-difluorobenzene (0.25 M, pre-cooled at the same temperature as the reaction). The vial was sealed and the reaction mixture was stirred at 1200 rpm at the appropriate temperature for 24–72 h. The crude mixture was then filtered through a small plug of silica (and eluted with cold CH_2Cl_2), evaporated to dryness under reduced pressure and directly purified by FCC (Pentane:Et_2O or Pentane:CH_2Cl_2 mixtures as eluent).

[*] The CsF employed was freshly ground prior to the reaction and used without any additional drying (Sigma-Aldrich, CsF 99.9% trace metal basis).

Non-linear Effect study

The non-linear effect study was conducted with (*R*) or (*S*) mixtures of catalyst **4h** by employing the previously described protocol for reaction optimization (see detailed conditions in scheme below). Under those standard conditions (rt), (*S*)-**4h** affords (*S*,*S*)-**3a** in 80% ee (90:10 e.r.). No background reaction observed under these conditions and the results shown are mean values of two sets of experiments.

Table S4. – Non-linear effect study

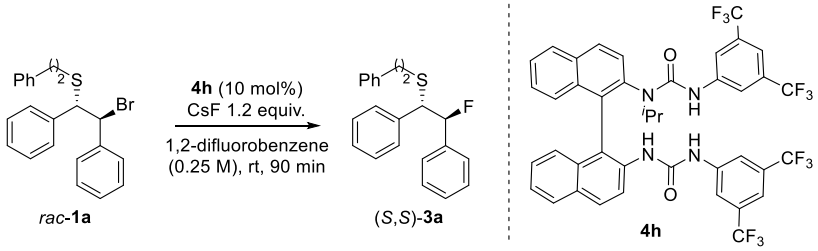

Entry	ee of catalyst*	ee of product†
1	1.0	0.6
2	19.2	13.7
3	38.9	29.2
4	58.1	44.6
5	77.2	61.0
6	99.9	80.0

* (*R*) and (*S*) mixtures of **4h** were premixed in a ratio between 50:50 and 0:100, respectively. The ee of the catalyst was calculated by comparing its optical rotation value with the one of the enantiopure form, which was assumed to have perfect ee (99.9% ee).

† The ee of the product was determined by HLPC analysis using a chiral stationary phase at 254 nm.

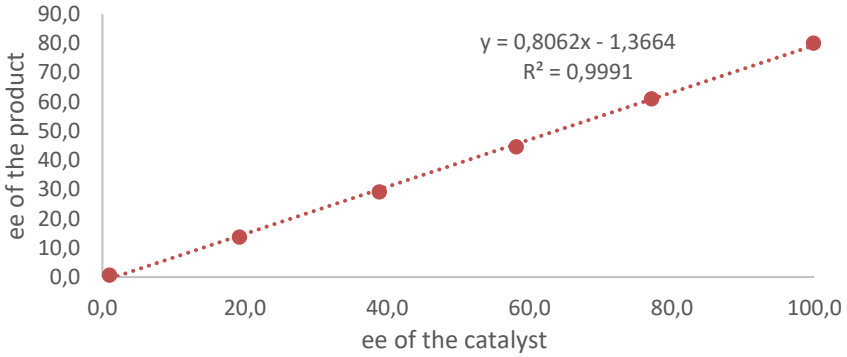

Figure S4. – Non-linear effect study

***Conclusion*:** No non-linear effect was observed. The experiment is thus consistent with the computed transition state model involving only one molecule of the urea catalyst.

Substrates Synthesis and Characterization

Bromo sulfides **1b**–**1j** and **1l** were prepared from the corresponding *meso*-epoxides (*43*). Bromo sulfides **1a** and **1k** were prepared *via* sulfenyl bromide addition to *cis*-stilbene, and the detailed experimental procedure is described in the single experiment. Chloro sulfide **1a'** and trichloroacetimidate **1a''** were prepared from alcohol **6a** according to reported literature procedures (detailed in the single experiment).

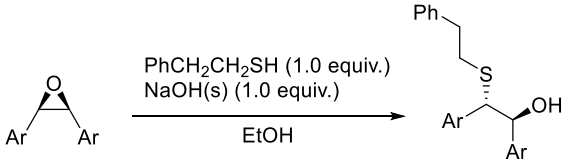

rac-**6a–6j**, *rac*-**6l**

Figure S5. – *Synthesis of hydroxy sulfides*

The appropriate *cis*-epoxide (1.0 equiv.) was dissolved in EtOH (0.1 M) in a round-bottom flask and $NaOH_{(S)}$ (1.0 equiv.), 2-phenylethane-1-thiol (1.0 equiv.) were added to the solution at room temperature. The reaction mixture was either stirred overnight at room temperature or reflux for the indicated time (monitored by TLC using hexane:CH_2Cl_2 = 80:20 as eluent). When TLC analysis showed no further conversion, the solvent was removed *in vacuo*. To the crude mixture residue was then added Et_2O and water, the layers were partitioned and the aqueous phase was extracted three times with Et_2O. The organic phases were combined, dried over $MgSO_4$, filtered and concentrated *in vacuo* to afford the crude product. The crude products were then purified by flash column chromatography (hexane/Et_2O) to afford pure hydroxy sulfides.

***rac*-2-(phenethylthio)-1,2-diphenylethan-1-ol (6a)**

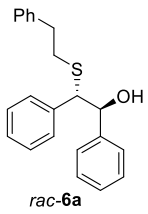

rac-**6a**

Alcohol **6a** was prepared according to the general procedure from *cis*-stilbene oxide (10.2 mmol, 2.00 g) and by stirring the reaction mixture at reflux for 2 h. **Purification** FCC, eluent = pentane:Et_2O (100:0 to 80:20 gradient), yellow oil, 3.19 g, 91% yield. **^{1}H NMR** (500 MHz, $CDCl_3$) δ = 7.32–7.26 (m, 2H), 7.25–7.17 (m, 7H), 7.16–7.12 (m, 4H), 7.12–7.08 (m, 2H), 4.86 (dd, J = 8.5, 2.7 Hz, 1H), 4.03 (d, J = 8.5 Hz, 1H), 3.17 (d, J = 2.7 Hz, 1H), 2.87–2.78 (m, 2H), 2.76–2.62 (m, 2H), **^{13}C NMR** (126 MHz, $CDCl_3$) δ = 141.1, 140.3, 139.6, 128.7, 128.6, 128.6, 128.4, 128.1, 127.8, 127.4, 126.8, 126.5, 77.4, 60.4, 36.3, 33.4, **IR** (thin layer film) ν = 3433, 3061, 3027, 2917, 1602, 1494, 1453, 1191, 1044, 1030, 756, 730 cm^{-1}; **HRMS** (ESIpos) m/z calculated for $C_{22}H_{22}ONaS$ $(M+Na)^+$ 357.1284, found 357.1285.

***rac*-1,2-bis(3-chlorophenyl)-2-(phenethylthio)ethan-1-ol (6b)**

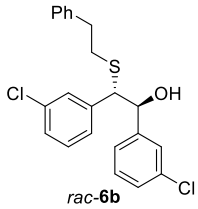

Alcohol **6b** was prepared according to the general procedure from the corresponding epoxide (8.1 mmol, 2.1 g) and by stirring the reaction mixture at reflux for 2 h. **Purification** FCC, eluent = hexane:Et_2O (100:0 to 80:20 gradient), yellow oil, 2.90 g, 89% yield. **^{1}H NMR** (500 MHz, $CDCl_3$) δ = 7.32–7.21 (m, 3H), 7.20–7.07 (m, 8H), 6.93 (dt, *J* = 7.5, 1.5 Hz, 1H), 6.88 (dt, *J* = 7.7, 1.4 Hz, 1H), 4.73 (d, *J* = 8.3 Hz, 1H), 3.83 (d, *J* = 8.3 Hz, 1H), 3.11 (s br, 1H), 2.81 (t, *J* = 7.5 Hz, 2H), 2.75–2.65 (m, 2H), **^{13}C NMR** (126 MHz, $CDCl_3$) [overlapping signals] δ = 142.7, 141.5, 140.0, 134.4, 134.2, 129.7, 129.4, 128.7, 128.7, 128.2 127.9, 126.9, 126.8, 126.7, 125.1, 76.7, 59.8, 36.3, 33.6; **IR** (thin layer film) ν = 3439, 3027, 2919, 1595, 1496, 1430, 1191, 1098, 1079, 884, 786, 771, 747, 696 cm^{-1}; **HRMS** (ESIpos) m/z calculated for $C_{22}H_{20}O_{35}Cl_2NaS$ $(M+Na)^+$ 425.0504, found 425.0504.

***rac*-1,2-bis(3-methoxyphenyl)-2-(phenethylthio)ethan-1-ol (6c)**

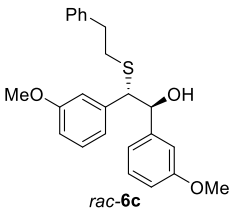

Alcohol **6c** was prepared according to the general procedure from the corresponding epoxide (8.3 mmol, 2.1 g) and by stirring the reaction mixture at reflux for 3 h. **Purification** FCC, eluent = hexane:Et_2O (100:0 to 70:30 gradient), yellow oil, 2.90 g, 88% yield. **^{1}H NMR** (400 MHz, $CDCl_3$) δ = 7.25–7.18 (m, 2H), 7.17–7.11 (m, 1H), 7.10–7.00 (m, 4H), 6.71–6.60 (m, 6H), 4.75 (dd, *J* = 8.3, 2.8 Hz, 1H), 3.91 (d, *J* = 8.3 Hz, 1H), 3.66 (s, 3H), 3.64 (s, 3H), 3.05 (d, *J* = 2.8 Hz, 1H), 2.78–2.72 (m, 2H), 2.68–2.58 (m, 2H), **^{13}C NMR** (101 MHz, $CDCl_3$) δ = 159.6, 159.4, 142.7, 141.2, 140.3, 129.3, 129.1, 128.7, 128.6, 126.5, 121.2, 119.2, 114.3, 113.7, 113.0, 112.1, 77.2, 60.2, 55.3, 55.3, 36.3, 33.5; **IR** (thin layer film) ν = 3455, 3026, 2536, 2835, 1599, 1585, 1489, 1454, 1259, 1150, 1042, 779, 732, 697 cm^{-1}; **HRMS** (ESIpos) m/z calculated for $C_{24}H_{26}O_3NaS$ $(M+Na)^+$ 417.1495, found 417.1491.

***rac*-2-(phenethylthio)-1,2-di-m-tolylethan-1-ol (6d)**

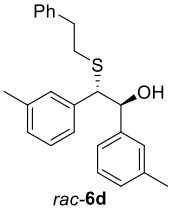

Alcohol **6d** was prepared according to the general procedure from the corresponding epoxide (11.6 mmol, 2.6 g) and by stirring the reaction mixture at reflux for 2 h. **Purification** FCC, eluent = hexane:Et_2O (100:0 to 80:20 gradient), yellow oil, 2.70 g, 60% yield. **^{1}H NMR** (400 MHz, $CDCl_3$) δ = 7.24–7.12 (m, 3H), 7.08–7.00 (m, 4H), 6.98–6.83 (m, 6H), 4.77 (d, *J* = 8.1 Hz, 1H), 3.94 (d, *J* = 8.1 Hz, 1H), 3.02 (s br, 1H), 2.78–2.70 (m, 2H), 2.68–2.55 (m, 2H), 2.23 (s, 3H), 2.22 (s, 3H), **^{13}C NMR** (101 MHz, $CDCl_3$) δ = 141.1, 140.4, 139.6, 138.0, 137.7, 129.4, 128.6, 128.6, 128.5, 128.2, 128.2, 127.9, 127.4, 126.5, 125.8, 124.0, 77.2, 60.1,

36.3, 33.4, 21.5, 21.5; **IR** (thin layer film) ν = 3442, 3026, 2918, 1605, 1489, 1454, 1378, 1152, 1044, 780, 729, 698 cm^{-1}; **HRMS** (ESIpos) m/z calculated for $C_{24}H_{26}ONaS$ $(M+Na)^+$ 385.1597, found 385.1598.

***rac*-1,2-bis(3-fluorophenyl)-2-(phenethylthio)ethan-1-ol (6e)**

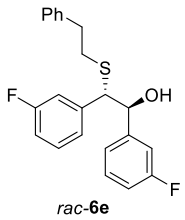

rac-**6e**

Alcohol **6e** was prepared according to the general procedure from the corresponding epoxide (12.6 mmol, 2.9 g) and by stirring the reaction mixture at reflux for 2 h. **Purification** FCC, eluent = hexane:Et_2O (100:0 to 80:20 gradient), yellow oil, 3.98 g, 85% yield. **^{1}H NMR** (400 MHz, $CDCl_3$) δ = 7.24–7.12 (m, 3H), 7.11–6.99 (m, 4H), 6.86–6.68 (m, 6H), 4.68 (d, J = 8.5, 1H), 3.80 (d, J = 8.4 Hz, 1H), 3.05 (s br, 1H), 2.74 (t, J = 7.3 Hz, 2H), 2.67–2.53 (m, 2H), **^{19}F NMR** (376 MHz, $CDCl_3$) δ = -112.7 (td, J = 9.0, 5.7 Hz, 1F), -113.0 (td, J = 9.3, 5.9 Hz, 1F), **^{13}C NMR** (101 MHz, $CDCl_3$) [overlapping signals] δ = 162.7 (d, $J_{C–F}$ = 246.2 Hz), 162.7 (d, $J_{C–F}$ = 246.2 Hz), 143.4 (d, $J_{C–F}$ = 7.3 Hz), 142.0 (d, $J_{C–F}$ = 7.3 Hz), 140.0, 130.0 (d, $J_{C–F}$ = 8.3 Hz), 129.6 (d, $J_{C–F}$ = 8.2 Hz), 128.6, 124.4 (d, $J_{C–F}$ = 2.9 Hz), 122.5 (d, $J_{C–F}$ = 2.9 Hz), 115.5 (d, $J_{C–F}$ = 22.0 Hz), 114.9 (d, $J_{C–F}$ = 21.1 Hz), 114.6 (d, $J_{C–F}$ = 21.1 Hz), 113.6 (d, $J_{C–F}$ = 22.2 Hz), 77.3 (d, $J_{C–F}$ = 1.8 Hz), 59.9 (d, $J_{C–F}$ = 1.8 Hz), 36.2, 33.5; **IR** (thin layer film) ν = 3432, 3028, 2918, 1613, 1589, 1487, 1448, 1254, 1160, 1045, 877, 782, 734, 694 cm^{-1}, **HRMS** (ESIpos) m/z calculated for $C_{22}H_{20}OF_2NaS$ $(M+Na)^+$ 393.1095, found 393.1095.

***rac*-1,2-bis(3,5-dimethylphenyl)-2-(phenethylthio)ethan-1-ol (6f)**

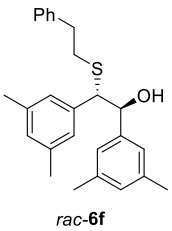

rac-**6f**

Alcohol **6f** was prepared according to the general procedure from the corresponding epoxide (12.4 mmol, 3.2 g) and by stirring the reaction mixture overnight at room temperature. **Purification** FCC, eluent = pentane:Et_2O (100:0 to 80:20 gradient), yellow oil, 982 mg, 20% yield (unoptimized). **^{1}H NMR** (400 MHz, $CDCl_3$) δ = 7.25–7.20 (m 2H), 7.19–7.13 (m, 1H), 7.06–7.00 (m, 2H), 6.82–6.78 (m, 2H), 6.78 (s, 4H), 4.77 (dd, J = 7.3, 3.4 Hz, 1H), 3.94 (d, J = 7.3 Hz, 1H), 2.98 (d, J = 3.5 Hz, 1H), 2.79–2.70 (m, 2H), 2.66–2.53 (m, 2H), 2.21 (s, 6H), 2.20 (s, 6H), **^{13}C NMR** (101 MHz, $CDCl_3$) δ = 141.3, 140.5, 139.7, 137.7, 137.4, 129.3, 129.1, 128.6, 128.5, 126.5, 126.4, 124.5, 76.8, 59.8, 36.3, 33.5, 21.4, 21.4; **IR** (thin layer film) ν = 3435, 3025, 2916, 1603, 1454, 1376, 1279, 1155, 1038, 852, 735, 697 cm^{-1}; **HRMS** (ESIpos) m/z calculated for $C_{26}H_{30}ONaS$ $(M+Na)^+$ 413.1910, found 413.1910.

***rac*-2-(phenethylthio)-1,2-di-p-tolylethan-1-ol (6g)**

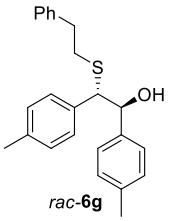

Alcohol **6g** was prepared according to the general procedure from the corresponding epoxide (12.7 mmol, 2.85 g) and by stirring the reaction mixture overnight at room temperature. **Purification** FCC, eluent = hexane:Et_2O (100:0 to 80:20 gradient), yellow oil, 2.99 g, 65% yield. **^{1}H NMR** (400 MHz, $CDCl_3$) δ = 7.33–7.27 (m, 2H), 7.26–7.21 (m, 1H), 7.14–7.09 (m, 2H), 7.09–7.01 (m, 8H), 4.86 (dd, J = 8.4, 2.8 Hz, 1H), 4.04 (d, J = 8.4 Hz, 1H), 3.11 (d, J = 2.8 Hz, 1H), 2.87–2.78 (m, 2H), 2.75–2.61 (m, 2H), 2.31 (s, 3H), 2.31 (s, 3H), **^{13}C NMR** (101 MHz, $CDCl_3$) δ = 140.5, 138.3, 137.3, 136.9, 136.6, 129.1, 128.8, 128.7, 128.6, 128.6, 126.8, 126.5, 77.0, 59.8, 36.3, 33.3, 21.3, 21.2; **IR** (thin layer film) ν = 3447, 3025, 2920, 2860, 1901, 1604, 1512, 1454, 1179, 1041, 814, 737, 698 cm^{-1}; **MP** 68–69 °C; **HRMS** (ESIpos) m/z calculated for $C_{24}H_{26}ONaS$ $(M+Na)^+$ 385.1597, found 385.1594.

***rac*-1,2-bis(4-chlorophenyl)-2-(phenethylthio)ethan-1-ol (6h)**

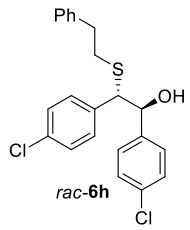

Alcohol **6h** was prepared according to the general procedure from the corresponding epoxide (7.2 mmol, 1.9 g) and by stirring the reaction mixture at reflux for 2 h. **Purification** FCC, eluent = hexane:Et_2O (100:0 to 80:20 gradient), yellow oil, 2.63 g, 92% yield. **^{1}H NMR** (400 MHz, $CDCl_3$) δ = 7.23–7.17 (m, 7H), 7.15–7.09 (m, 2H), 7.06–6.99 (m, 4H), 4.65 (dd, J = 8.6, 2.5 Hz, 1H), 3.79 (d, J = 8.6 Hz, 1H), 3.10 (d, J = 2.5 Hz, 1H), 2.74 (t, J = 7.3 Hz, 2H), 2.64–2.55 (m, 2H), **^{13}C NMR** (101 MHz, $CDCl_3$) [overlapping signals] δ = 140.0, 139.2, 137.8, 133.6, 133.3, 130.0, 128.7,128.7, 128.4, 128.2, 126.7, 76.7, 59.7, 36.2, 33.4; **IR** (thin layer film) ν = 3432, 3027, 2916, 1901, 1596, 1489, 1454, 1407, 1180, 1089, 1014, 834, 747, 697 cm^{-1}; **HRMS** (ESIpos) m/z calculated for $C_{22}H_{20}OCl_2NaS$ $(M+Na)^+$ 425.0504, found 425.0505.

***rac*-1,2-bis(4-fluorophenyl)-2-(phenethylthio)ethan-1-ol (6i)**

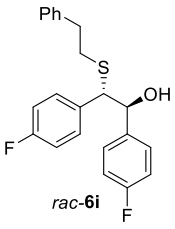

Alcohol **6i** was prepared according to the general procedure from the corresponding epoxide (5.16 mmol, 1.2 g) and by stirring the reaction mixture at reflux for 2 h. **Purification** FCC, eluent = hexane:Et_2O (100:0 to 80:20 gradient), yellow oil, 800 mg, 60% yield. **^{1}H NMR** (400 MHz, $CDCl_3$) δ = 7.31–7.19 (m, 3H), 7.11–7.07 (m, 2H), 7.05–6.99 (m, 4H), 6.92–6.84 (m, 4H), 4.73 (d, J = 8.8 Hz, 1H), 3.88 (d, J = 8.8 Hz, 1H), 3.09 (s br, 1H), 2.81 (t, J = 7.3 Hz, 2H), 2.74–2.62 (m, 2H), **^{19}F NMR** (376 MHz, CDCl3) δ = -114.2–-114.3 (m, 1F), -114.5–-114.6 (m, 1F), **^{13}C NMR** (101 MHz, $CDCl_3$) [overlapping signals] δ = 164.4 (d, $J_{C–F}$ = 246.6 Hz), 162.0 (d, $J_{C–F}$ = 245.7 Hz), 140.1, 135.5 (d, $J_{C–F}$ = 3.7 Hz), 135.2 (d, $J_{C–F}$ = 3.7 Hz), 130.2 (d, $J_{C–F}$ = 8.1 Hz), 128.7, 128.5, 128.4 (d, $J_{C–F}$ = 8.1 Hz), 126.6, 115.4 (d, $J_{C–F}$ = 21.4 Hz), 115.1 (d, $J_{C–F}$ = 21.5 Hz), 77.0,

59.7, 36.2, 33.4; **IR** (thin layer film) ν = 3433, 2919, 1603, 1507, 1221, 1157, 1095, 832, 804, 746, 698 cm^{-1}; **HRMS** (ESIpos) m/z calculated for $C_{22}H_{20}OF_2NaS$ $(M+Na)^+$ 393.1095, found 393.1095.

***rac*-1,2-di(naphthalen-2-yl)-2-(phenethylthio)ethan-1-ol (6j)**

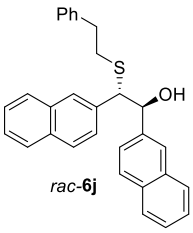

rac-**6j**

Alcohol **6j** was prepared according to the general procedure from the corresponding epoxide (2.87 mmol, 850 mg) and by stirring the reaction mixture at reflux for 5 h. **Purification** FCC, eluent = hexane:Et_2O (100:0 to 80:20 gradient), yellow oil, 1.13 g, 91% yield. **^{1}H NMR** (500 MHz, $CDCl_3$) δ = 7.79–7.62 (m, 7H), 7.54 (s, 1H), 7.46–7.35 (m, 5H), 7.30–7.16 (m, 4H), 7.07–7.01 (m, 2H), 5.16 (d, *J* = 8.3 Hz, 1H), 4.30 (d, *J* = 8.3 Hz, 1H), 3.28 (s br, 1H), 2.87–2.76 (m, 2H), 2.75–2.61 (m, 2H), **^{13}C NMR** (126 MHz, $CDCl_3$) [overlapping signals] δ = 140.2, 138.6, 137.0, 133.1, 133.1, 132.8, 128.7, 128.6, 128.3, 128.1, 127.9, 127.9, 127.7, 127.7, 127.7, 126.5, 126.5, 126.2, 126.1, 126.0, 126.0, 126.0, 124.6, 77.1, 60.3, 36.3, 33.4; **IR** (thin layer film) ν = 3427, 3056, 3025, 2916,1631, 1508, 1496, 1454, 1364, 1271, 1048, 906, 820, 747, 698 cm^{-1}; **MP** 48–52 °C, **HRMS** (ESIpos) m/z calculated for $C_{30}H_{26}ONaS$ $(M+Na)^+$ 457.1597, found 457.1597.

***rac*-2-(methylthio)-1,2-di-m-tolylethan-1-ol (6l)**

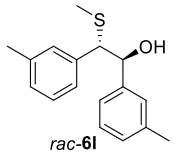

rac-**6l**

The corresponding epoxide (4.4 mmol, 1.0 g, 1.0 equiv.) and sodium methanethiolate (2.0 equiv.) were dissolved in EtOH (0.1 M) in a round-bottom flask at room temperature. The mixture was then refluxed until TLC analysis showed no further conversion (hexane:CH_2Cl_2 = 80:20 as eluent). The reaction vessel was then cooled to room temperature and the solvent was removed *in vacuo*. The residue was then treated with Et_2O and water, the layers were partitioned and the aqueous phase was extracted three times with Et_2O. The organic phases were combined, dried over $MgSO_4$, filtered and concentrated *in vacuo*. The crude product was then purified by flash column chromatography (hexane:Et_2O 100:0 to 80:20 gradient), to afford **6l** as a yellow oil (1.00 g, 83% yield). **^{1}H NMR** (500 MHz, $CDCl_3$) δ = 7.09 (q, *J* = 7.6 Hz, 2H), 7.04–6.92 (m, 6H), 4.87 (d, *J* = 8.1 Hz, 1H), 3.94 (d, *J* = 8.1 Hz, 1H), 3.08 (s br, 1H), 2.27 (s, 3H), 2.26 (s, 3H), 1.97 (s, 3H), **^{13}C NMR** (126 MHz, $CDCl_3$) δ = 141.1, 139.1, 138.0, 137.7, 129.4, 128.6, 128.2, 128.0, 127.4, 125.8, 124.0, 76.6, 61.4, 21.5, 14.9; **IR** (thin layer film) ν = 3421, 3023, 2916, 1606, 1488, 1436, 1044, 778, 732, 699 cm^{-1}; **HRMS** (ESIpos) m/z calculated for $C_{17}H_{20}ONaS$ $(M+Na)^+$ 295.1127, found 295.1127.

Synthesis of bromo sulfides with TMSBr (method A)

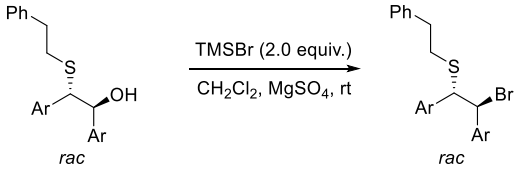

Figure S6. – *Synthesis of bromide substrates (method A)*

The employed protocol followed a slightly modified literature procedure (*44*).

In a vial equipped with a magnetic stirring bar, the appropriate hydroxy sulfide was dissolved in CH_2Cl_2 (1.0 M), and anhydrous $MgSO_4$ was added (500 mg/mmol), followed by dropwise addition of TMSBr (2 equiv.). After stirring at rt for 1 h, the crude mixture was filtered over celite and the solvent was evaporated *in vacuo* thus affording the desired compounds without any further purification (96–99% purity).

Synthesis of bromo sulfides via PBr_3 bromination (method B)

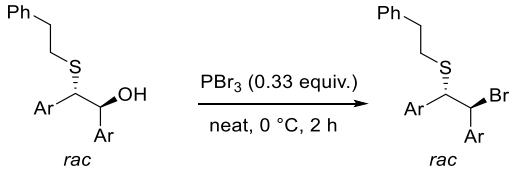

Figure S7. – *Synthesis of bromide substrates (method B)*

In a flame-dried round-bottom flask equipped with a magnetic stirring bar and under inert atmosphere, the appropriate hydroxy sulfide (neat for liquid alcohols, 1 M CH_2Cl_2 solution for solids) was cooled to 0 °C in an ice-bath and PBr_3 (0.33 equiv.) was added dropwise. The solution was then stirred at this temperature for 2 h. After this time, the reaction was quenched by the addition of ice-cold water and diluted with cold Et_2O. The layers were partitioned and the aqueous phase was extracted three times with Et_2O. The organic phases were combined, dried over Na_2SO_4, filtered and concentrated *in vacuo* to afford the desired bromide without any further purification (96–99% purity).

N.B. The bromides starting materials were unstable on silica gel and proved to be unstable for MS analysis with a variety of ionization methods (HRMS of the molecular ion was therefore not recorded). To prevent any decomposition, they were always stored in the fridge.

***rac*-2-bromo-1,2-diphenylethyl(phenethyl)sulfane (1a)**

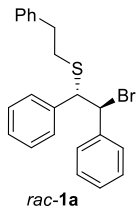

Bromide **1a** was prepared from *cis*-stilbene according to a modified literature procedure (*45*). In a flame-dried round-bottom flask filled with argon and equipped with a magnetic stirring bar, diphenylethyl disulfide (3 mmol, 814 mg, 1.0 equiv.) was dissolved in 7 ml of anhydrous CH_2Cl_2. The solution was cooled to 0 °C and a solution of Br_2 (6 ml, 0.5 M in CH_2Cl_2, 3 mmol, 1.0 equiv.) was added dropwise. The solution was stirred at 0 °C for 2 h protected from light, forming an orange/yellow solution. After this time, *cis*-stilbene (1 ml, 6 mmol, 2.0 equiv.) was added neat at 0 °C and stirring was continued at the same temperature. Once the orange/yellow colour had disappeared (approx. 1 h), the crude mixture was evaporated to dryness and the residue was stirred in hexane:Et_2O (20:1) to afford a solid which was then recrystallized in hexane:Et_2O (20:1) to afford **1a** as a white solid (800 mg, 33% yield). **^{1}H NMR** (400 MHz, $CDCl_3$) δ = 7.27–7.04 (m, 15H), 5.24 (d, J = 9.0 Hz, 1H), 4.48 (d, J = 9.0 Hz, 1H), 2.89–2.73 (m, 2H), 2.60–2.53 (m, 2H), **^{13}C NMR** (100 MHz, $CDCl_3$) δ = 140.3, 139.6, 138.5, 128.9, 128.5, 128.5, 128.4, 128.3, 128.3 128.2, 127.8, 126.3, 58.1, 58.0, 36.0, 33.6; **MP** 64–65 °C, **IR** (thin layer film) ν = 3657, 2980, 2888, 1473, 1462, 1383, 1252, 1152, 1073, 955, 695 cm^{-1}; **HRMS** (APCIpos) m/z calculated for $C_{22}H_{21}S$ $(M\text{-}Br)^+$ 317.1358, found 317.1355.

***rac*-2-chloro-1,2-diphenylethyl)(phenethyl)sulfane (1a')**

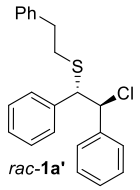

Chloride **1a'** was prepared according to a reported procedure (*46*). Alcohol **6a** (500 mg, 1.45 mmol) was dissolved in anhydrous CH_2Cl_2 (7.2 ml) under inert atmosphere and the solution was cooled to 0 °C. At this temperature, anhydrous *N*,*N*-dimethylformamide (5.0 mol%) and thionyl chloride (160 μL, 2.18 mmol, 1.5 equiv.) were sequentially added and the reaction mixture was stirred for 30 min at 0 °C. The volatiles were then evaporated *in vacuo* to afford **1a'** as a pale yellow solid (400 mg, 79% yield). **^{1}H NMR** (500 MHz, $CDCl_3$) δ = 7.30–7.04 (m, 15H), 5.19 (d, J = 8.4 Hz, 1H), 4.39 (d, J = 8.4 Hz, 1H), 2.89–2.73 (m, 2H), 2.59 (t, J = 7.9 Hz, 2H), **^{13}C NMR** (126 MHz, $CDCl_3$) δ = 140.5, 139.1, 138.5, 129.1, 128.6, 128.6, 128.4, 128.3, 128.1, 128.0, 127.8, 126.5, 67.0, 58.7, 36.2, 33.6; **MP** 58–60 °C; **IR** (thin layer film) ν = 3061, 3028, 2918, 2850, 1602, 1494, 1453, 1074, 1030, 748, 698 cm^{-1}; **HRMS** (EI) m/z calculated for $C_{22}H_{20}S$ $(M\text{-}HCl)^{+\cdot}$ 316.1276, found 316.1276.

***rac*-2-(phenethylthio)-1,2-diphenylethyl 2,2,2-trichloroacetimidate (1a'')**

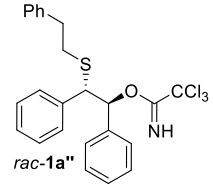

Trichloroacetimidate **1a''** was synthesised according to a reported procedure (*21*). Under inert atmosphere, alcohol **6a** (500 mg, 1.45 mmol) was dissolved in anhydrous CH_2Cl_2 (7.2 ml) and the solution was cooled to 0 °C. At this temperature, trichloroacetonitrile (290 μL, 2.9 mmol, 2 equiv.) and sodium hydride (12 mg, 0.3

mmol, 0.2 equiv.) were added sequentially and the reaction mixture was stirred overnight at 0 °C. The reaction was quenched by addition of water, the layers were separated and the aqueous one was extracted three times with EtOAc. The organic layers were then combined, washed with brine and dried over $MgSO_4$. After removal of the solvent under reduced pressure, the crude product was purified by FCC (hexane: AcOEt = 98: 2 with 1% NEt_3) and subsequently recrystalized in hexane to afford **1a''** as a white solid (430 mg, 62% yield). **^{1}H NMR** (500 MHz, $CDCl_3$) δ = 8.35 (s, 1H), 7.28–7.10 (m, 13H), 7.09–7.04 (m, 2H), 6.12 (d, *J* = 7.6 Hz, 1H), 4.32 (d, *J* = 7.7 Hz, 1H), 2.85–2.75 (m, 2H), 2.73–2.62 (m, 2H), **^{13}C NMR** (126 MHz, $CDCl_3$) δ = 161.2, 140.6, 138.1, 137.3, 129.3, 128.7, 128.5, 128.3, 128.2, 127.9, 127.7, 127.3, 126.4, 91.6, 83.5, 55.7, 36.3, 33.4, **MP** 92–93 °C; **IR** (thin layer film) ν = 3338, 3062, 3029, 2918, 1664, 1495, 1454, 1289, 1073, 992, 824, 795,697, 649 cm^{-1}; **HRMS** (EI) m/z calculated for $C_{22}H_{20}S$ $(M\text{-}C_2Cl_3NH_2O)^{+\cdot}$ 316.1276, found 316.1276.

***rac*-2-bromo-1,2-bis(3-chlorophenyl)ethyl(phenethyl)sulfane (1b)**

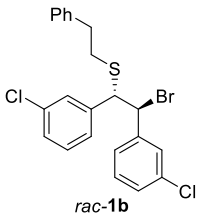

rac-**1b**

Bromide **1b** was prepared according to the general procedure (method B) by employing alcohol **6b** (3.4 mmol, 1.4 g) as starting material. Yellow solid, 1.4 g, 89% yield. **^{1}H NMR** (500 MHz, $CDCl_3$) δ = 7.32–7.23 (m, 3H), 7.21–7.09 (m, 8H), 7.01 (ddt, *J* = 24.9, 7.6, 1.5 Hz, 2H), 5.12 (d, *J* = 8.2 Hz, 1H), 4.28 (d, *J* = 8.2 Hz, 1H), 2.92–2.81 (m, 2H), 2.67–2.57 (m, 2H), **^{13}C NMR** (126 MHz, $CDCl_3$) [overlapping signals] δ = 140.9, 140.4, 140.1, 134.2, 134.0, 129.5, 129.4, 128.9, 128.7, 128.6, 128.6, 128.1, 127.2, 126.6, 126.5, 57.5, 56.1, 36.1, 33.7; **MP** 86–88 °C; **IR** (thin layer film) ν = 3063, 3026, 2955, 2933, 1571, 1475, 1430, 1077, 885, 863, 795, 712, 689 cm^{-1}.

***rac*-2-bromo-1,2-bis(3-methoxyphenyl)ethyl(phenethyl)sulfane (1c)**

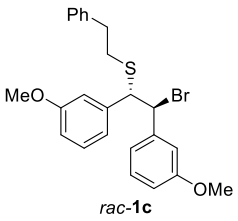

rac-**1c**

Bromide **1c** was prepared according to the general procedure (method A) by employing alcohol **6c** (2.9 mmol, 1.2 g) as starting material. Brown oil, 835 mg, 63% yield.**^{1}H NMR** (400 MHz, $CDCl_3$) δ = 7.30–7.16 (m, 4H), 7.13–7.06 (m, 3H), 6.78 (d, *J* = 7.8 Hz, 1H), 6.75–6.67 (m, 5H), 5.19 (d, *J* = 8.8 Hz, 1H), 4.40 (d, *J* = 8.8 Hz, 1H), 3.70 (s, 3H), 3.69 (s, 3H), 2.89–2.69 (m, 2H), 2.64–2.49 (m, 2H), **^{13}C NMR** (101 MHz, $CDCl_3$) δ = 159.3, 159.1, 140.9, 140.3, 140.1, 129.1, 129.1, 128.6, 128.4, 126.3, 121.4, 120.6, 114.3, 114.0, 113.9, 113.3, 58.1, 57.9, 55.2, 55.2, 36.0, 33.6; **IR** (thin layer film) ν = 3059, 3025, 3001, 2935, 2834, 1598, 1584, 1489, 1464, 1260, 1148, 1044 870, 776, 742, 732, 696 cm^{-1}.

***rac*-2-bromo-1,2-di-*m*-tolylethyl(phenethyl)sulfane (1d)**

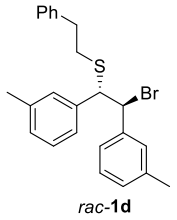

rac-**1d**

Bromide **1d** was prepared according to the general procedure (method A) by employing alcohol **6d** (3.5 mmol, 1.5 g) as starting material. Brown solid, 1.4 g, 94% yield. **^{1}H NMR** (500 MHz, $CDCl_3$) δ = 7.29–7.20 (m, 3H), 7.13–7.05 (m, 4H), 7.09–6.90 (m, 6H), 5.24 (d, J = 8.7 Hz, 1H), 4.45 (d, J = 8.7 Hz, 1H), 2.85-2.75 (m, 2H), 2.58 (t, J = 7.9 Hz, 2H), 2.26 (s, 6H), **^{13}C NMR** (126 MHz, $CDCl_3$) δ = 140.4, 139.5, 138.5, 137.7, 137.6, 129.5, 129.0, 129.0, 128.5, 128.4, 128.4, 128.0, 127.9, 126.3, 126.0, 125.3, 58.4, 58.0, 36.1, 33.6, 21.3, 21.3; **MP** 56–58 °C; **IR** (thin layer film) ν = 3023, 2917, 2851, 1603, 1585, 1488, 1451, 1408, 1374, 1313, 1254, 1226, 1213, 1165, 1156, 1097, 1029, 997, 961, 902, 888,823, 791, 784, 763, 749, 736, 700 cm^{-1}.

***rac*-2-bromo-1,2-bis(3-fluorophenyl)ethyl(phenethyl)sulfane (1e)**

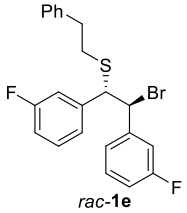

rac-**1e**

Bromide **1e** was prepared according to the general procedure (method A) by employing alcohol **6e** (1.3 mmol, 500 mg) as starting material, and stirring the reaction for 6 h in the presence of 4 equiv. of TMSBr. Brown oil, 350 mg, 62% yield. **^{1}H NMR** (500 MHz, $CDCl_3$) δ = 7.31–7.20 (m, 3H), 7.20–7.10 (m, 4H), 6.95–6.87 (m, 6H), 5.14 (d, J = 8.7 Hz, 1H), 4.34 (d, J = 8.7 Hz, 1H), 2.88–2.76 (m, 2H), 2.60 (m, 2H), **^{19}F NMR** (470 MHz, $CDCl_3$) δ = -112.4–-112.5 (m, 2F), **^{13}C NMR** (126 MHz, $CDCl_3$) δ = 162.5 (d, $J_{C–F}$ = 246.9 Hz), 162.3 (d, $J_{C–F}$ = 246.8 Hz), 141.5 (d, $J_{C–F}$ = 7.4 Hz), 141.0 (d, $J_{C–F}$ = 7.0 Hz), 140.0, 129.7 (d, $J_{C–F}$ = 8.3 Hz), 129.7 (d, $J_{C–F}$ = 8.2 Hz), 128.6, 128.53, 126.5, 124.6 (d, $J_{C–F}$ = 2.9 Hz), 123.9 (d, $J_{C–F}$ = 3.1 Hz), 115.6 (d, $J_{C–F}$ = 22.3 Hz), 115.5 (d, $J_{C–F}$ = 21.0 Hz), 115.3 (d, $J_{C–F}$ = 22.6 Hz), 114.9 (d, $J_{C–F}$ = 21.3 Hz), 57.6 (d, $J_{C–F}$ = 1.8 Hz), 56.2 (d, $J_{C–F}$ = 2.0 Hz), 36.0, 33.6; **IR** (thin layer film) ν = 3062, 3027, 2917, 2849, 1613, 1589, 1523, 1487, 1447, 1254, 1138, 953, 878, 782, 737, 709, 696 cm^{-1}.

***rac*-2-bromo-1,2-bis(3,5-dimethylphenyl)ethyl(phenethyl)sulfane (1f)**

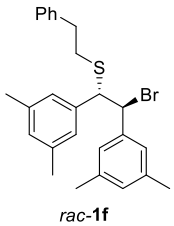

rac-**1f**

Bromide **1f** was prepared according to the general procedure (method A) by employing alcohol **6f** (1.2 mmol, 460 mg) as starting material. Yellow solid, 300 mg, 60% yield. **^{1}H NMR** (400 MHz, $CDCl_3$) δ = 7.28–7.18 (m, 3H), 7.09–7.06 (m, 2H), 6.81 (s, 2H), 6.79 (d, J = 3.3 Hz, 2H), 6.74 (s, 2H), 5.20 (d, J = 8.2 Hz, 1H), 4.38 (d, J = 8.2 Hz, 1H), 2.88–2.68 (m, 2H), 2.62–2.50 (m, 2H), 2.22 (s, 12H), **^{13}C NMR** (101 MHz, $CDCl_3$) δ = 140.5, 139.3, 138.4, 137.4, 137.4, 129.9, 129.2, 128.5, 128.4, 126.8, 126.3, 126.2, 58.7, 57.7, 36.1, 33.7, 21.2, 21.1; **MP** 101–103 °C; **IR** (thin layer film) ν = 3023, 2916, 2856, 1599, 1495, 1453, 1374, 1159, 997, 850, 793, 769, 753, 734, 720, 695, 632, cm^{-1}.

***rac*-2-bromo-1,2-di-*p*-tolylethyl(phenethyl)sulfane (1g)**

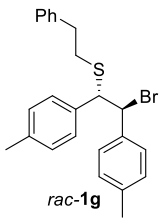

Bromide **1g** was prepared according to the general procedure (method B) by employing alcohol **6g** (3.3 mmol, 1.2 g) as starting material. Brown solid, 800 mg, 57% yield. **^{1}H NMR** (400 MHz, $CDCl_3$) δ = 7.32–7.18 (m, 3H), 7.11–6.97 (m, 10H), 5.26 (d, J = 8.9 Hz, 1H), 4.47 (d, J = 8.9 Hz, 1H), 2.89–2.73 (m, 2H), 2.58–2.52 (m, 2H), 2.28 (s, 6H), **^{13}C NMR** (101 MHz, $CDCl_3$) δ = 140.4, 138.0, 137.2, 136.7, 135.5, 128.9, 128.8, 128.7, 128.5, 128.4, 128.1, 126.3, 58.4, 57.7, 36.1, 33.6, 21.2, 21.1; **MP** 67–69 °C; **IR** (thin layer film) ν = 3051, 2954, 2854, 1603, 1513, 1496, 1478, 1446, 1412, 1376, 1323, 1298, 1270, 1229, 1199, 1184, 1163, 1111, 1070, 1040, 1021, 970, 912, 868, 784, 764, 738, 722, 707, 696 cm^{-1}.

***rac*-2-bromo-1,2-bis(4-chlorophenyl)ethyl(phenethyl)sulfane (1h)**

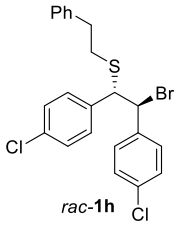

Bromide **1h** was prepared according to the general procedure (method A) by employing alcohol **6h** (1.2 mmol, 500 mg) as starting material, and stirring the reaction for 6 h in the presence of 4 equiv. of TMSBr. Brown oil, 380 mg, 75% yield. **^{1}H NMR** (400 MHz, $CDCl_3$) δ = 7.30–6.99 (m, 13H), 5.13 (d, J = 8.3 Hz, 1H), 4.31 (d, J = 8.2 Hz, 1H), 2.80 (dd, J = 8.4, 5.6 Hz, 2H), 2.56 (t, J = 7.7 Hz, 2H), **^{13}C NMR** (101 MHz, $CDCl_3$) δ = 140.0, 137.4, 136.6, 134.2, 133.6, 130.3, 129.7, 128.5, 128.5, 128.4, 128.3, 126.5, 57.3, 56.3, 36.0, 33.6; **IR** (thin layer film) ν = 3084, 3062, 3026, 2918, 2849, 1650, 1456, 1406, 1315, 1029, 826, 764, 742, 623 cm^{-1}.

***rac*-2-bromo-1,2-bis(4-fluorophenyl)ethyl(phenethyl)sulfane (1i)**

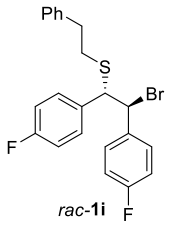

Bromide **1i** was prepared according to the general procedure (method B) by employing alcohol **6i** (3.2 mmol, 1.2 mg) as starting material. Brown solid, 800 mg, 60% yield. **^{1}H NMR** (500 MHz, $CDCl_3$) δ = 7.45–7.30 (m, 3H), 7.25–7.13 (m, 6H), 6.99 (q, J = 8.6 Hz, 4H), 5.28 (d, J = 8.4 Hz, 1H), 4.47 (d, J = 8.4 Hz, 1H), 2.92 (td, J = 7.5, 4.6 Hz, 2H), 2.68 (t, J = 8.0 Hz, 2H), **^{19}F NMR** (470 MHz, $CDCl_3$) δ = -112.8 (ddd, J = 13.7, 8.6, 5.3 Hz, 1F), -113.7 (ddd, J = 14.1, 8.9, 5.2 Hz, 1F), **^{13}C NMR** (126 MHz, $CDCl_3$) δ = 162.3 (d, $J_{C–F}$ = 248.1 Hz), 162.0 (d, $J_{C–F}$ = 247.3 Hz), 140.1, 135.0 (d, $J_{C–F}$ = 3.3 Hz), 133.9 (d, $J_{C–F}$ = 3.3 Hz), 130.6 (d, $J_{C–F}$ = 8.1 Hz), 130.1 (d, $J_{C–F}$ = 8.4 Hz), 128.6, 128.5, 126.5, 115.2 (d, $J_{C–F}$ = 17.8 Hz), 115.0 (d, $J_{C–F}$ = 18.1 Hz), 57.5, 56.8, 36.0, 33.7; **MP** 54–56 °C; **IR** (thin layer film) ν = 3062, 3024, 2958, 2925, 1601, 1508, 1240, 1220, 1158, 1147, 1072, 1031, 835, 802, 767, 727, 647 cm^{-1}.

***rac*-2-bromo-1,2-di(naphthalen-2-yl)ethyl(phenethyl)sulfane (1j)**

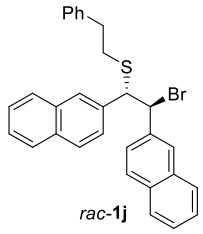

rac-**1j**

Bromide **7j** was prepared according to the general procedure (method A) by employing alcohol **6j** (0.9 mmol, 390 mg) as starting material, brown solid, 400 mg, 89% yield. **^{1}H NMR** (400 MHz, $CDCl_3$) δ = 7.76–7.62 (m, 6H), 7.60 (s, 1H), 7.52 (s, 1H), 7.44–7.34 (m, 6H), 7.25–7.17 (m, 3H), 7.03 (d, *J* = 6.3 Hz, 2H), 5.57 (d, *J* = 8.9 Hz, 1H), 4.75 (d, *J* = 8.9 Hz, 1H), 2.91–2.73 (m, 2H), 2.56 (t, *J* = 7.7 Hz, 2H), **^{13}C NMR** (101 MHz, $CDCl_3$) δ = 140.2, 136.7, 135.8, 132.9, 132.8, 132.8, 132.6, 128.6, 128.4, 128.3, 128.2, 128.1, 128.1, 127.8, 127.6, 127.6, 127.4, 126.4, 126.3, 126.2, 126.2, 126.1, 125.9, 125.7, 58.2, 58.0, 36.1, 33.6; **MP** 35–37 °C; **IR** (thin layer film) ν = 3056, 2917, 1700, 1507, 1496, 1453, 1366, 1271, 1156, 1123, 1073, 1218, 960, 893, 859, 816, 796, 745, 697, 622 cm^{-1}.

***rac*-2-bromo-1,2-diphenylethyl(methyl)sulfane (1k)**

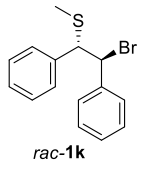

rac-**1k**

Bromide **1k** was prepared from *cis*-stilbene according to a modified literature procedure (*45*). In a flame-dried argon filled round-bottom flask equipped with a magnetic stirring bar, dimethyl disulfide (5.5 mmol, 0.49 ml, 1.1 equiv.) was dissolved in anhydrous CH_2Cl_2 (15 mL). The solution was cooled to 0 °C and a solution of Br_2 (10 ml, 0.5 M in CH_2Cl_2, 5 mmol, 1.0 equiv.) was added dropwise. The solution was stirred at 0 °C for 2 h protected from light. After this time, *cis*-stilbene (1.7 ml, 10 mmol, 2.0 equiv) was added neat at 0 °C and stirring was continued at the same temperature. Once the orange/yellow colour had disappeared (~1 h), the crude mixture was evaporated to dryness and the residue stirred in hexane:Et_2O (20:1) to afford a solid that was then recrystallized in hexane:Et_2O (20:1) to afford **1k** as a white solid (1.2 g, 40% yield). **^{1}H NMR** (500 MHz, $CDCl_3$) δ = 7.24–7.14 (m, 10H), 5.29 (d, *J* = 9.1 Hz, 1H), 4.43 (d, *J* = 9.1 Hz, 1H), 1.91(s, 3H), **^{13}C NMR** (126 MHz, $CDCl_3$) [overlapping signals] δ = 139.6, 138.3, 128.7, 128.3, 128.2, 128.1, 127.6, 60.0, 58.0, 15.5; **MP** 58–59 °C; **IR** (thin layer film) ν = 3735, 3649, 2981, 2888, 1456, 1382, 1252, 1151, 1073, 955, 695, 689 cm^{-1}.

***rac*-2-bromo-1,2-di-(*m*-tolylethyl)(methyl)sulfane (1l)**

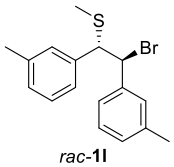

rac-**1l**

Bromide **1l** was prepared according to the general procedure (method B) by employing alcohol **6l** (3.7 mmol, 1.0 g) as starting material, brown solid, 1.0 g, 80% yield. **^{1}H NMR** (500 MHz, $CDCl_3$) δ = 7.11–7.02 (m, 4H), 7.00–6.91 (m, 4H), 5.28 (d, *J* = 8.8 Hz, 1H), 4.39 (d, *J* = 8.8 Hz, 1H), 2.25 (s, 6H), 1.92 (s, 3H), **^{13}C NMR** (126 MHz, $CDCl_3$) δ = 139.6, 138.3, 137.8, 137.7, 129.4, 129.0, 129.0, 128.3, 127.9, 127.9, 125.9, 125.3, 59.6, 58.3, 21.4, 21.3, 15.6; **MP** 79–80 °C; **IR** (thin layer film) ν = 3007, 2961, 2921, 1601, 1585, 1173, 1154, 1089, 1064, 1039, 998, 814, 701, 669 cm^{-1}.

Products Characterization

((1*S*,2*S*)-2-fluoro-1,2-diphenylethyl)(phenethyl)sulfane (3a)

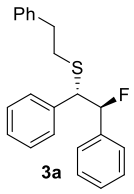

Product **3a** was prepared according to the general procedure by employing 0.2 mmol of substrate (79.5 mg) and the reaction was stirred at –30 °C for 72 h. **Purification** FCC eluent = pentane:Et_2O (100:0 to 99:1 gradient), white solid, 55.0 mg, 83% yield, e.r. = 95.5:4.5. **^{1}H NMR** (400 MHz, $CDCl_3$) δ = 7.30–7.19 (m, 9H), 7.17–7.14 (m, 2H), 7.11–7.09 (m, 4H), 5.67 (dd, J = 46.3, 7.5 Hz, 1H), 4.22 (dd, J = 13.6, 7.5 Hz, 1H), 2.88–2.62 (m, 4H), **^{19}F NMR** (376 MHz, $CDCl_3$) δ = -172.6 (dd, J = 46.3, 13.6 Hz, 1F), **^{13}C NMR** (101 MHz, $CDCl_3$) δ = 140.5, 137.8 (d, $J_{C–F}$ = 4.8 Hz), 137.6 (d, $J_{C–F}$ = 21.1 Hz), 129.1, 128.7, 128.6 (d, $J_{C–F}$ = 2.4 Hz), 128.5, 128.5, 128.1, 127.8, 126.4 (d, $J_{C–F}$ = 7.0 Hz), 126.4, 97.1 (d, $J_{C–F}$ = 180.3 Hz), 56.4 (d, $J_{C–F}$ = 23.9 Hz), 36.5, 33.4; **MP** 34–36 °C; **IR** (thin layer film) ν = 3029, 2922, 1602, 1495, 1453, 1211, 1049, 1030, 998, 755, 732, 697, 627 cm^{-1}; **HRMS** (EI) m/z calculated for $C_{22}H_{20}S$ $(M\text{-}HF)^{+\cdot}$ 316.128, found 316.1281; **$[\alpha]_D^{25\,°C}$** +104.7 ° (c = 1.0, $CHCl_3$, e.r. = 95.5:4.5); **HPLC** DAICEL CHIRALPAK® IC-3, Heptane:EtOH = 99.75:0.25, 1 ml/min, t_1 = 5.8 (major), t_2 = 6.8 (minor).

The opposite enantiomer (*1R,2R*)-**3a** (**$[\alpha]_D^{25\,°C}$** –97.2 ° – c = 1.0, $CHCl_3$, e.r. = 95:5) was prepared following the same protocol using (*R*)-**4h** as catalyst (81% yield, e.r. = 95:5).

((1*S*,2*S*)-1,2-bis(3-chlorophenyl)-2-fluoroethyl)(phenethyl)sulfane (3b)

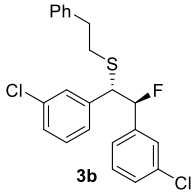

Product **3b** was prepared according to the general procedure by employing 0.2 mmol of substrate (93.2 mg) and the reaction was stirred at rt for 72 h. **Purification** FCC, eluent = pentane:Et_2O (100:0 to 99:1 gradient), white solid, 79.4 mg, 98% yield, e.r. = 97:3. **^{1}H NMR** (500 MHz, $CDCl_3$) δ = 7.34–7.09 (m, 11H), 7.02 (d, J = 7.6 Hz, 1H), 6.95 (d, J = 7.7 Hz, 1H), 5.62 (dd, J = 46.0, 6.6 Hz, 1H), 4.08 (dd, J = 15.6, 6.6 Hz, 1H), 2.88–2.78 (m, 2H), 2.79–2.63 (m, 2H), **^{19}F NMR** (470 MHz, $CDCl_3$) δ = -174.9 (dd, J = 46.0, 15.5 Hz, 1F), **^{13}C NMR** (126 MHz, $CDCl_3$) δ = 140.1, 139.6 (d, $J_{C–F}$ = 3.7 Hz), 139.0 (d, $J_{C–F}$ = 21.3 Hz), 134.3, 134.1, 129.7, 129.3, 129.0, 128.8 (d, $J_{C–F}$ = 1.2 Hz), 128.6, 128.5, 128.1, 127.2, 126.5, 126.3 (d, $J_{C–F}$ = 7.6 Hz), 124.4 (d, $J_{C–F}$ = 7.1 Hz), 95.5 (d, $J_{C–F}$ = 182.9 Hz), 55.5 (d, $J_{C–F}$ = 24.0 Hz), 36.2, 33.3 (d, $J_{C–F}$ = 1.8 Hz); **MP:** 44–45 °C; **IR** (thin layer film) ν = 3062, 3027, 2918, 2849, 1595, 1573, 1495, 1476, 1453, 1430, 1209, 1188, 1098, 1080, 1051, 999, 882, 785, 773, 746, 694 cm^{-1}; **HRMS** (EI) m/z calculated for $C_{22}H_{18}Cl_2S$ $(M\text{-}HF)^{+\cdot}$ 384.0501, found 384.0501; **$[\alpha]_D^{25\,°C}$** +83.4 ° (c = 1.0, $CHCl_3$, e.r. = 97:3); **HPLC** DAICEL CHIRALPAK® IB-3, Heptane:EtOH 99.9:0.1, 1 ml/min, t_1: 14.5 min (minor), t_2: 15.8 min (major).

((1*S*,2*S*)-2-fluoro-1,2-bis(3-methoxyphenyl)ethyl)(phenethyl)sulfane (3c)

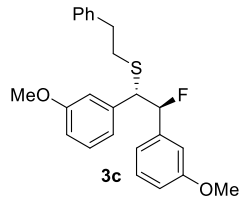

Product **3c** was prepared according to the general procedure by employing 0.2 mmol of substrate (91.5 mg) and the reaction was stirred at 0 °C for 72 h. **Purification** FCC, eluent = pentane:Et_2O (100:0 to 80:20 gradient), colourless oil, 70.5 mg, 89% yield, e.r. = 96:4. **^{1}H NMR** (500 MHz, $CDCl_3$) δ = 7.32–7.09 (m, 7H), 6.84–6.64 (m, 6H), 5.66 (dd, J = 46.4, 7.2 Hz, 1H), 4.18 (dd, J = 14.1, 7.2 Hz, 1H), 3.75 (s, 3H), 3.73 (s, 3H), 2.89–2.77 (m, 2H), 2.76–2.68 (m, 2H), **^{19}F NMR** (470 MHz, $CDCl_3$) δ = -173.1 (dd, J = 46.4, 14.1 Hz, 1F), **^{13}C NMR** (126 MHz, $CDCl_3$) [overlapping signals] δ = 159.5, 159.2, 140.4, 139.3 (d, $J_{C–F}$ = 4.3 Hz), 139.0 (d, $J_{C–F}$ = 21.0 Hz), 129.3, 129.0, 128.5, 128.4, 126.3, 121.4, 118.6 (d, $J_{C–F}$ = 7.0 Hz), 114.3 (d, $J_{C–F}$ = 2.9 Hz), 114.3, 113.4, 111.6 (d, $J_{C–F}$ = 7.5 Hz), 96.7 (d, $J_{C–F}$ = 181.0 Hz), 56.2 (d, $J_{C–F}$ = 23.8 Hz), 55.2, 36.2, 33.3 (d, $J_{C–F}$ = 2.0 Hz); **IR** (thin layer film) ν = 3060, 3026, 2935, 2835, 1600, 1585, 1490, 1464, 1453, 1434, 1319, 1261, 1153, 1042, 995, 874, 780, 734, 696 cm^{-1}; **HRMS** (EI) m/z calculated for $C_{24}H_{25}FO_2S$ $(M)^{+\cdot}$ 396.1554, found 396.1561; **$[\alpha]_D^{25\ °C}$** +74.0 ° (c = 1.0, $CHCl_3$, e.r. = 96:4); **HPLC** DAICEL CHIRALPAK® IF-3, Heptane:EtOH 99.5:0.5, 1 ml/min, t_1: 10.7 min (major), t_2: 12.3 min (minor).

((1S,2S)-2-fluoro-1,2-di-*m*-tolylethyl)(phenethyl)sulfane (3d)

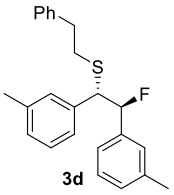

Product **3d** was prepared according to the general procedure by employing 0.2 mmol of substrate (85 mg) and the reaction was stirred at –30 °C for 72 h. **Purification** FCC, eluent = pentane:Et_2O (100:0 to 99:1 gradient), white solid, 50 mg , 69% yield, e.r. = 97:3. **Gram scale** Product **3d** was prepared according to the general procedure by employing 2.35 mmol of substrate (1 g) and the reaction was stirred at –10 °C for 72 h; **Purification** FCC, eluent = pentane:Et_2O (100:0 to 99:1 gradient followed by 25:75 to recover the catalyst), white solid, 531 mg , 62% yield, e.r. = 94:6; 99% recovered catalyst. After recrystallization in hexane (82% yield), e.r. > 99.9:0.1. **^{1}H NMR** (500 MHz, $CDCl_3$) δ = 7.34–7.20 (m, 3H), 7.19–6.88 (m, 10H), 5.66 (dd, J = 46.5, 7.2 Hz, 1H), 4.19 (dd, J = 14.5, 7.2 Hz, 1H), 2.92–2.76 (m, 2H), 2.71 (m, 2H), 2.31 (s, 3H), 2.31 (s, 3H), **^{19}F NMR** (470 MHz, $CDCl_3$) δ = -173.4 (dd, J = 46.4, 14.5 Hz, 1F), **^{13}C NMR** (126 MHz, $CDCl_3$) [overlapping signals] δ = 140.5, 138.0, 137.8 ($J_{C–F}$ = 4.3 Hz), 137.6, 137.6 ($J_{C–F}$ = 20.7 Hz), 129.5, 129.2, 129.1, 128.5, 128.4, 128.2, 127.8, 126.9, ($J_{C–F}$ = 6.8 Hz), 126.3, 126.0, 123.4 ($J_{C–F}$ = 6.9 Hz), 97.0 ($J_{C–F}$ = 180.0 Hz), 56.2 ($J_{C–F}$ = 23.7 Hz), 36.2, 33.3 ($J_{C–F}$ = 2.1 Hz), 21.4; **MP:** 84–86 °C; **IR** (thin layer film) ν = 3026, 2920, 1605, 1494, 1453, 1378, 1312, 1281, 1158, 1094, 1052, 999, 908, 883, 781, 731, 697, 636, 611 cm^{-1}; **HRMS** (EI) m/z calculated for $C_{24}H_{24}S$ $(M\text{-}HF)^{+\cdot}$ 344.1593, found 344.1587; **$[\alpha]_D^{25\ °C}$** +86.1 ° (c = 1.0, $CHCl_3$, e.r. = 97:3); **HPLC** DAICEL CHIRALPAK® IC-3, Heptane:EtOH 99.75:0.25, 1 ml/min, t_1: 4.4 min (major), t_2: 5.2 min (minor).

Single Crystal Data for **3d**: $C_{24}H_{25}FS$, Mr =364.53. 150 K – monoclinic, P21, a = 11.4021(3) Å, b = 7.21710(10) Å, c = 12.6576(3) Å, V = 987.66(4) Å, Data/restraints/parameters – 4088/1/236, Flack = 0.011(12) for 1862 Friedel pairs and Hooft = 0.012(3) for 1855 Friedel pairs, P2(correct) > 99.9999%, P3(correct), Rint = 0.033, Final R1 = 0.0318, wR2 = 0.0841 (I>2σ(I)).

((1*S*,2*S*)-2-fluoro-1,2-bis(3-fluorophenyl)ethyl)(phenethyl)sulfane (3e)

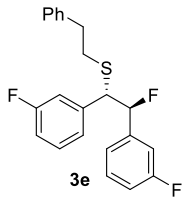

Product **3e** was prepared according to the general procedure by employing 0.2 mmol of substrate (86.6 mg) and the reaction was stirred at rt for 72 h. **Purification** FCC, eluent = pentane:Et_2O (100:0 to 99:1 gradient), colourless oil, 56 mg, 75% yield, e.r. = 94:6. **^{1}H NMR** (500 MHz, $CDCl_3$) δ = 7.33–7.18 (m, 5H), 7.12 (dd, J = 7.0, 1.7 Hz, 2H), 7.03–6.81 (m, 6H), 5.64 (dd, J = 46.1, 6.9 Hz, 1H), 4.12 (dd, J = 14.8, 6.9 Hz, 1H), 2.88–2.82 (m, 2H), 2.78–2.64 (m, 2H), **^{19}F NMR** (470 MHz, $CDCl_3$) δ = -112.4 –-112.5 (m, 1F), -112.6–-112.7 (m, 1F), -173.8 (dd, J = 46.0, 14.8 Hz, 1F), **^{13}C NMR** (126 MHz, $CDCl_3$) δ = 162.8 (d, $J_{C–F}$ = 246.5 Hz), 162.5 (d, $J_{C–F}$ = 247.0 Hz), 140.2, 140.1 (dd, $J_{C–F}$ = 8.0, 4.3 Hz), 139.7 (dd, $J_{C–F}$ = 21.4, 7.1 Hz), 130.1 (d, $J_{C–F}$ = 8.0 Hz), 129.8 (d, $J_{C–F}$ = 8.0 Hz), 128.7, 128.6, 126.6, 124.7 (d, $J_{C–F}$ = 2.0 Hz), 122.0 (dd, $J_{C–F}$ = 7.3, J = 3.2 Hz), 116.0 (d, $J_{C–F}$ = 22.3 Hz), 115.7 (d, $J_{C–F}$ = 21.4 Hz), 115.0 (d, $J_{C–F}$ = 20.7 Hz), 113.4 (dd, $J_{C–F}$ = 22.6, 8.2 Hz), 95.8 (d, $J_{C–F}$ = 186.0 Hz), 55.7 (d, $J_{C–F}$ = 23.9 Hz), 36.3, 33.4 (d, $J_{C–F}$ = 1.9 Hz); **IR** (thin layer film) ν = 3064, 3026, 2920, 2850, 1614, 1591, 1488, 1449, 1257, 1142, 1075, 1051, 1004, 955, 919, 878, 784, 738, 696 cm^{-1}; **HRMS** (EI) m/z calculated for $C_{22}H_{18}F_2S$ $(M\text{-}HF)^{+\cdot}$ 352.1092, found 352.1087; **$[\alpha]_D^{25\,°C}$** +91.4 ° (c = 0.5, $CHCl_3$, e.r. = 94:6); **HPLC** DAICEL CHIRALPAK® IB-3, Heptane:EtOH 99.75:0.25, 1 ml/min, t_1: 6.9 min (minor), t_2: 7.6 min (major).

((1*S*,2*S*)-1,2-bis(3,5-dimethylphenyl)-2-fluoroethyl)(phenethyl)sulfane (3f)

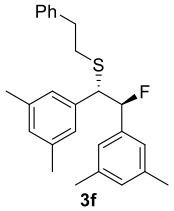

Product **3f** was prepared according to the general procedure by employing 0.2 mmol of substrate (90.6 mg) and the reaction was stirred at rt for 24 h. **Purification** FCC, eluent = pentane:Et_2O (100:0 to 99:1 gradient), colourless oil, 57 mg, 73% yield, e.r. = 96.5:3.5. **^{1}H NMR** (500 MHz, $CDCl_3$) δ = 7.30–7.25 (m, 3H), 7.24–7.19 (m, 1H), 7.10 (d, J = 7.9 Hz, 1H), 6.91 (s, 1H), 6.87 (s, 1H), 6.81 (s, 2H), 6.77 (s, 2H), 5.63 (dd, J = 46.6, 6.7 Hz, 1H), 4.13 (dd, J = 16.0, 6.7 Hz, 1H), 2.87–2.74 (m, 2H), 2.74–2.57 (m, 2H), 2.27 (s, 12H), **^{19}F NMR** (470 MHz, $CDCl_3$) δ = -174.6 (dd, J = 46.5, 16.1 Hz, 1F), **^{13}C NMR** (126 MHz, $CDCl_3$) δ = 140.7, 138.1 (d, $J_{C–F}$ = 4.0 Hz), 137.9, 137.8 (d, $J_{C–F}$ = 20.2 Hz), 137.5, 130.1 (d, $J_{C–F}$ = 1.7 Hz), 129.4, 128.7, 128.5, 126.8, 126.4, 124.2 (d, $J_{C–F}$ = 7.1 Hz), 97.0 (d, $J_{C–F}$ = 179.8 Hz), 56.2 (d, $J_{C–F}$ = 23.4 Hz), 36.4, 33.5 (d, $J_{C–F}$ = 2.2 Hz), 21.4, 21.3; **IR** (thin layer film) ν = 3025, 2917, 2860, 1605, 1495, 1454, 1377, 1227, 1161, 1030. 920, 853, 799, 745, 698 cm^{-1}; **HRMS** (EI) m/z calculated for $C_{26}H_{28}S$ $(M\text{-}HF)^{+\cdot}$ 372.1906, found 372.1912;

[α]$_D^{25\ °C}$ +84.5 ° (c = 0.5, $CHCl_3$, e.r. = 96.5:3.5); **HPLC** DAICEL CHIRALPAK® ID-3, Heptane:EtOH 99.8:0.2, 1 ml/min, t_1: 4.7 min (minor), t_2: 5.4 min (major).

((1*S*,2*S*)-2-fluoro-1,2-di-*p*-tolylethyl)(phenethyl)sulfane (3g)

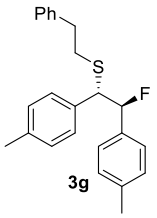

Product **3g** was prepared according to the general procedure by employing 0.2 mmol of substrate (85 mg) and the reaction was stirred at –30 °C for 72 h. **Purification** FCC, eluent = pentane:Et_2O (100:0 to 99:1 gradient), white solid, 44 mg , 60% yield, e.r. = 91:9. **^{1}H NMR** (400 MHz, $CDCl_3$) δ = 7.31–7.14 (m, 3H), 7.12–6.95 (m, 10H), 5.62 (dd, J = 46.3, 7.6 Hz, 1H), 4.19 (dd, J = 13.3, 7.6 Hz, 1H), 2.84–2.73 (m, 2H), 2.72–2.60 (m, 2H), 2.29 (s, 3H), 2.29 (s, 3H), **^{19}F NMR** (376 MHz, $CDCl_3$) δ = -171.0 (dd, J = 46.3, 13.2 Hz, 1F); **^{13}C NMR** (101 MHz, $CDCl_3$) δ = 140.6, 138.3 (d, $J_{C–F}$ = 1.9 Hz), 137.4, 134.8 (d, $J_{C–F}$ = 21.3 Hz), 134.8 (d, $J_{C–F}$ = 5.3 Hz), 129.2, 128.9, 128.8, 128.7, 128.5, 126.4 (d, $J_{C–F}$ = 6.7 Hz), 126.3, 97.1 (d, $J_{C–F}$ = 179.1 Hz), 56.0 (d, $J_{C–F}$ = 24.0 Hz), 36.4, 33.4 (d, $J_{C–F}$ = 2.3 Hz), 21.3, 21.2; **MP** 60–62 °C; **IR** (thin layer film) ν = 3027, 2945, 2869, 1602, 1514, 1496, 1448, 1074, 946, 908, 816, 738, 718, 702 cm^{-1}; **HRMS** (EI) m/z calculated for $C_{24}H_{24}S$ $(M\text{-}HF)^{+\cdot}$ 344.1593, found 344.1595; **[α]$_D^{25\ °C}$** +85.0 ° (c = 0.5, $CHCl_3$, e.r. = 91:9); **HPLC** DAICEL CHIRALPAK® IF-3, Heptane:EtOH 99.8:0.2, 1 ml/min, t_1: 9.4 min (minor), t_2: 10.1 min (major).

((1*S*,2*S*)-1,2-bis(4-chlorophenyl)-2-fluoroethyl)(phenethyl)sulfane (3h)

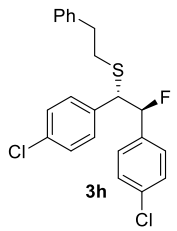

Product **3h** was prepared according to the general procedure by employing 0.2 mmol of substrate (93.2 mg) and the reaction was stirred at 0 °C for 72 h. **Purification** FCC, eluent = pentane:Et_2O (100:0 to 99:1 gradient), white solid, 40.0 mg, 53% yield, e.r. = 93:7. **^{1}H NMR** (400 MHz, $CDCl_3$) δ = 7.32–7.15 (m, 7H), 7.10–7.05 (m, 2H), 7.02 (d, J = 8.4 Hz, 2H), 6.97 (d, J = 8.4 Hz, 2H), 5.58 (dd, J = 45.8, 7.0 Hz, 1H), 4.09 (dd, J = 13.8, 7.0 Hz, 1H), 2.90–2.76 (m, 2H), 2.73–2.56 (m, 2H), **^{19}F NMR** (376 MHz, $CDCl_3$) δ = -172.4 (dd, J = 45.9, 13.9 Hz, 1F), **^{13}C NMR** (101 MHz, $CDCl_3$) δ = 140.2, 135.9 (d, $J_{C–F}$ = 4.0 Hz), 135.6 (d, $J_{C–F}$ = 21.4 Hz), 134.7 (d, $J_{C–F}$ = 1.9 Hz), 133.8, 130.4, 128.7, 128.7, 128.6, 128.4, 127.8 (d, $J_{C–F}$ = 6.9 Hz), 126.6, 95.9 (d, $J_{C–F}$ = 181.7 Hz), 55.4 (d, $J_{C–F}$ = 24.4 Hz), 36.2, 33.4 (d, $J_{C–F}$ = 1.8 Hz); **MP** 68-70 °C; **IR** (thin layer film) ν = 3062, 3027, 2922, 2850, 1601, 1491, 1453, 1408, 1276, 1209, 1179, 1091, 1052, 1014, 862, 836, 822, 771, 748, 720, 698 cm^{-1}; **HRMS** (EI) m/z calculated for $C_{22}H_{18}Cl_2S$ $(M\text{-}HF)^{+\cdot}$ 384.0501, found 384.0499; **[α]$_D^{25\ °C}$** +83.7 ° (c = 0.5, $CHCl_3$, e.r. = 93:7); **HPLC** DAICEL CHIRALPAK® IC-3, Heptane:EtOH 99.9:0.1, 1 ml/min, t_1: 8.1 min (minor), t_2: 9.3 min (major).

((1*S*,2*S*)-1,2-bis(4-fluorophenyl)-2-fluoroethyl)(phenethyl)sulfane (3i)

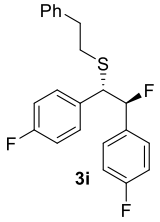

Product **3i** was prepared according to the general procedure by employing 0.2 mmol of substrate (86.7 mg) and the reaction was stirred at 0 °C for 72 h. **Purification**: FCC, eluent = pentane:Et_2O (100:0 to 99:1 gradient), colourless oil, 43.2 mg , 58% yield, e.r. = 94:6. **^{1}H NMR** (400 MHz, $CDCl_3$) δ = 7.30–7.19 (m, 3H), 7.14–6.99 (m, 6H), 6.98–6.89 (m, 4H), 5.60 (dd, *J* = 45.8, 7.3 Hz, 1H), 4.15 (dd, *J* = 13.2, 7.3 Hz, 1H), 2.90–2.78 (m, 2H), 2.75–2.65 (m, 2H), **^{19}F NMR** (470 MHz, $CDCl_3$) δ = -112.0–-114.0 (m, 1F), -112.6–-112.7 (m, 1F),-170.3 (dd, *J* = 46.7, 11.2 Hz, 1F), **^{13}C NMR** (101 MHz, $CDCl_3$) δ =162.7 (dd, $J_{C–F}$ = 247.0, 1.9 Hz), 162.1 (d, $J_{C–F}$ = 247.0 Hz), 140.2, 133.1 (d, $J_{C–F}$ = 3.4 Hz), 133.0 (dd, $J_{C–F}$ = 18 Hz, *J* = 3.2 Hz), 130.6 (d, $J_{C–F}$ = 8.1 Hz), 128.5, 128.5, 128.1 (t, $J_{C–F}$ = 7.1 Hz), 126.4, 115.3 (d, $J_{C–F}$ = 21.5 Hz), 115.0 (d, $J_{C–F}$ = 21.5 Hz), 96.1 (d, $J_{C–F}$ = 181.2 Hz), 55.3 (d, $J_{C–F}$ = 24.8 Hz), 36.2, 33.3 (d, $J_{C–F}$ = 2.0 Hz); **IR** (thin layer film) ν = 3063, 3028, 2922, 2851, 1604, 1508, 1454, 1417, 1298, 1224, 1158, 1096, 1052, 1013, 937, 834, 806, 749, 722, 698 cm^{-1}; **HRMS** (EI) m/z calculated for $C_{22}H_{18}F_2S$ $(M\text{-}HF)^{+\cdot}$ 352.1092, found 352.1094; **$[\alpha]_D^{25\,°C}$** +65.2 ° (c = 0.5, $CHCl_3$, e.r. = 94:6); **HPLC** DAICEL CHIRALPAK® IC-3, Heptane:EtOH 99.9:0.1, 1ml/min, t_1: 12.5 min (major), t_2: 15.0 min (minor).

((1*S*,2*S*)-2-fluoro-1,2-di(naphthalen-2-yl)ethyl)(phenethyl)sulfane (3j)

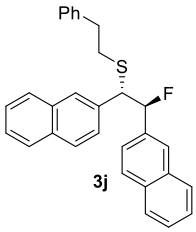

Product **3j** was prepared according to the general procedure by employing 0.05 mmol of substrate (25.0 mg) and the reaction was stirred at rt for 24 h. **Purification** Preparative TLC, eluent = pentane:CH_2Cl_2 (80:20), white solid, 13.2 mg, 61% yield, e.r. = 95.5:4.5. **^{1}H NMR** (500 MHz, $CDCl_3$) δ = 7.82–7.69 (m, 6H), 7.66 (s, 1H), 7.60 (s, 1H), 7.50–7.43 (m, 4H), 7.38 (dd, *J* = 8.5, 1.8 Hz, 1H), 7.26–7.17 (m, 4H), 7.10–7.02 (m, 2H), 5.98 (dd, *J* = 46.1, 7.1 Hz, 1H), 4.50 (dd, *J* = 14.4, 7.2 Hz, 1H), 2.92–2.76 (m, 2H), 2.76–2.63 (m, 2H), **^{19}F NMR** (470 MHz, $CDCl_3$) δ = -172.3 (dd, J = 46.0, 14.2 Hz, 1F), **^{13}C NMR** (126 MHz, $CDCl_3$) [overlapping signals] δ = 139.3, 134.2 (d, $J_{C–F}$ = 4.1 Hz), 134.0, 133.9 (d, $J_{C–F}$ = 20.5 Hz), 132.2, 132.0, 131.7, 127.5, 127.4, 127.3, 127.1, 127.0, 126.8 (d, $J_{C–F}$ = 3.6 Hz), 126.6 (d, $J_{C–F}$ = 4.2 Hz), 125.5, 125.3 (d, $J_{C–F}$ = 3.3 Hz), 125.2 (d, $J_{C–F}$ = 3.0 Hz), 125.0, 124.9 (d, $J_{C–F}$ = 8.0 Hz), 122.7 (d, $J_{C–F}$ = 5.9 Hz), 95.8 (d, $J_{C–F}$ = 180.4 Hz), 55.3 (d, $J_{C–F}$ = 23.9 Hz), 35.2, 32.2 (d, $J_{C–F}$ = 1.9 Hz); **MP** 105–106 °C; **IR** (thin layer film) ν = 3057, 3025, 2919, 2850, 1601, 1508, 1496, 1453, 1368, 1331, 1270, 1188, 1143, 1124, 1053, 1018, 950, 896, 860, 819, 805, 748, 697 cm^{-1}; **HRMS** (EI) m/z calculated for $C_{30}H_{24}S$ $(M\text{-}HF)^{+\cdot}$ 416.1593, found 416.1605; **$[\alpha]_D^{25\,°C}$** +59.5 ° (c = 0.4, $CHCl_3$, e.r. = 95.5:4.5); **HPLC** DAICEL CHIRALPAK® IB-3, Heptane:EtOH 99.85:0.15, 1ml/min, t_1: 26.2 min (major), t_2: 30.2 min (minor).

(1*S*,2*S*)-(2-fluoro-1,2-diphenylethyl)(methyl)sulfane (3k)

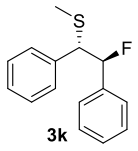

Product **3k** was prepared according to the general procedure by employing 0.2 mmol of substrate (49.6 mg) and the reaction was stirred at –30 °C for 72 h. **Purification** FCC, eluent = pentane:Et_2O (100:0 to 99:1 gradient), colourless oil, 35.5 mg, 72% yield, e.r. = 91:9. **^{1}H NMR** (400 MHz, $CDCl_3$) δ = 7.19–7.11 (m, 6H), 7.09 (dd, J = 7.5, 2.0 Hz, 2H), 7.07–7.02 (m, 2H), 5.62 (dd, J = 46.3, 7.4 Hz, 1H), 4.07 (dd, J = 13.9, 7.4 Hz, 1H), 1.93 (d, J = 0.8 Hz, 3H), **^{19}F NMR** (376.5 MHz, $CDCl_3$) δ = -173.2 (dd, J = 46.4, 13.9 Hz, 1F), **^{13}C NMR** (101 MHz, $CDCl_3$) δ = 137.8 (d, $J_{C–F}$ = 16.5 Hz), 137.6, 129.0, 128.6 (d, $J_{C–F}$ = 1.5 Hz), 128.5, 128.2, 127.8, 126.4 (d, $J_{C–F}$ = 7.1 Hz), 97.1 (d, $J_{C–F}$ = 180.2 Hz), 58.1 (d, $J_{C–F}$ = 23.8 Hz), 15.5; **IR** (thin layer film) ν = 3031, 2918, 1493, 1453, 1212, 1075, 1051, 998, 916, 756, 737, 696, 627 cm^{-1}; **HRMS** (EI) m/z calculated for $C_{15}H_{15}FS$ $(M)^{+\cdot}$ 246.0873, found 246.0878; **$[\alpha]_D^{25\,°C}$** +74.1 ° (c = 0.5, $CHCl_3$, e.r. = 91:9) **HPLC** DAICEL CHIRALPAK® IC-3, Heptane:EtOH 99.9:0.1, 1 ml/min, t_1: 8.0 min (major), t_2: 9.1 min (minor).

((1*S*,2*S*)-2-fluoro-1,2-di-*m*-tolylethyl)(methyl)sulfane (3l)

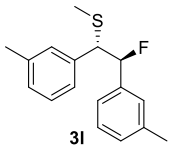

Product **3l** was prepared according to the general procedure by employing 0.2 mmol of substrate (67.0 mg) and the reaction was stirred at –10 ° for 72 h. **Purification** FCC, eluent = pentane:Et_2O (100:0 to 99:1 gradient), colourless liquid, 43.2 mg , 87% yield, e.r. = 92.5:7.5. **^{1}H NMR** (500 MHz, $CDCl_3$) δ = 7.21–6.86 (m, 8H), 5.69 (dd, J = 46.4, 7.0 Hz, 1H), 4.10 (dd, J = 15.0, 7.1 Hz, 1H), 2.29 (s, 6H), 2.01 (s, 3H), **^{19}F NMR** (470 MHz, $CDCl_3$) δ = -174.1 (dd, J = 46.6, 14.9 Hz, 1F), **^{13}C NMR** (126 MHz, $CDCl_3$) [overlapping signals] δ = 138.0, 137.7 (d, $J_{C–F}$ = 12.0 Hz), 137.6, 137.6 (d, $J_{C–F}$ = 3.8 Hz), 129.5, 129.2 (d, $J_{C–F}$ = 1.8 Hz), 128.2, 127.8, 126.9 (d, $J_{C–F}$ = 6.8 Hz), 126.0, 123.4 (d, $J_{C–F}$ = 7.0 Hz), 96.9 (d, $J_{C–F}$ = 179.8 Hz), 57.9 (d, $J_{C–F}$ = 23.7 Hz), 21.4, 15.4 (d, $J_{C–F}$ = 2.6 Hz); **IR** (thin layer film) ν = 3025, 2918, 2864, 1607, 1590, 1488, 1437, 1379, 1313, 1247, 1191, 1159, 1094, 1056, 999, 883, 780, 735, 700 cm^{-1}; **HRMS** (EI) m/z calculated for $C_{17}H_{19}FS$ $(M)^{+\cdot}$ 274.1186, found 274.1181; **$[\alpha]_D^{25\,°C}$** +63.7 ° (c = 1.0, $CHCl_3$, e.r. = 92.5:7.5); **HPLC** DAICEL CHIRALPAK® IC-3, Heptane:EtOH 99.75:0.25, 1 ml/min, t_1: 3.9 min (major), t_2: 4.3 min (minor).

***rac*-2-(phenethylthio)-1,2-diphenylethyl-N,N'-bis(3,5-bis(trifluoromethyl)phenyl)carbamimidothioate (3m)**

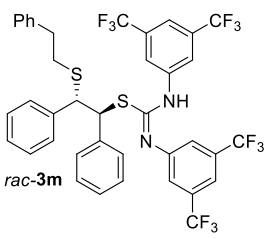

The thiourea degradation product **3m** was prepared by dissolving bromo sulfide **1a** (0.2 mmol, 79.5 mg, 1 equiv.) and thiourea **2d** (0.2 mmol, 100.0 mg, 1 equiv.) in CH_2Cl_2 (0.25M). After stirring for 1h, the solvent was removed *in vacuo* and the crude product was purified by FCC (pentane:CH_2Cl_2, 95:5 to 85:15 gradient) to afford a dense sticky oil (57.2 mg, 0.07 mmol, 35% yield). **^{1}H NMR** (500

MHz, DMSO-d_6) δ = 10.09 (s, 1H), 8.06 (s br, 2H), 7.78 (s br, 1H), 7.64 (s br, 1H), 7.20–7.09 (m, 9H), 7.08–7.01 (m, 4H), 7.00–6.94 (m, 4H), 5.29 (d, J = 11.0 Hz, 1H), 4.40 (d, J = 11.0 Hz, 1H), 2.72–2.56 (m, 2H), 2.50–2.38 (m, 2H),), **^{19}F NMR** (470 MHz, DMSO-d_6) δ = –61.3 (s, 6F), –61.7 (s, 6F), **^{13}C NMR** (126 MHz, DMSO-d_6) [overlapping signals] δ = 151.0, 150.8, 142.3, 140.7, 140.2, 139.7, 131.2 (q, $J_{C–F}$ = 32.6 Hz), 131.1 (q, $J_{C–F}$ = 32.6 Hz), 128.9, 128.8, 128.6, 128.4, 128.0, 127.9, 127.6, 126.5, 123.7 (q, $J_{C–F}$ = 272.7 Hz), 123.6 (q, $J_{C–F}$ = 272.7 Hz), 122.8, 119.7, 116.6, 115.9, 56.6, 53.4, 35.4, 32.9; **IR** (thin layer film) ν = 2989, 2883, 1632, 1603, 1532, 1470, 1455, 1433, 1372, 1277, 1173, 1134, 1107, 1030, 970, 885, 847, 721, 700, 683, 668, 642, 616, 606 cm^{-1}; **HRMS** (ESIpos) m/z calculated for $C_{39}H_{29}N_2F_{12}S_2$ $(M+H)^+$ 817.15751, found 817.15729.

Determination of binding constants

A stock solution of **4h** (5 μM) in CH_2Cl_2 (spectrophotometric grade) was prepared by weighing out the solid urea catalyst. A TBAF·$3H_2O$ solution (0.2 mM) was prepared by weighing out commercially available TBAF·$3H_2O$ in a vial purged with Ar and dissolving it in the previously prepared solution of **4h** (5 μM). The exact fluoride concentration was determined following a reported procedure (*47*). A TBAB solution (0.2 mM) was prepared by weighing out commercially available TBAB and dissolving it in the previously prepared solution of **4h** (5 μM). 0.8 ml of the stock solution of **4h** were subsequently used as sample for the UV-Vis titration to which an increasing amount of the TBAF or TBAB solution was added (0–10 equiv.). After every addition a UV-Vis spectrum was recorded, a bathochromic shift of the band with a maximum at 255 nm was observed, and the absorption at the new maximum (273 nm or 269 nm, respectively) was plotted against the concentration of the added halide. The association constants were determined by non-linear least squares regression using DynaFit 4 (*48*); the model fits well when analysed on the basis of 1:1 complexation between the urea and fluoride or bromide ions ($K_{a\ (4h:X-)}$).

$K_{a\ (4h:F-)} = 1.7 \pm 0.2 \times 10^6\ M^{-1}$

$K_{a\ (4h:Br-)} = 3.3 \pm 0.3 \times 10^5\ M^{-1}$

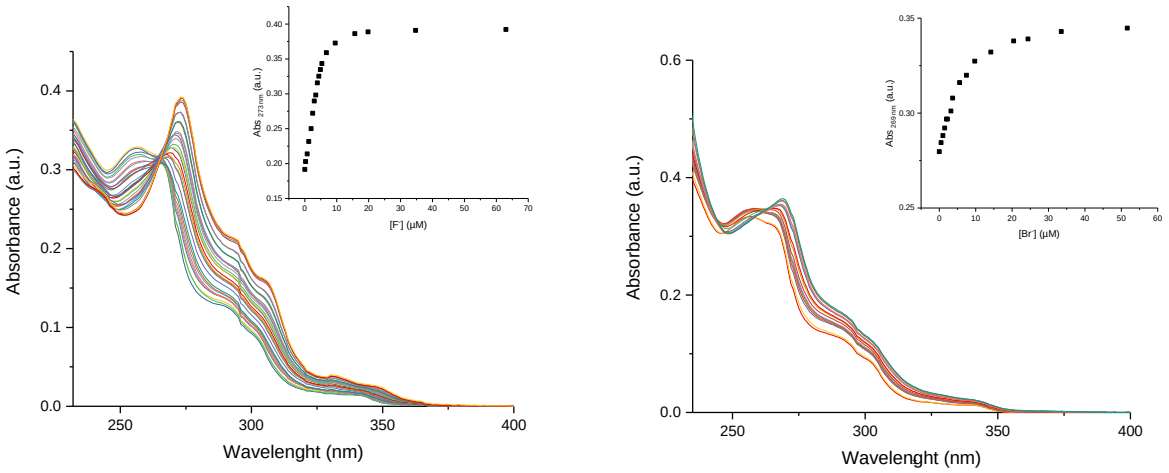

Figure S8: Stacked UV-Vis spectra for the titration of **4h** (5μM) vs. TBAF·$3H_2O$ (0.2 mM) in CH_2Cl_2 (left), and TBAB (0.2 mM) (right). Inset: titration profile at the absorption maximum.

Computational Methods

All computational work was undertaken using S-methylated substrate **1k**, in dichloromethane solvent (ε = 8.93), with Gibbs free energies evaluated at 298.15 K unless otherwise stated. Distances are quoted in Å and angles in degrees.

Density Functional Theory (DFT)

Density functional theory (DFT) geometry optimizations and frequency analyses were performed using the Gaussian 09, Revision D.01 software package (*49*). The M06-2X (*50*) functional was used with ultrafine (99,590) integration grid in combination with a mixed basis set, with Ahlrichs type def2-TZVPPD applied to non-catalyst heteroatoms, and def2-SVP applied to all other atoms, herein referred to as the def2-SVP(TZVPPD) basis set (*51-53*). The def2-TZVPPD basis set includes an effective core potential (ECP) description for Cs (*54*). Geometry optimizations were performed in dichloromethane solvent using the conductor-like polarizable continuum model (CPCM) of solvation (*55–57*), due to the presence of many charged species. Vibrational frequencies were used to classify stationary points. Stationary points with all real frequencies were classified as minima, and those with a single imaginary frequency as a transition state (TS). Thermochemistry was evaluated at the solution standard state of 1 mol dm^{-3} and temperature of 298.15 K unless otherwise stated. Gas phase species were evaluated at standard pressure of 1 bar. Gibbs free energies were calculated using vibrational frequencies with *GoodVibes* (*58*) python script employing a quasi-harmonic approximation for entropy calculation with a free-rotor description below 100 cm^{-1}, as proposed by Grimme (*59*). *GoodVibes* was used to implement concentration corrections, but vibrational frequencies were not scaled. Non-covalent interactions (NCI) were computed using the non-covalent interaction index from the optimization density (*60, 61*).

Energies were corrected with single point calculations using the ORCA 3.0.3 software package (*62*). The ωB97X-D3 functional, which incorporates Grimme's D3 dispersion correction, was used with default integration grid and tight SCF criteria (*63–65*). The (ma)-def2-TZVPP basis set refers to ma-def2-TZVPP (*66*) on heteroatoms, and def2-TZVPP on all others, with corresponding ECP for Cs. Solvation in dichloromethane was modelled using the conductor-like screening model (COSMO) (*67*). This level of theory most accurately reproduced DLPNO-CCSD(T) (*68*) S_N2 and E2 activation barriers in unpublished benchmarking studies.

Conformational sampling for simple molecules (starting materials and products) was performed using Spartan '16 (*69*). Rotatable dihedral bonds were systematically scanned, and energies evaluated using the

Merck molecular force field (MMFF) (*70*). DFT single point energies (optimization level of theory) were evaluated for each structure and those within a 40 kJ/mol window were fully optimized.

DFT Basis Set Benchmarking

The use of a mixed basis set was found to be essential to accurately reproduce large basis set benchmark geometries, at viable computational cost. We benchmarked urea-fluoride geometries (**Table S5**) and bromide and fluoride TSs (**Table S6**) comparing def2-SVP(TZVPPD) to def2-TZVPP(D). Geometry optimization methods were also benchmarked relative to MP2 (*71*) geometries in unpublished work. Use of a small basis set on all atoms results in deprotonation of the catalyst by fluoride, and, in some cases, loss of TSs for fluoride delivery. Use of diffuse basis functions on the catalyst structure resulted in density convergence issues.

Table S5. – *Key bond lengths of **2a-F**$^-$ complex with basis set*

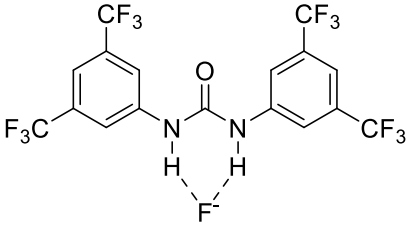

Functional	Basis Set	Average Key Bond Distances (Å)			RMSD
		N-F	N-H	H-F	
M06-2X	def2-TZVPP(D)	2.589	1.045	1.599	-
M06-2X	def2-SVP(TZVPPD)	2.587	1.051	1.591	0.006
M06-2X	def2-SVP		Deprotonated		(0.115)

Table S6. – *Key bond lengths of TSs in non-asymmetric reaction pathway*

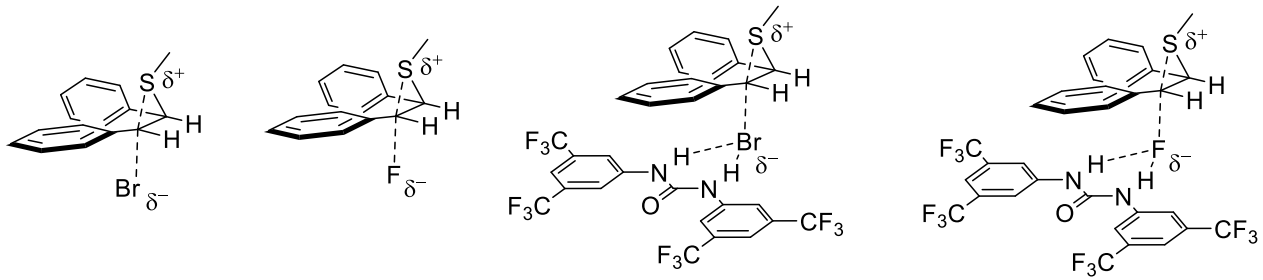

TS_{Br} **TS_F** **TS_{Br}(2a)** **TS_F(2a)**

Functional	Basis Set	Uncoordinated (Å)				Coordinated (Å)										RMSD
		TS_{Br}		TS_F		TS_{Br}(2a)					TS_F(2a)					
		C-Br	C-S	C-F	C-S	C-Br	C-S	N-Br	N-H	H-Br	C-F	C-S	N-F	N-H	H-F	
M06-2X	def2-TZVPP(D)	2.715	2.261	2.238	2.067	2.670	2.296	3.453	1.016	2.471	2.093	2.233	2.700	1.027	1.734	-
M06-2X	def2-SVP(TZVPPD)	2.713	2.256	2.238	2.065	2.672	2.283	3.431	1.021	2.499	2.099	2.229	2.690	1.034	1.719	0.011
M06-2X	def2-SVP	2.809	2.192	2.254	2.009	2.727	2.248	3.420	1.023	2.461	2.180	2.163	2.630	1.042	1.649	0.059

Molecular Dynamics (MD)

Conformational sampling of catalyst-CsF complexes and ion pairs was performed using the GROMACS (version 5.1.4) molecular dynamics package (*72–77*) with optimized potential for liquid simulations (OPLS-AA 2005) forcefield (*78*, *79*). Compatible parameters were generated from Schrodinger Maestro software (ffld_server utility, version 14) (*80*), with restrained electrostatic potential (RESP) charges (*81*, *82*). Parameters for the episulfonium ion were adapted from those generated for the corresponding dimethyl aziridinium ion in a manner similar to Duarte and Paton (*83*). RESP charges were fitted to HF/6-31G(d) electrostatic potential using Ambertools (*84*). Simulations were performed in explicit dichloromethane solvent with topology obtained from virtualchemistry.org (*85*, *86*).

The species of interest was first centered in a cubic box, with 3-dimensional periodic boundary conditions (PBC), and minimum species-boundary distance of 15 Å. Simulations involving a cesium cation made use of the *genion* command to insert the cation into the box in a random position. A 1 nm cut-off was used for both Van der Waals interactions and the particle mesh Ewald method (*87*). Simulations made use of the linear constraint solver algorithm (LINCS) (*88*). System temperature was maintained using the velocity rescaling method, with time constant of 100 fs (*89*), and constant pressure was maintained (NPT simulations) using the Parrinello-Rahman barostat, with time constant of 2 ps, reference pressure of 1 bar, and compressibility of 4.5×10^{-5} bar $^{-1}$ (*90*, *91*).

Each system was minimized by steepest-descents method for 5000 steps, before generation of initial random velocities according to a 173 K Maxwell-Boltzmann distribution. The system was equilibrated under constant volume (NVT), with 1 fs timestep, and heavy atom position restraints. During NVT, system temperature was raised to that required for the NPT production run, followed by an equilibration period, totaling 200 ps. The system was then equilibrated for 400 ps under constant pressure (NPT) with 2 fs timestep. During this equilibration, it was verified that the volume of the system had stabilized. An NPT production run was then performed, from which data was derived.

MD trajectories were analyzed using clustering, performed by heavy atom root-mean-square deviation (RMSD) using the GROMOS algorithm (*92*) in GROMACS. RMSD between frames was calculated, accounting for automorphism arising from molecular symmetry, using an in-house python script. Fluorine atoms in CF_3 groups were omitted to reduce automorphs 81-fold.

We used classical MD simulations to investigate catalyst-fluoride binding modes, and to generate catalyst-fluoride-episulfonium ion pair conformations in an approach similar to that by Duarte and Paton (*83*). In order to effectively sample different conformations and binding modes of catalyst; simulations of catalyst alone, and with fluoride were performed at elevated temperature of 373 K. Additionally, it was also found

that the presence of an explicit Cs^+ counter-ion was essential to facilitate interconversion of fluoride binding modes over the simulation timescale. Simulations of the reactive ion pair with episulfonium were performed at reaction temperature of 298 K.

Computation – Non-asymmetric Catalytic System

Herein we describe the methods used to investigate the non-asymmetric pathway, using achiral catalyst, and also the hypothetical uncatalyzed reaction.

Phase-Transfer

In order to generate a free energy profile for the reaction involving catalyst **2a**, a description of the phase-transfer step is required. We applied a thermodynamic approach, combining computed solution phase energies with literature experimental data in an anion-exchange step. A similar approach has been employed by Pliego and Riveros (*93*, *94*) for solid-liquid phase-transfer with crown ethers. Enthalpy changes were calculated using a Hess cycle with experimental data published in the CRC Handbook of Chemistry and Physics 97th Edition (**Figure S9**, **Table S7**) (*95*). Molar entropies of ionic salts and gaseous ion entropies were used in combination with computed entropy changes to calculate the corresponding entropy change for the process (**Table S8**). Gaseous ion entropies were those determined by Marcus and Loewenschuss (*96*). Values of ΔG with illustrative metal cations, catalysts and leaving groups are given in **Table S9**.

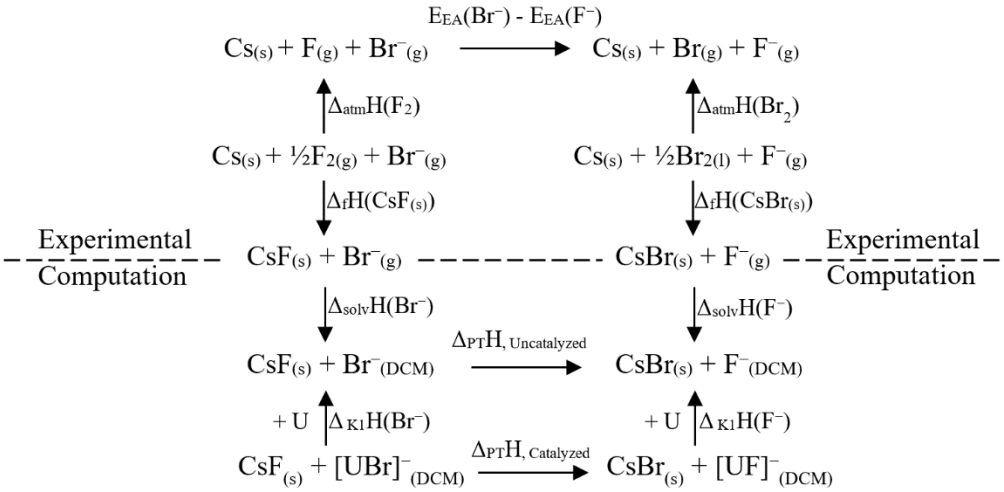

Figure S9. – *Hess cycle for calculation of thermochemical values for phase-transfer model*

Table S7. – *Standard enthalpy and entropy changes at 298.15 K*

	Source	ΔH (kJ/mol)	ΔS (J/K/mol)
$\Delta_f(CsF_{(s)})$	Ref (*95*)	-553.5	-
$\Delta_f(CsBr_{(s)})$	Ref (*95*)	-405.8	-
$\Delta_f(CsCl_{(s)})$	Ref (*95*)	-443.0	-
$\Delta_{atm}(F_2)$	Ref (*95*)	+79.38	-
$\Delta_{atm}(Br_2)$	Ref (*95*)	+111.87	-
$\Delta_{atm}(Cl_2)$	Ref (*95*)	+121.301	-
$E_{EA}(F)$	Ref (*95*)	+328.1649	-
$E_{EA}(Br)$	Ref (*95*)	+324.5369	-
$E_{EA}(Cl)$	Ref (*95*)	+348.5750	-
$\Delta_{solv}(F^-)$	Computed	-317.8	-26.7*
$\Delta_{solv}(Br^-)$	Computed	-240.6	-26.7*
$\Delta_{solv}(Cl^-)$	Computed	-257.8	-26.7*
K1 (F^-) **2a**	Computed	+103.0	+88.7
K1 (Br^-) **2a**	Computed	+51.51	+85.2
K1 (Cl^-) **2a**	Computed	+58.65	+86.3
K1 (F^-) **2f**	Computed	+83.30	+76.7
K1 (Br^-) **2f**	Computed	+39.05	+83.3
K1 (F^-) **2d**	Computed	+104.5	+75.9
K1 (Br^-) **2d**	Computed	+49.2	+73.8

* Entropy change associated with a change in standard state from 1 bar to 1 M.

Table S8. – *Standard molar entropies at 298.15 K*

	Source	S (J/K/mol)
$CsF_{(s)}$	Ref (*95*)	92.8
$CsBr_{(s)}$	Ref (*95*)	113.1
$CsCl_{(s)}$	Ref (*95*)	101.2
$F^-_{(g)}$	Ref (*96*)	145.59
$Br^-_{(g)}$	Ref (*96*)	163.57
$Cl^-_{(g)}$	Ref (*96*)	154.40

Table S9. – *Solubility model standard thermochemical values evaluated at 298.15 K*

Catalyst	Cation	Leaving Group	$\Delta_{PT}G$ (kJ/mol)	$\Delta_{PT}H$ (kJ/mol)	$\Delta_{PT}S$ (J/K/mol)
Uncatalyzed	Cs	Br	+33.7	+34.4	+2.31
Uncatalyzed	K	Br	+57.5	+60.8	+11.3
Uncatalyzed	Na	Br	+93.6	+98.8	+17.7
2a	Cs	Br	-16.7	-17.1	-1.16
2a	K	Br	+7.00	+9.33	-7.84
2a	Na	Br	+43.1	+47.3	-14.2
2f	Cs	Br	-7.02	-8.30	-4.29
2f	K	Br	+16.7	+18.1	+4.71
2f	Na	Br	+52.8	+56.1	+11.1
Thiourea **2d**	Cs	Br	-21.0	-20.9	+0.29
Uncatalyzed	Cs	Cl	+29.2	+29.0	-0.52
2a	Cs	Cl	-14.5	-15.4	-2.96

Catalyst 2a

Stationary points along the uncatalyzed pathway, and that catalyzed by urea **2a** are shown in **Figure S10**. Key geometric parameters are tabulated in **Table S10**. Conformational sampling of starting material and product was undertaken with Spartan.

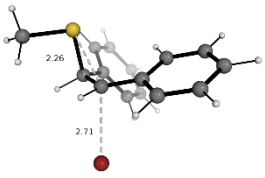

TS_{Br}(uncat)

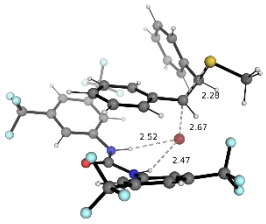

TS_{Br}(2a)

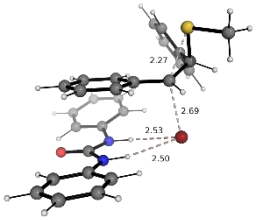

TS_{Br}(2f)

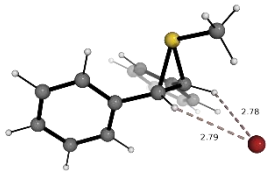

IP$_{Br}$(uncat)

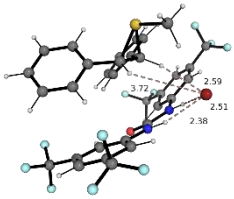

IP$_{Br}$(2a)

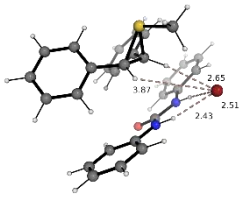

IP$_{Br}$(2f)

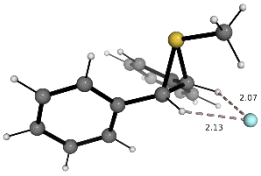

IP$_{F}$(uncat)

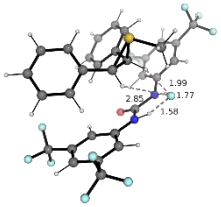

IP$_{F}$(2a)

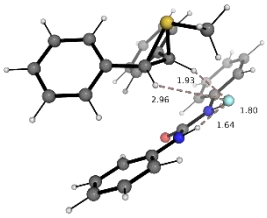

IP$_{F}$(2f)

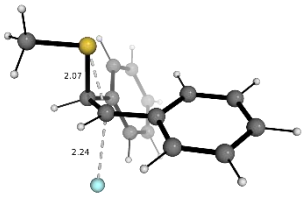

TS$_{F}$(uncat)

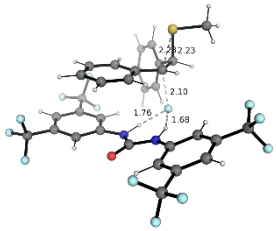

TS$_{F}$(2a)

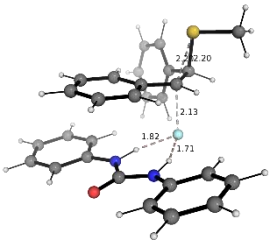

TS$_{F}$(2f)

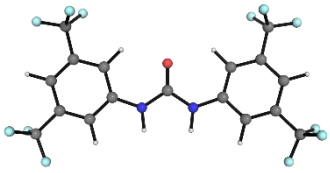

2a$_{aa}$ (G_{rel} = 0 kJ/mol)

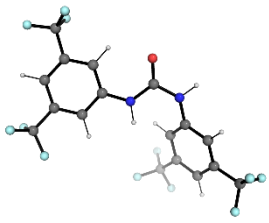

2a$_{as}$ (G_{rel} = +11.8 kJ/mol)

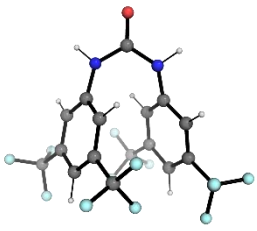

2a$_{ss}$ (G_{rel} = +35.4 kJ/mol)

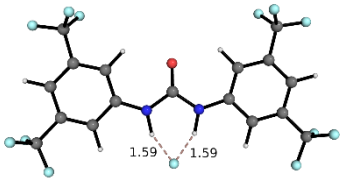

2a-F

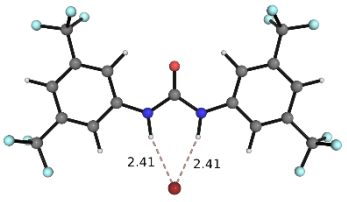

2a-Br

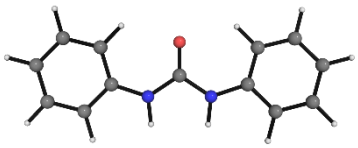

$2f_{aa}$ (G_{rel} = 0 kJ/mol)

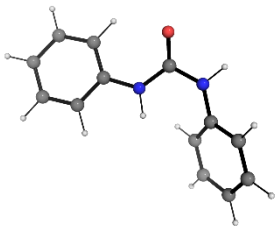

$2f_{as}$ (G_{rel} = +1.7 kJ/mol)

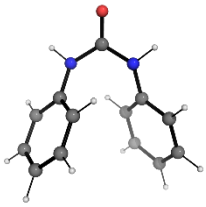

$2f_{ss}$ (G_{rel} = +10.9 kJ/mol)

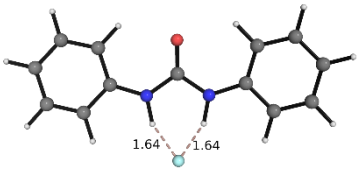

2f-F

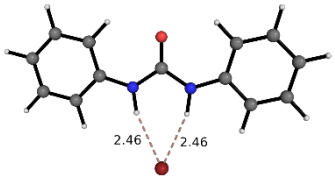

2f-Br

Figure S10. – *Geometries of key species on non-asymmetric pathway*

Table S10. – *Key geometric parameters for stationary points on non-asymmetric pathway*

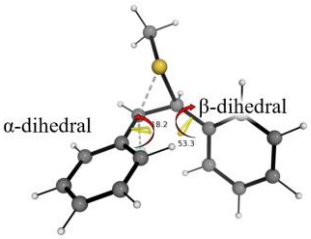

	k imag	Key Distances (Å)				Key Angles (°)	
		C-X	C-S	H-bond 1	H-bond 2	α-Dihedral†	β-Dihedral†
2a	-	-	-	-	-	-	-
2a-F	-	-	-	1.591	1.591	-	-
2a-Br	-	-	-	2.408	2.408	-	-
2f	-	-	-	-	-	-	-
2f-F	-	-	-	1.641	1.641	-	-
2f-Br	-	-	-	2.464	2.464	-	-
TS_{Br}(uncat)	-330.27	2.713	2.256	-	-	3.4	-41.0
TS_{Br}(2a)	-327.44	2.672	2.283	2.523	2.475	-41.2	83.9
TS_{Br}(2f)	-327.94	2.694	2.266	2.531	2.498	-33.7	82.7
Epi	-	-	1.834*	-	-	-	-
IP_{Br}(uncat)	-	-	-	-	-	-	-
IP_{Br}(2a)	-	-	-	2.378	2.507	-	-
IP_{Br}(2f)	-	-	-	2.433	2.517	-	-
IP_{F}(uncat)	-	-	-	-	-	-	-
IP_{F}(2a)	-	-	-	1.580	1.771	-	-
IP_{F}(2f)	-	-	-	1.645	1.805	-	-
TS_{F}(uncat)	-296.87	2.238	2.065	-	-	18.2	-53.3
TS_{F}(2a)	-394.36	2.099	2.229	1.760	1.678	-4.8	-66.5
TS_{F}(2f)	-369.13	2.133	2.198	1.818	1.705	-12.2	-69.4

* Average value. †Phenyl ring dihedrals measured relative to C-C bond.

Unsubstituted Urea 2f

The achiral reaction pathway was also computed with the **catalyst 2f** for comparison with **catalyst 2a** (**Figure S11**). Consistent with previously reported experimental results (*25*), substitution of the aromatic rings of diarylureas leads to subtle modulation of hydrogen bond donor ability of the catalyst, and relatively

small variation in solution phase Gibbs free energy barriers for S_N2 reactions. In contrast, we find larger Gibbs free energy differences in steps involving phase transfer (**iii-iv**), with differences of up to 19.6 kJ/mol, demonstrating that the unsubstituted catalyst is inferior at phase-transfer, arising from inferior H-bond donor ability.

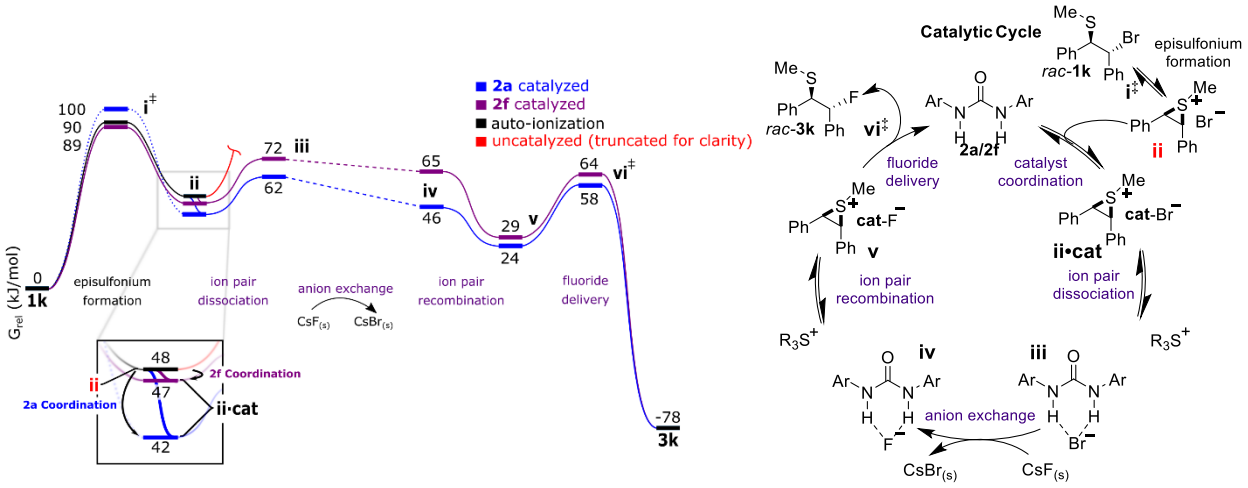

Figure S11. – *Gibbs free energy profile comparing urea **2f** with catalyst **2a***

Episulfonium Isomers

We considered the episulfonium methyl group both *syn* and *anti* to the phenyl substituents (**Figure S12**).

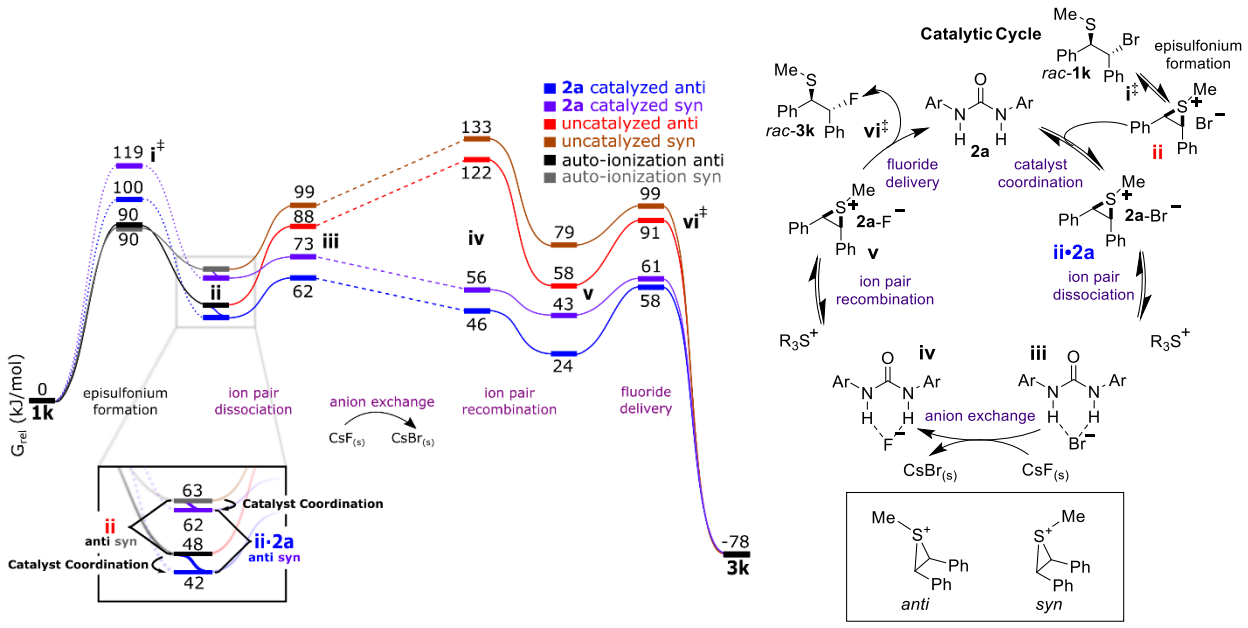

Figure S12. – *Gibbs free energy profile comparing syn and anti episulfonium isomers*

For both the catalyzed and uncatalyzed pathways, the *syn* isomer is disfavored, notably for the ion pairs **ii** and **v**. Aryl group atropisomerism was considered and discounted in the *syn* isomer with a dihedral scan indicating an (uncorrected) barrier to interconversion of less than 20 kJ/mol. The barrier to formation of both episulfonium isomers (uncoordinated) is 90.3 kJ/mol, indicating no kinetic preference to formation. The thermodynamic preference for *anti* episulfonium-bromide ion pairs is 14.4 kJ/mol (Boltzmann factor (298.15 K) = 3 x 10^{-3}), and greater when coordinated by urea. In the case of a chiral urea, the rate-limiting step of the catalyzed reaction is prior to the enantiodetermining step and so the more thermodynamically stable *anti* isomer is used in this work.

Stationary points along the non-asymmetric pathway with methyl group *syn* are illustrated in **Figure S13** with key geometric parameters tabulated in **Table S11**.

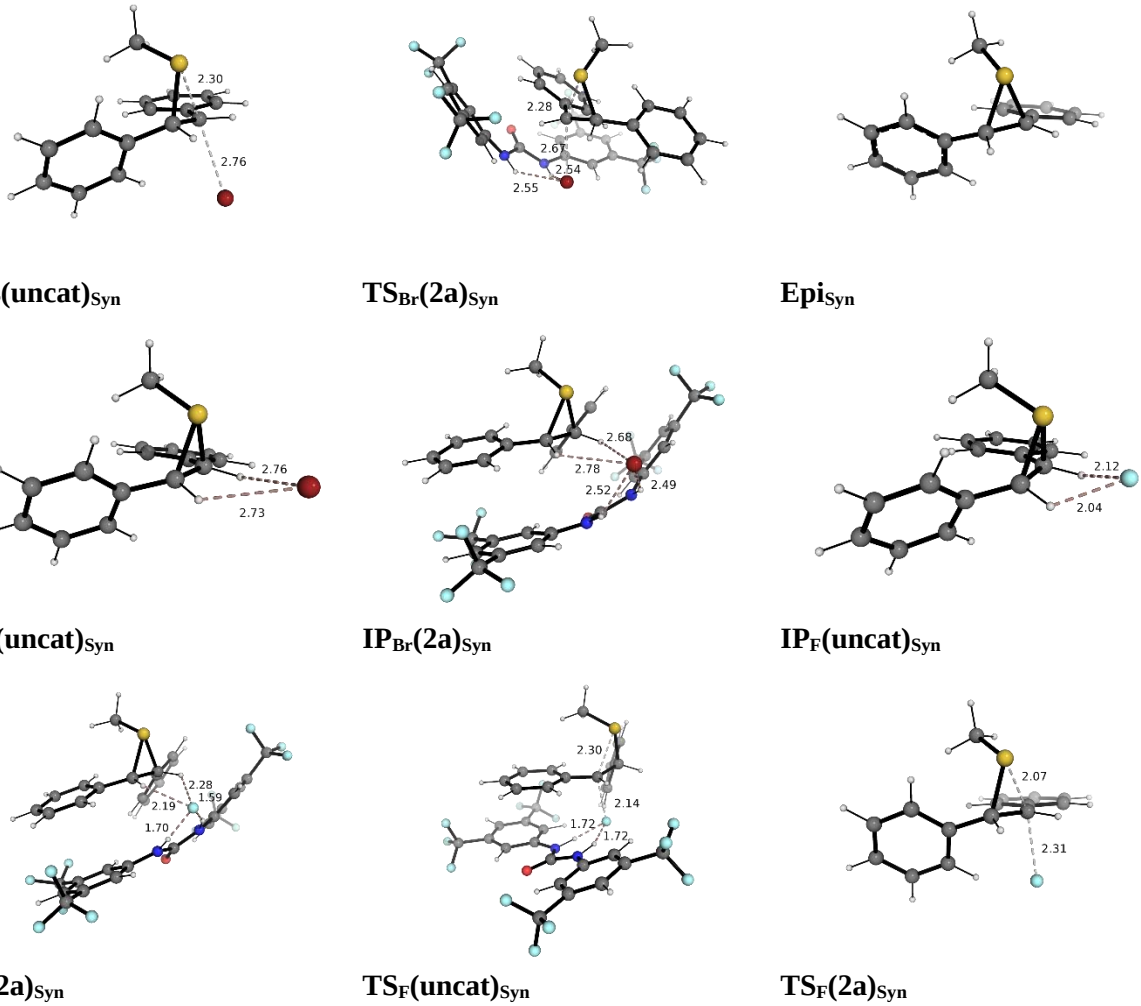

$TS_{Br}(uncat)_{Syn}$ **$TS_{Br}(2a)_{Syn}$** **Epi_{Syn}**

$IP_{Br}(uncat)_{Syn}$ **$IP_{Br}(2a)_{Syn}$** **$IP_{F}(uncat)_{Syn}$**

$IP_{F}(2a)_{Syn}$ **$TS_{F}(uncat)_{Syn}$** **$TS_{F}(2a)_{Syn}$**

Figure S13. – *Geometries of key species with episulfonium methyl syn*

Table S11. – *Key geometric parameters for stationary points with episulfonium methyl syn*

	k imag	Key Distances (Å)				Key Angles (°)	
		C-X	C-S	H-bond 1	H-bond 2	α-Dihedral†	β-Dihedral†
$TS_{Br}(uncat)_{Syn}$	-292.83	2.758	2.295	-	-	-9.4	-9.4
$TS_{Br}(2a)_{Syn}$	-348.72	2.665	2.285	2.547	2.540	-49.7	-49.7
Epi_{Syn}	-	-	1.866*	-	-	-	-
$IP_{Br}(uncat)_{Syn}$	-	-	-	-	-	-	-
$IP_{Br}(2a)_{Syn}$	-	-	-	2.519	2.486	-	-
$IP_{F}(uncat)_{Syn}$	-	-	-	-	-	-	-
$IP_{F}(2a)_{Syn}$	-	-	-	1.699	1.587	-	-
$TS_{F}(uncat)_{Syn}$	-209.16	2.309	2.068	-	-	-0.1	-49.1
$TS_{F}(2a)_{Syn}$	-350.45	2.136	2.299	1.719	1.717	-12.9	-47.9

* Average value. †Phenyl ring dihedrals measured relative to C-C bond.

Leaving Groups

The reaction was also studied with the chloride and trichloroacetimidate (TCA) leaving groups. The Gibbs energy barrier to formation of the episulfonium from the corresponding chloride at 104 kJ/mol is slightly higher than from the bromide at 90 kJ/mol. The barrier to ionization of the trichloroacetimidate is, however, prohibitively higher at 143 kJ/mol, in the absence of a promoter (**Figure S14**). These computed barriers are consistent with the reactivity observed experimentally (**Figure S1**).

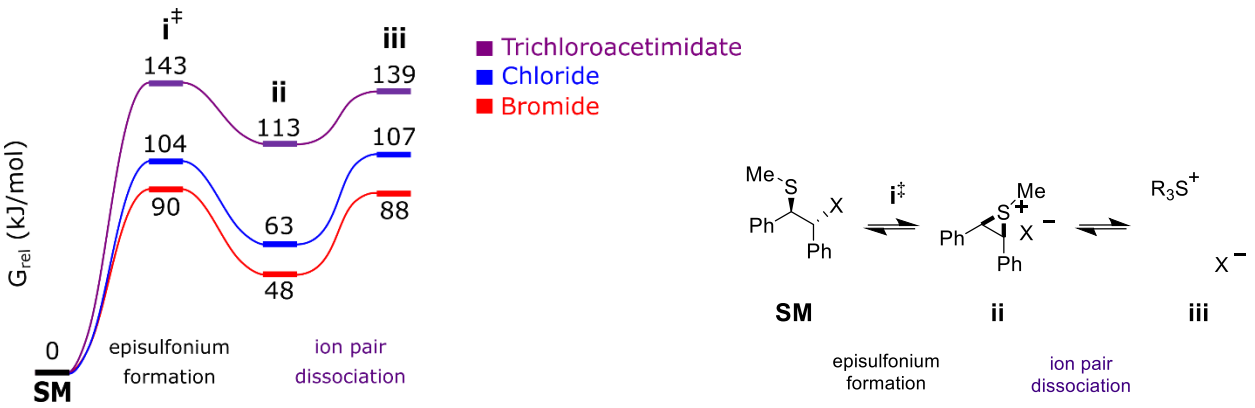

Figure S14. – *Gibbs free energy profile comparing starting material leaving groups*

The full reaction Gibbs free energy profiles for bromide and chloride starting materials is given in **Figure S15**. Generation of the episulfonium ion from the chloride starting material (**i‡-iii**) is less favorable than for

the bromide, but not prohibitively so. Phase-transfer (**iii-iv**) remains unfavorable in the absence of catalyst ($\Delta_{PT}G$ = +29.2 kJ/mol, *c.f.* $\Delta_{PT}G$ = +33.7 for bromide) and favorable in the presence of catalyst ($\Delta_{PT}G$ = -14.5 kJ/mol, *c.f.* $\Delta_{PT}G$ = -16.7 for bromide). Overall, the reaction is slightly less exergonic, by 15 kJ/mol. In the case of a chiral urea, the influence of the leaving group concludes prior to the enantiodetermining step and therefore does not influence the level of enantioinduction, as observed experimentally.

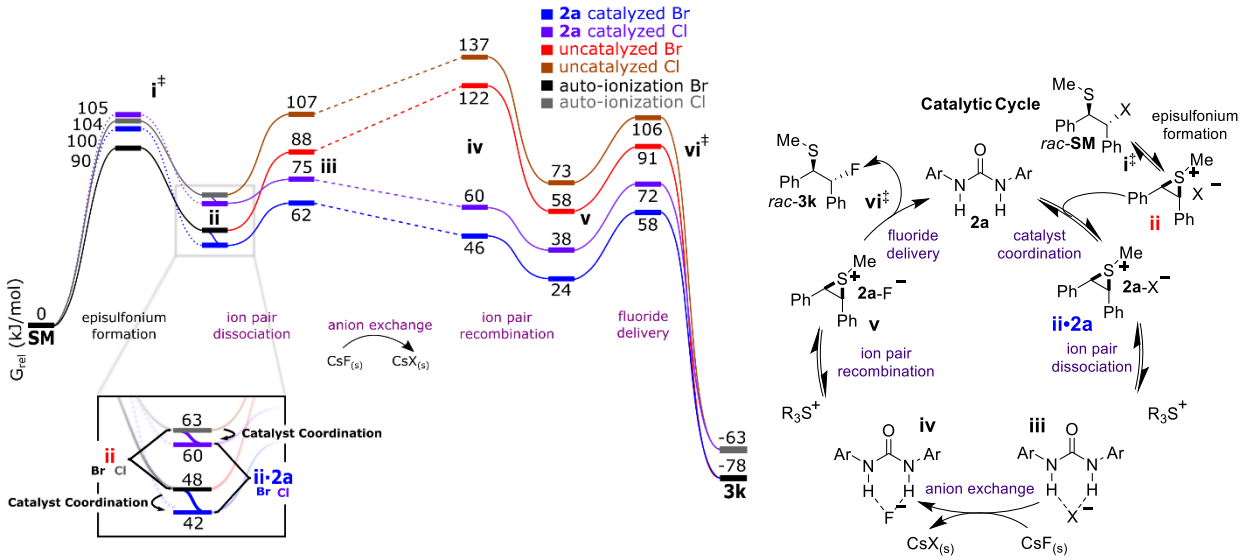

Figure S15. – *Full reaction Gibbs free energy profile comparing bromide and chloride leaving groups*

Stationary points with chloride and trichloroacetimidate leaving groups are illustrated in **Figure S16** with key geometric parameters tabulated in **Table S12**.

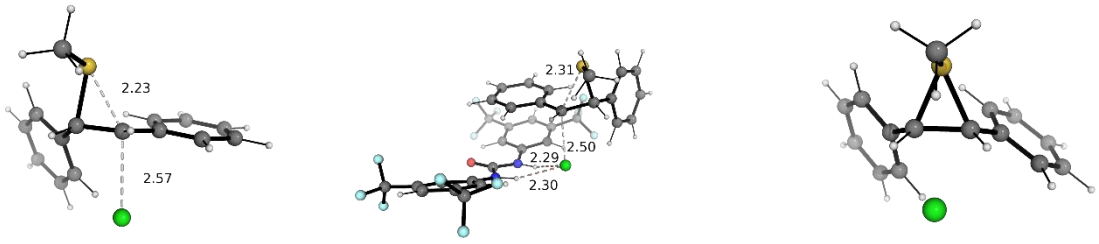

TS_{Cl}(uncat) **TS_{Cl}(2a)** **IP_{Cl}(uncat)**

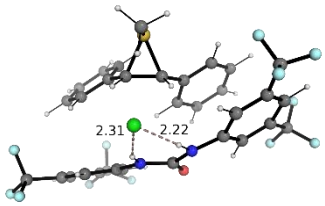

IP_{Cl}(2a)

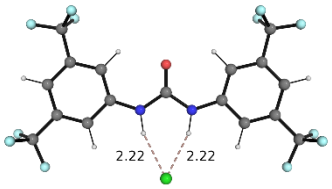

2a-Cl

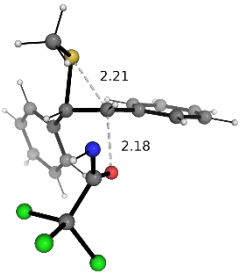

TS_{TCA}(uncat)

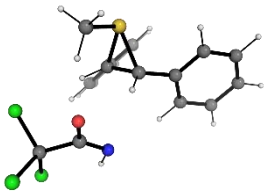

IP_{TSA}(uncat)

Figure S16. – *Geometries of key species with different leaving groups*

Table S12. – *Key geometric parameters for stationary points with different leaving groups*

	k imag	Key Distances (Å)				Key Angles (°)	
		C-X	C-S	H-bond 1	H-bond 2	α-Dihedral†	β-Dihedral†
TS_{Cl}(uncat)	-359.36	2.571	2.233	-	-	5.6	-43.4
TS_{Cl}(2a)	-349.94	2.498	2.315	2.305	2.292	-12.5	-69.8
IP_{Cl}(2a)	-	-	-	2.306	2.220	-	-
2a-Cl	-	-	-	2.219	2.218	-	-
TS_{TCA}(uncat)	-411.32	2.182	2.206	-	-	12.0	-47.9

†Phenyl ring dihedrals measured relative to C-C bond.

Thiourea 2d

Thiourea **2d** is an ineffective catalyst for the reported HB PTC reaction due to reaction of the catalyst with the starting material (**Figure S3**). Evaluation of the thermodynamics of phase-transfer (**Table S9**), however, suggest that the thiourea is suitable for phase-transfer, with $\Delta_{PT}G$ = -21.0 kJ/mol, slightly more favorable than for urea **2a** at $\Delta_{PT}G$ = -16.7 kJ/mol.

Stationary points with thiourea **2d** are illustrated in **Figure S17** with key geometric parameters tabulated in **Table S13**.

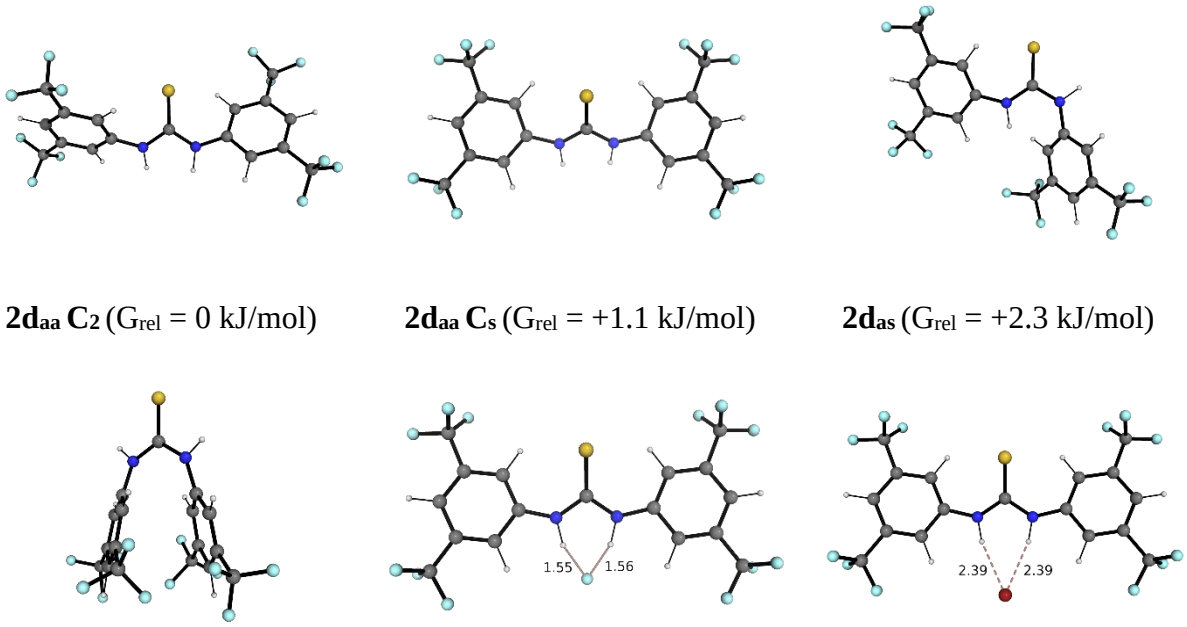

2d$_{aa}$ C$_2$ (G_{rel} = 0 kJ/mol) **2d$_{aa}$ C$_s$** (G_{rel} = +1.1 kJ/mol) **2d$_{as}$** (G_{rel} = +2.3 kJ/mol)

2d$_{ss}$ (G_{rel} = +15.0 kJ/mol) **2d-F** **2d-Br**

Figure S17. – *Geometries of key thiourea species*

Table S13. – *Key geometric parameters for thiourea stationary points*

	Key Distances (Å)	
	H-bond 1	**H-bond 2**
2d	-	-
2d-F	1.554	1.556
2d-Br	2.387	2.387

Computation – Asymmetric Catalytic System

For the asymmetric reaction, we initially considered the tetradentate catalyst, **4a**. After the advent of alkylated catalysts, we performed conformational sampling and TS analysis on the methylated catalyst, **4f**. A more specific and detailed analysis of selectivity is then undertaken for the isopropylated catalyst, **4h**.

Tetradentate Catalyst, 4a

Binding modes of tetradentate catalyst, **4a**, to fluoride with Cs^+ counterion, **IP 4a-F Cs**, were investigated using MD simulations. We initially envisaged two binding modes i) 'bis', with all 4 N-H donors coordinated to fluoride and ii) 'cooperative' with one urea simultaneously acting as a hydrogen bond donor to fluoride and acceptor to the other urea (**Figure S18 A**).

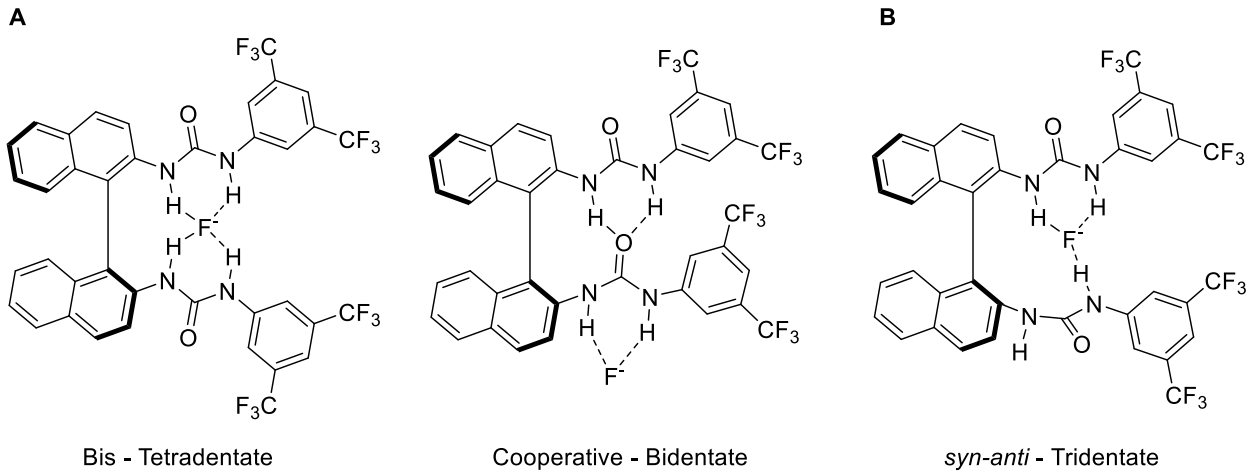

Figure S18. *–Binding modes of catalyst **4a** with fluoride A) Initially envisaged B) Arising from simulation*

We simulated the complex for a total of 120 ns (3 x 20 ns trajectories with 'bis' and 'cooperative' starting points respectively) and clustered frames for each trajectory with RMSD cut-off of 0.15 nm (**Table S14**). No 'cooperative' binding mode persisted through equilibration to the production runs. Populations of the binding modes were not found to depend strongly on initial binding mode over 60 ns total simulation. Of significance was the high weighting of a binding mode with one urea *syn-anti* isomerized adjacent to the BINAM backbone, resulting in tridentate binding (**Figure S18 B**).

Table S14. – *Summary of binding modes from MD simulations of **IP 4a-F Cs***

Run #	Starting point	Binding mode weightings		
		Bis	**Cooperative**	***syn-anti***
1	Cooperative	3 %	0 %	96 %
2	Cooperative	73 %	0 %	27 %
3	Cooperative	100 %	0 %	0 %
4	Bis	77 %	0 %	22 %
5	Bis	30 %	0 %	69 %
6	Bis	65 %	0 %	34 %
Average	Cooperative	59 %	0 %	41 %
Average	Bis	57 %	0 %	42 %
	Overall	58 %	0 %	42 %

On the basis of these results, we optimized two analogous TSs, using DFT, with fluoride coordinated by i) 4 N-H donors, **TS 4a-F epi tetra** and ii) 3 N-H donors, **TS 4a-F epi tri**, with *syn-anti* isomerized urea (**Figure S19**). We found that the tetradentate TS was unable to maintain all 4 H-bonds to fluoride, and was 23.8 kJ/mol higher in (non-single point corrected) Gibbs free energy than the tridentate TS (**Table S15**).

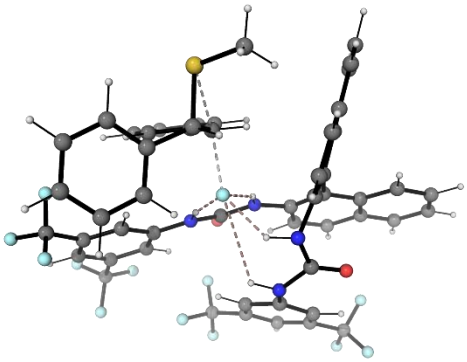

TS 4a-F epi tetra

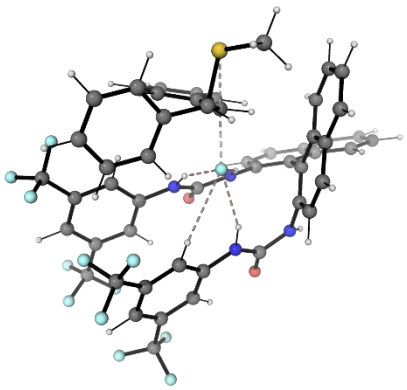

TS 4a-F epi tri

Figure S19. – *Preliminary TSs with catalyst **4a***

Table S15. – *Preliminary TS geometric parameters*

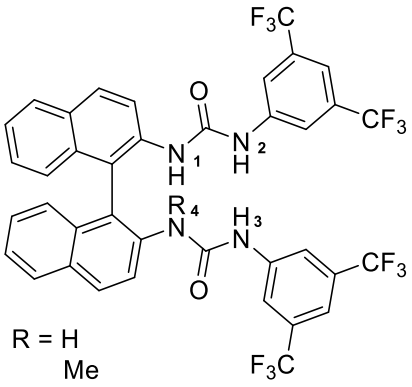

	G rel (kJ/mol)	H-bond Lengths (N-H --- F) (Å)				H-bond Angles (N-H---F) (°)				TS Distances (Å)	
		1	2	3	4	1	2	3	4	C - F	C - S
TS 4a-F epi tetra	23.8	1.882	1.699	3.218	1.917	150.5	158.1	125.5	134.4	2.069	2.242
TS 4a-F epi tri	0.0	1.867	1.741	2.186	-	152.5	152.8	151.4	-	2.108	2.259

We therefore reasoned that a catalyst mono-methylated on a single nitrogen proximal to the binaphthyl core, **4f**, would be equally active (i.e. comparable yield), to **4a** and that, due to vastly reduced conformational space, would lead to more rationalizable structure activity relationships. Pleasingly this prediction was borne out experimentally with preserved yield (> 95 %), and additionally resulted in a more enantioselective catalyst.

Methylated Tridentate Catalyst, 4f

MD Conformational Sampling Protocol

Uncoordinated **4f** was simulated for 100 ns to generate conformers. The 20 most populous clusters (0.7 Å RMSD) were optimized using DFT, resulting in 16 distinct conformers.

The CsF complex, **IP 4f-F Cs** was simulated for 100 ns and tricoordination was found to dominate the 100 ns simulation (96 % frames) and to be stable once formed. RMSD clustering resulted in only two conformationally similar high weight clusters (1.1 Å RMSD), which were optimized with DFT.

The ion pair of **4f**-fluoride complex with episulfonium intermediate, **IP 4f-F epi**, was simulated at reaction temperature of 298 K for 100 ns. Every fifth frame was clustered with cut-off of 0.1 nm, resulting in 40 clusters. The 12 most populated episulfonium urea-fluoride ion pairs (91 % of frames, cluster weighting >

1.5 %) were then optimized using DFT. To ensure that novel modes were not lost, clusters down to 0.5 % weighting were manually checked and found to be qualitative duplicates of higher weighted clusters.

Each DFT optimized ion pair was used as the starting point for generating TSs by advancing the substrate forward to align fluoride with the C-S σ*. A total of 16 unique TSs were obtained using DFT (9 to (*S*,*S*) product with (*S*) catalyst, 7 to (*R*,*R*)), resulting in an ensemble with energetic span of 42.2 kJ/mol.

*Uncoordinated **4f***

The 16 primary conformations of **4f** are illustrated in **Figure S20**, with relative Gibbs free energies.

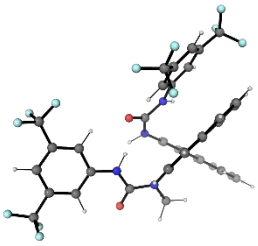

4f 1
+ 0.0 kJ/mol

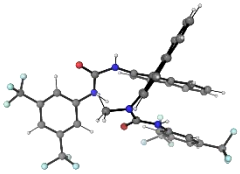

4f 2
+ 1.4 kJ/mol

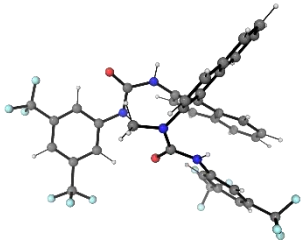

4f 3
+ 1.6 kJ/mol

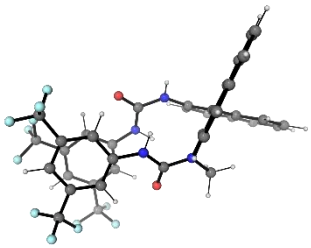

4f 4
+ 12.9 kJ/mol

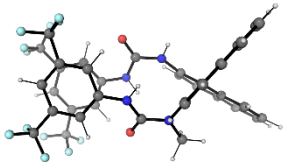

4f 5
+ 14.2 kJ/mol

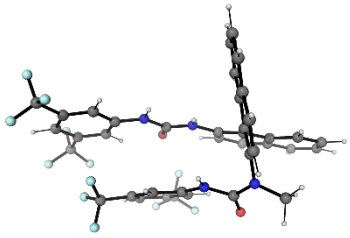

4f 6
+ 14.6 kJ/mol

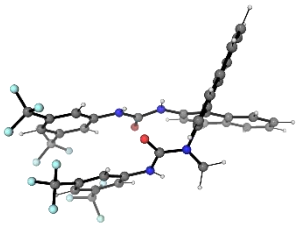

4f 7
+ 14.9 kJ/mol

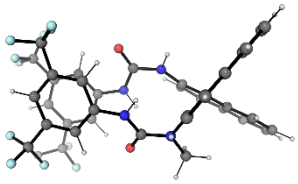

4f 8
+ 15.2 kJ/mol

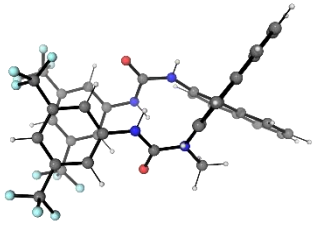

4f 9
+ 16.6 kJ/mol

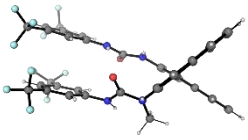

4f 10
+ 16.7 kJ/mol

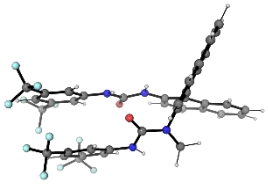

4f 11
+ 16.8 kJ/mol

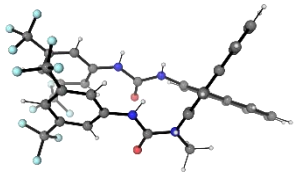

4f 12
+ 17.1 kJ/mol

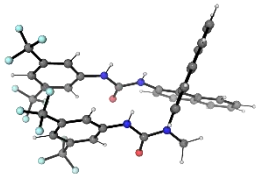

4f 13
+ 18.5 kJ/mol

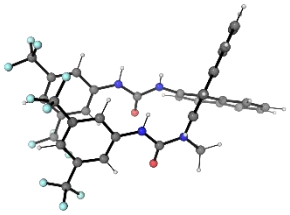

4f 14
+ 19.6 kJ/mol

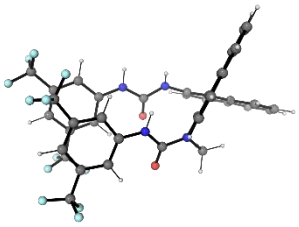

4f 15
+ 20.3 kJ/mol

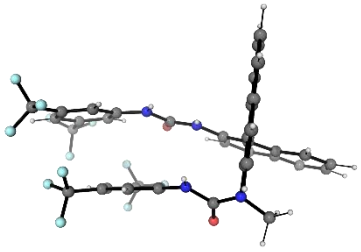

4f 16
+ 22.5 kJ/mol

Figure S20. – *Conformations of catalyst **4f** and relative Gibbs free energies*

***4f** Complexes*

Complex geometries and energies of **4f** coordinating fluoride alone, and with Cs^+ cation are shown in **Figure S21**. Relative Gibbs free energies are given with cesium cation at infinite separation, for fluoride only complexes. Additionally, the lowest energy ion pair with **4f** was used to optimize an ion pair with isopropylated catalyst **4h**, for comparison with the x-ray structure.

Complexes of catalyst **4f** were also optimized with chloride and bromide anions (**Figure S21**). **4f** binding free energies with fluoride, chloride and bromide in dichloromethane are given in **Table S16**, along with corresponding equilibrium constants. Binding of the catalyst to fluoride is computed to be stronger than to the other halides. This trend is consistent with the experimentally determined binding constants for fluoride

and bromide with catalyst **4h** and TBAF/TBAB, but with a far larger magnitude (Page S38). The discrepancy is likely due to the presence of water in TBAF experimentally, and also the presence of the TBA counter-ion. To estimate the influence of water on the binding of fluoride, we computed a conformer of fluoride coordinating **4f** and a single water molecule (**4f-F•H_2O**). This reduces the equilibrium constant to a value more comparable with experiment (**Table S16**). Key geometric parameters are given in **Table S17**.

Table S16. – *Anion binding of catalyst **4f***

Bound Species	ΔG	K
Br^-	-21.9	5 x 10^3
Cl^-	-28.9	1 x 10^5
F^-	-76.1	2 x 10^{13}
$F^- \bullet (H_2O)^{\dagger}$	-49.4	2 x 10^8
CsF*	-31.6	-

Equilibrium constants computed from ensemble of conformers. †K estimated from single conformers. *Binding of a solvated CsF ion pair by catalyst **4f**.

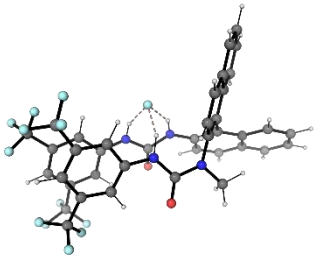

4f-F 1
+ 0.0 kJ/mol

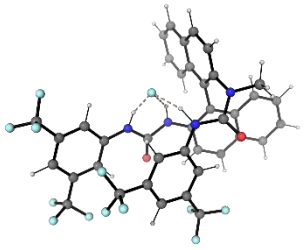

4f-F 2
+ 1.7 kJ/mol

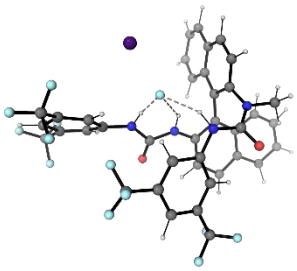

IP 4f-F Cs 1
- 37.7 kJ/mol

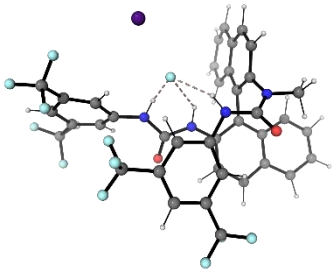

IP 4f-F Cs 2
- 36.8 kJ/mol

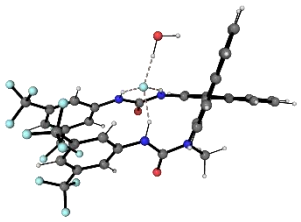

4f-F•H_2O

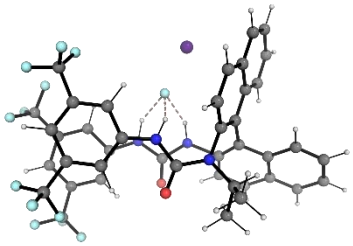

IP 4h-F Cs 1

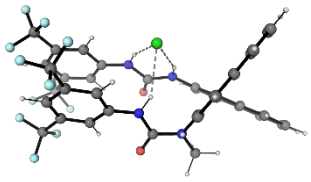

4f-Cl 1
+ 0.0 kJ/mol

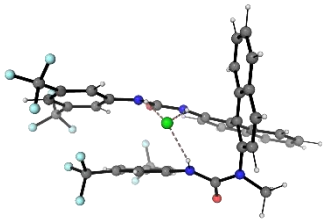

4f-Cl 2
+ 0.0 kJ/mol

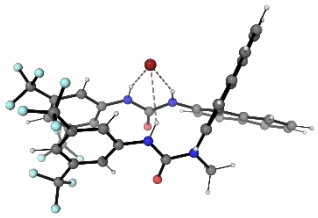

4f-Br 1
+ 0.0 kJ/mol

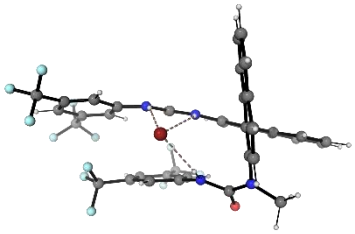

4f-Br 2
+ 1.5 kJ/mol

Figure S21. – *Anion binding modes of catalyst **4f** and relative Gibbs free energies*

Table S17. – *Key geometric parameters for complexes of catalyst **4f***

	Key Distances (Å)				Key Angles (°)	
	H-bond 1	**H-bond 2**	**H-bond 3**	**Cs - F**	**H-bond 3**	**Backbone**
4f-F 1	1.779	1.649	1.670	-	154.1	68.8
4f-F 2	1.894	1.566	1.664	-	159.9	108.8
4f-F•H_2O	1.786	1.736	1.744	-	151.4	70.0
IP 4f-F Cs 1	1.781	1.753	1.740	2.720	152.0	69.8
IP 4f-F Cs 2	1.814	1.641	1.851	2.759	144.5	99.3
IP 4h-F Cs 1	1.738	1.795	1.756	2.716	152.7	72.2
4f-Cl 1	2.354	2.208	2.354	-	145.1	69.7
4f-Cl 2	2.494	2.154	2.362	-	154.8	109.2
4f-Br 1	2.543	2.384	2.662	-	144.0	69.8
4f-Br 2	2.712	2.344	2.562	-	154.6	109.4

__4f__-Fluoride Episulfonium Ion Pairs

The structures of the twelve DFT optimized ion pairs of episulfonium intermediate with **4f-F** complex are illustrated in **Figure S22**, along with relative Gibbs free energies.

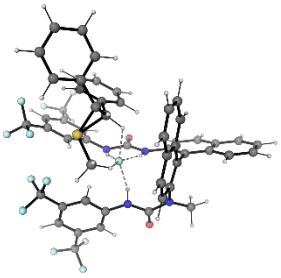

IP 4f-F epi 1
0.0 kJ/mol

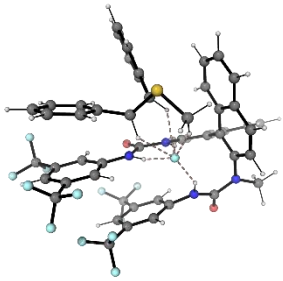

IP 4f-F epi 2
+ 1.2 kJ/mol

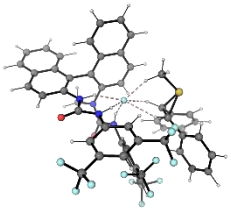

IP 4f-F epi 3
+ 2.3 kJ/mol

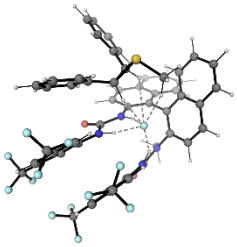

IP 4f-F epi 4
+ 6.0 kJ/mol

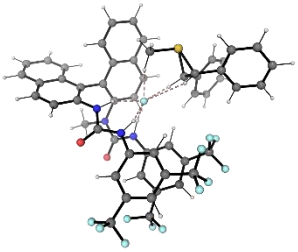

IP 4f-F epi 5
+ 7.2 kJ/mol

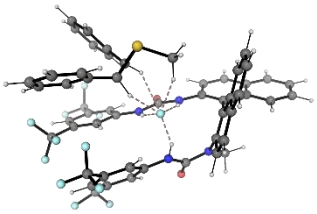

IP 4f-F epi 6
+ 9.7 kJ/mol

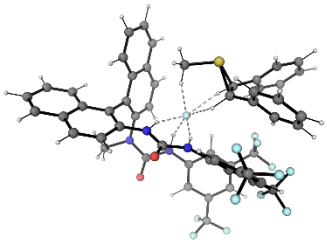

IP 4f-F epi 7
+ 12.3 kJ/mol

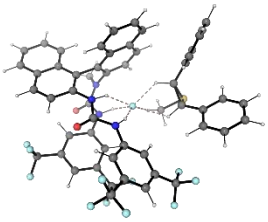

IP 4f-F epi 8
+ 13.7 kJ/mol

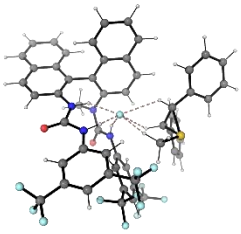

IP 4f-F epi 9
+ 19.2 kJ/mol

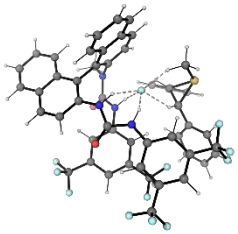

IP 4f-F epi 10
+ 21.5 kJ/mol

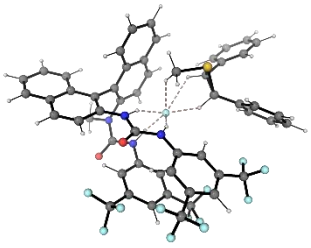

IP 4f-F epi 11
+ 26.1 kJ/mol

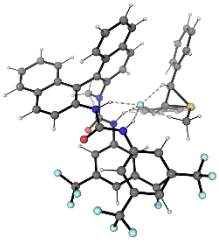

IP 4f-F epi 12
+ 28.3 kJ/mol

Figure S22. – *Geometries and relative Gibbs free energies of **4f-F** complex with episulfonium ion*

***4f** Transition States and Enantioselectivity*

Boltzmann weighting of TSs with S-methylated substrate **1k** and methylated catalyst **4f** at 243.15 K (in CH_2Cl_2) gives an e.r. of 92.5:7.5 with *(S)*-catalyst affording *(S,S)* as major product (91:9 at 298.15 K). From our model, we infer that substrates with differing sulfur protecting groups will produce the same enantiomer of product, with minor modulation of catalyst-substrate docking pose. The distribution of TSs affording major and minor product is shown in **Figure S23**. TS geometries and relative Gibbs free energies are illustrated in **Figure S24**, with key geometric parameters tabulated in **Table S18**.

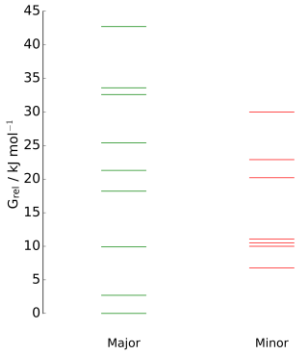

Figure S23. – *Distribution of TS free energies at 243.15 K*

TSs forming major enantiomer

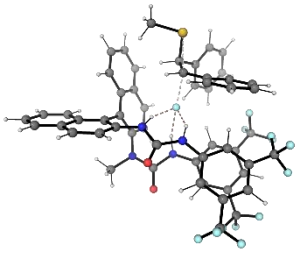

TS 4f-F epi major 1
298.15 K: + 0.0 kJ/mol
243.15 K: + 0.0 kJ/mol

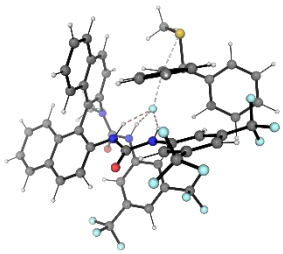

TS 4f-F epi major 2
298.15 K: + 2.8 kJ/mol
243.15 K: + 2.7 kJ/mol

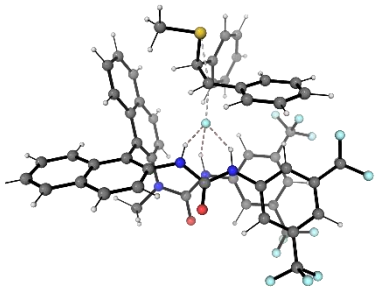

TS 4f-F epi major 3
298.15 K: + 9.9 kJ/mol
243.15 K: + 9.9 kJ/mol

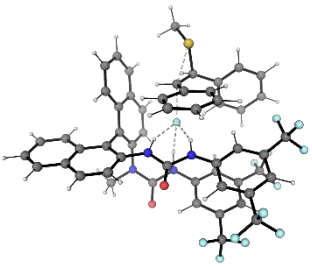

TS 4f-F epi major 4
298.15 K: + 18.4 kJ/mol
243.15 K: + 18.2 kJ/mol

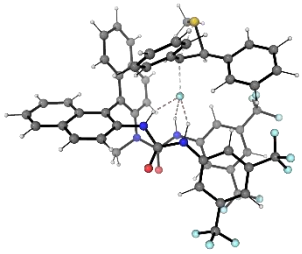

TS 4f-F epi major 5
298.15 K: + 21.1 kJ/mol
243.15 K: + 21.3 kJ/mol

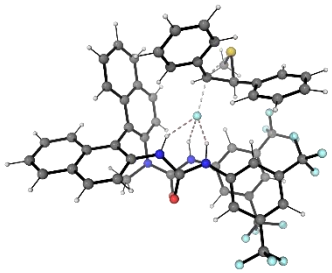

TS 4f-F epi major 6
298.15 K: + 25.7 kJ/mol
243.15 K: + 25.4 kJ/mol

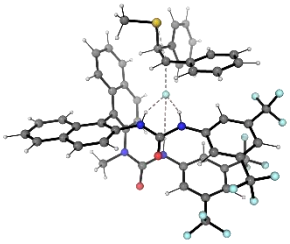

TS 4f-F epi major 7
298.15 K: + 32.6 kJ/mol
243.15 K: + 32.6 kJ/mol

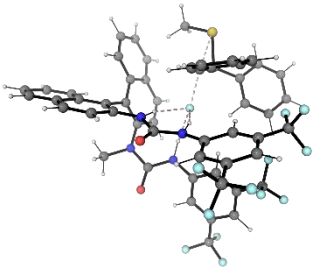

TS 4f-F epi major 8
298.15 K: + 32.9 kJ/mol
243.15 K: + 33.6 kJ/mol

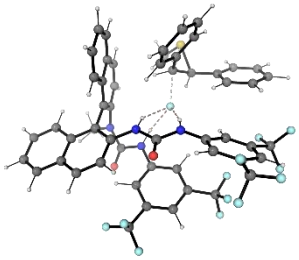

TS 4f-F epi major 9
298.15 K: + 42.2 kJ/mol
243.15 K: + 42.7 kJ/mol

TSs forming minor enantiomer

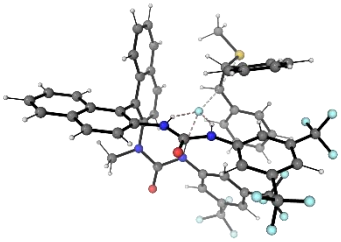

TS 4f-F epi minor 1
298.15 K: + 6.0 kJ/mol
243.15 K: + 6.8 kJ/mol

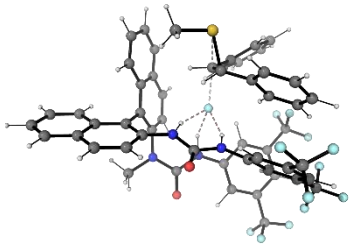

TS 4f-F epi minor 2
298.15 K: + 10.0 kJ/mol
243.15 K: + 10.0 kJ/mol

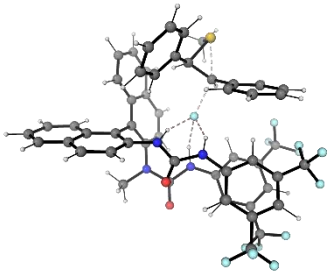

TS 4f-F epi minor 3
298.15 K: + 10.6 kJ/mol
243.15 K: + 10.5 kJ/mol

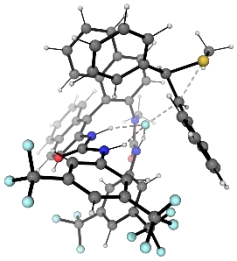

TS 4f-F epi minor 4
298.15 K: + 10.7 kJ/mol
243.15 K: + 11.1 kJ/mol

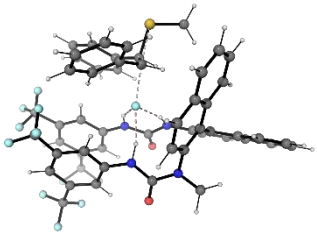

TS 4f-F epi minor 5
298.15 K: + 20.4 kJ/mol
243.15 K: + 20.2 kJ/mol

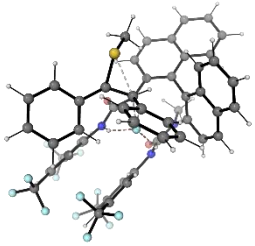

TS 4f-F epi minor 6
298.15 K: + 23.0 kJ/mol
243.15 K: + 22.9 kJ/mol

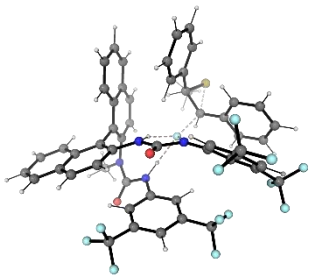

TS 4f-F epi minor 7
298.15 K: + 29.7 kJ/mol
243.15 K: + 30.0 kJ/mol

Figure S24. – *TSs with catalyst **4f** and substrate **1k**. $\Delta\Delta G^{\ddagger}$ values given relative to lowest energy TS at given temperature*

We also considered removal of bromide from the starting material, assisted by **4f**; reducing the barrier to bromide dissociation from 90.2 kJ/mol to 82.7 kJ/mol at 298.15 K. The lowest energy TS for fluoride delivery was used as starting point for the optimization, with no further conformational searching (**TS Br 4f 1k**, **Figure S25**).

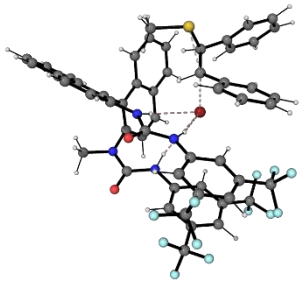

TS Br 4f 1k

Figure S25. – *Example TS for **4f** assisted bromide removal from substrate **1k***

Table S18. – *Key **4f** TS geometric parameters*

TS	k imag	Key Distances (Å)						Key Angles (°)			
		C-F	C-S	α-C-H	H-bond 1	H-bond 2	H-bond 3	H-bond 3	α-Dihedral†	β-Dihedral†	Backbone
TS 4f-F epi major 1	-418.30	2.070	2.210	1.091	1.734	1.839	1.854	149.5	-20.5	-71.4	68.4
TS 4f-F epi major 2	-387.71	2.071	2.268	1.089	1.840	1.795	1.871	152.8	4.7	-59.4	113.2
TS 4f-F epi major 3	-406.05	2.083	2.205	1.091	1.679	1.906	1.879	149.4	-19.6	-72.3	67.6
TS 4f-F epi major 4	-292.68	2.186	2.240	1.091	1.778	1.749	1.933	151.7	-8.6	-76.5	73.2
TS 4f-F epi major 5	-426.00	2.058	2.253	1.090	1.761	1.841	1.898	146.9	13.1	-33.2	64.0
TS 4f-F epi major 6	-424.89	2.066	2.265	1.089	1.938	1.683	2.021	145.5	22.0	-35.4	67.3
TS 4f-F epi major 7	-398.95	2.097	2.205	1.090	1.743	1.633	2.788	140.8	-14.7	-57.5	69.7
TS 4f-F epi major 8	-452.00	2.027	2.289	1.090	1.944	1.658	1.921	165.6	-2.8	-49.1	66.8
TS 4f-F epi major 9	-433.42	2.053	2.277	1.087	2.002	1.643	1.927	152.9	26.4	-26.3	111.6
TS 4f-F epi minor 1	-365.95	2.109	2.225	1.090	1.800	1.728	1.711	172.8	-6.3	90.6	76.9
TS 4f-F epi minor 2	-429.11	2.055	2.243	1.090	1.827	1.803	1.793	148.2	22.2	-26.1	73.6
TS 4f-F epi minor 3	-415.48	2.075	2.196	1.089	1.728	1.808	1.880	147.9	-40.7	86.6	65.2
TS 4f-F epi minor 4	-397.02	2.075	2.224	1.088	1.771	1.877	1.800	151.2	-4.1	-63.2	112.4
TS 4f-F epi minor 5	-438.90	2.068	2.184	1.093	1.748	1.789	1.889	148.1	-52.7	50.9	69.1
TS 4f-F epi minor 6	-426.40	2.068	2.252	1.090	1.734	1.872	2.131	137.0	15.6	-34.0	64.6
TS 4f-F epi minor 7	-412.25	2.068	2.252	1.088	1.902	1.715	1.839	159.2	-21.0	-64.8	112.3
TS Br 4f 1k	-340.66	2.640*	2.265	1.092	2.620	2.350	2.779	133.6	-50.4	74.1	71.2

*C-Br distance. †Phenyl ring dihedrals measured relative to C-C bond.

Isopropylated Catalyst, 4h

Transition States and Enantioselectivity

We used the **4f** TSs as starting points for locating TSs for the isopropylated catalyst, **4h**, on the basis of limited conformation change upon changing the alkyl group. Due to the impact of Boltzmann weighting, and the absence of **4f** TSs between +11.0 and +18.0 kJ/mol, we used only the 7 TSs with relative energy + 11.0 kJ/mol and below. Optimizations from **TS 4f-F epi major 1** demonstrated that the favored orientation of the iPr group was with hydrogen pointing towards the BINAM core, and methyl groups straddling the urea carbonyl oxygen. This conformation was later supported by the determination of a crystal structure of **4h** with TBAF. We also considered at least one minor rotamer for each TS, but only in the case of **TS 4f-F epi major 1** was this energetically competitive. A total of 6 TSs were located within +10.7 kJ/mol of the lowest, with a considerable jump to the next TS at +16.2 kJ/mol. The lowest 6 TSs were therefore used for Boltzmann weighting and further analysis.

Comparison of relative Gibbs free energies of the **4h** TSs with its corresponding parent **4f** TS shows nearly all TSs are destabilized relative to the major TS on changing Me to iPr (**Figure S26**). A notable exception is **TS 4f-F epi minor 3 → TS 4h-F epi major 2**, becoming the new minor TS.

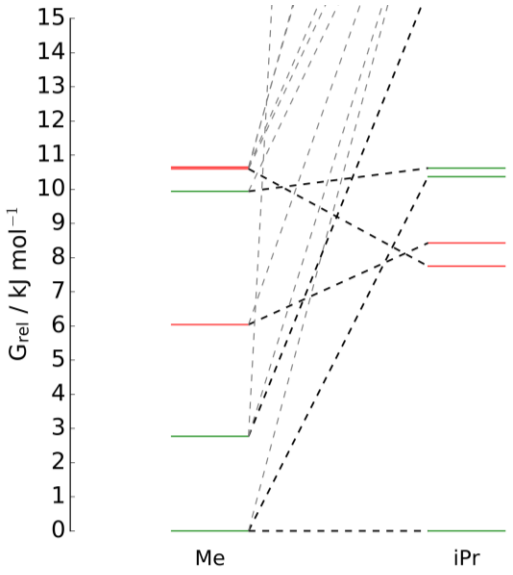

Figure S26. – *Correlation of relative TS free energies on replacement of catalyst Me group with iPr*

Boltzmann weighting of TSs at 243.15 K (in CH_2Cl_2) gives an er of 96.5:3.5 with *(S)* catalyst affording *(S,S)* as major product (92:8 at 298.15 K).

All TSs involving **4h** are illustrated in **Figure S27**, with relative Gibbs free energies. TSs that were used in enantioselectivity calculations are shown in bold. Key geometric parameters are given in **Table S19**.

TSs forming major enantiomer

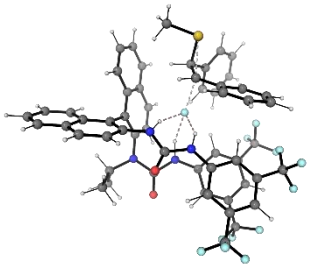

TS 4h-F epi major 1
298.15 K: + 0.0 kJ/mol
243.15 K: + 0.0 kJ/mol

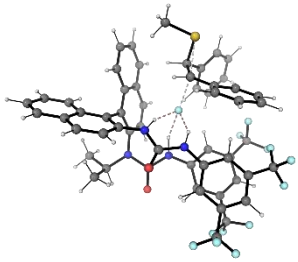

TS 4h-F epi major 2
298.15 K: + 10.4 kJ/mol
243.15 K: + 10.0 kJ/mol

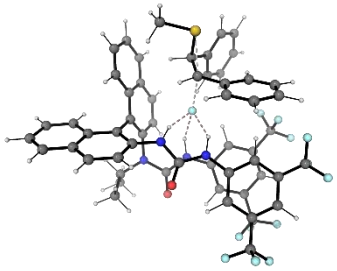

TS 4h-F epi major 3
298.15 K: + 10.6 kJ/mol
243.15 K: + 10.7 kJ/mol

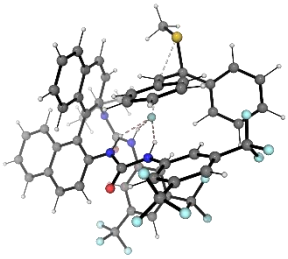

TS 4h-F epi major 4
298.15 K: + 15.9 kJ/mol
243.15 K: + 16.2 kJ/mol

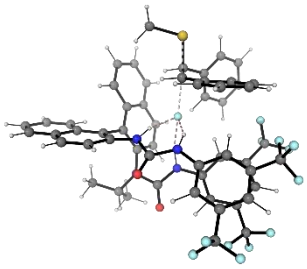

TS 4h-F epi major 5
298.15 K: + 19.8 kJ/mol
243.15 K: + 19.3 kJ/mol

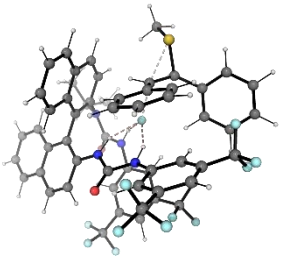

TS 4h-F epi major 6
298.15 K: + 19.7 kJ/mol
243.15 K: + 19.7 kJ/mol

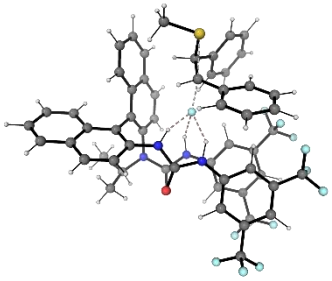

TS 4h-F epi major 7
298.15 K: + 20.9 kJ/mol
243.15 K: + 20.6 kJ/mol

TSs forming minor enantiomer

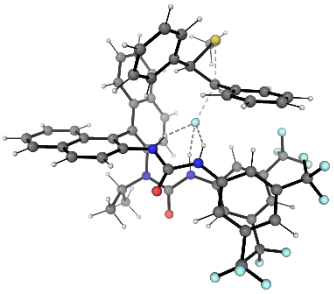

TS 4h-F epi Minor 1
298.15 K: + 7.8 kJ/mol
243.15 K: + 7.8 kJ/mol

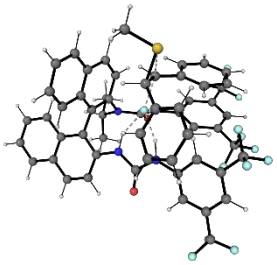

TS 4h-F epi Minor 2
298.15 K: +8.4 kJ/mol
243.15 K: + 9.1 kJ/mol

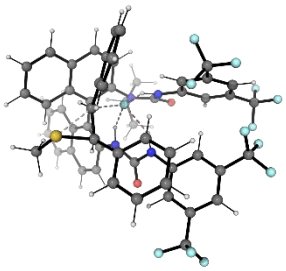

TS 4h-F epi Minor 3
298.15 K: + 10.4 kJ/mol
243.15 K: + 10.6 kJ/mol

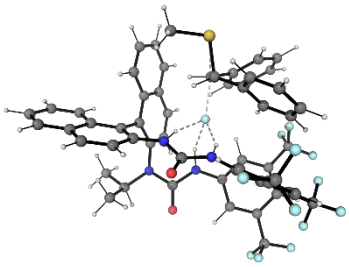

TS 4h-F epi Minor 4
298.15 K: + 20.0 kJ/mol
243.15 K: + 20.0 kJ/mol

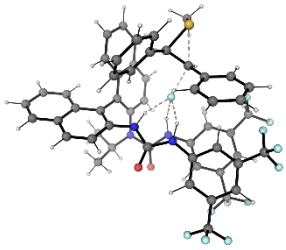

TS 4h-F epi Minor 5
298.15 K: + 21.8 kJ/mol
243.15 K: + 21.4 kJ/mol

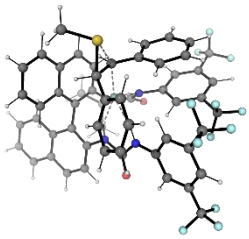

TS 4h-F epi Minor 6
298.15 K: + 21.1 kJ/mol
243.15 K: +21.4 kJ/mol

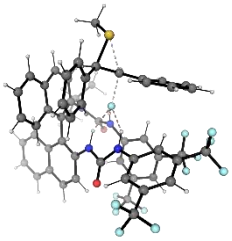

TS 4h-F epi Minor 7
298.15 K: + 22.9 kJ/mol
243.15 K: + 23.8 kJ/mol

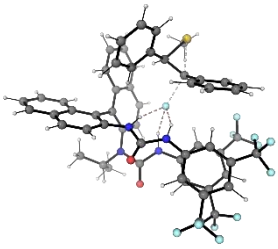

TS 4h-F epi Minor 8
298.15 K: +30.1 kJ/mol
243.15 K: + 29.6 kJ/mol

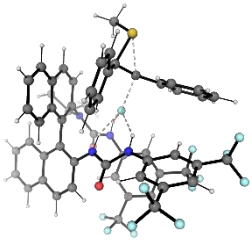

TS 4h-F epi Minor 9
298.15 K: 29.6 kJ/mol
243.15 K: + 30.2 kJ/mol

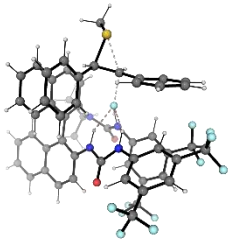

TS 4h-F epi Minor 10
298.15 K: + 40.6 kJ/mol
243.15 K: + 41.1 kJ/mol

Figure S27. – *TSs with catalyst **4h** and substrate **1k**. $\Delta\Delta G^{\ddagger}$ values given relative to lowest energy TS at given temperature*

Table S19. – *Key **4h** TS geometric parameters*

TS	k imag	Key Distances (Å)						Key Angles (º)			
		C-F	C-S	α-C-H	H-bond 1	H-bond 2	H-bond 3	H-bond 3	α-Dihedral	β-Dihedral	Backbone
TS 4h-F epi major 1	-415.39	2.069	2.213	1.090	1.728	1.831	1.870	150.4	-20.9	-70.6	71.7
TS 4h-F epi major 2	-408.62	2.078	2.208	1.090	1.706	1.855	1.888	146.5	-18.0	-72.3	68.5
TS 4h-F epi major 3	-406.40	2.082	2.208	1.091	1.680	1.887	1.903	150.4	-20.6	-70.6	71.3
TS 4h-F epi major 4	-385.12	2.073	2.272	1.088	1.857	1.785	1.865	153.0	5.5	-59.1	111.0
TS 4h-F epi major 5	-408.30	2.077	2.211	1.090	1.705	1.856	1.884	147.5	-17.5	-73.2	68.0
TS 4h-F epi major 6	-375.93	2.082	2.273	1.088	1.840	1.787	1.918	150.3	5.2	-59.2	111.7
TS 4h-F epi major 7	-398.20	2.091	2.202	1.091	1.655	1.938	1.901	147.4	-17.1	-73.0	67.7
TS 4h-F epi minor 1	-416.48	2.073	2.195	1.089	1.726	1.800	1.884	149.5	-40.5	86.6	68.2
TS 4h-F epi minor 2	-364.96	2.113	2.227	1.090	1.791	1.732	1.724	171.0	-7.1	90.2	79.9
TS 4h-F epi minor 3	-421.87	2.060	2.248	1.090	1.811	1.807	1.802	148.9	22.3	-25.4	76.7
TS 4h-F epi minor 4	-416.62	2.066	2.238	1.090	1.771	1.852	1.804	145.8	24.0	-21.9	71.9
TS 4h-F epi minor 5	-418.25	2.075	2.198	1.089	1.731	1.796	1.922	143.9	-41.8	-87.8	65.2
TS 4h-F epi minor 6	-338.12	2.136	2.219	1.090	1.765	1.751	1.713	170.7	-4.2	-91.3	74.3
TS 4h-F epi minor 7	-395.39	2.078	2.227	1.088	1.797	1.852	1.795	150.9	-4.6	-61.7	109.3
TS 4h-F epi minor 8	-417.88	2.075	2.203	1.089	1.734	1.791	1.925	144.1	-41.6	-86.7	64.6
TS 4h-F epi minor 9	-392.96	2.084	2.226	1.088	1.778	1.863	1.838	149.2	-3.5	-67.6	110.4
TS 4h-F epi minor 10	-391.12	2.088	2.236	1.088	1.875	1.789	1.851	144.3	-8.6	-54.6	95.2

[†]Phenyl ring dihedrals measured relative to C-C bond.

Transition State Analysis

Catalyst Conformation

The conformation of the **4h** in the major TS was found to be in very good agreement with the subsequently determined experimental crystal structure (**Figure S28**). Whilst slightly different structures are expected, the following similarities are of note i) the binding mode of the catalyst with fluoride is as predicted from MD simulations, with coordination by three hydrogen bonds, ii) the broad conformation of the catalyst, such as BINAM angle and orientation of the ureas, iii) the orientation of the isopropyl group, iv) the episulfonium substrate sits in the position of the TBA cation of the crystal structure.

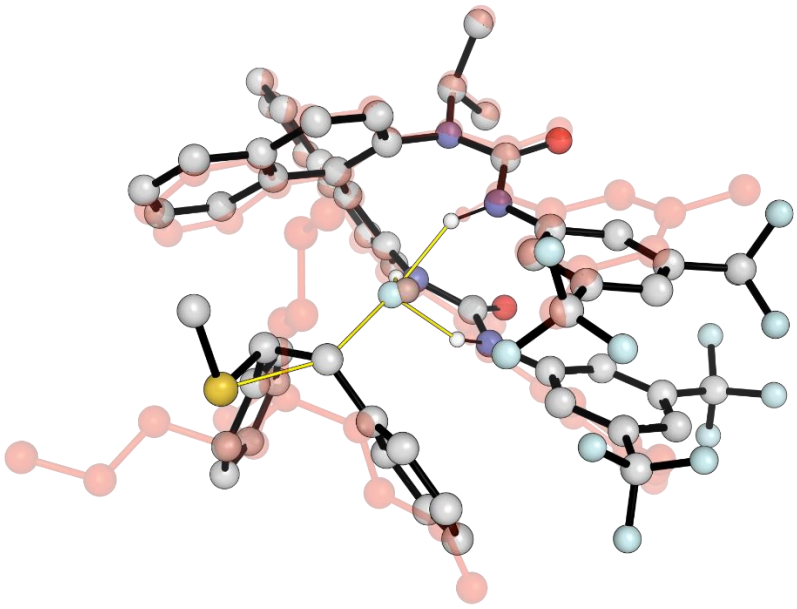

Figure S28. – *Superposition of crystal structure of **4h** coordinating TBAF, and the major TS*

Substrate Conformation

In the TSs for uncoordinated fluoride delivery, and when coordinated by an achiral urea, we note a preference for the substrate phenyl ring to be orthogonal to the forming and breaking bonds (α-dihedrals of -4.8, -12.2 and 18.2 degrees). We attribute this preference primarily to the well-known effects of *β*-unsaturation on the rate of S_N2 reactions. To estimate the energetic contribution of this effect, a dihedral scan on **TS_F(2a)** with fixed C-S and C-F bond distances was run (**Figure S29**).

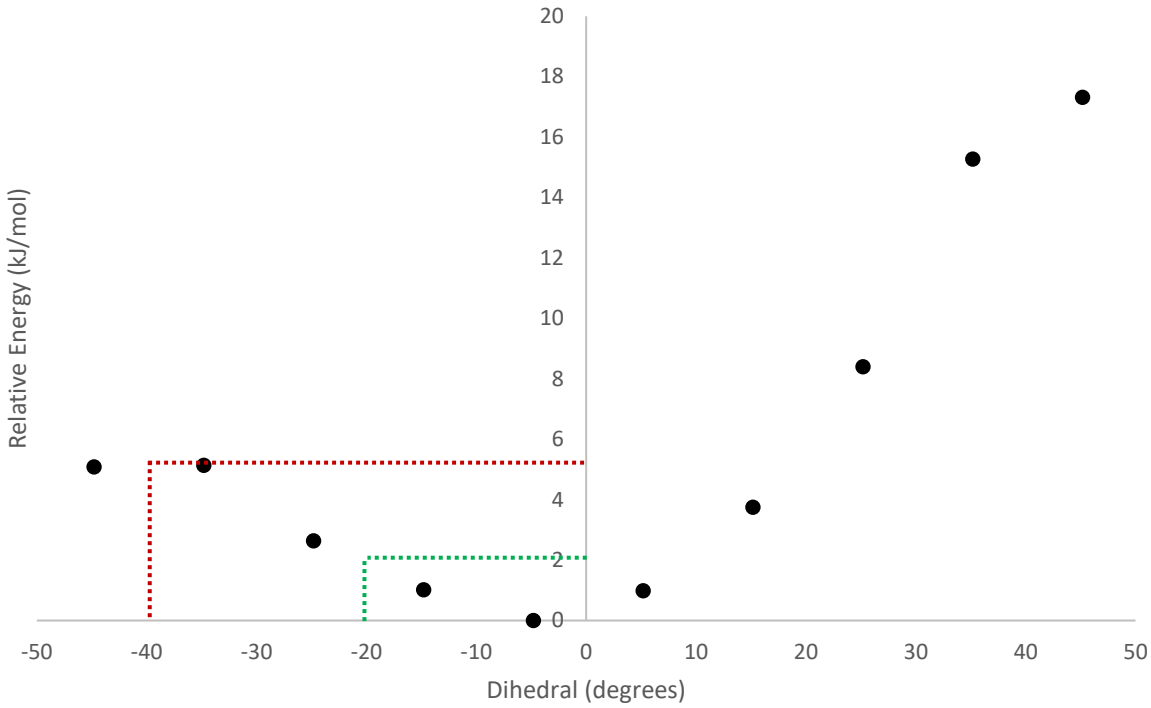

Figure S29. – *Energetic preference (uncorrected) for α-dihedral in fluoride delivery TS*

The conformation of the substrate, in the majority of low energy TSs with chiral urea, **4h**, has a small α-dihedral. A notable exception is in the case of the lowest energy minor TS, **TS 4h-F epi minor 1**, where this angle is –40.5 º (See **Table S10** for definitions).

Comparing the dihedral values in the lowest energy major and minor TSs, the dihedral scan estimates an energetic contribution of approximately 3 kJ/mol to a $\Delta\Delta G^{\ddagger}$ of 7.8 kJ/mol. An alternative approach was also taken, looking at the distortion of the episulfonium + fluoride unit in the chiral TSs. Single point energies were evaluated on this unit (i.e. with catalyst removed), revealing an increased distortion in the minor TS by 4 kJ/mol.

Non-covalent Interactions

Within all optimized TSs, the catalyst forms three hydrogen bonds to fluoride, and the episulfonium forms a cation-π interaction, to varying degrees, with the naphthyl ring of the BINAM core. In the major TS, the cation-π distance is 0.05 Å shorter than in the minor. The minor TS, however, has some π - π stacking of substrate and BINAM backbone, which partially compensates for the loss of planarity of the substrate α-dihedral.

The non-covalent interactions in the lowest major and minor TSs were visualized using the non-covalent interaction index (**Figure S30**). Key additional non-covalent interactions common to both TSs are as i) sandwich intramolecular π - π stacking within the catalyst itself, ii) CH-π interaction from catalyst ortho C-H bond to substrate phenyl ring.

TS 4h-F epi major 1

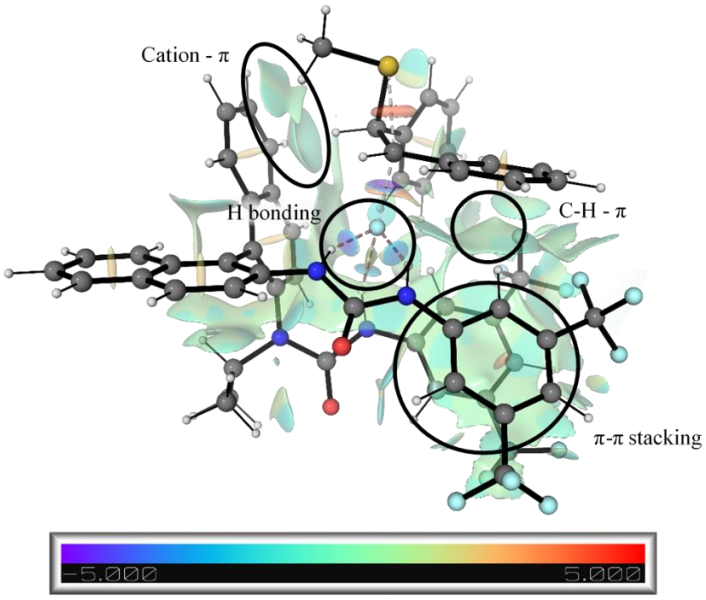

TS 4h-F epi minor 1

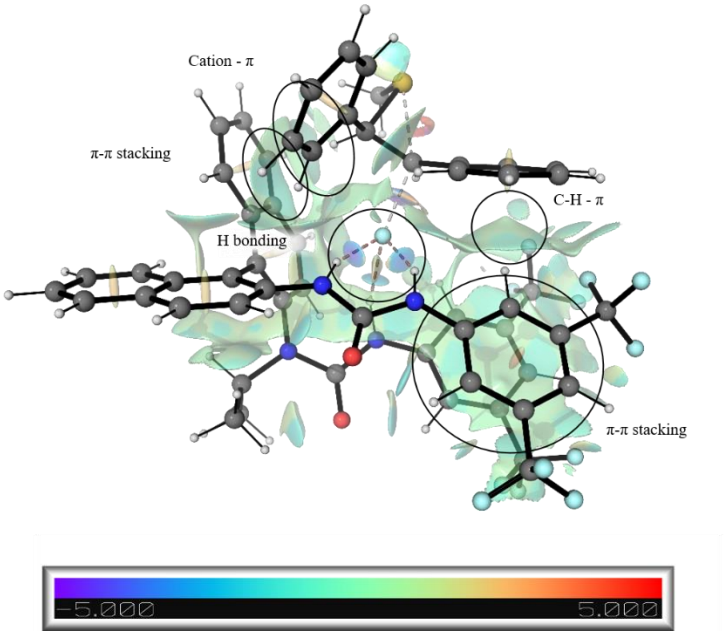

Figure S30. – *Non-covalent interaction plots for lowest energy major and minor TSs*

Analysis of key geometric parameters over the intrinsic reaction coordinate (IRC) pathway was performed for the **4f** TSs corresponding to **TS 4h-F epi major 1** and **TS 4h-F epi minor 1**. Distances are plotted relative to the IRC (defined as C-S distance minus C-F distance) in **Figure S31**.

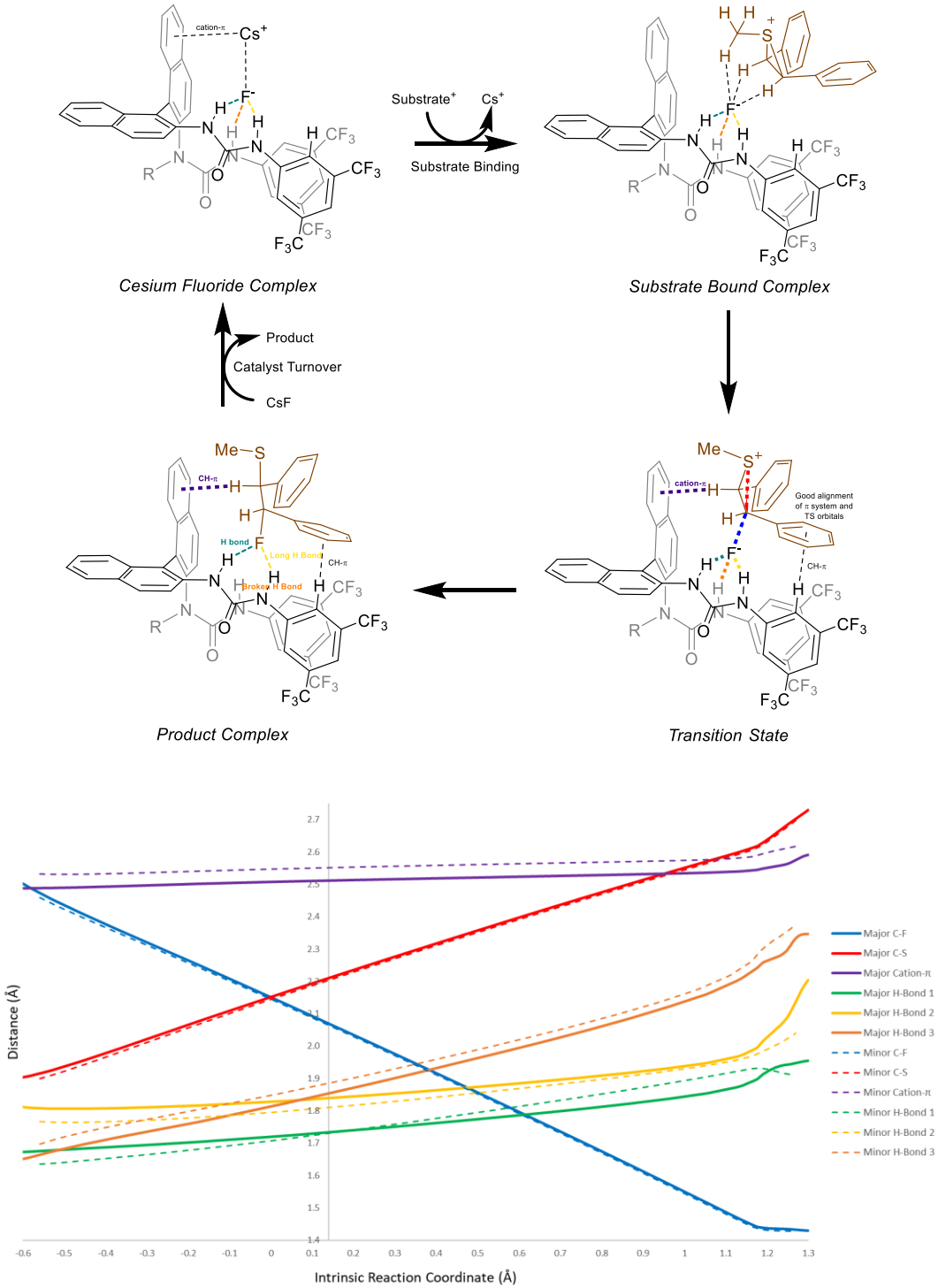

Figure S31. – *Key distances over the lowest energy intrinsic reaction coordinate pathways*

The y-axis intercepts the x-axis at 0.14 Å - the major TS position (*c.f.* 0.12 Å for the minor). The graph falls into two distinct domains, -0.5 < IRC < 1.2 and 1.2 < IRC < 1.3. The former describes the main bond breaking/forming process, and the latter describes substrate relaxation (note that C-F distance remains constant in the latter region). Change in distances with respect to the IRC in the first domain are roughly linear. All gradients quoted in the following analysis were evaluated for -0.5 < IRC < 1.0.

C–S and C–F distances behave similarly along the IRC pathway for both TSs, with the IRC pathway to major product slightly looser. The largest consistent difference in distances between the pathways is the shorter (stronger) cation-π interaction in the pathway leading to major product.

All H-bonds lengthen along the IRC pathways, however, due to the early TS position, all remain bonded at the TS (<1.9 Å). After the TS, all H-bonds continue to elongate, with this most significant for H-bond 3 with gradient of 0.30 for both pathways (0.12 average gradient for all other H-bonds). For the pathway to major product there is also a significant lengthening of H-bond 2 during product relaxation, resulting in only one dominant H-bond in the product complex. This behavior of the H-bonds over the IRC pathway parallels the fluorinase enzyme, with the bidentate urea (H-bonds 1 and 2) mimicking Ser 158A and the third H-bond mimicking the role of Thr 80A (*27*, *28*, *97*).

Computation – Tabulated Thermochemical Data

Table S20. – *Non-asymmetric pathway*

	Energies (Ha)				
	E (opt)	**G (opt)**	**G-qh (opt)**	**E (sp)**	**G-qh (sp)**
$2a_{aa}$	-2033.353700	-2033.169216	-2033.159297	-2035.910612	-2035.716209
$2a_{as}$	-2033.349097	-2033.163487	-2033.154014	-2035.906815	-2035.711732
$2a_{ss}$	-2033.353644	-2033.159334	-2033.154211	-2035.902173	-2035.702740
2a-F	-2133.373665	-2133.191831	-2133.181208	-2135.938385	-2135.745928
2a-Br	-4607.746838	-4607.568062	-4607.556044	-4610.320359	-4610.129565
$2f_{aa}$	-686.592580	-686.403598	-686.400697	-687.441567	-687.249684
$2f_{as}$	-686.590424	-686.401679	-686.398774	-687.440712	-687.249062
$2f_{ss}$	-686.586950	-686.396627	-686.394565	-687.437932	-687.245547
2f-F	-786.604866	-786.418795	-786.415088	-787.461699	-787.271921
2f-Br	-3260.981282	-3260.798779	-3260.793709	-3261.846836	-3261.659263
TS_{Br}(uncat)	-3552.313308	-3552.099059	-3552.096054	-3553.071744	-3552.854490
TS_{Br}(2a)	-5585.700428	-5585.277217	-5585.262671	-5589.004716	-5588.566959
TS_{Br}(2f)	-4238.934182	-4238.510177	-4238.502137	-4240.536668	-4240.104623
Epi	-977.934363	-977.715799	-977.713498	-978.672665	-978.451800
IP_{Br}(uncat)	-3552.327903	-3552.114714	-3552.110708	-3553.087609	-3552.870414
IP_{Br}(2a)	-5585.720703	-5585.299111	-5585.283707	-5589.026043	-5588.589047
IP_{Br}(2f)	-4238.951489	-4238.527116	-4238.519030	-4240.553001	-4240.120542
IP_{F}(uncat)	-1077.944669	-1077.728265	-1077.725249	-1078.696148	-1078.476728
IP_{F}(2a)	-3111.351814	-3110.924654	-3110.911336	-3114.646474	-3114.205996
IP_{F}(2f)	-1764.581152	-1764.152806	-1764.145923	-1766.172929	-1765.737700
TS_{F}(uncat)	-1077.931232	-1077.714931	-1077.712483	-1078.682835	-1078.464086
TS_{F}(2a)	-3111.333561	-3110.907849	-3110.893899	-3114.632833	-3114.193171
TS_{F}(2f)	-1764.563519	-1764.136424	-1764.128860	-1766.158998	-1765.724339
$TS_{Br}(uncat)_{Syn}$	-3552.314667	-3552.098689	-3552.096189	-3553.072956	-3552.854478
$TS_{Br}(2a)_{Syn}$	-5585.695928	-5585.270984	-5585.256659	-5588.999015	-5588.559746
Epi_{Syn}	-977.932392	-977.711698	-977.709984	-978.670160	-978.447752
$IP_{Br}(uncat)_{Syn}$	-3552.325789	-3552.110440	-3552.107121	-3553.083582	-3552.864914
$IP_{Br}(2a)_{Syn}$	-5585.721447	-5585.294962	-5585.281452	-5589.021329	-5588.581334

$IP_F(uncat)_{Syn}$	-1077.930972	-1077.713062	-1077.710892	-1078.681477	-1078.461397
$IP_F(2a)_{Syn}$	-1077.940540	-1077.721570	-1077.719401	-1078.689932	-1078.468793
$TS_F(uncat)_{Syn}$	-3111.333036	-3110.906408	-3110.892635	-3114.632407	-3114.192006
$TS_F(2a)_{Syn}$	-1077.930518	-1077.712361	-1077.710403	-1078.681423	-1078.461308
2a-Cl	-2493.745562	-2493.564446	-2493.553453	-2496.312863	-2496.120754
$IP_{Cl}(uncat)$	-1438.325448	-1438.110886	-1438.107288	-1439.078804	-1438.860644
$IP_{Cl}(2a)$	-3471.722329	-3471.295377	-3471.282386	-3475.017991	-3474.578048
$TS_{Cl}(uncat)$	-1438.310957	-1438.095721	-1438.092884	-1439.063141	-1438.845068
$TS_{Cl}(2a)$	-3471.698687	-3471.275025	-3471.260681	-3474.998817	-3474.560811
$IP_{TCA}(uncat)$	-2565.401972	-2565.163174	-2565.156926	-2566.275419	-2566.030373
$TS_{TCA}(uncat)$	-2565.390450	-2565.150917	-2565.145234	-2566.264159	-2566.018943
$2d_{aa}$ C_s	-2356.242028	-2356.059599	-2356.050146	-2358.849266	-2358.657384
$2d_{aa}$ C_2	-2356.242176	-2356.059864	-2356.050464	-2358.849507	-2358.657795
$2d_{as}$	-2356.241488	-2356.059100	-2356.049303	-2358.849116	-2358.656931
$2d_{ss}$	-2356.250239	-2356.059190	-2356.053767	-2358.848538	-2358.652066
2d-F	-2456.264202	-2456.087093	-2456.075591	-2458.877728	-2458.689117
2d-Br	-4930.635637	-4930.461170	-4930.448352	-4933.258430	-4933.071145

Table S21. – *Starting material and product conformers*

	Energies (Ha)				
	E (opt)	**G (opt)**	**G-qh (opt)**	**E (sp)**	**G-qh (sp)**
1k 1	-3552.349602	-3552.134441	-3552.130859	-3553.107610	-3552.888867
1k 2	-3552.340139	-3552.122829	-3552.120101	-3553.096913	-3552.876875
1k 3	-3552.347694	-3552.132204	-3552.128731	-3553.105749	-3552.886786
1k 4	-3552.345284	-3552.129334	-3552.126041	-3553.102214	-3552.882971
1k 5	-3552.348631	-3552.131856	-3552.129023	-3553.105882	-3552.886274
1k 6	-3552.342835	-3552.126177	-3552.123292	-3553.099249	-3552.879706
1k 7	-3552.341024	-3552.123968	-3552.121118	-3553.098766	-3552.878860
1k 8	-3552.345270	-3552.127062	-3552.124525	-3553.102599	-3552.881854
1k 9	-3552.341424	-3552.123633	-3552.121115	-3553.097556	-3552.877247
1k 10	-3552.338915	-3552.121719	-3552.118829	-3553.095400	-3552.875314
1k 11	-3552.339750	-3552.121824	-3552.119351	-3553.096422	-3552.876023

1k 12	-3552.340139	-3552.122829	-3552.120101	-3553.096910	-3552.876872
1k 13	-3552.339750	-3552.121828	-3552.119355	-3553.096421	-3552.876026
3k 1	-1078.003107	-1077.783673	-1077.780394	-1078.747642	-1078.52493
3k 2	-1078.00365	-1077.784834	-1077.781383	-1078.748316	-1078.52605
3k 3	-1078.004291	-1077.785309	-1077.781913	-1078.750116	-1078.52774
3k 4	-1078.005161	-1077.786005	-1077.782736	-1078.750915	-1078.52849
3k 5	-1078.003503	-1077.783251	-1077.780522	-1078.747937	-1078.52496
3k 6	-1078.005080	-1077.785660	-1077.782468	-1078.749839	-1078.52723
3k 7	-1078.002886	-1077.783190	-1077.780074	-1078.748758	-1078.52595
3k 8	-1078.004062	-1077.784577	-1077.781462	-1078.748790	-1078.52619
3k 9	-1078.000578	-1077.778922	-1077.776482	-1078.745884	-1078.52179
3k 10	-1077.996285	-1077.776270	-1077.773407	-1078.740453	-1078.51758
3k 11	-1077.997826	-1077.776618	-1077.773935	-1078.742626	-1078.51874
SM Cl 1	-1438.355099	-1438.138131	-1438.134843	-1439.104987	-1438.884731
SM Cl 2	-1438.352819	-1438.136176	-1438.132757	-1439.102935	-1438.882873
SM Cl 3	-1438.354862	-1438.136916	-1438.134003	-1439.103661	-1438.882802
SM Cl 4	-1438.354204	-1438.136447	-1438.133509	-1439.103351	-1438.882656
SM Cl 5	-1438.353043	-1438.135978	-1438.132596	-1439.102907	-1438.882460
SM Cl 6	-1438.352750	-1438.135472	-1438.132232	-1439.101679	-1438.881161
SM Cl 7	-1438.352484	-1438.133881	-1438.131336	-1439.101090	-1438.879942
SM Cl 8	-1438.350730	-1438.130977	-1438.128611	-1439.100052	-1438.877933
SM Cl 9	-1438.350529	-1438.132376	-1438.129609	-1439.098830	-1438.877910
SM Cl 10	-1438.346536	-1438.127877	-1438.125169	-1439.095915	-1438.874548
SM Cl 11	-1438.347454	-1438.128950	-1438.126160	-1439.095528	-1438.874234
SM Cl 12	-1438.346298	-1438.128144	-1438.125299	-1439.094311	-1438.873312
SM Cl 13	-1438.344664	-1438.125056	-1438.122806	-1439.093324	-1438.871466
SM TCA 1	-2565.452546	-2565.210573	-2565.204218	-2566.321590	-2566.073262
SM TCA 2	-2565.451583	-2565.209240	-2565.203206	-2566.321064	-2566.072687
SM TCA 3	-2565.452862	-2565.208848	-2565.203461	-2566.321230	-2566.071829
SM TCA 4	-2565.450169	-2565.208660	-2565.202090	-2566.319761	-2566.071682
SM TCA 5	-2565.451754	-2565.208442	-2565.202762	-2566.320487	-2566.071495
SM TCA 6	-2565.449840	-2565.209075	-2565.201866	-2566.319271	-2566.071297
SM TCA 7	-2565.451039	-2565.208409	-2565.202371	-2566.319940	-2566.071272
SM TCA 8	-2565.451922	-2565.207890	-2565.202498	-2566.320477	-2566.071053

SM TCA 9	-2565.451867	-2565.208237	-2565.202586	-2566.319886	-2566.070605
SM TCA 10	-2565.451575	-2565.207986	-2565.202434	-2566.319448	-2566.070307
SM TCA 11	-2565.449238	-2565.206793	-2565.200882	-2566.318648	-2566.070292
SM TCA 12	-2565.452287	-2565.207971	-2565.202570	-2566.319860	-2566.070143
SM TCA 13	-2565.450265	-2565.205579	-2565.200497	-2566.318061	-2566.068293
SM TCA 14	-2565.449122	-2565.205836	-2565.200102	-2566.317297	-2566.068277
SM TCA 15	-2565.449624	-2565.205375	-2565.200122	-2566.317239	-2566.067737
SM TCA 16	-2565.449020	-2565.204895	-2565.199666	-2566.316768	-2566.067414
SM TCA 17	-2565.450488	-2565.205095	-2565.200112	-2566.316998	-2566.066622
SM TCA 18	-2565.447862	-2565.203157	-2565.197780	-2566.316399	-2566.066317
SM TCA 19	-2565.446923	-2565.203405	-2565.197655	-2566.315160	-2566.065892
SM TCA 20	-2565.449467	-2565.202916	-2565.198553	-2566.316618	-2566.065704
SM TCA 21	-2565.446408	-2565.201964	-2565.196582	-2566.313927	-2566.064101
SM TCA 22	-2565.445298	-2565.200455	-2565.195433	-2566.313748	-2566.063883
SM TCA 23	-2565.444836	-2565.200389	-2565.194871	-2566.313149	-2566.063184
SM TCA 24	-2565.443789	-2565.201120	-2565.194997	-2566.311557	-2566.062765
SM TCA 25	-2565.441691	-2565.197287	-2565.192180	-2566.307937	-2566.058426

Table S22. – *Tetradentate catalyst, **4a***

Index	Energies (Ha)				
	E (opt)	G (opt)	G-qh (opt)	E (sp)	G-qh (sp)
TS 4a-F epi tetra	-4103.703284	-4102.991767	-4102.974341	-	-
TS 4a-F epi tri	-4103.714953	-4102.998148	-4102.983416	-	-

Table S23. – *Uncoordinated **4f***

Index	Energies (Ha)				
	E (opt)	G (opt)	G-qh (opt)	E (sp)	G-qh (sp)
4f 1	-3064.986424	-3064.490460	-3064.476912	-3068.773763	-3068.264251
4f 2	-3064.987219	-3064.490110	-3064.476928	-3068.773999	-3068.263708
4f 3	-3064.986698	-3064.489846	-3064.476566	-3068.773786	-3068.263654
4f 4	-3064.994152	-3064.492587	-3064.481799	-3068.771678	-3068.259325
4f 5	-3064.992995	-3064.491042	-3064.480778	-3068.771067	-3068.258850
4f 6	-3064.986817	-3064.489007	-3064.476686	-3068.768822	-3068.258691
4f 7	-3064.994705	-3064.493090	-3064.482298	-3068.770990	-3068.258583
4f 8	-3064.994058	-3064.491212	-3064.481279	-3068.771259	-3068.258480
4f 9	-3064.991288	-3064.488805	-3064.478575	-3068.770634	-3068.257921
4f 10	-3064.995184	-3064.491055	-3064.481609	-3068.771466	-3068.257891
4f 11	-3064.995991	-3064.491813	-3064.482275	-3068.771581	-3068.257865
4f 12	-3064.991921	-3064.489612	-3064.479813	-3068.769863	-3068.257755
4f 13	-3064.990429	-3064.489078	-3064.478726	-3068.768912	-3068.257209
4f 14	-3064.990818	-3064.487932	-3064.478080	-3068.769520	-3068.256782
4f 15	-3064.991178	-3064.489268	-3064.479018	-3068.768666	-3068.256506
4f 16	-3064.988637	-3064.487813	-3064.476789	-3068.767538	-3068.255690

Table S24. – ***4f** complexes*

	Energies (Ha)				
	E (opt)	G (opt)	G-qh (opt)	E (sp)	G-qh (sp)
4f-F 1	-3165.019236	-3164.518732	-3164.507896	-3168.805120	-3168.293780
4f-F 2	-3165.014392	-3164.515957	-3164.503978	-3168.803552	-3168.293138

IP 4f-F Cs 1	-3185.082242	-3184.582209	-3184.571139	-3188.943324	-3188.432221
IP 4f-F Cs 2	-3185.079080	-3184.583659	-3184.570500	-3188.940455	-3188.431875
4f-F•H_2O	-3241.469500	-3240.947941	-3240.936300	-3245.274813	-3244.741613
4f-Cl 1	-3525.39086	-3524.89129	-3524.88019	-3529.177920	-3528.667249
4f-Cl 2	-3525.385259	-3524.889117	-3524.876315	-3529.176182	-3528.667238
4f-Br 1	-5639.39259	-5638.89422	-5638.88265	-5643.185958	-5642.676018
4f-Br 2	-5639.38687	-5638.89211	-5638.87873	-5643.183590	-5642.675449

Table S25. – ***4f****-fluoride episulfonium ion pairs*

	Energies (Ha)				
	E (opt)	**G (opt)**	**G-qh (opt)**	**E (sp)**	**G-qh (sp)**
IP 4f-F epi 1	-4142.993600	-4142.255848	-4142.238021	-4147.517967	-4146.762388
IP 4f-F epi 2	-4142.993974	-4142.253725	-4142.237081	-4147.518838	-4146.761945
IP 4f-F epi 3	-4142.986996	-4142.249185	-4142.231444	-4147.517049	-4146.761497
IP 4f-F epi 4	-4142.996868	-4142.253311	-4142.238222	-4147.518733	-4146.760087
IP 4f-F epi 5	-4142.992901	-4142.253274	-4142.236590	-4147.515959	-4146.759648
IP 4f-F epi 6	-4142.988950	-4142.250082	-4142.232630	-4147.515032	-4146.758712
IP 4f-F epi 7	-4142.988601	-4142.248683	-4142.232097	-4147.514225	-4146.757721
IP 4f-F epi 8	-4142.983972	-4142.246189	-4142.228540	-4147.512619	-4146.757187
IP 4f-F epi 9	-4142.980129	-4142.241181	-4142.224249	-4147.510941	-4146.755061
IP 4f-F epi 10	-4142.988032	-4142.246282	-4142.230455	-4147.511781	-4146.754204
IP 4f-F epi 11	-4142.986052	-4142.242718	-4142.228058	-4147.510436	-4146.752442
IP 4f-F epi 12	-4142.983498	-4142.243063	-4142.226290	-4147.508809	-4146.751601

Table S26. – ***4f*** *TSs and enantioselectivity*

Index	Energies (Ha)					
	E (opt)	**G (opt)**	**G-qh (opt)**	**E (sp)**	**G-qh (sp)**	**G-qh 243.15 K (sp)**
TS 4f-F epi major 1	-4142.982972	-4142.240007	-4142.224875	-4147.507966	-4146.749869	-4146.726778
TS 4f-F epi major 2	-4142.976870	-4142.234393	-4142.218967	-4147.506718	-4146.748815	-4146.725767
TS 4f-F epi major 3	-4142.979913	-4142.238243	-4142.222399	-4147.503595	-4146.746081	-4146.723007
TS 4f-F epi major 4	-4142.974862	-4142.231326	-4142.216940	-4147.500783	-4146.742861	-4146.719857
TS 4f-F epi major 5	-4142.974597	-4142.233207	-4142.217164	-4147.499259	-4146.741826	-4146.718677
TS 4f-F epi major 6	-4142.973872	-4142.230443	-4142.215939	-4147.498024	-4146.740091	-4146.717086
TS 4f-F epi major 7	-4142.972144	-4142.229100	-4142.214755	-4147.494836	-4146.737447	-4146.714362
TS 4f-F epi major 8	-4142.964220	-4142.224090	-4142.207050	-4147.494490	-4146.737320	-4146.713977
TS 4f-F epi major 9	-4142.961376	-4142.221118	-4142.204790	-4147.490373	-4146.733787	-4146.710501
TS 4f-F epi minor 1	-4142.971969	-4142.233025	-4142.216508	-4147.503029	-4146.747568	-4146.724197
TS 4f-F epi minor 2	-4142.974176	-4142.231943	-4142.216583	-4147.503648	-4146.746055	-4146.722981
TS 4f-F epi minor 3	-4142.980133	-4142.236252	-4142.221542	-4147.504421	-4146.745830	-4146.722789
TS 4f-F epi minor 4	-4142.969500	-4142.229719	-4142.213057	-4147.502255	-4146.745812	-4146.722557
TS 4f-F epi minor 5	-4142.976723	-4142.233558	-4142.218614	-4147.500221	-4146.742112	-4146.719087
TS 4f-F epi minor 6	-4142.975739	-4142.233099	-4142.217823	-4147.499007	-4146.741091	-4146.718064
TS 4f-F epi minor 7	-4142.966408	-4142.225070	-4142.209160	-4147.495812	-4146.738564	-4146.715339
TS Br 4f 1k	-6617.344967	-6616.606991	-6616.590423	-6621.876134	-6621.121590	-

Table S27. – ***4h****: TSs and enantioselectivity*

Index	Energies (Ha)					
	E (opt)	G (opt)	G-qh (opt)	E (sp)	G-qh (sp)	G-qh 243.15 K (sp)
TS 4h-F epi major 1	-4221.515301	-4220.717951	-4220.702774	-4226.149514	-4225.336987	-4225.313215
TS 4h-F epi major 2	-4221.513746	-4220.714222	-4220.699884	-4226.146899	-4225.333037	-4225.309402
TS 4h-F epi major 3	-4221.512162	-4220.715512	-4220.699979	-4226.145124	-4225.332941	-4225.309148
TS 4h-F epi major 4	-4221.503969	-4220.709103	-4220.692304	-4226.142614	-4225.330949	-4225.307045
TS 4h-F epi major 5	-4221.509583	-4220.710273	-4220.695429	-4226.143581	-4225.329427	-4225.305846
TS 4h-F epi major 6	-4221.503864	-4220.707918	-4220.691489	-4226.141861	-4225.329486	-4225.305697
TS 4h-F epi major 7	-4221.510403	-4220.711598	-4220.696967	-4226.142467	-4225.329031	-4225.305383
TS 4h-F epi minor 1	-4221.512146	-4220.714976	-4220.699766	-4226.146414	-4225.334034	-4225.310226
TS 4h-F epi minor 2	-4221.504642	-4220.710922	-4220.694430	-4226.143989	-4225.333777	-4225.309732
TS 4h-F epi minor 3	-4221.506389	-4220.710996	-4220.694746	-4226.144666	-4225.333023	-4225.309159
TS 4h-F epi minor 4	-4221.504242	-4220.707763	-4220.691809	-4226.141803	-4225.329370	-4225.305593
TS 4h-F epi minor 5	-4221.510668	-4220.710656	-4220.696231	-4226.143123	-4225.328686	-4225.305067
TS 4h-F epi minor 6	-4221.500602	-4220.705226	-4220.689368	-4226.140188	-4225.328954	-4225.305058
TS 4h-F epi minor 7	-4221.496899	-4220.704826	-4220.686655	-4226.138524	-4225.328280	-4225.304133
TS 4h-F epi minor 8	-4221.506543	-4220.706992	-4220.692146	-4226.139923	-4225.325526	-4225.301953
TS 4h-F epi minor 9	-4221.496203	-4220.702901	-4220.685220	-4226.136704	-4225.325721	-4225.301711
TS 4h-F epi minor 10	-4221.492108	-4220.698086	-4220.681046	-4226.132594	-4225.321532	-4225.297565

Table S28. – *Miscellaneous species*

Index	Energies (Ha)				
	E (opt)	**G (opt)**	**G-qh (opt)**	**E (sp)**	**G-qh (sp)**
Br(g)*	-2574.27728	-2574.290436	-2574.290436	-2574.298613	-2574.311769
$Br(CH_2Cl_2)$				-2574.39026	-2574.403416
F(g)*	-99.854602	-99.865742	-99.865742	-99.868379	-99.879519
$F(CH_2Cl_2)$				-99.989411	-100.000551
$F•H_2O$	-176.428994	-176.426887	-176.426888	-176.4606374	-176.4585314
Cl(g)*	-460.266789	-460.278793	-460.278793	-460.281805	-460.293809
$Cl(CH_2Cl_2)$				-460.379998	-460.392002
Cs(g)*	-19.934066	-19.947960	-19.947960	-20.013829	-20.027723
$Cs(CH_2Cl_2)$				-20.110183	-20.124077
(*Z*)-TCA	-1587.435872	-1587.432886	-1587.432227	-1587.572235	-1587.568590
(*E*)-TCA	-1587.434039	-1587.431808	-1587.430707	-1587.571196	-1587.567864
CsBr(g)*	-2594.377610	-2594.400681	-2594.40066	-2594.475060	-2594.498110
$CsBr(CH_2Cl_2)$	-2594.422237	-2594.445944	-2594.445749	-2594.525198	-2594.548710
CsF(g)*	-120.001129	-120.021281	-120.021283	-120.088507	-120.108661
$CsF(CH_2Cl_2)$	-120.040461	-120.061202	-120.061202	-120.135181	-120.155922

* Evaluated at 1M concentration

Computation – Coordinates and MD Input Files

Coordinates for DFT stationary points and MD input files are available as part of the supporting information, and are uploaded separately.

Copies of NMR-spectra

Achiral Catalysts

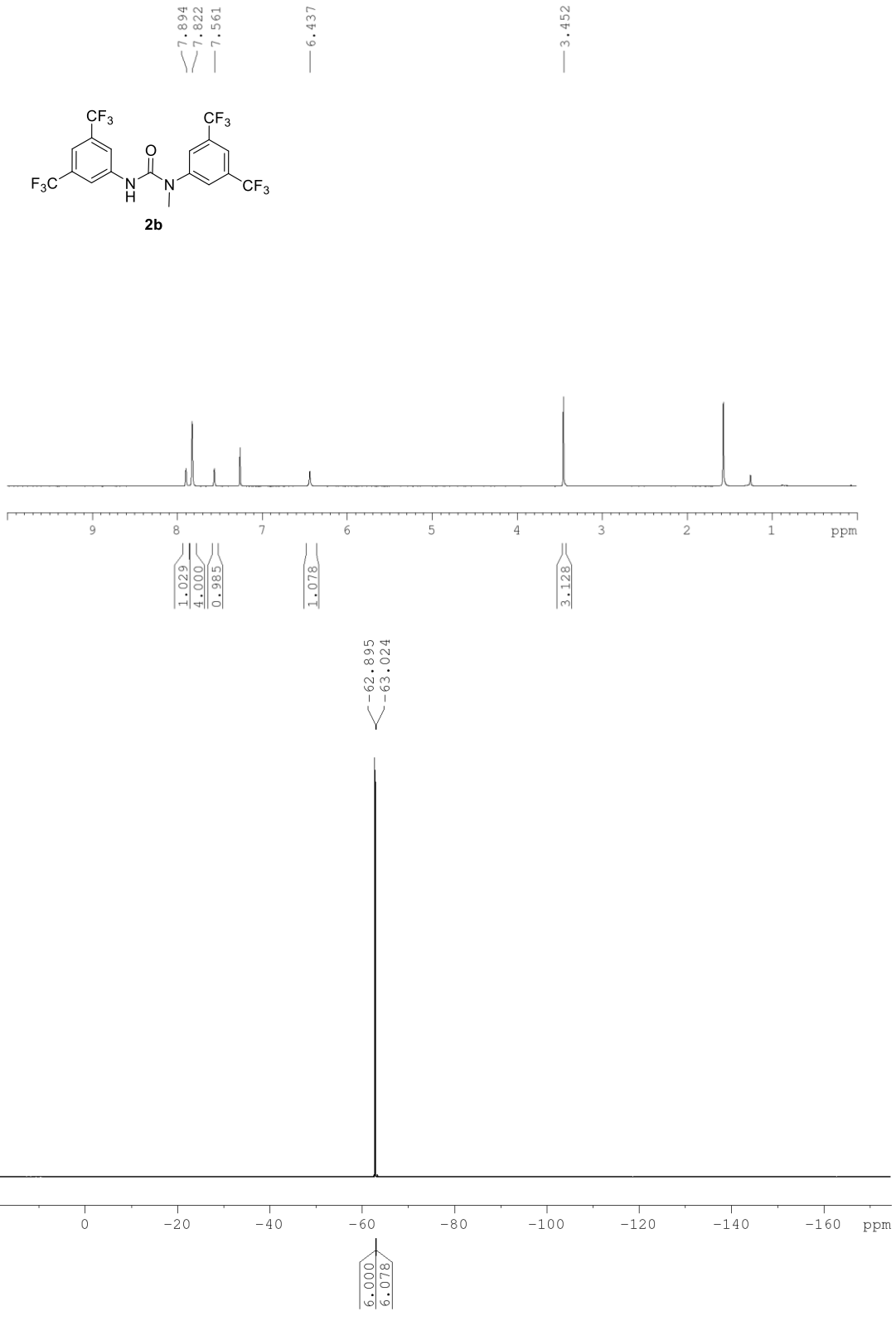

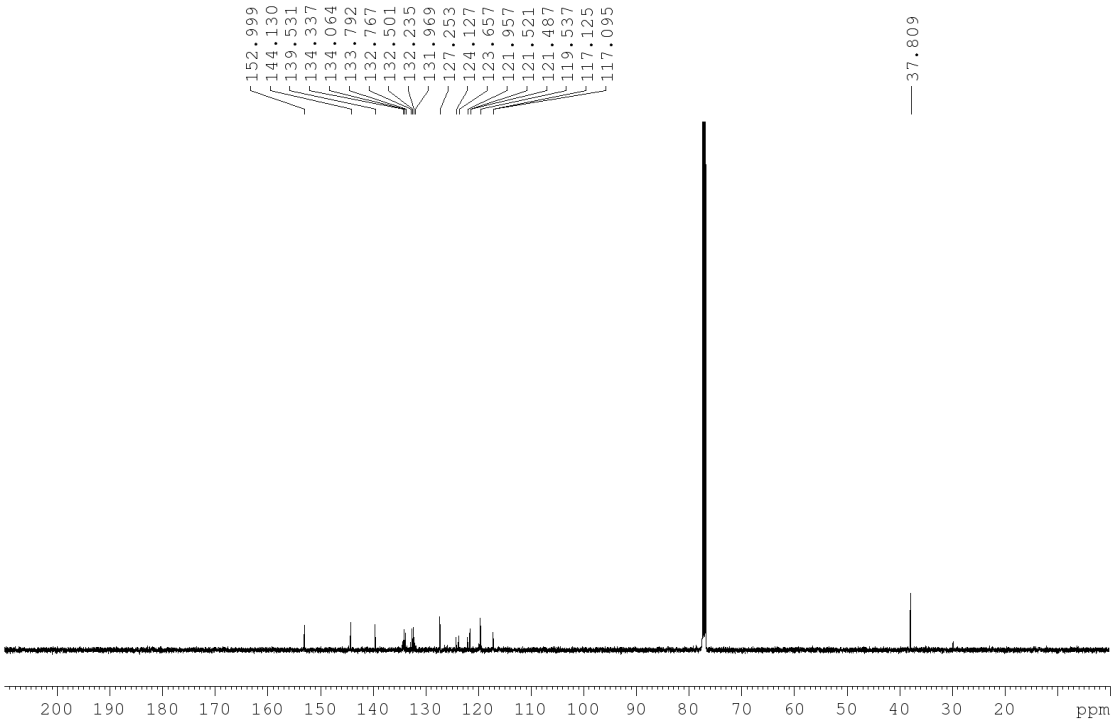
152.999
144.130
139.531
134.337
134.064
133.792
132.767
132.501
132.235
131.969
127.253
124.127
123.657
121.957
121.521
121.487
119.537
117.125
117.095
37.809
200 190 180 170 160 150 140 130 120 110 100 90 80 70 60 50 40 30 20 ppm

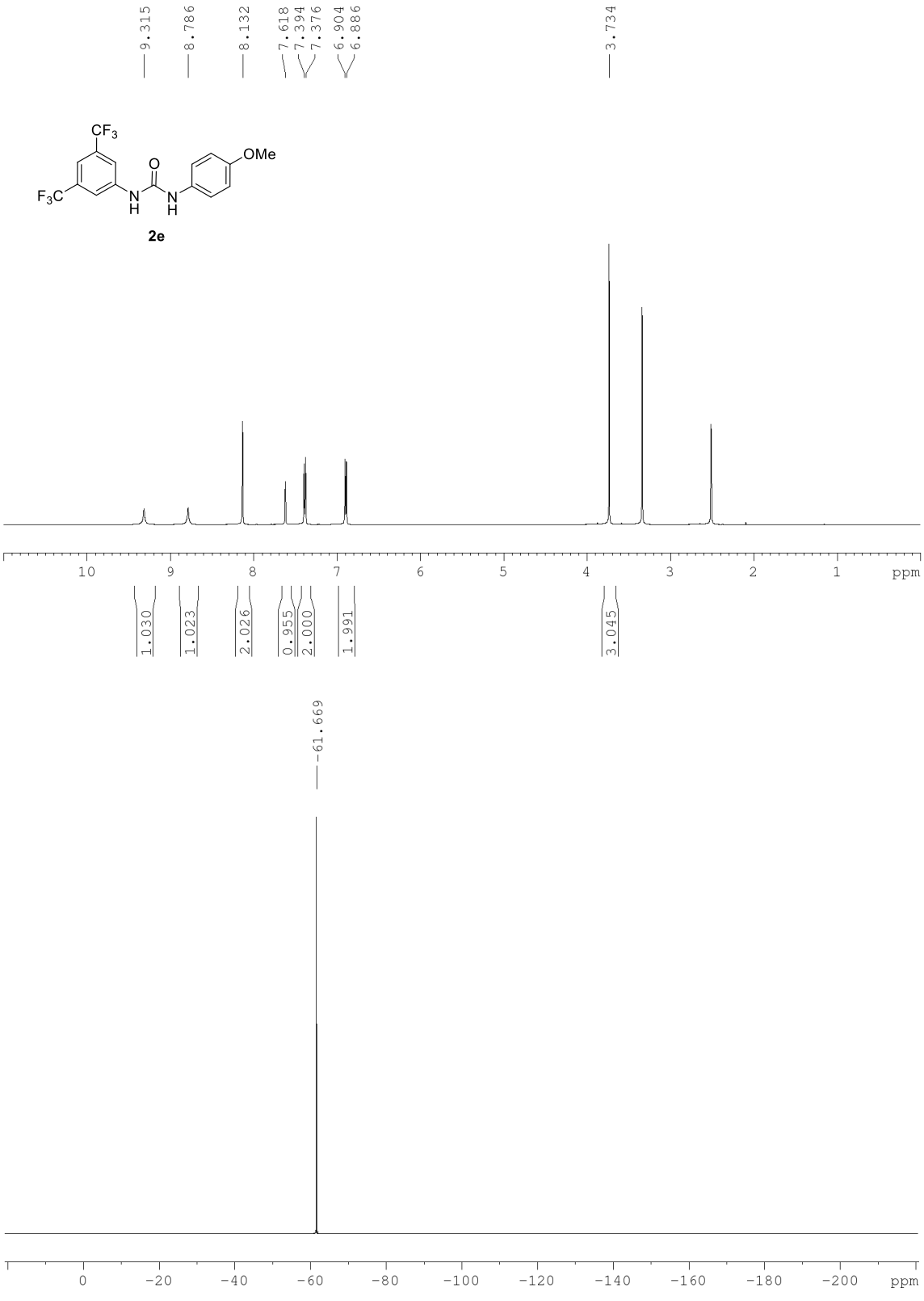
9.315
8.786
8.132
7.618
7.394
7.376
6.904
6.886
3.734
CF3
F3C
O
N
H
N
H
OMe
2e
10
9
8
7
6
5
4
3
2
1
ppm
1.030
1.023
2.026
0.955
2.000
1.991
3.045
-61.669
0
-20
-40
-60
-80
-100
-120
-140
-160
-180
-200
ppm

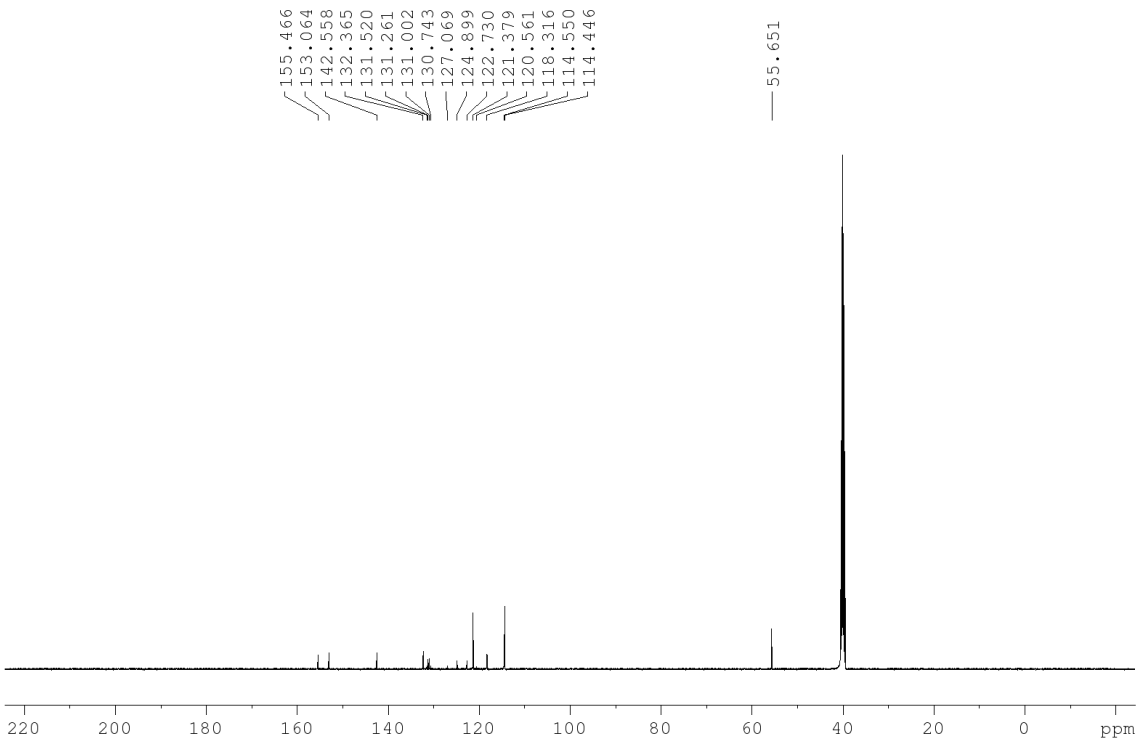
155.466
153.064
142.558
132.365
131.520
131.261
131.002
130.743
127.069
124.899
122.730
121.379
120.561
118.316
114.550
114.446
55.651
220
200
180
160
140
120
100
80
60
40
20
0
ppm

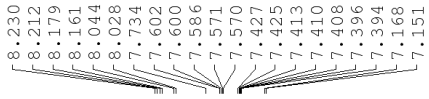
8.230
8.212
8.179
8.161
8.044
8.028
7.734
7.602
7.600
7.586
7.571
7.570
7.427
7.425
7.413
7.410
7.408
7.396
7.394
7.168
7.151

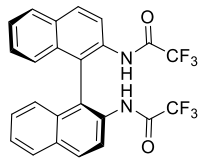
O
N
H
H
N
CF3
CF3
O

5a

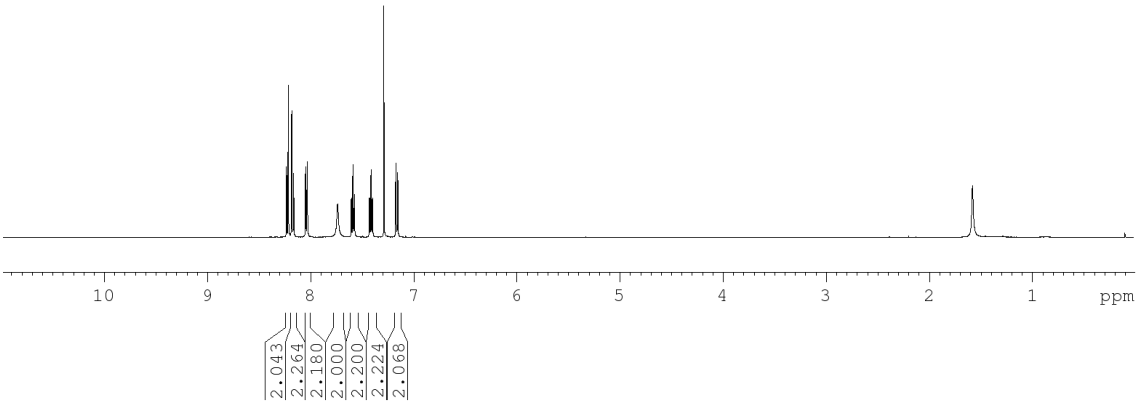
10
9
8
7
6
5
4
3
2
1
ppm
2.043
2.264
2.180
2.000
2.200
2.224
2.068

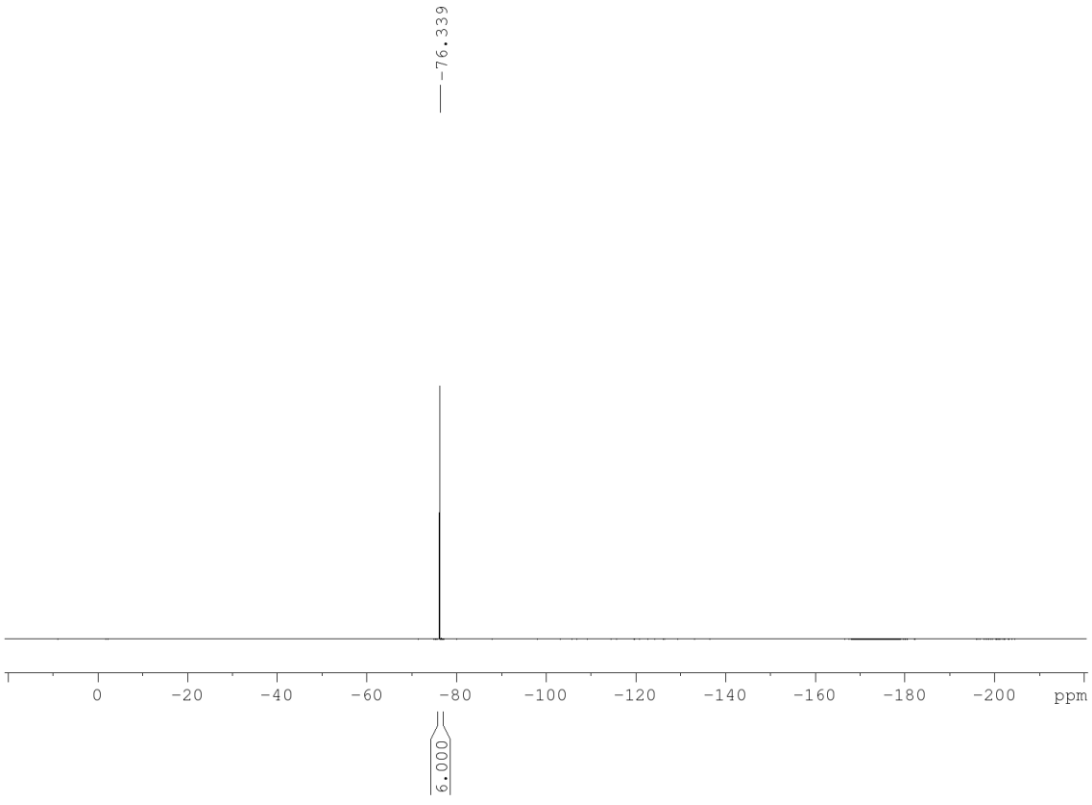
-76.339
0
-20
-40
-60
-80
-100
-120
-140
-160
-180
-200
ppm
6.000

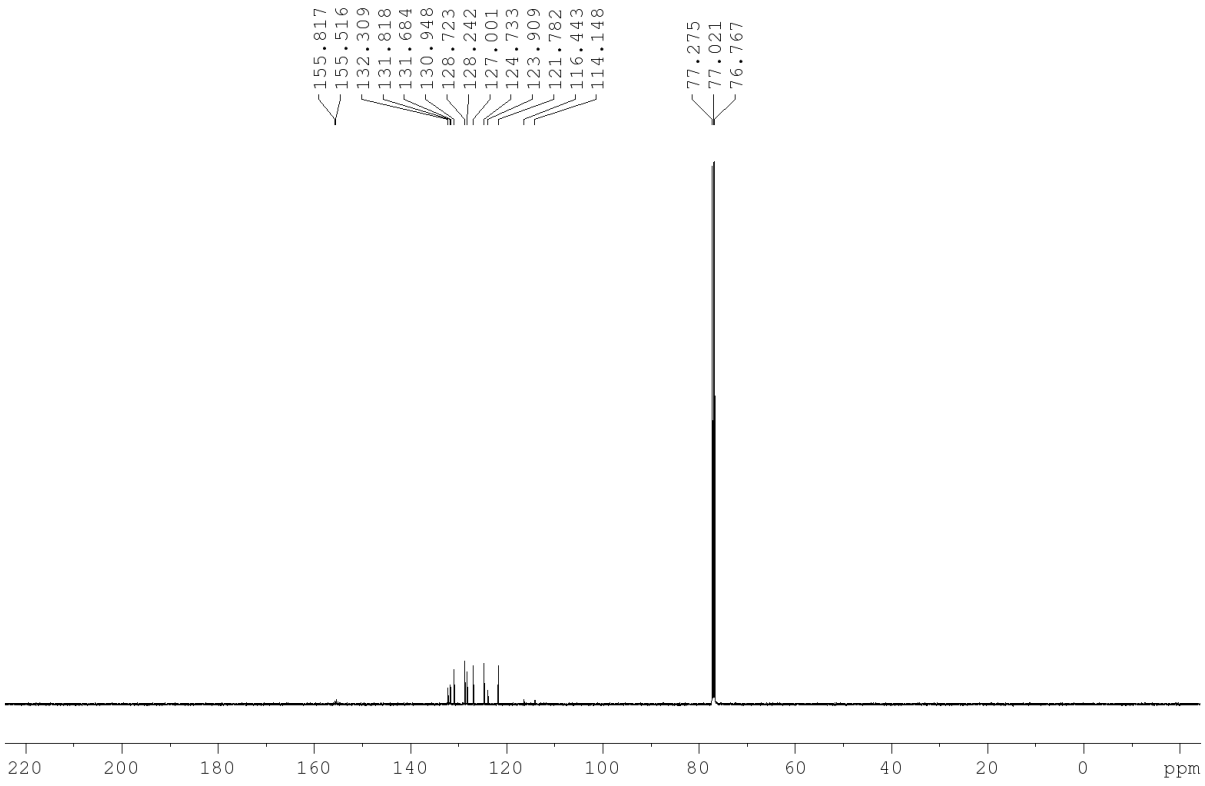
155.817
155.516
132.309
131.818
131.684
130.948
128.723
128.242
127.001
124.733
123.909
121.782
116.443
114.148
77.275
77.021
76.767
220
200
180
160
140
120
100
80
60
40
20
0
ppm

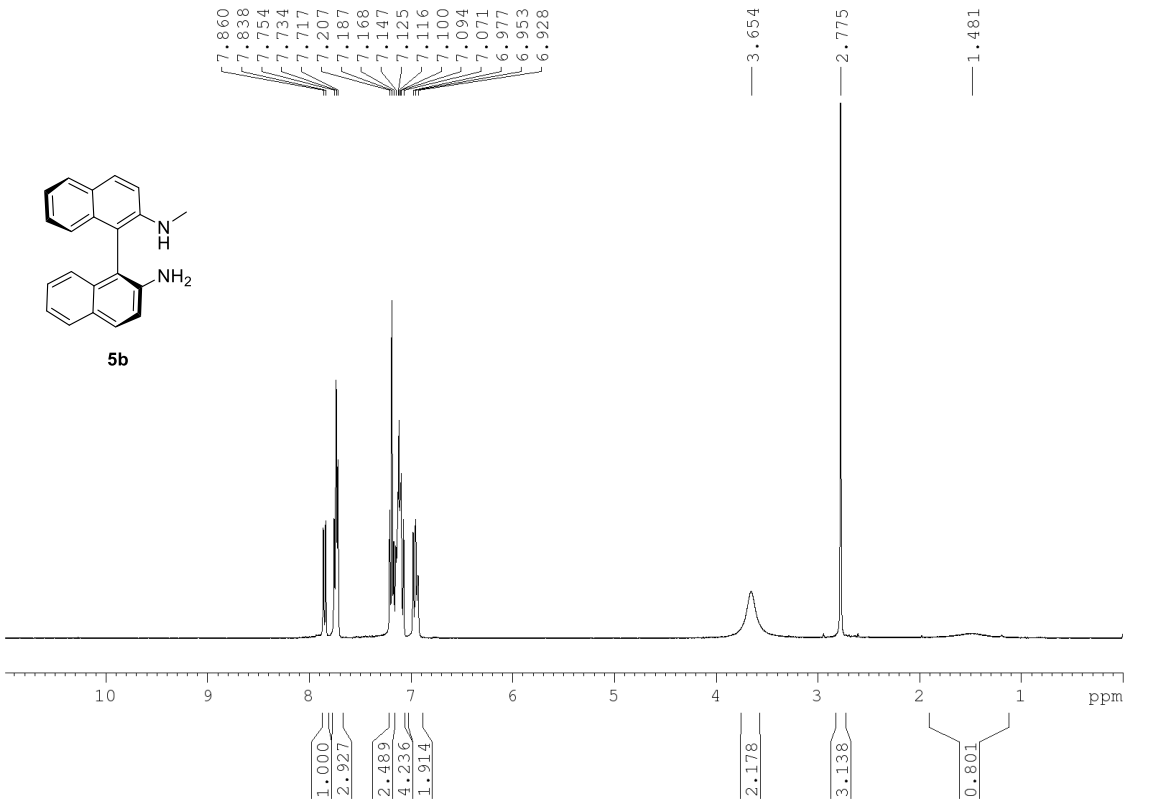
7.860
7.838
7.754
7.734
7.717
7.207
7.187
7.168
7.147
7.125
7.116
7.100
7.094
7.071
6.977
6.953
6.928
3.654
2.775
1.481
N
H
NH2
5b
10
9
8
7
6
5
4
3
2
1
ppm
1.000
2.927
2.489
4.236
1.914
2.178
3.138
0.801

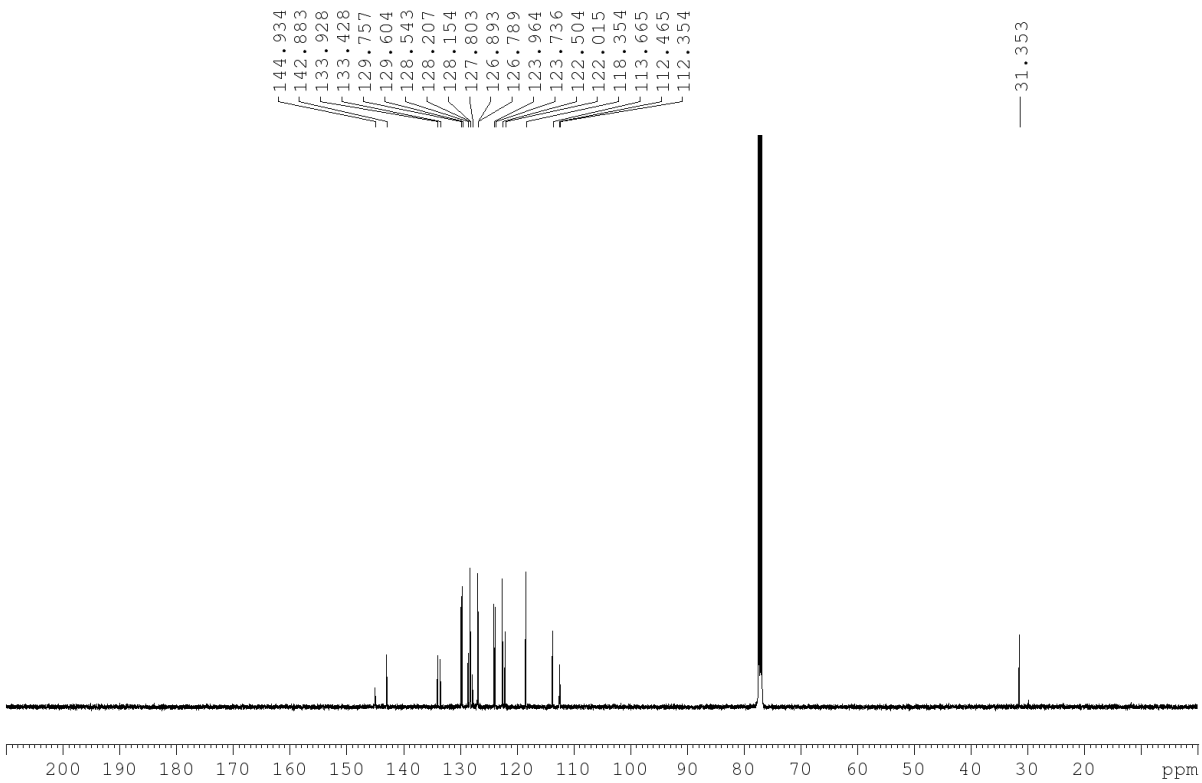
144.934
142.883
133.928
133.428
129.757
129.604
128.543
128.207
128.154
127.803
126.893
126.789
123.964
123.736
122.504
122.015
118.354
113.665
112.465
112.354
31.353
200
190
180
170
160
150
140
130
120
110
100
90
80
70
60
50
40
30
20
ppm

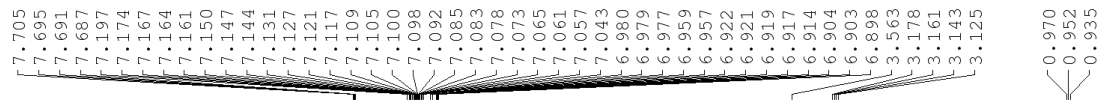
7.705
7.695
7.691
7.687
7.197
7.174
7.167
7.164
7.161
7.150
7.147
7.144
7.131
7.127
7.121
7.117
7.109
7.105
7.100
7.098
7.092
7.085
7.083
7.078
7.073
7.065
7.061
7.057
7.043
6.980
6.979
6.977
6.959
6.957
6.922
6.921
6.919
6.917
6.914
6.904
6.903
6.898
3.563
3.178
3.161
3.143
3.125
0.970
0.952
0.935

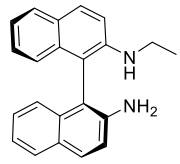
N
H
NH2

5c

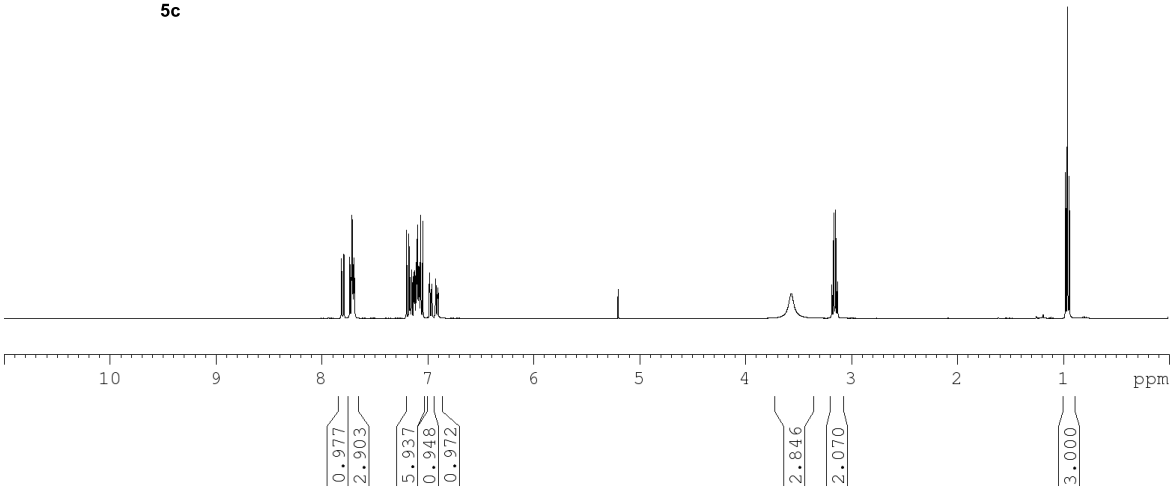
10
9
8
7
6
5
4
3
2
1
ppm
0.977
2.903
5.937
0.948
0.972
2.846
2.070
3.000

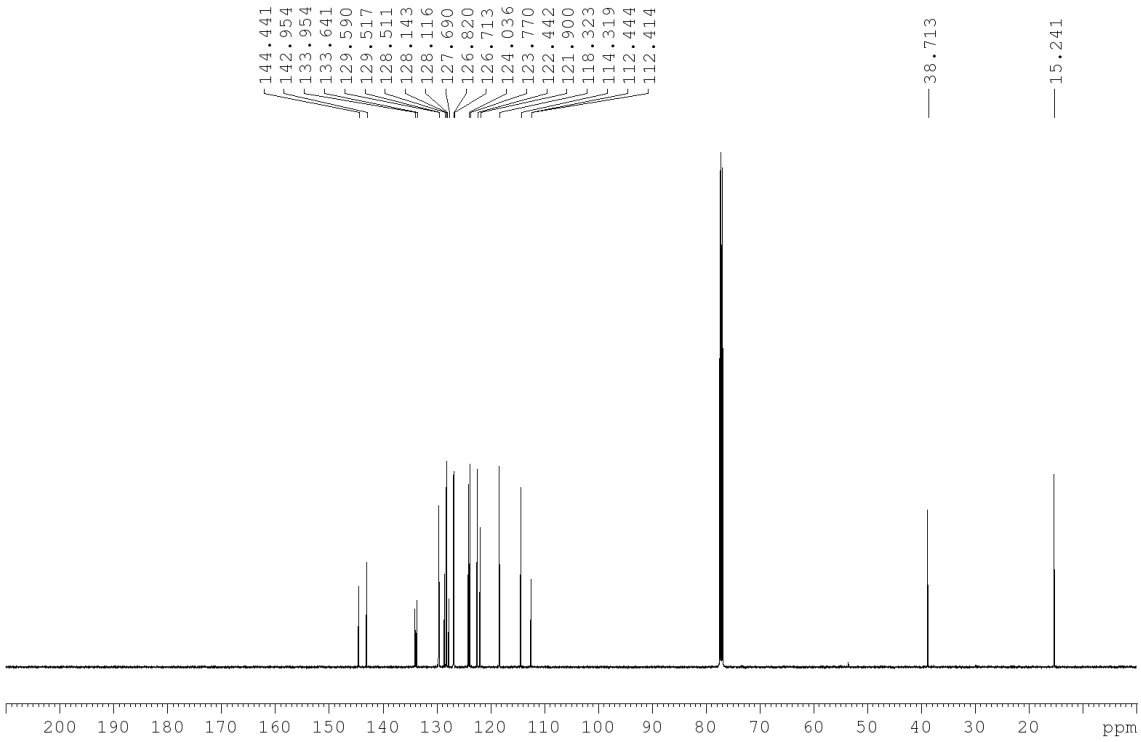
144.441
142.954
133.954
133.641
129.590
129.517
128.511
128.143
128.116
127.690
126.820
126.713
124.036
123.770
122.442
121.900
118.323
114.319
112.444
112.414
38.713
15.241
200
190
180
170
160
150
140
130
120
110
100
90
80
70
60
50
40
30
20
ppm

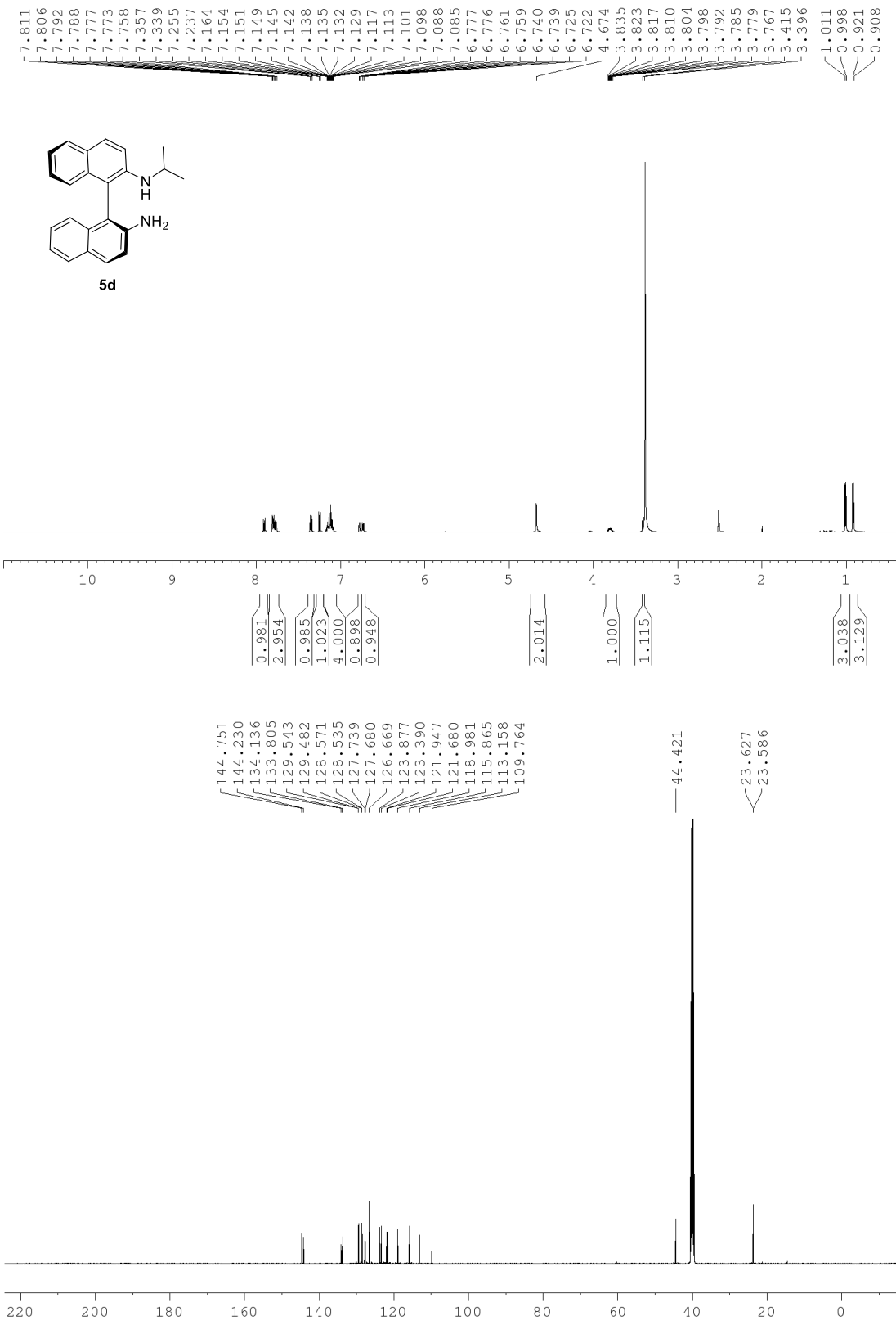
7.811
7.806
7.792
7.788
7.777
7.773
7.758
7.357
7.339
7.255
7.237
7.164
7.154
7.151
7.149
7.145
7.142
7.138
7.135
7.132
7.129
7.117
7.113
7.101
7.098
7.088
7.085
6.777
6.776
6.761
6.759
6.740
6.739
6.725
6.722
4.674
3.835
3.823
3.817
3.810
3.804
3.798
3.792
3.785
3.779
3.767
3.415
3.396
1.011
0.998
0.921
0.908
NH
NH2
5d
10
9
8
7
6
5
4
3
2
1
ppm
0.981
2.954
0.985
1.023
4.000
0.898
0.948
2.014
1.000
1.115
3.038
3.129
144.751
144.230
134.136
133.805
129.543
129.482
128.571
128.535
127.739
127.680
126.669
123.877
123.390
121.947
121.680
118.981
115.865
113.158
109.764
44.421
23.627
23.586
220
200
180
160
140
120
100
80
60
40
20
0
ppm

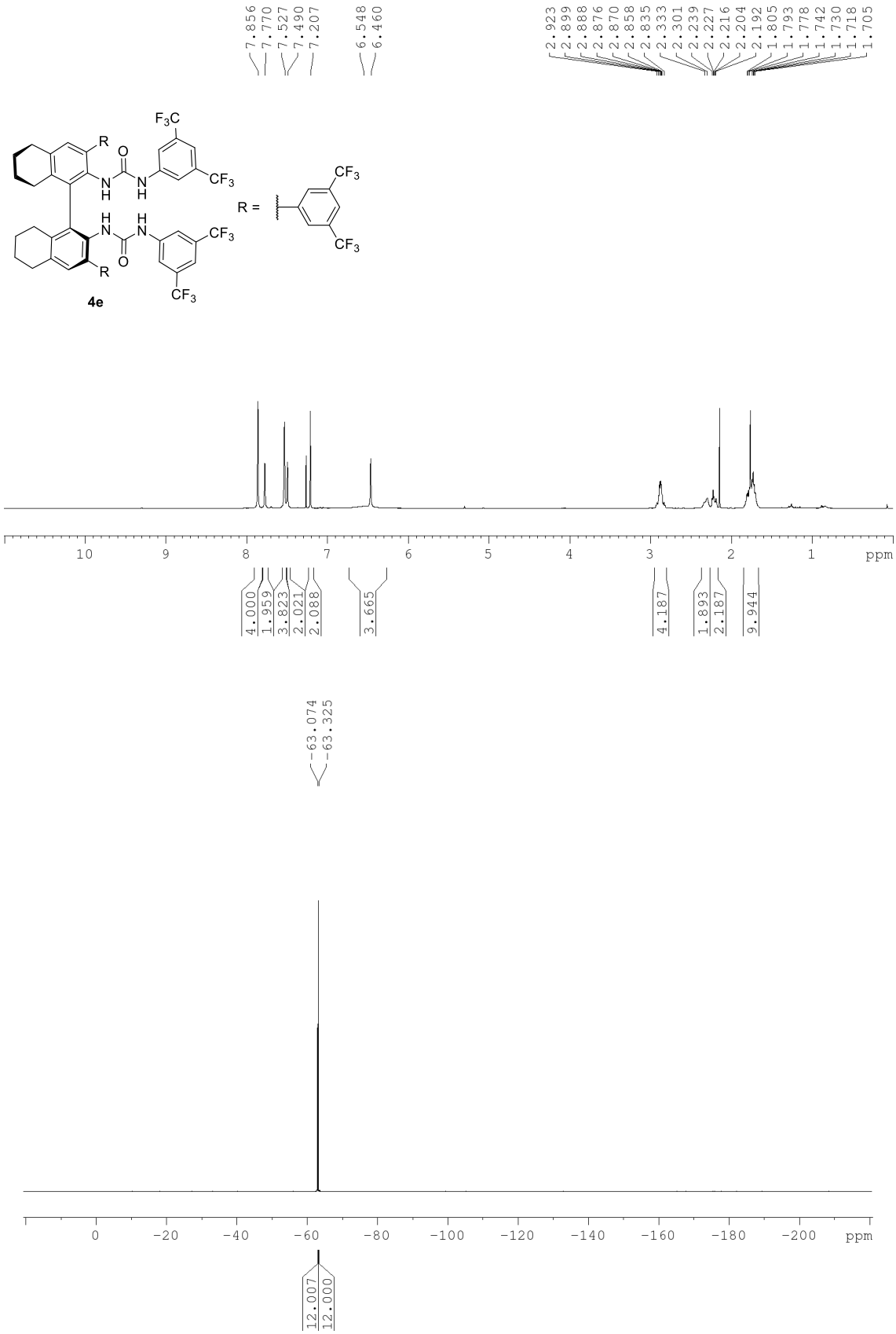
7.856
7.770
7.527
7.490
7.207
6.548
6.460
2.923
2.899
2.888
2.876
2.870
2.858
2.835
2.333
2.301
2.239
2.227
2.216
2.204
2.192
1.805
1.793
1.778
1.742
1.730
1.718
1.705
F3C
CF3
R
O
N
H
R =
4e
10
9
8
7
6
5
4
3
2
1
ppm
4.000
1.959
3.823
2.021
2.088
3.665
4.187
1.893
2.187
9.944
-63.074
-63.325
0
-20
-40
-60
-80
-100
-120
-140
-160
-180
-200
ppm
12.007
12.000

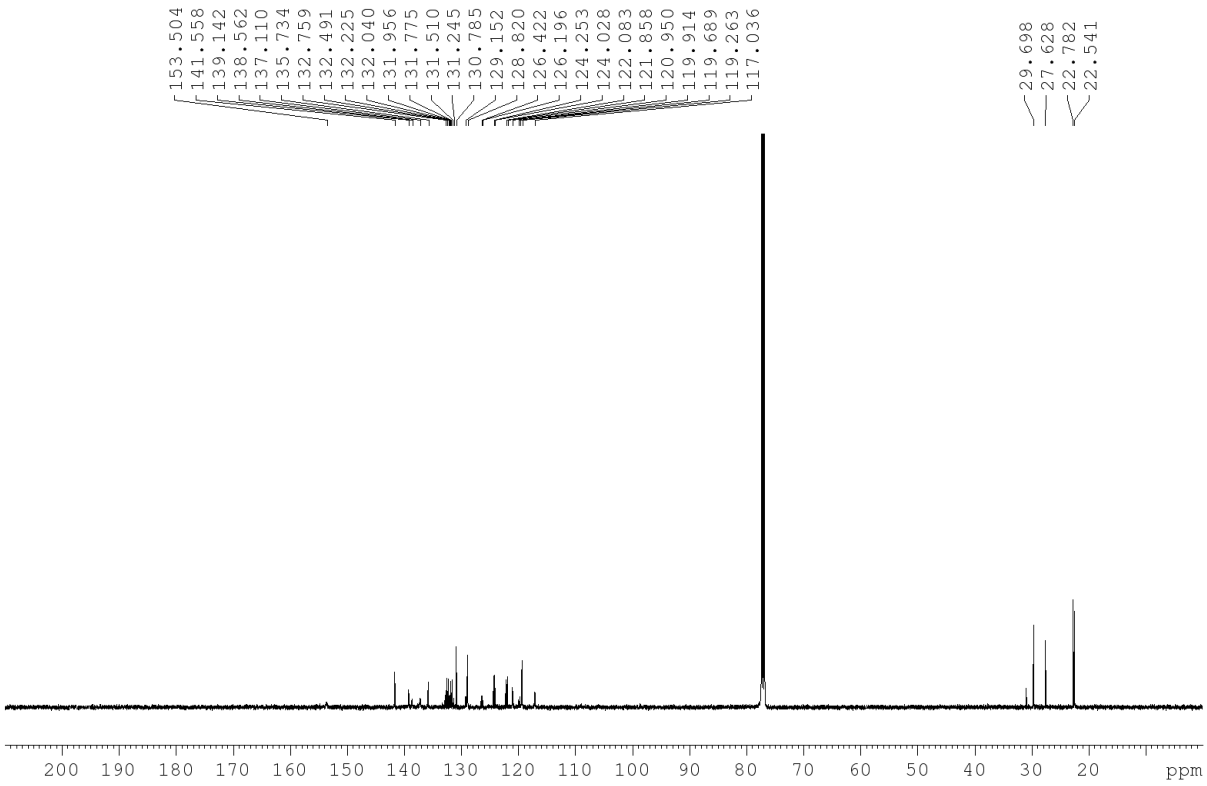
153.504
141.558
139.142
138.562
137.110
135.734
132.759
132.491
132.225
132.040
131.956
131.775
131.510
131.245
130.785
129.152
128.820
126.422
126.196
124.253
124.028
122.083
121.858
120.950
119.914
119.689
119.263
117.036
29.698
27.628
22.782
22.541
200 190 180 170 160 150 140 130 120 110 100 90 80 70 60 50 40 30 20 ppm

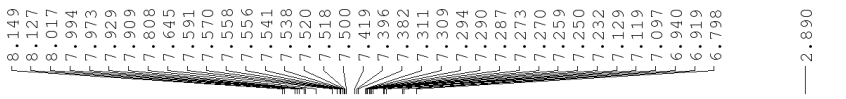
8.149
8.127
8.017
7.994
7.973
7.929
7.909
7.808
7.645
7.591
7.570
7.558
7.556
7.541
7.538
7.520
7.518
7.500
7.419
7.396
7.382
7.311
7.309
7.294
7.290
7.287
7.273
7.270
7.259
7.250
7.232
7.129
7.119
7.097
6.940
6.919
6.798
2.890

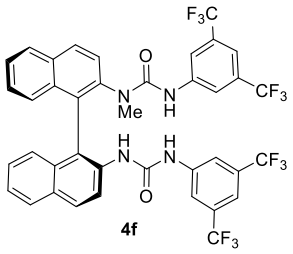
F3C
O
N
Me
N
H
CF3
H
N
H
N
CF3
O
CF3

4f

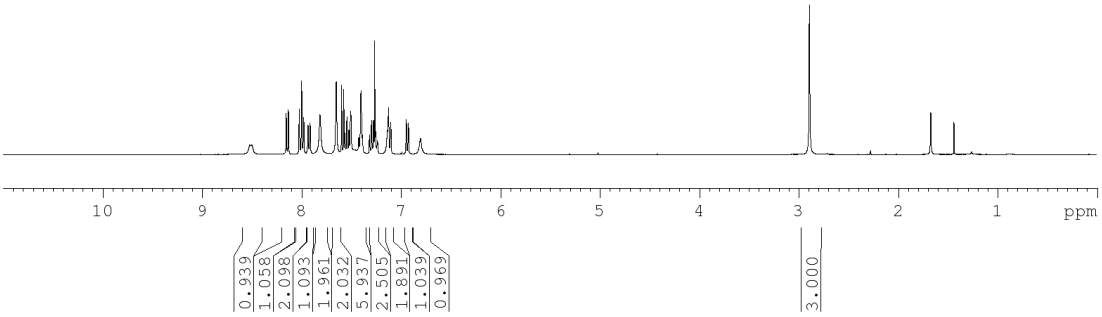
10
9
8
7
6
5
4
3
2
1
ppm
0.939
1.058
2.098
1.093
1.961
2.032
5.937
2.505
1.891
1.039
0.969
3.000

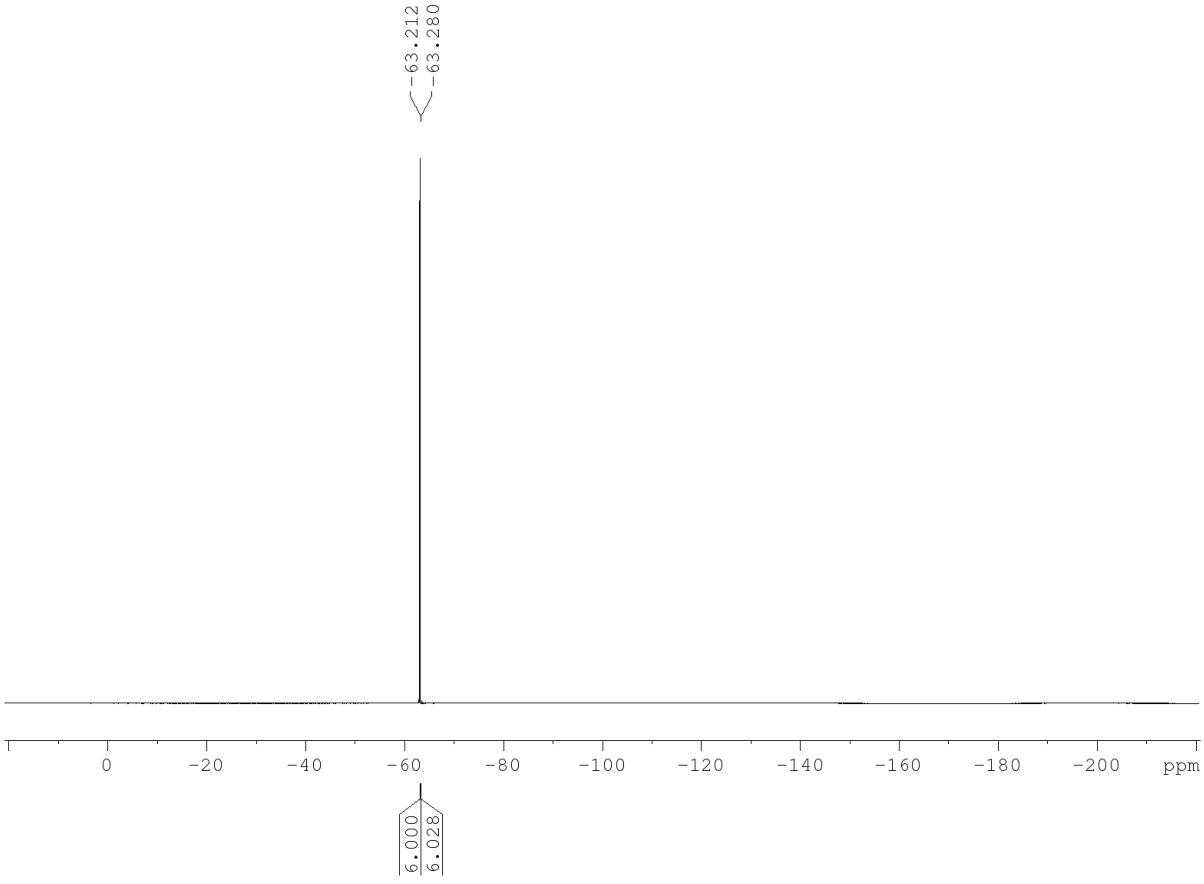
-63.212
-63.280
0
-20
-40
-60
-80
-100
-120
-140
-160
-180
-200
ppm
6.000
6.028

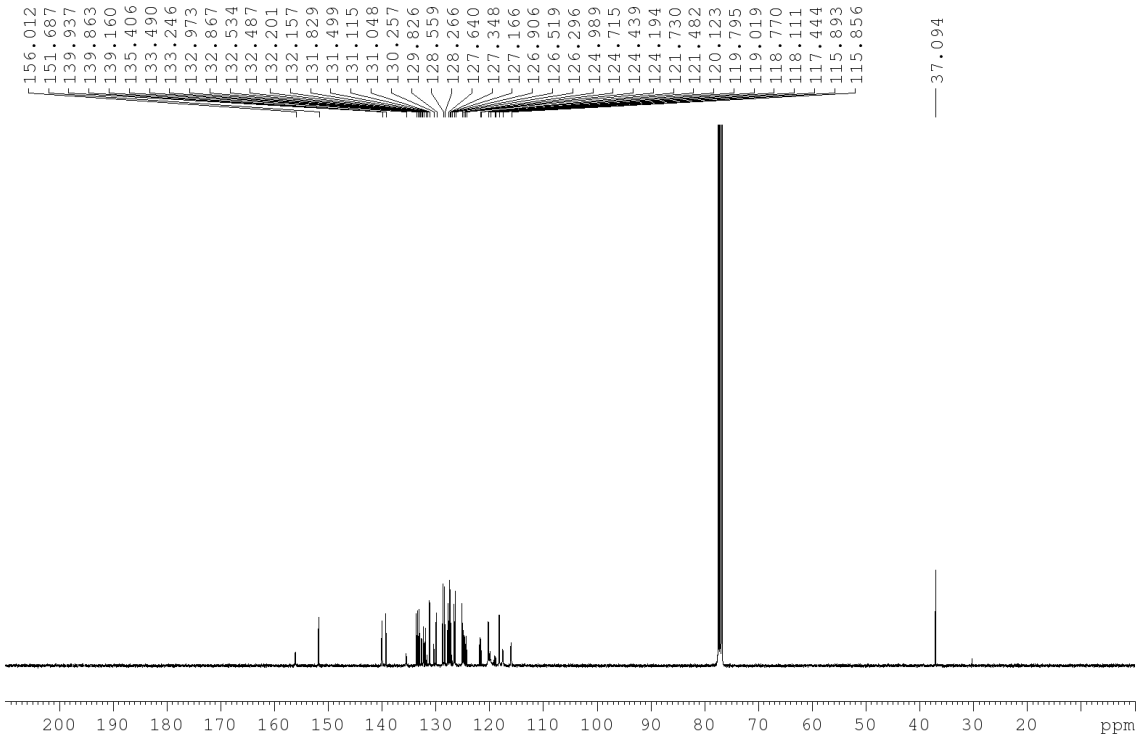
156.012
151.687
139.937
139.863
139.160
135.406
133.490
133.246
132.973
132.867
132.534
132.487
132.201
132.157
131.829
131.499
131.115
131.048
130.257
129.826
128.559
128.266
127.640
127.348
127.166
126.906
126.519
126.296
124.989
124.715
124.439
124.194
121.730
121.482
120.123
119.795
119.019
118.770
118.111
117.444
115.893
115.856
37.094
200 190 180 170 160 150 140 130 120 110 100 90 80 70 60 50 40 30 20 ppm

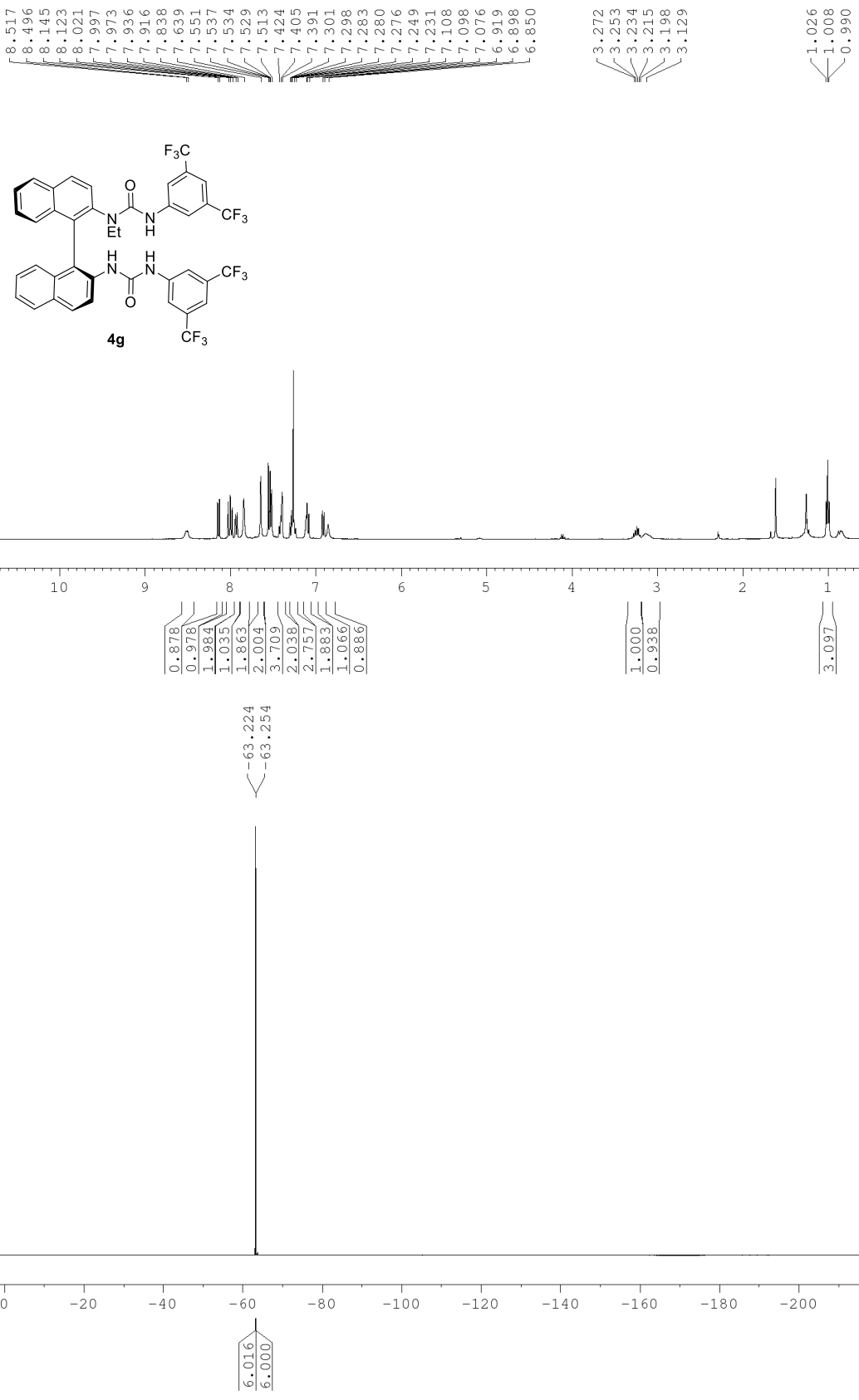
8.517
8.496
8.145
8.123
8.021
7.997
7.973
7.936
7.916
7.838
7.639
7.551
7.537
7.534
7.529
7.513
7.424
7.405
7.391
7.301
7.298
7.283
7.280
7.276
7.249
7.231
7.108
7.098
7.076
6.919
6.898
6.850
3.272
3.253
3.234
3.215
3.198
3.129
1.026
1.008
0.990
F3C
CF3
CF3
CF3
Et
4g
10
9
8
7
6
5
4
3
2
1
ppm
0.878
0.978
1.984
1.035
1.863
2.004
3.709
2.038
2.757
1.883
1.066
0.886
1.000
0.938
3.097
-63.224
-63.254
0
-20
-40
-60
-80
-100
-120
-140
-160
-180
-200
ppm
6.016
6.000

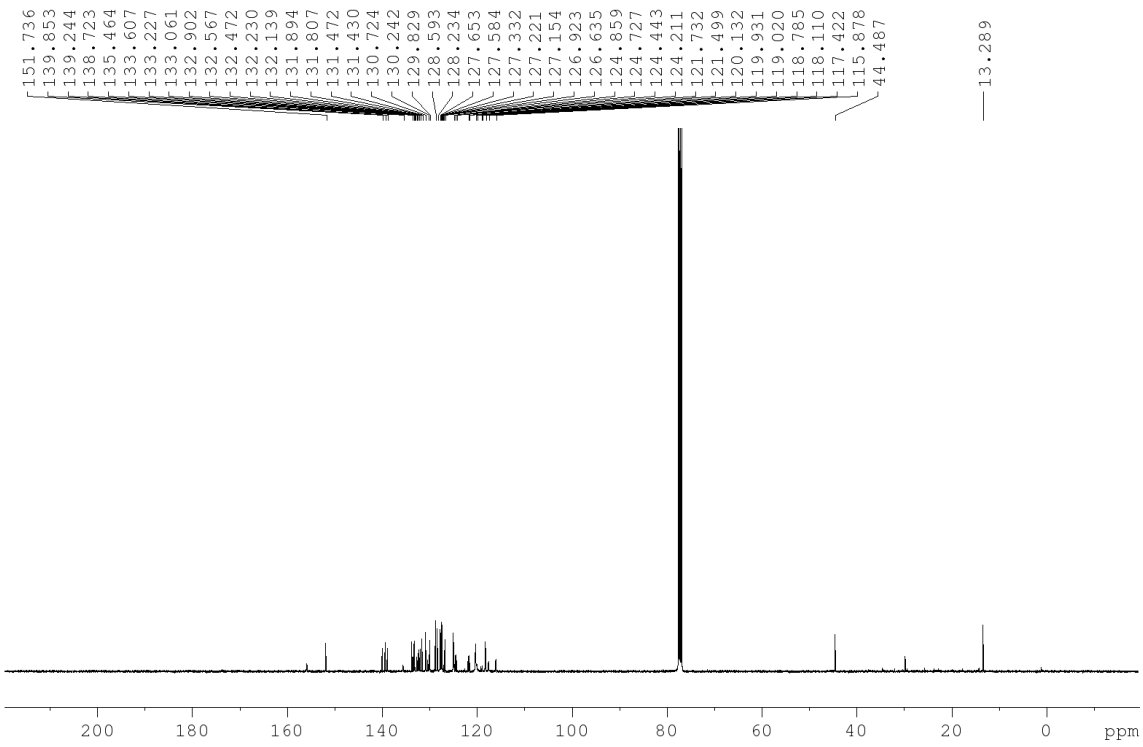
151.736
139.853
139.244
138.723
135.464
133.607
133.227
133.061
132.902
132.567
132.472
132.230
132.139
131.894
131.807
131.472
131.430
130.724
130.242
129.829
128.593
128.234
127.653
127.584
127.332
127.221
127.154
126.923
126.635
124.859
124.727
124.443
124.211
121.732
121.499
120.132
119.931
119.020
118.785
118.110
117.422
115.878
44.487
13.289
200
180
160
140
120
100
80
60
40
20
0
ppm

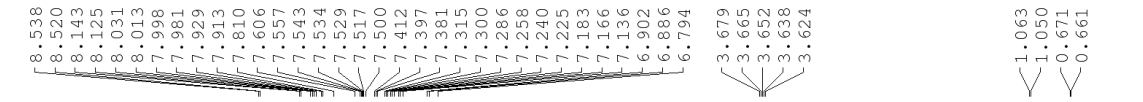
8.538
8.520
8.143
8.125
8.031
8.013
7.998
7.981
7.929
7.913
7.810
7.606
7.557
7.543
7.534
7.529
7.517
7.500
7.412
7.397
7.381
7.315
7.300
7.286
7.258
7.240
7.225
7.183
7.166
7.136
6.902
6.886
6.794
3.679
3.665
3.652
3.638
3.624
1.063
1.050
0.671
0.661

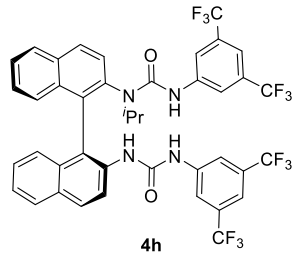
F3C
O
N
iPr
N
H
CF3
H
N
H
N
CF3
O
CF3

4h

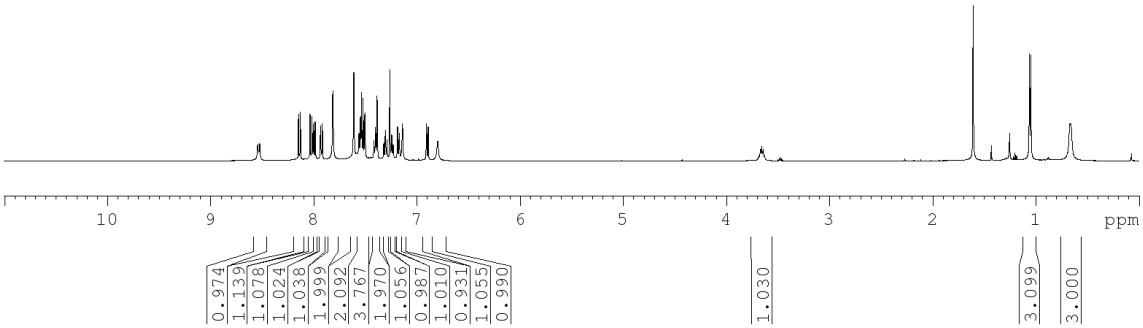
10
9
8
7
6
5
4
3
2
1
ppm
0.974
1.139
1.078
1.024
1.038
1.999
2.092
3.767
1.970
1.056
0.987
1.010
0.931
1.055
0.990
1.030
3.099
3.000

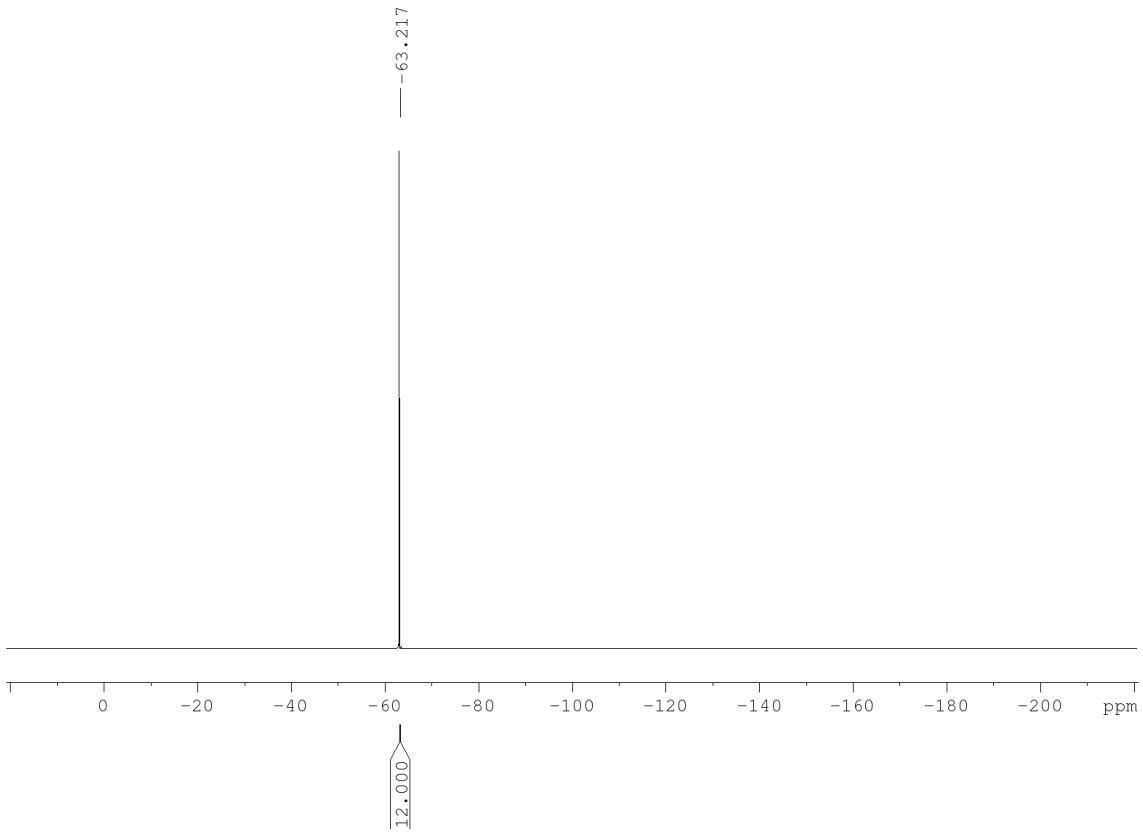
-63.217
0
-20
-40
-60
-80
-100
-120
-140
-160
-180
-200
ppm
12.000

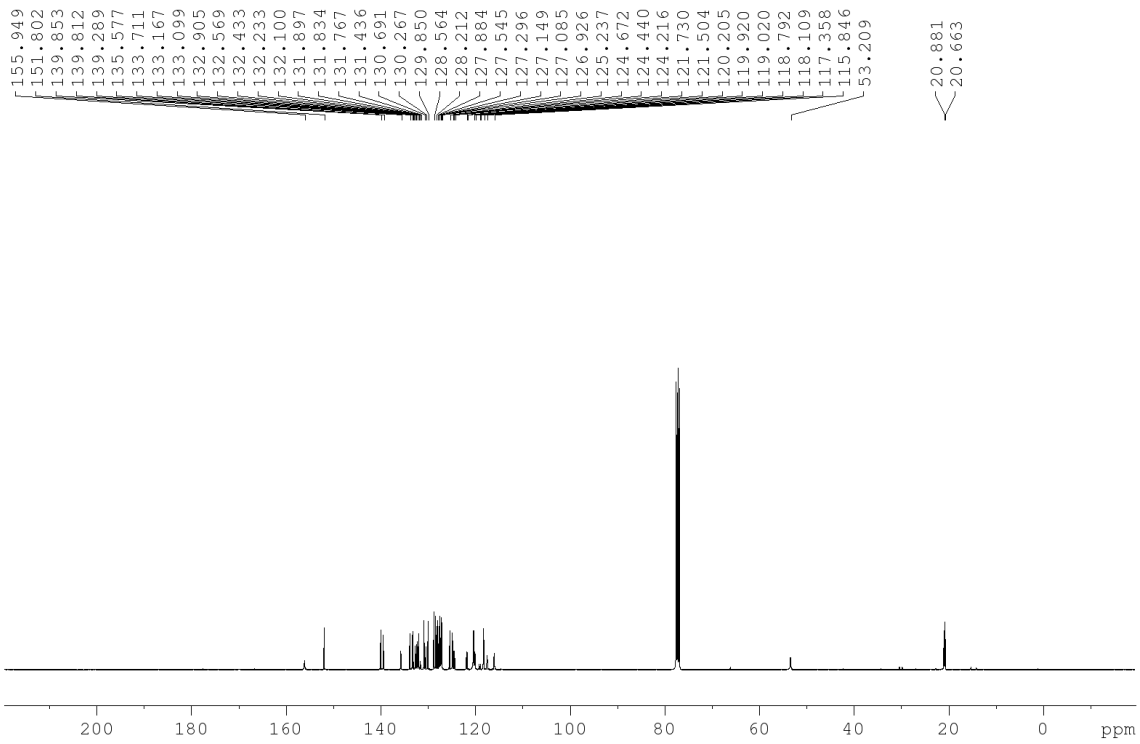
155.949
151.802
139.853
139.812
139.289
135.577
133.711
133.167
133.099
132.905
132.569
132.433
132.233
132.100
131.897
131.834
131.767
131.436
130.691
130.267
129.850
128.564
128.212
127.884
127.545
127.296
127.149
127.085
126.926
125.237
124.672
124.440
124.216
121.730
121.504
120.205
119.920
119.020
118.792
118.109
117.358
115.846
53.209
20.881
20.663
200
180
160
140
120
100
80
60
40
20
0
ppm

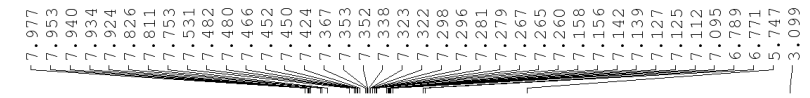
7.977
7.953
7.940
7.934
7.924
7.826
7.811
7.753
7.531
7.482
7.480
7.466
7.452
7.450
7.424
7.367
7.353
7.352
7.338
7.323
7.322
7.298
7.296
7.281
7.279
7.267
7.265
7.260
7.158
7.156
7.142
7.139
7.127
7.125
7.112
7.095
6.789
6.771
5.747
3.099

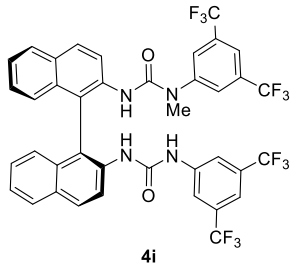
F3C
O
N
H
N
Me
CF3
H
N
H
N
O
CF3
CF3

4i

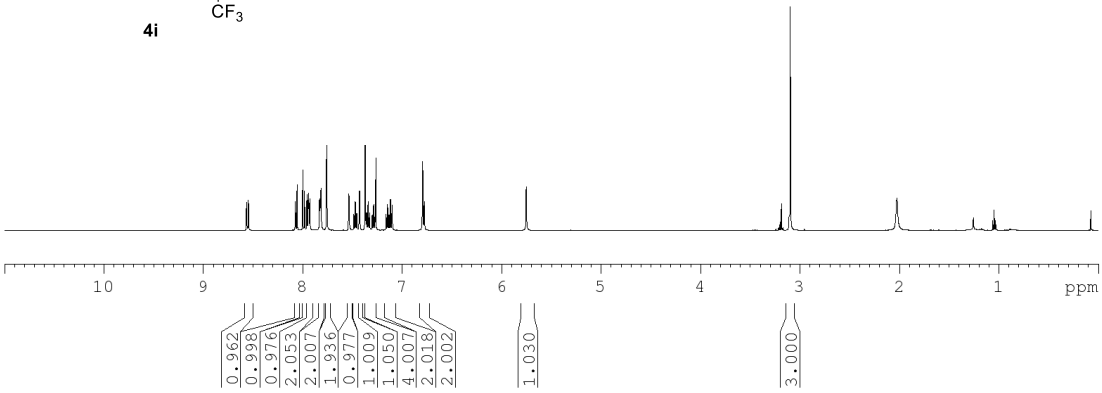
10
9
8
7
6
5
4
3
2
1
ppm
0.962
0.998
0.976
2.053
2.007
1.936
0.977
1.009
1.050
4.007
2.018
2.002
1.030
3.000

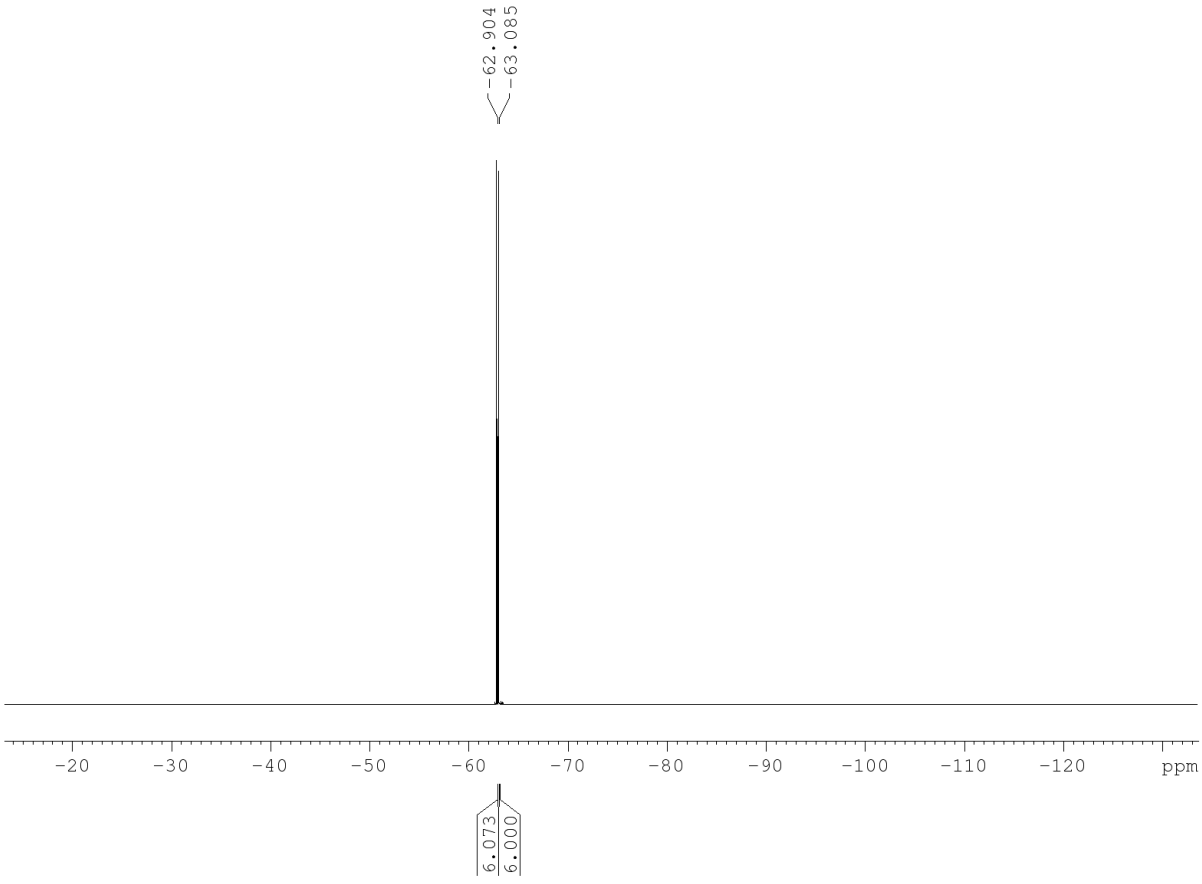
-62.904
-63.085
-20
-30
-40
-50
-60
-70
-80
-90
-100
-110
-120
ppm
6.073
6.000

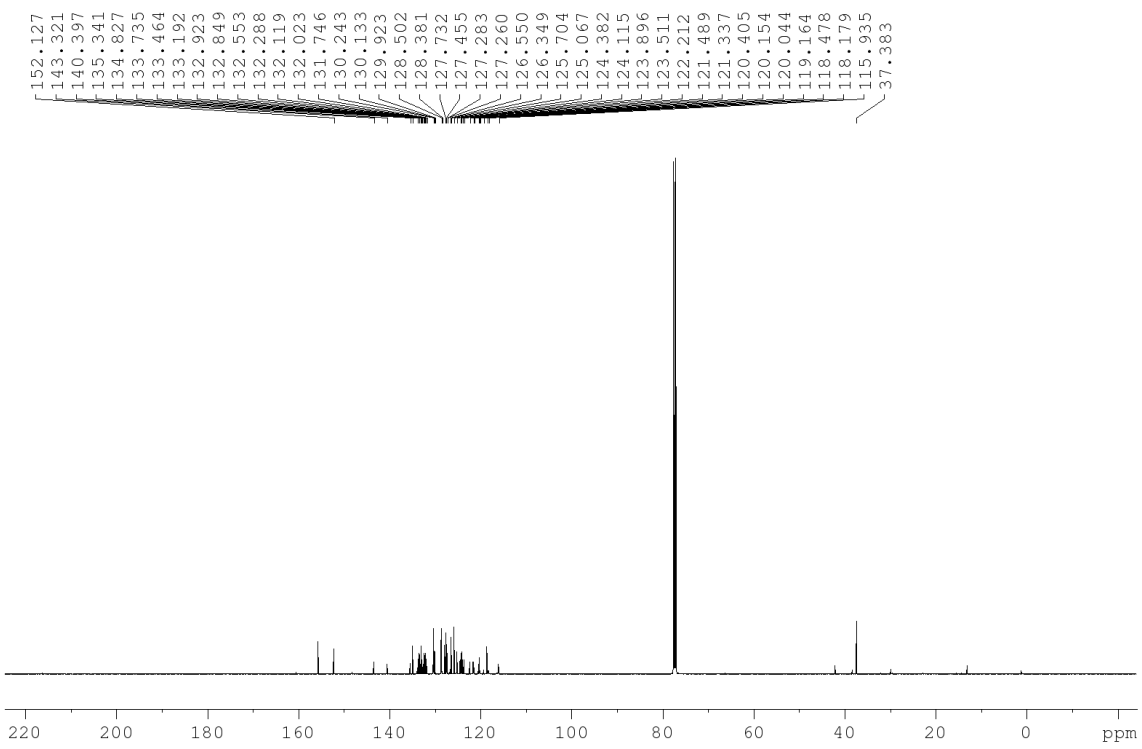
152.127
143.321
140.397
135.341
134.827
133.735
133.464
133.192
132.923
132.849
132.553
132.288
132.119
132.023
131.746
130.243
130.133
129.923
128.502
128.381
127.732
127.455
127.283
127.260
126.550
126.349
125.704
125.067
124.382
124.115
123.896
123.511
122.212
121.489
121.337
120.405
120.154
120.044
119.164
118.478
118.179
115.935
37.383
220
200
180
160
140
120
100
80
60
40
20
0
ppm

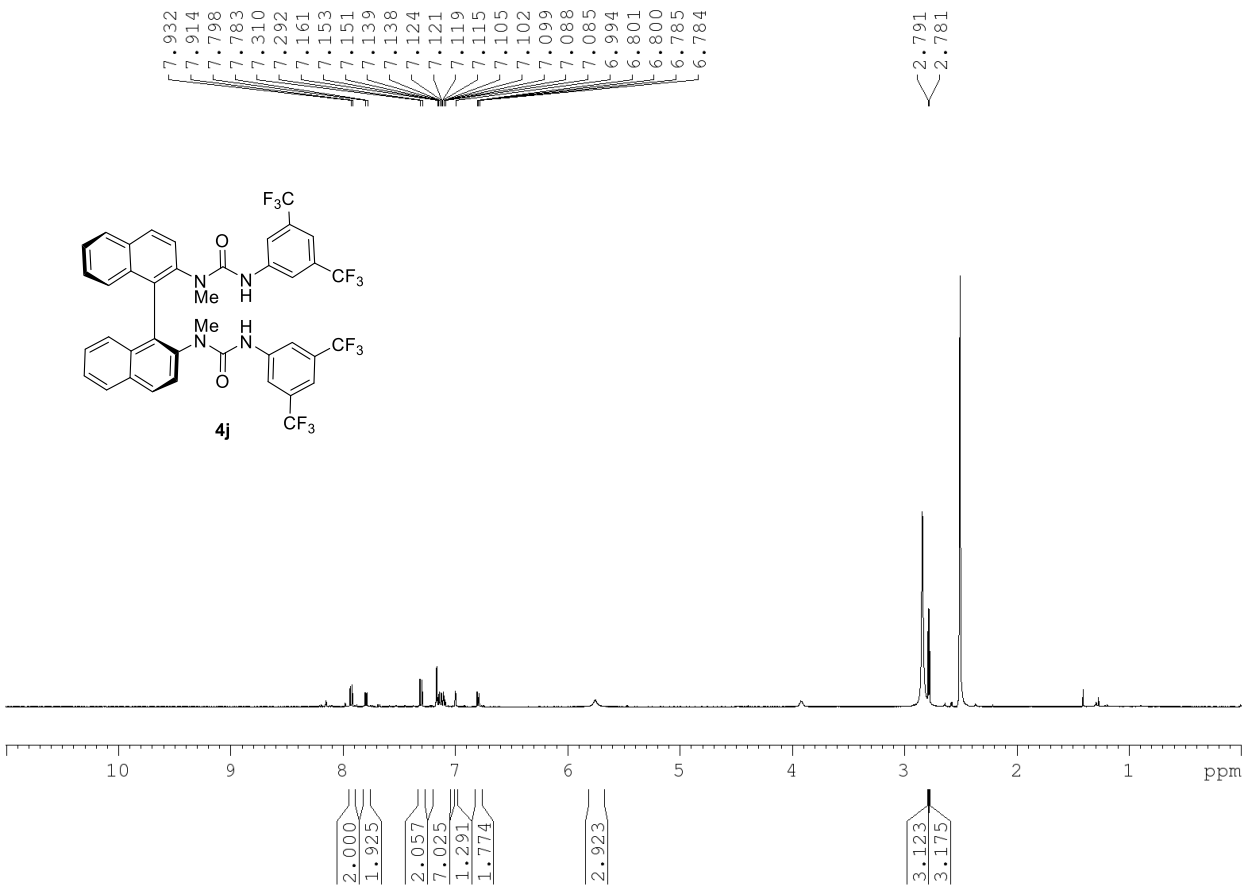
7.932
7.914
7.798
7.783
7.310
7.292
7.161
7.153
7.151
7.139
7.138
7.124
7.121
7.119
7.115
7.105
7.102
7.099
7.088
7.085
6.994
6.801
6.800
6.785
6.784
2.791
2.781
F3C
CF3
CF3
CF3
Me
H
4j
10
9
8
7
6
5
4
3
2
1
ppm
2.000
1.925
2.057
7.025
1.291
1.774
2.923
3.123
3.175

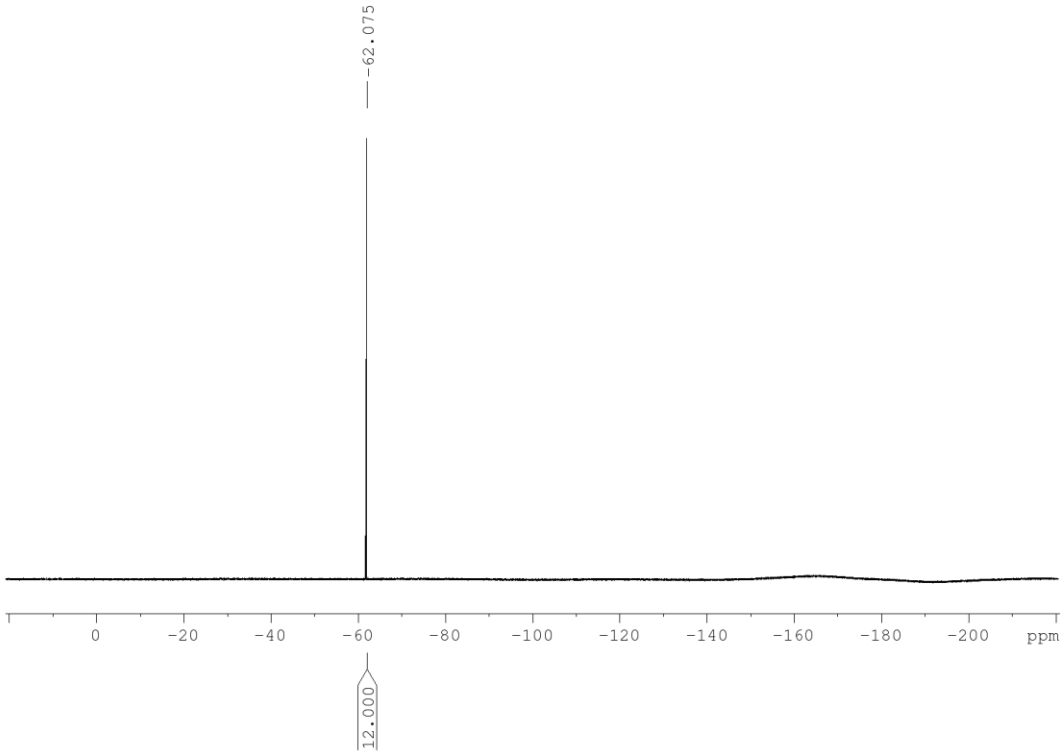
-62.075
0
-20
-40
-60
-80
-100
-120
-140
-160
-180
-200
ppm
12.000

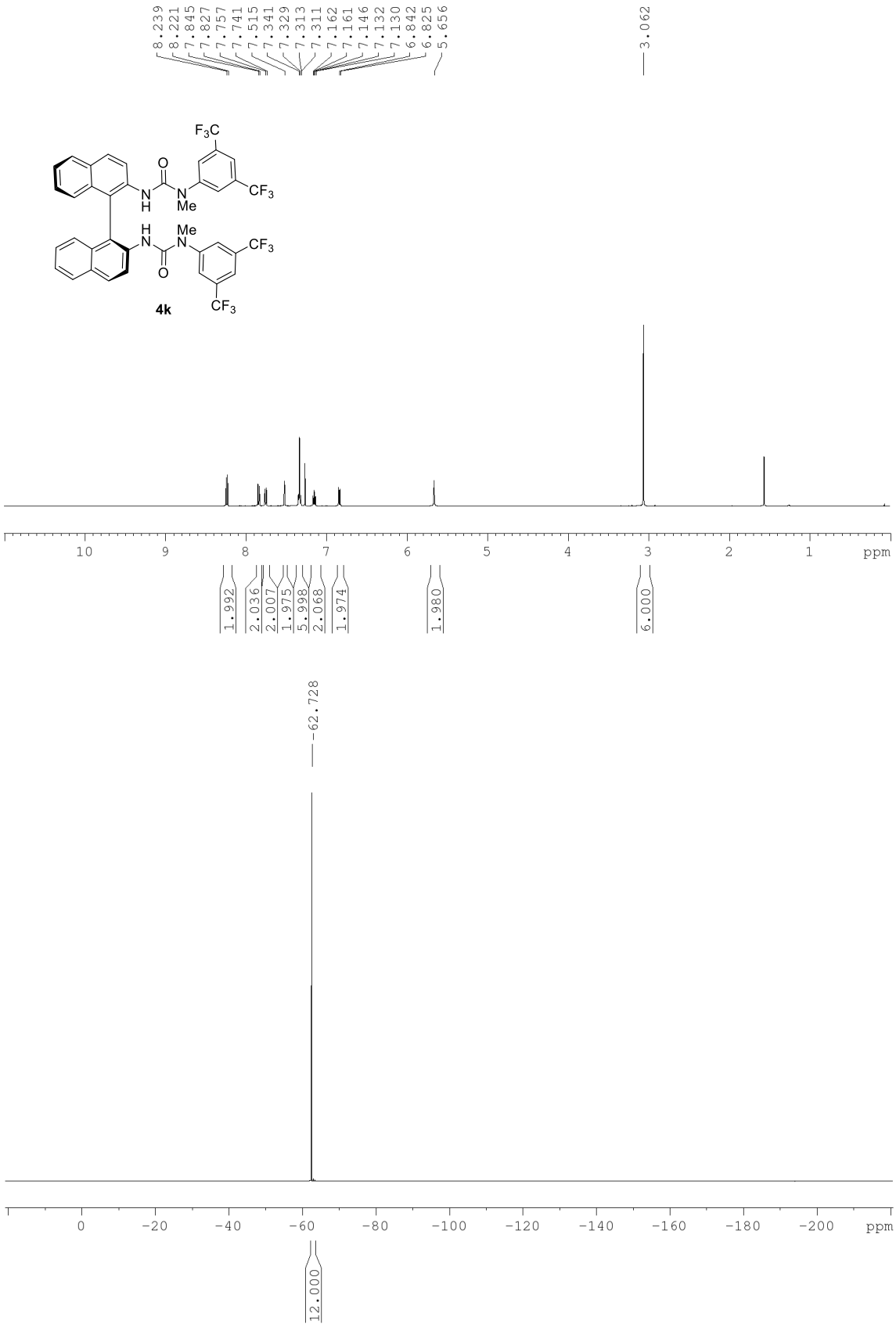
8.239
8.221
7.845
7.827
7.757
7.741
7.515
7.341
7.329
7.313
7.311
7.162
7.161
7.146
7.132
7.130
6.842
6.825
5.656
3.062
F3C
CF3
N
H
O
N
Me
H
N
Me
N
CF3
O
CF3
4k
10
9
8
7
6
5
4
3
2
1
ppm
1.992
2.036
2.007
1.975
5.998
2.068
1.974
1.980
6.000
-62.728
0
-20
-40
-60
-80
-100
-120
-140
-160
-180
-200
ppm
12.000

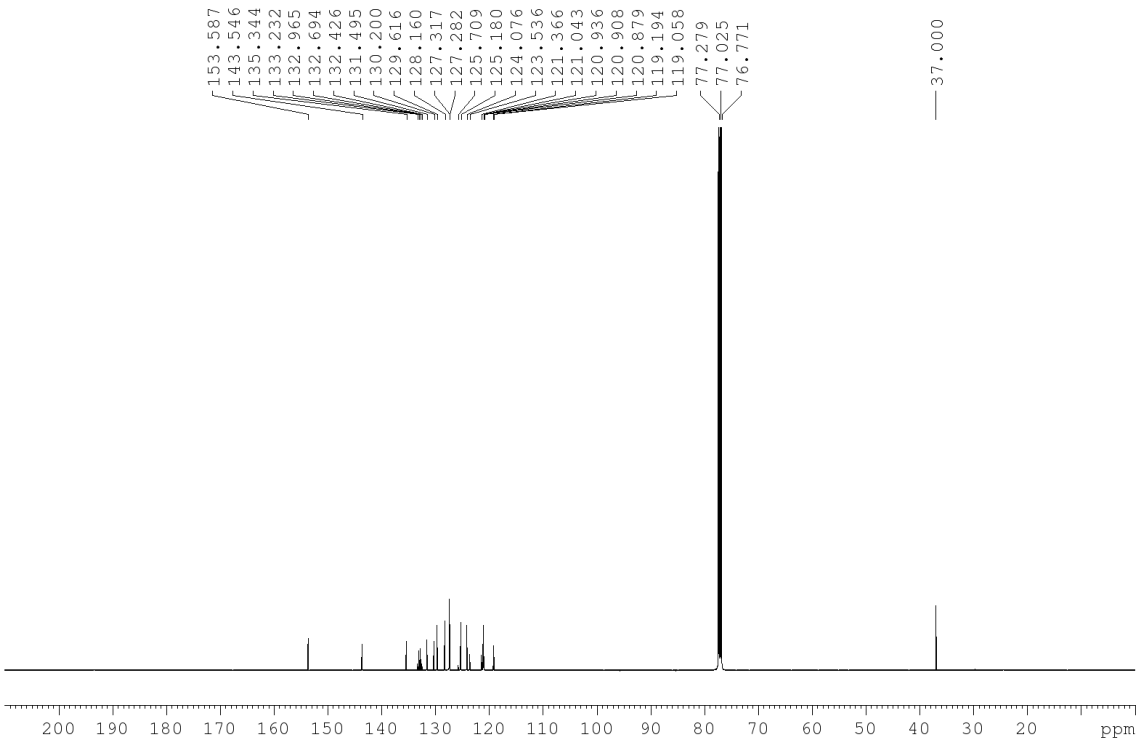
153.587
143.546
135.344
133.232
132.965
132.694
132.426
131.495
130.200
129.616
128.160
127.317
127.282
125.709
125.180
124.076
123.536
121.366
121.043
120.936
120.908
120.879
119.194
119.058
77.279
77.025
76.771
37.000
200 190 180 170 160 150 140 130 120 110 100 90 80 70 60 50 40 30 20 ppm

Substrates precursors (alcohols)

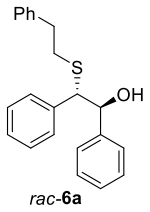

rac-**6a**

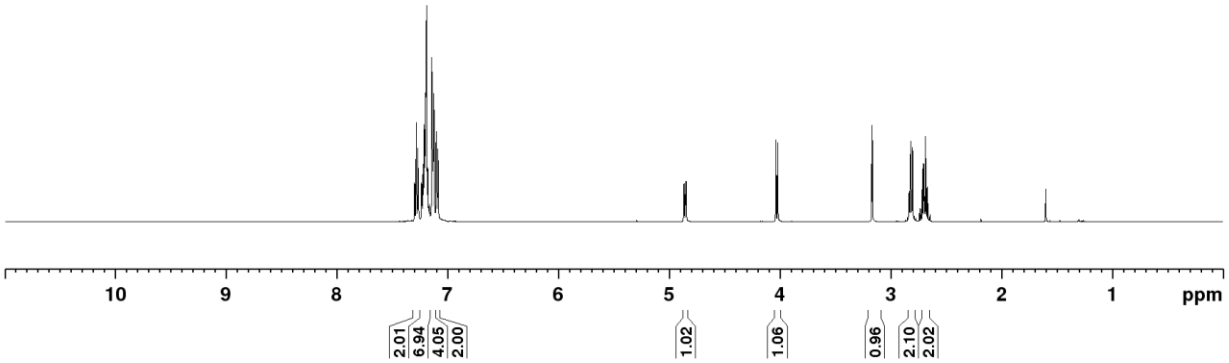

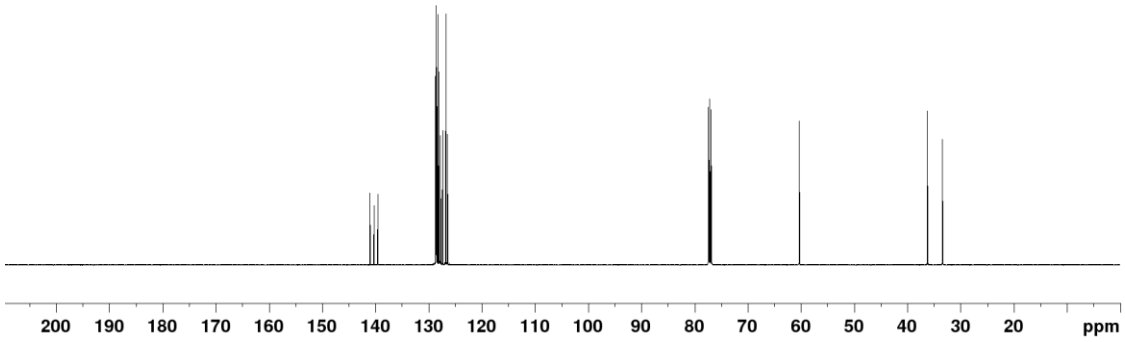

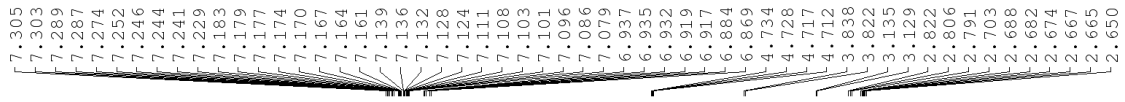
7.305
7.303
7.289
7.287
7.274
7.252
7.246
7.244
7.241
7.229
7.183
7.179
7.177
7.174
7.170
7.167
7.164
7.161
7.139
7.136
7.132
7.128
7.124
7.111
7.108
7.103
7.101
7.096
7.086
7.079
6.937
6.935
6.932
6.919
6.917
6.884
6.869
4.734
4.728
4.717
4.712
3.838
3.822
3.135
3.129
2.822
2.806
2.791
2.703
2.688
2.682
2.674
2.667
2.665
2.650

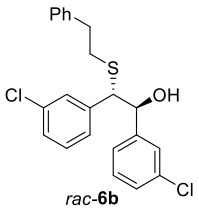
Ph
S
Cl
OH
Cl

rac-**6b**

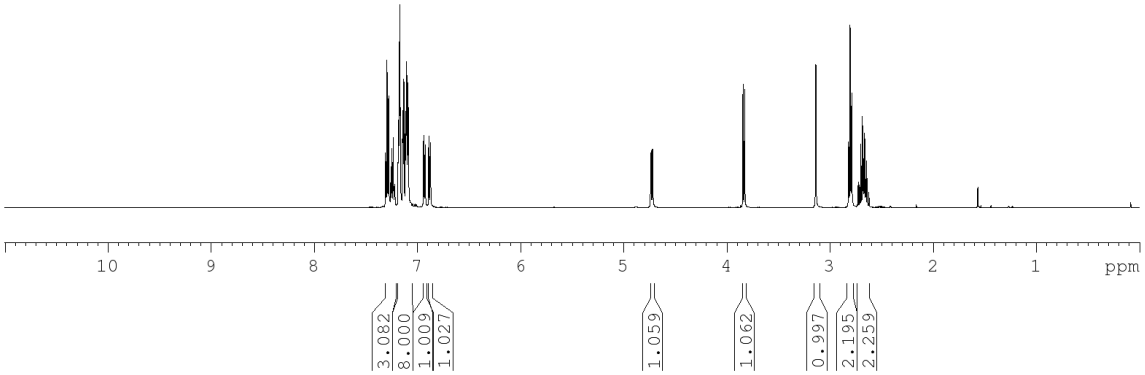
10
9
8
7
6
5
4
3
2
1
ppm
3.082
8.000
1.009
1.027
1.059
1.062
0.997
2.195
2.259

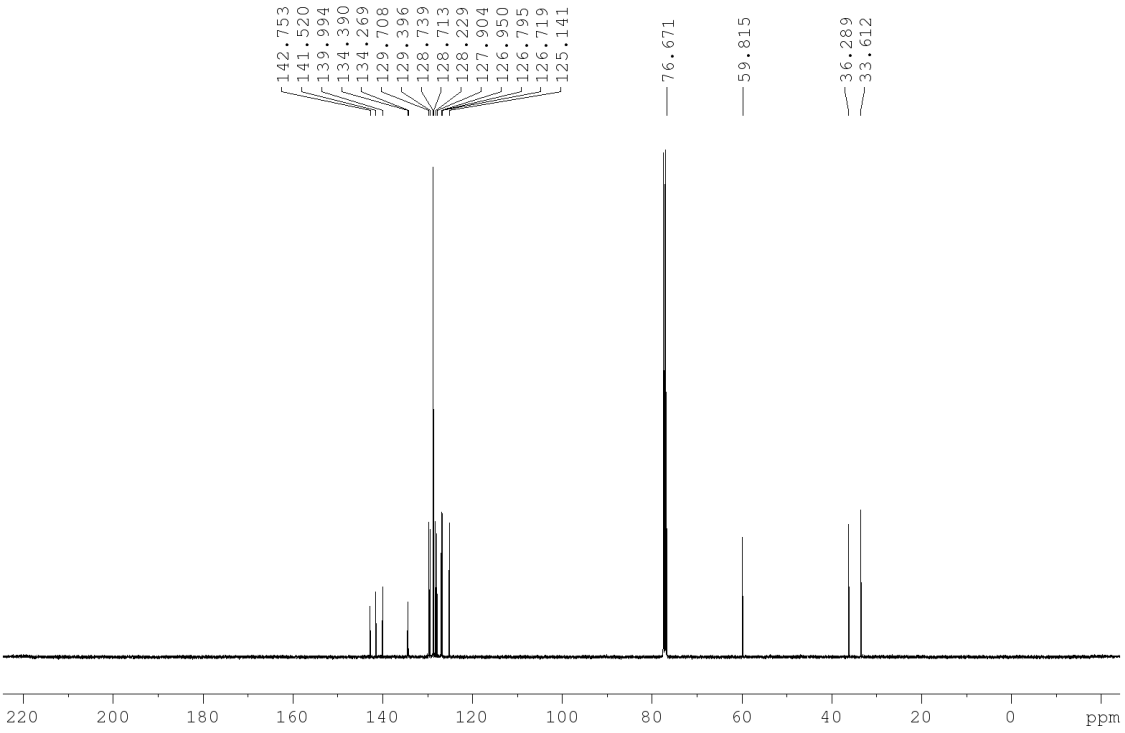
142.753
141.520
139.994
134.390
134.269
129.708
129.396
128.739
128.713
128.229
127.904
126.950
126.795
126.719
125.141
76.671
59.815
36.289
33.612
220
200
180
160
140
120
100
80
60
40
20
0
ppm

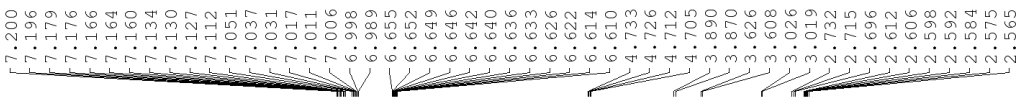
7.200
7.196
7.179
7.176
7.166
7.164
7.160
7.134
7.130
7.127
7.112
7.051
7.037
7.031
7.017
7.011
7.006
6.998
6.989
6.655
6.652
6.649
6.646
6.642
6.640
6.636
6.633
6.626
6.622
6.614
6.610
4.733
4.726
4.712
4.705
3.890
3.870
3.626
3.608
3.026
3.019
2.732
2.715
2.696
2.612
2.606
2.598
2.592
2.584
2.575
2.565

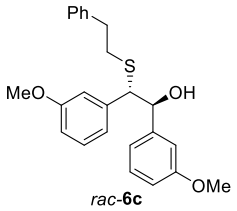
Ph
S
MeO
OH
OMe

rac-**6c**

10
9
8
7
6
5
4
3
2
1
ppm
2.147
1.012
4.007
5.983
1.000
0.999
6.048
0.992
2.007
2.060

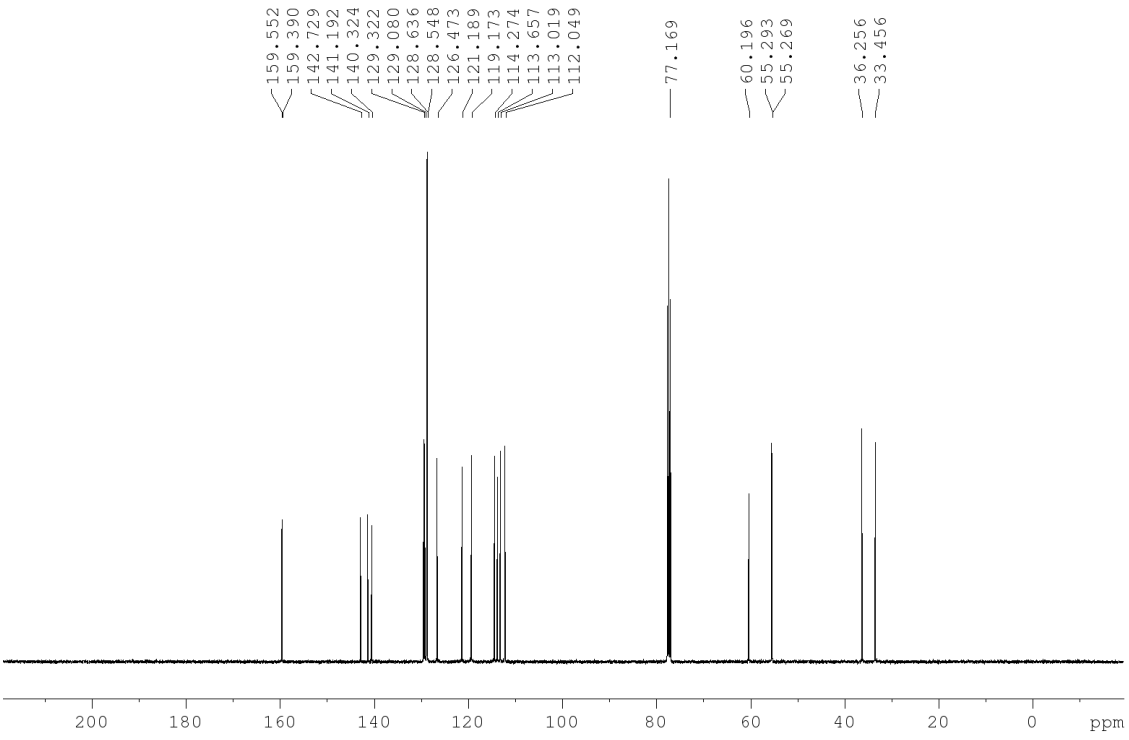
159.552
159.390
142.729
141.192
140.324
129.322
129.080
128.636
128.548
126.473
121.189
119.173
114.274
113.657
113.019
112.049
77.169
60.196
55.293
55.269
36.256
33.456
200
180
160
140
120
100
80
60
40
20
0
ppm

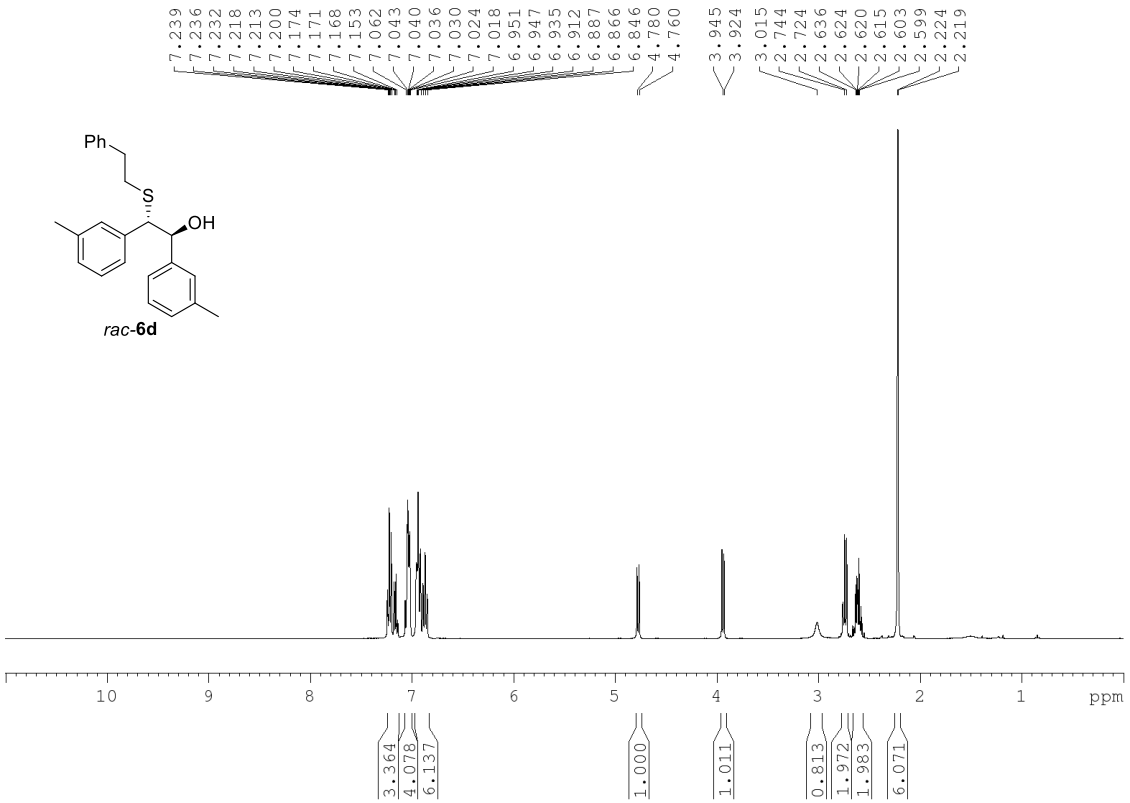
7.239
7.236
7.232
7.218
7.213
7.200
7.174
7.171
7.168
7.153
7.062
7.043
7.040
7.036
7.030
7.024
7.018
6.951
6.947
6.935
6.912
6.887
6.866
6.846
4.780
4.760
3.945
3.924
3.015
2.744
2.724
2.636
2.624
2.620
2.615
2.603
2.599
2.224
2.219
Ph
S
OH
rac-6d
10
9
8
7
6
5
4
3
2
1
ppm
3.364
4.078
6.137
1.000
1.011
0.813
1.972
1.983
6.071

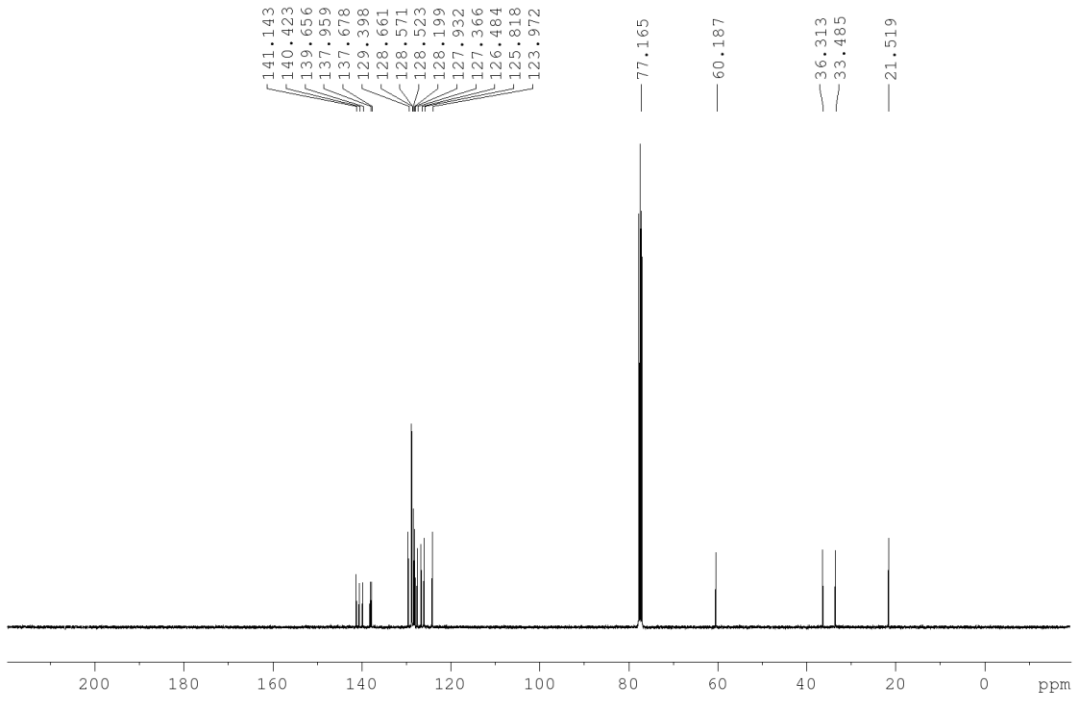
141.143
140.423
139.656
137.959
137.678
129.398
128.661
128.571
128.523
128.199
127.932
127.366
126.484
125.818
123.972
77.165
60.187
36.313
33.485
21.519
200
180
160
140
120
100
80
60
40
20
0
ppm

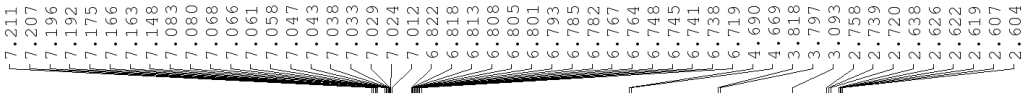
7.211
7.207
7.196
7.192
7.175
7.166
7.163
7.148
7.083
7.080
7.068
7.066
7.061
7.058
7.047
7.043
7.038
7.033
7.029
7.024
7.012
6.822
6.818
6.813
6.808
6.805
6.801
6.793
6.785
6.782
6.767
6.764
6.748
6.745
6.741
6.738
6.719
4.690
4.669
3.818
3.797
3.093
2.758
2.739
2.720
2.638
2.626
2.622
2.619
2.607
2.604

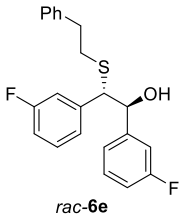
Ph
S
F
OH
F

rac-**6e**

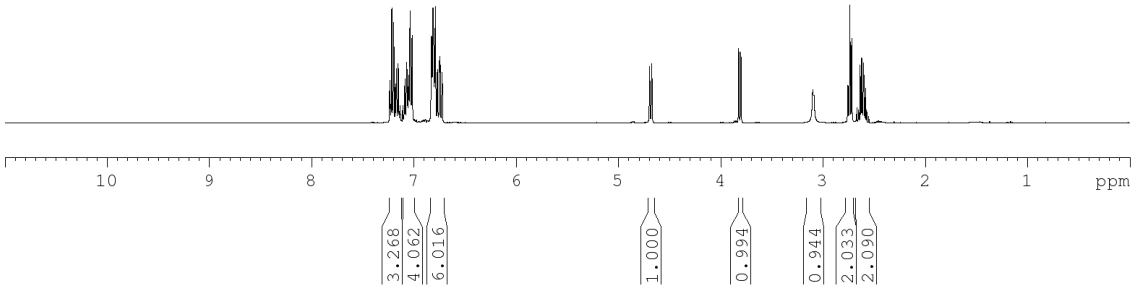
10
9
8
7
6
5
4
3
2
1
ppm
3.268
4.062
6.016
1.000
0.994
0.944
2.033
2.090

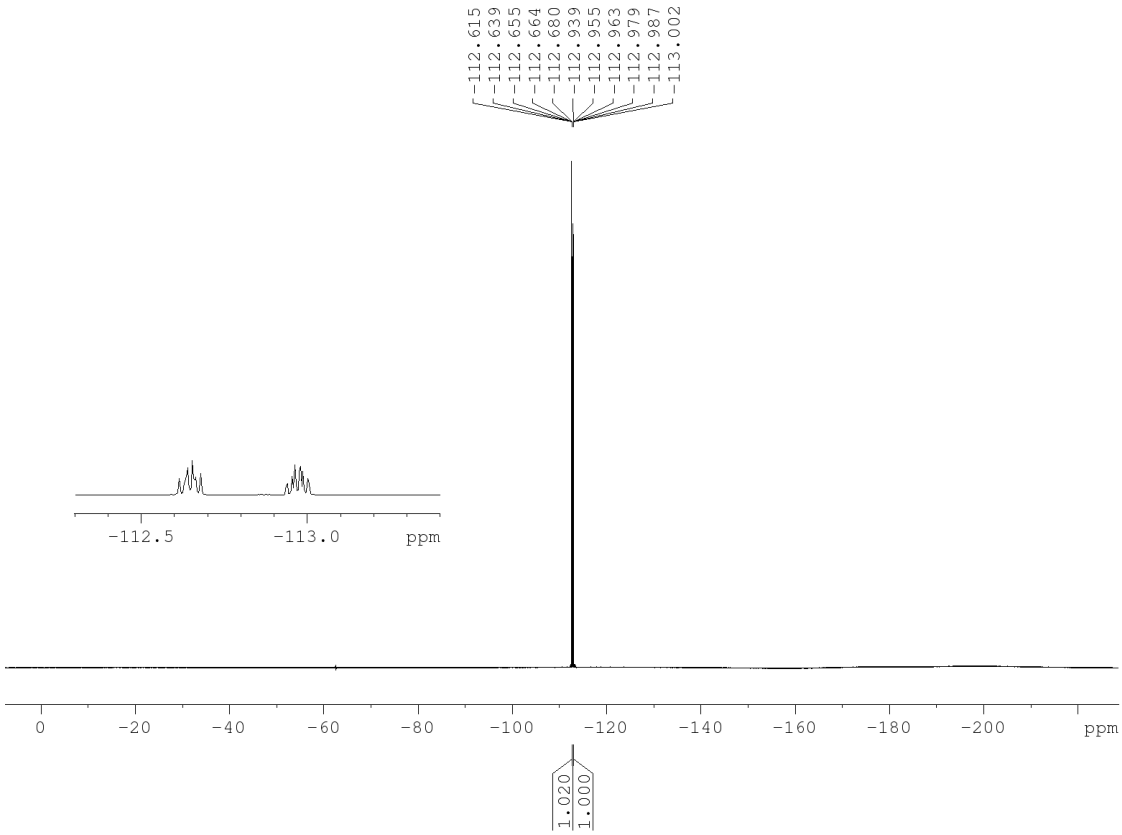
-112.615
-112.639
-112.655
-112.664
-112.680
-112.939
-112.955
-112.963
-112.979
-112.987
-113.002
-112.5
-113.0
ppm
0
-20
-40
-60
-80
-100
-120
-140
-160
-180
-200
ppm
1.020
1.000

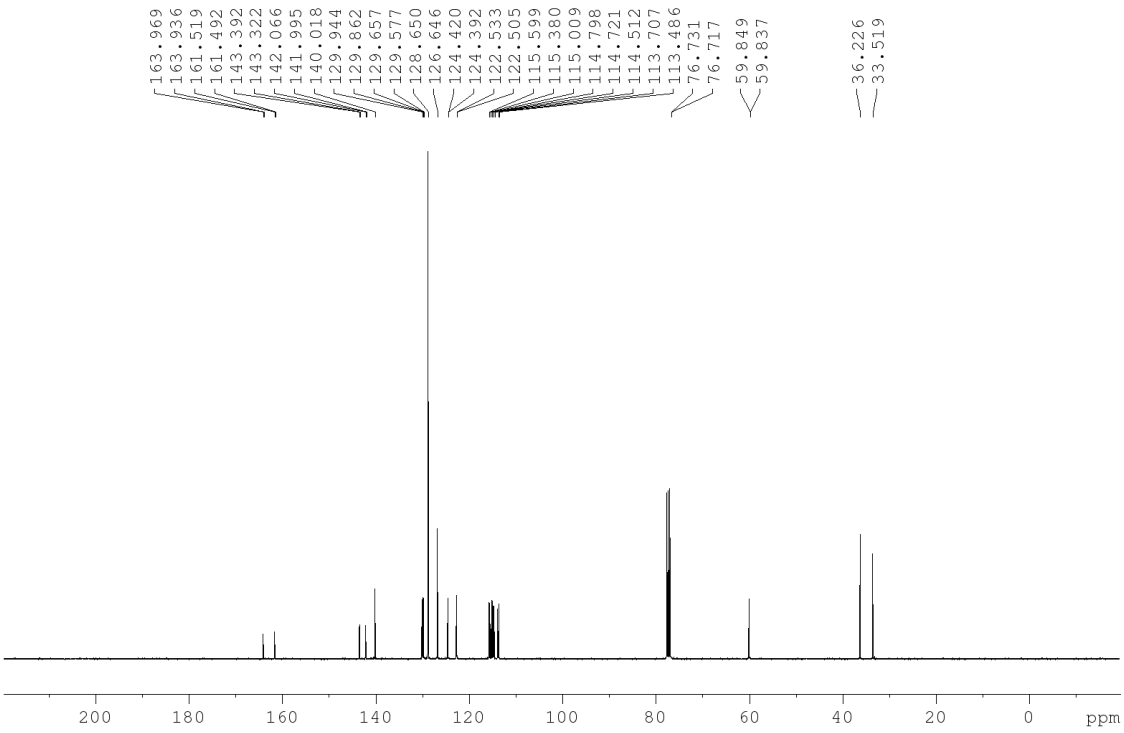
163.969
163.936
161.519
161.492
143.392
143.322
142.066
141.995
140.018
129.944
129.862
129.657
129.577
128.650
126.646
124.420
124.392
122.533
122.505
115.599
115.380
115.009
114.798
114.721
114.512
113.707
113.486
76.731
76.717
59.849
59.837
36.226
33.519
200
180
160
140
120
100
80
60
40
20
0
ppm

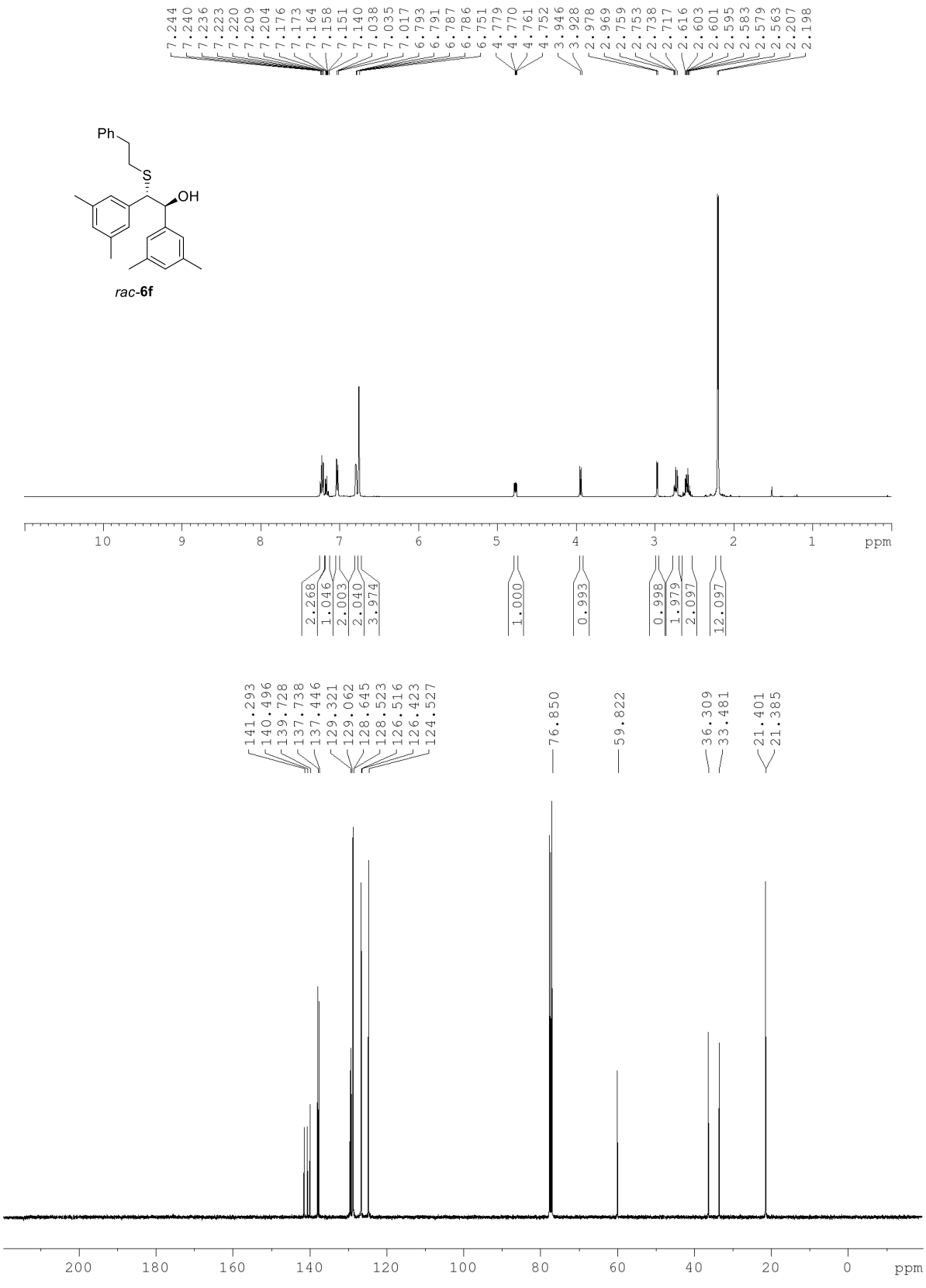
7.244
7.240
7.236
7.223
7.220
7.209
7.204
7.176
7.173
7.164
7.158
7.151
7.140
7.038
7.035
7.017
6.793
6.791
6.787
6.786
6.751
4.779
4.770
4.761
4.752
3.946
3.928
2.978
2.969
2.759
2.753
2.738
2.717
2.616
2.603
2.601
2.595
2.583
2.579
2.563
2.207
2.198
Ph
S
OH
rac-6f
10
9
8
7
6
5
4
3
2
1
ppm
2.268
1.046
2.003
2.040
3.974
1.000
0.993
0.998
1.979
2.097
12.097
141.293
140.496
139.728
137.738
137.446
129.321
129.062
128.645
128.523
126.516
126.423
124.527
76.850
59.822
36.309
33.481
21.401
21.385
200
180
160
140
120
100
80
60
40
20
0
ppm

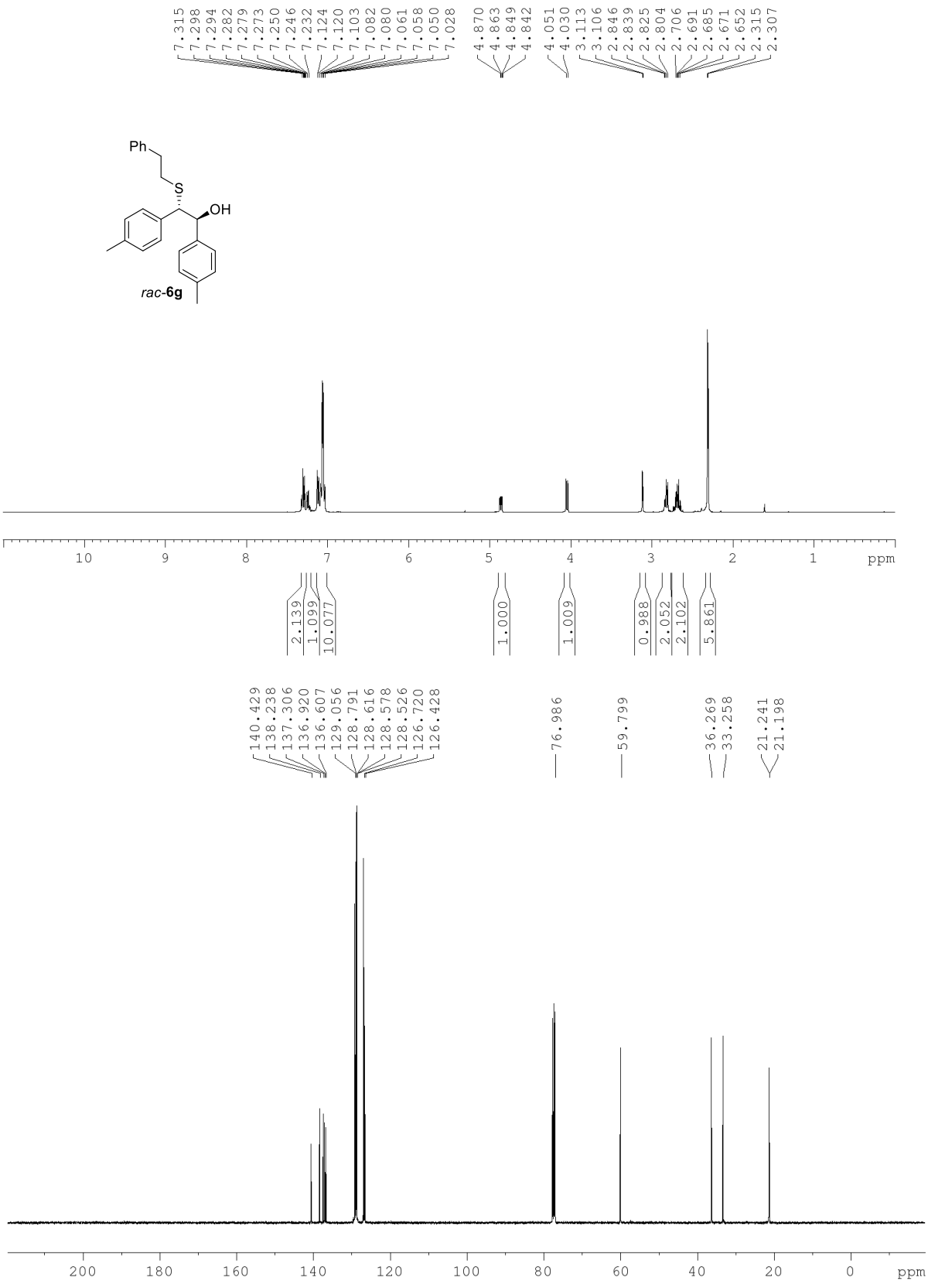
7.315
7.298
7.294
7.282
7.279
7.273
7.250
7.246
7.232
7.124
7.120
7.103
7.082
7.080
7.061
7.058
7.050
7.028
4.870
4.863
4.849
4.842
4.051
4.030
3.113
3.106
2.846
2.839
2.825
2.804
2.706
2.691
2.685
2.671
2.652
2.315
2.307
Ph
S
OH
rac-6g
10
9
8
7
6
5
4
3
2
1
ppm
2.139
1.099
10.077
1.000
1.009
0.988
2.052
2.102
5.861
140.429
138.238
137.306
136.920
136.607
129.056
128.791
128.616
128.578
128.526
126.720
126.428
76.986
59.799
36.269
33.258
21.241
21.198
200
180
160
140
120
100
80
60
40
20
0
ppm

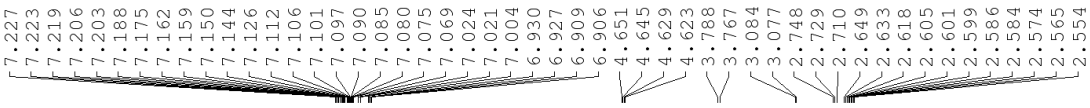
7.227
7.223
7.219
7.206
7.203
7.188
7.175
7.162
7.159
7.150
7.144
7.126
7.112
7.106
7.101
7.097
7.090
7.085
7.080
7.075
7.069
7.024
7.021
7.004
6.930
6.927
6.909
6.906
4.651
4.645
4.629
4.623
3.788
3.767
3.084
3.077
2.748
2.729
2.710
2.649
2.633
2.618
2.605
2.601
2.599
2.586
2.584
2.574
2.565
2.554

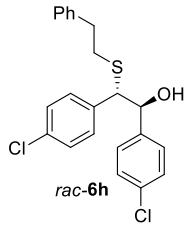
Ph
S
OH
Cl
Cl

rac-**6h**

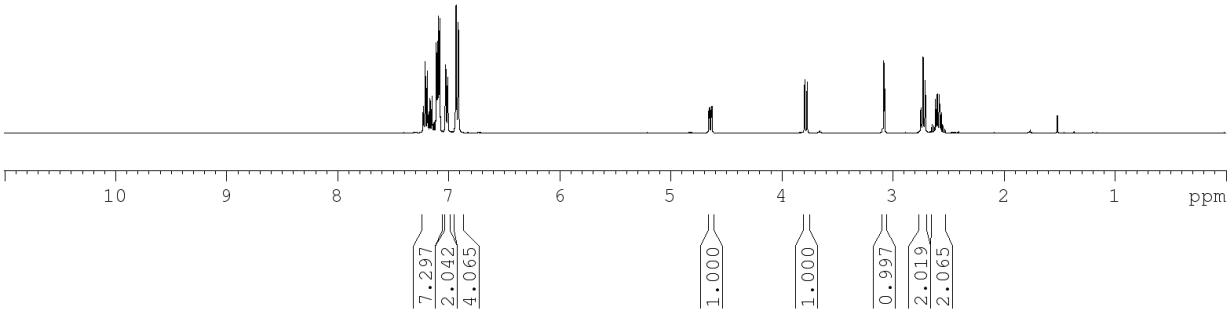
10
9
8
7
6
5
4
3
2
1
ppm
7.297
2.042
4.065
1.000
1.000
0.997
2.019
2.065

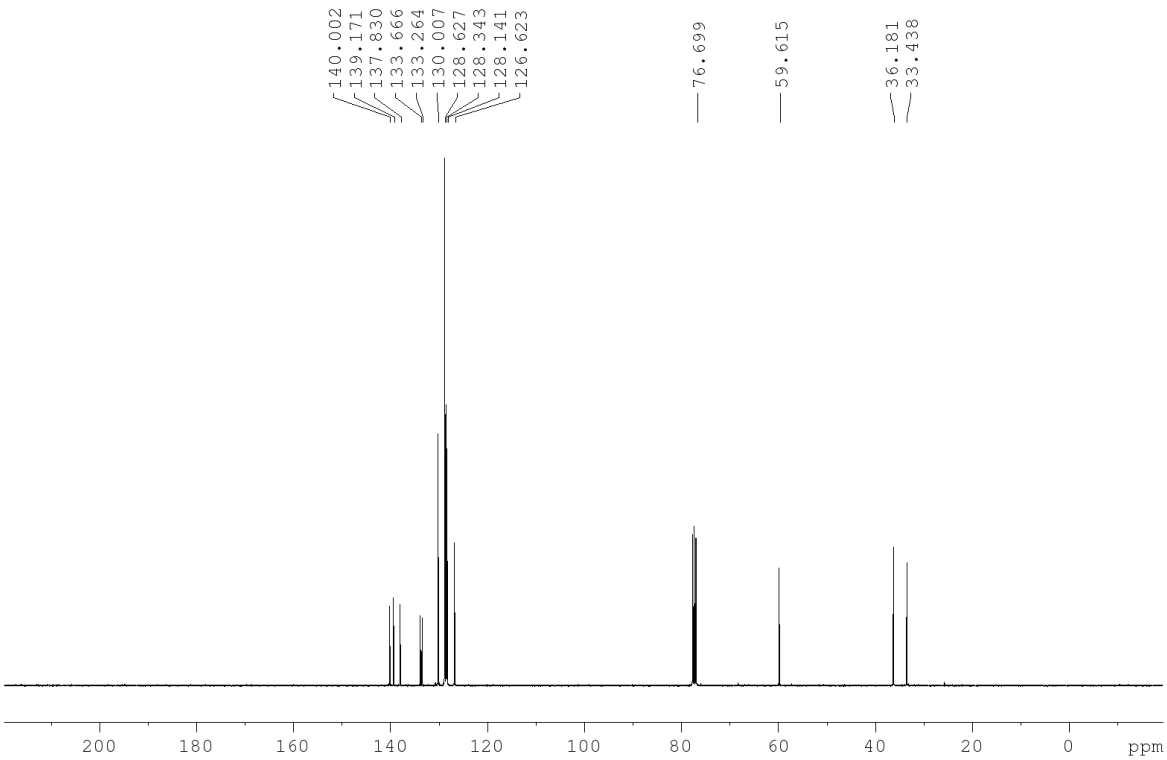
140.002
139.171
137.830
133.666
133.264
130.007
128.627
128.343
128.141
126.623
76.699
59.615
36.181
33.438
200
180
160
140
120
100
80
60
40
20
0
ppm

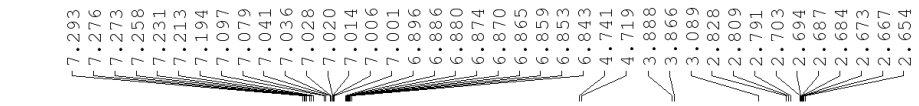
7.293
7.276
7.273
7.258
7.231
7.213
7.194
7.097
7.079
7.041
7.036
7.028
7.020
7.014
7.006
7.001
6.896
6.886
6.880
6.874
6.870
6.865
6.859
6.853
6.843
4.741
4.719
3.888
3.866
3.089
2.828
2.809
2.791
2.703
2.694
2.687
2.684
2.673
2.667
2.654

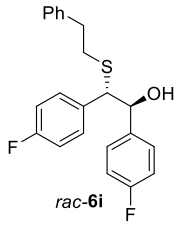
Ph
S
OH
F
F

rac-**6i**

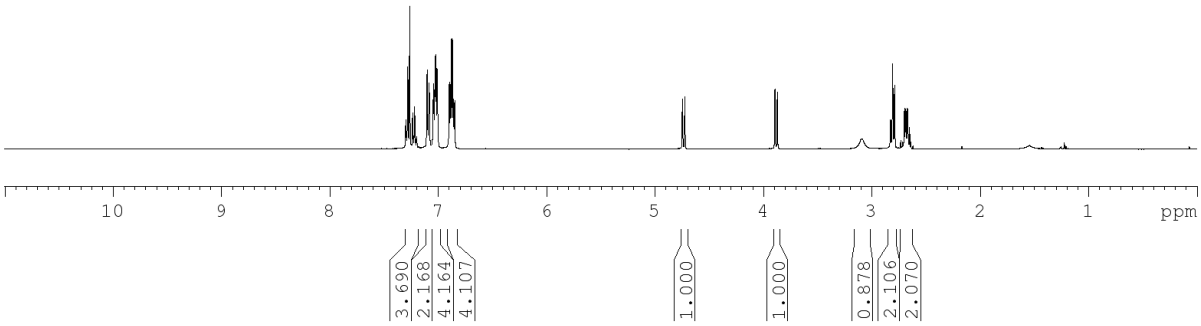
10
9
8
7
6
5
4
3
2
1
ppm
3.690
2.168
4.164
4.107
1.000
1.000
0.878
2.106
2.070

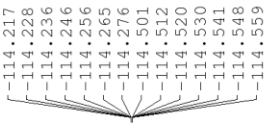
-114.217
-114.228
-114.236
-114.246
-114.256
-114.265
-114.276
-114.501
-114.512
-114.520
-114.530
-114.541
-114.548
-114.559

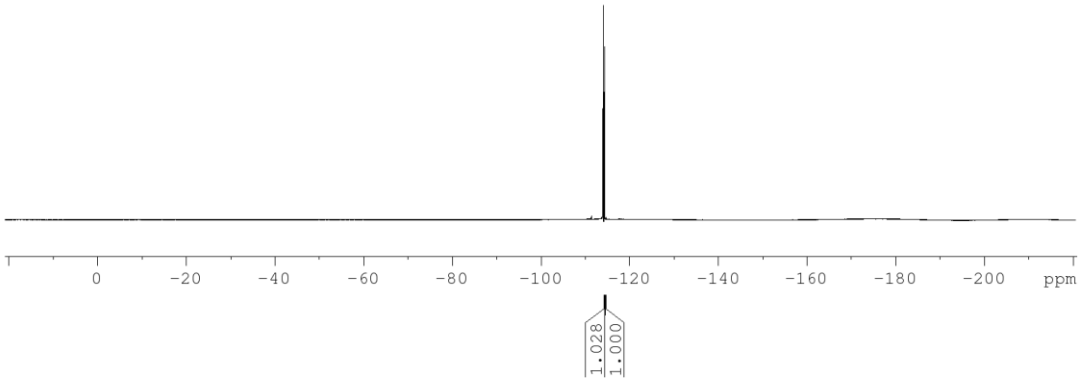
0
-20
-40
-60
-80
-100
-120
-140
-160
-180
-200
ppm
1.028
1.000

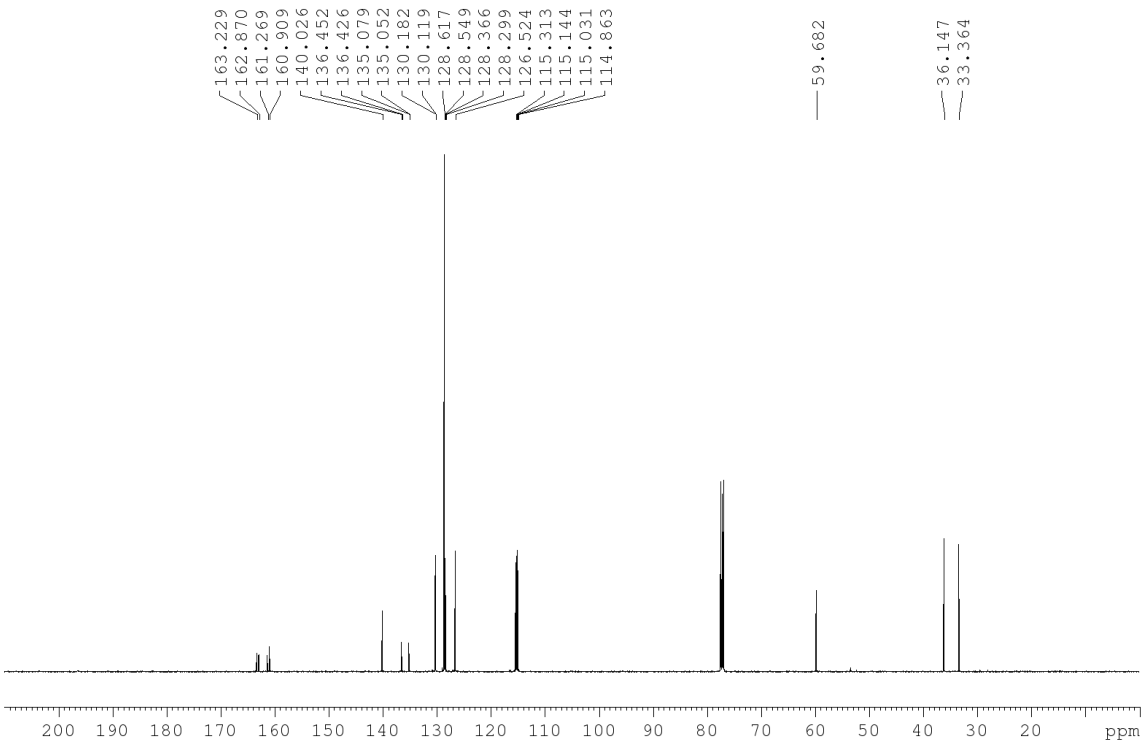
163.229
162.870
161.269
160.909
140.026
136.452
136.426
135.079
135.052
130.182
130.119
128.617
128.549
128.366
128.299
126.524
115.313
115.144
115.031
114.863
59.682
36.147
33.364
200 190 180 170 160 150 140 130 120 110 100 90 80 70 60 50 40 30 20
ppm

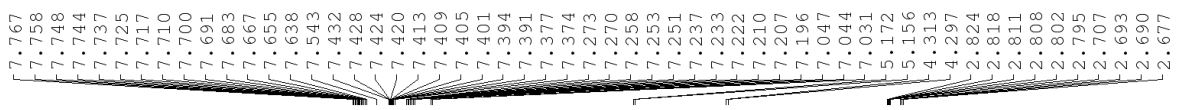
7.767
7.758
7.748
7.744
7.737
7.725
7.717
7.710
7.700
7.691
7.683
7.667
7.655
7.638
7.543
7.432
7.428
7.424
7.420
7.413
7.409
7.405
7.401
7.394
7.391
7.377
7.374
7.273
7.270
7.258
7.253
7.251
7.237
7.233
7.222
7.210
7.207
7.196
7.047
7.044
7.031
5.172
5.156
4.313
4.297
2.824
2.818
2.811
2.808
2.802
2.795
2.707
2.693
2.690
2.677

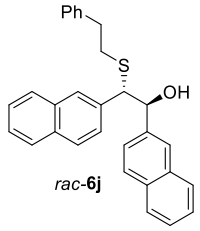
Ph
S
OH

rac-**6j**

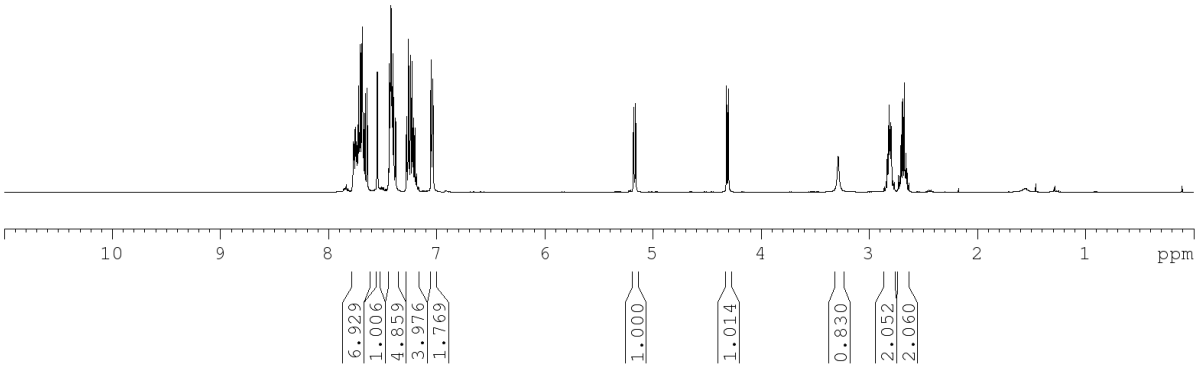
10
9
8
7
6
5
4
3
2
1
ppm
6.929
1.006
4.859
3.976
1.769
1.000
1.014
0.830
2.052
2.060

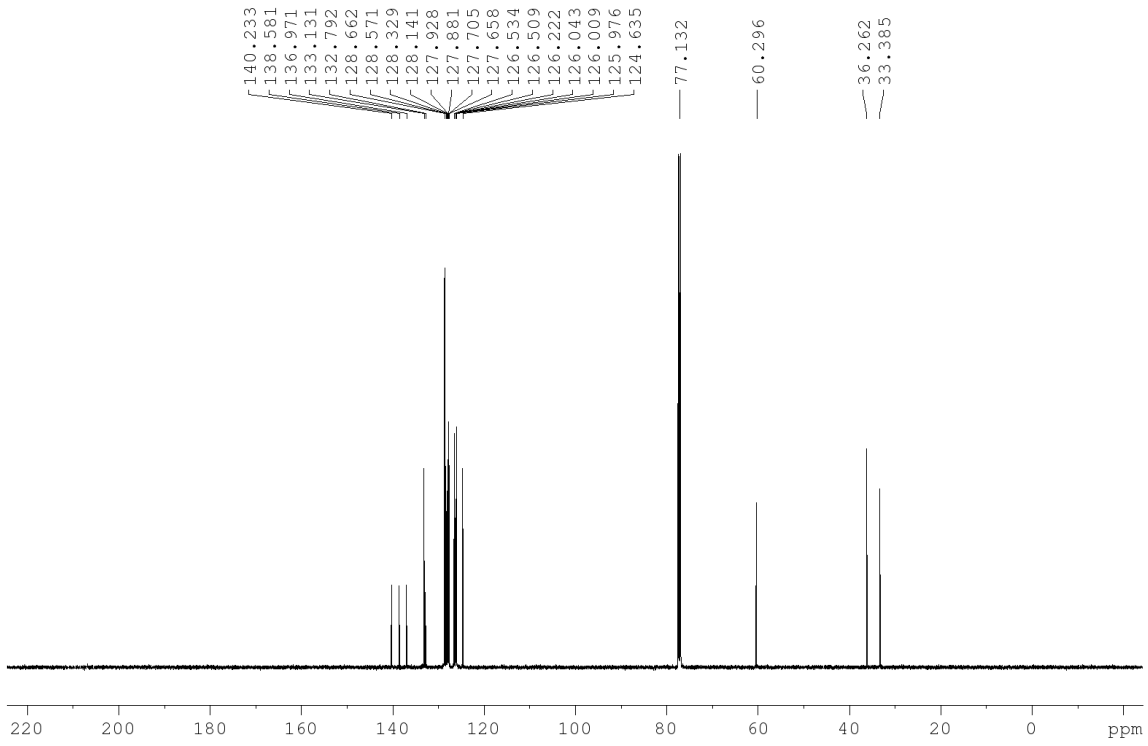
140.233
138.581
136.971
133.131
132.792
128.662
128.571
128.329
128.141
127.928
127.881
127.705
127.658
126.534
126.509
126.222
126.043
126.009
125.976
124.635
77.132
60.296
36.262
33.385
220
200
180
160
140
120
100
80
60
40
20
0
ppm

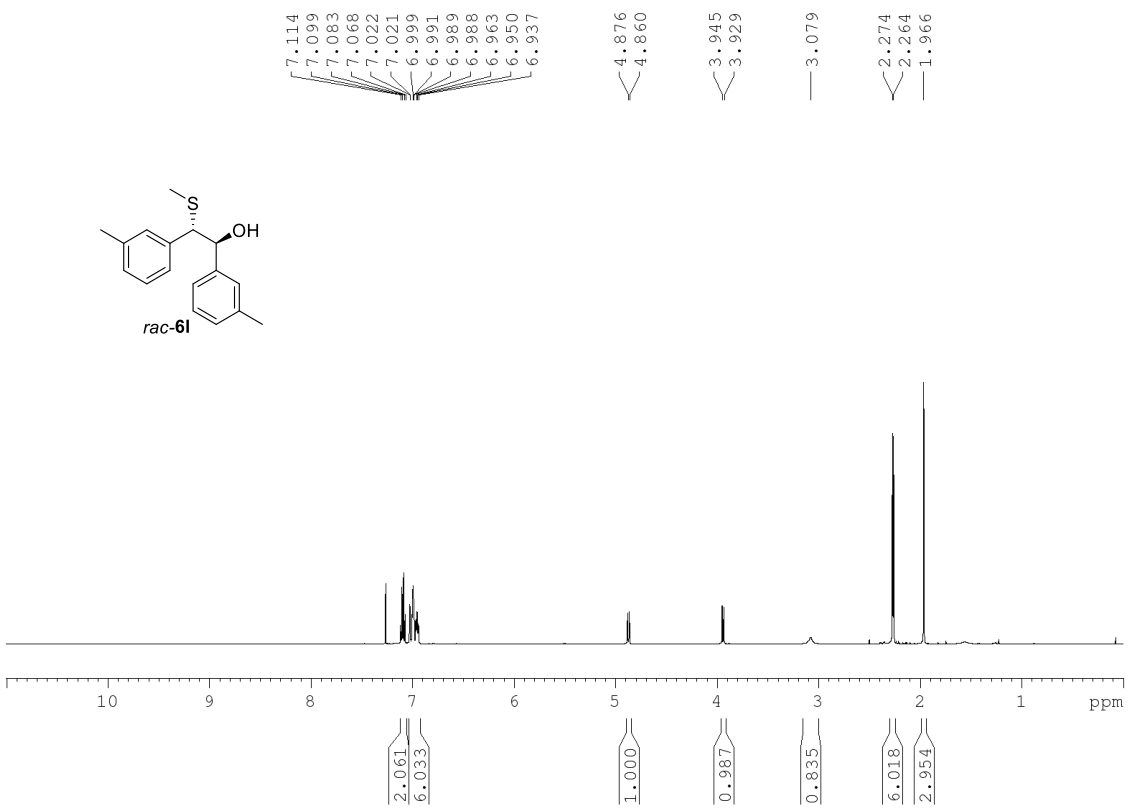
7.114
7.099
7.083
7.068
7.022
7.021
6.999
6.991
6.989
6.988
6.963
6.950
6.937
4.876
4.860
3.945
3.929
3.079
2.274
2.264
1.966
S
OH
rac-6l
10
9
8
7
6
5
4
3
2
1
ppm
2.061
6.033
1.000
0.987
0.835
6.018
2.954

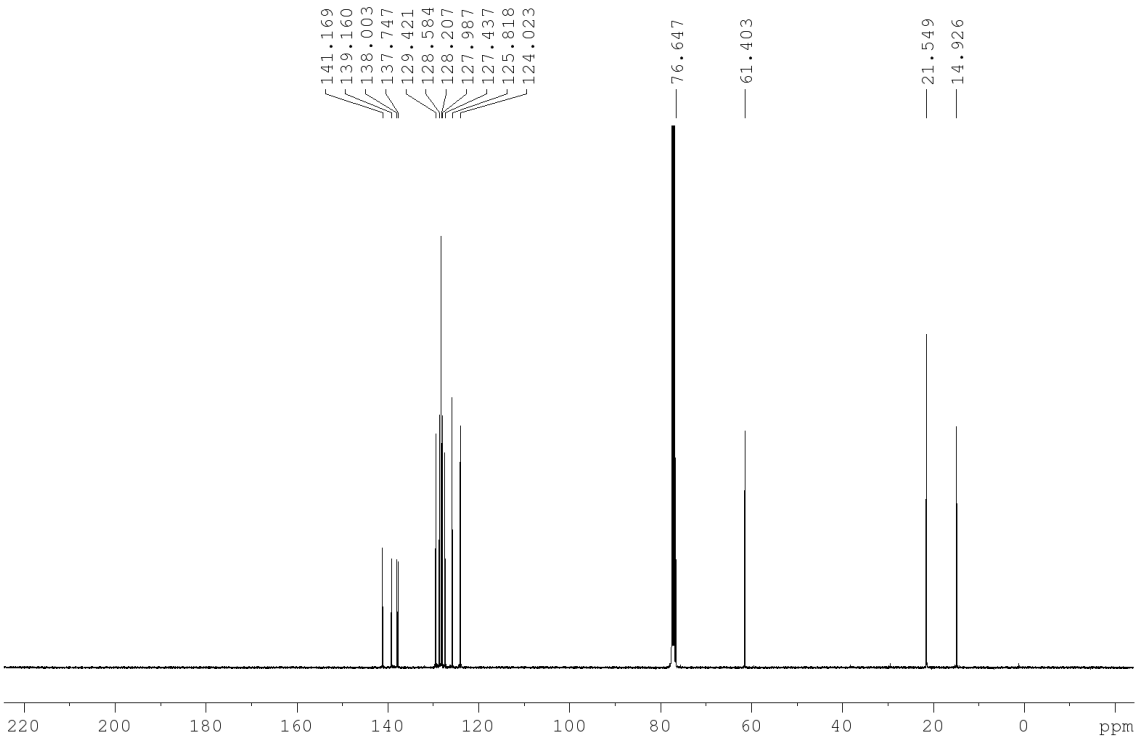
141.169
139.160
138.003
137.747
129.421
128.584
128.207
127.987
127.437
125.818
124.023
76.647
61.403
21.549
14.926
220
200
180
160
140
120
100
80
60
40
20
0
ppm

Starting materials

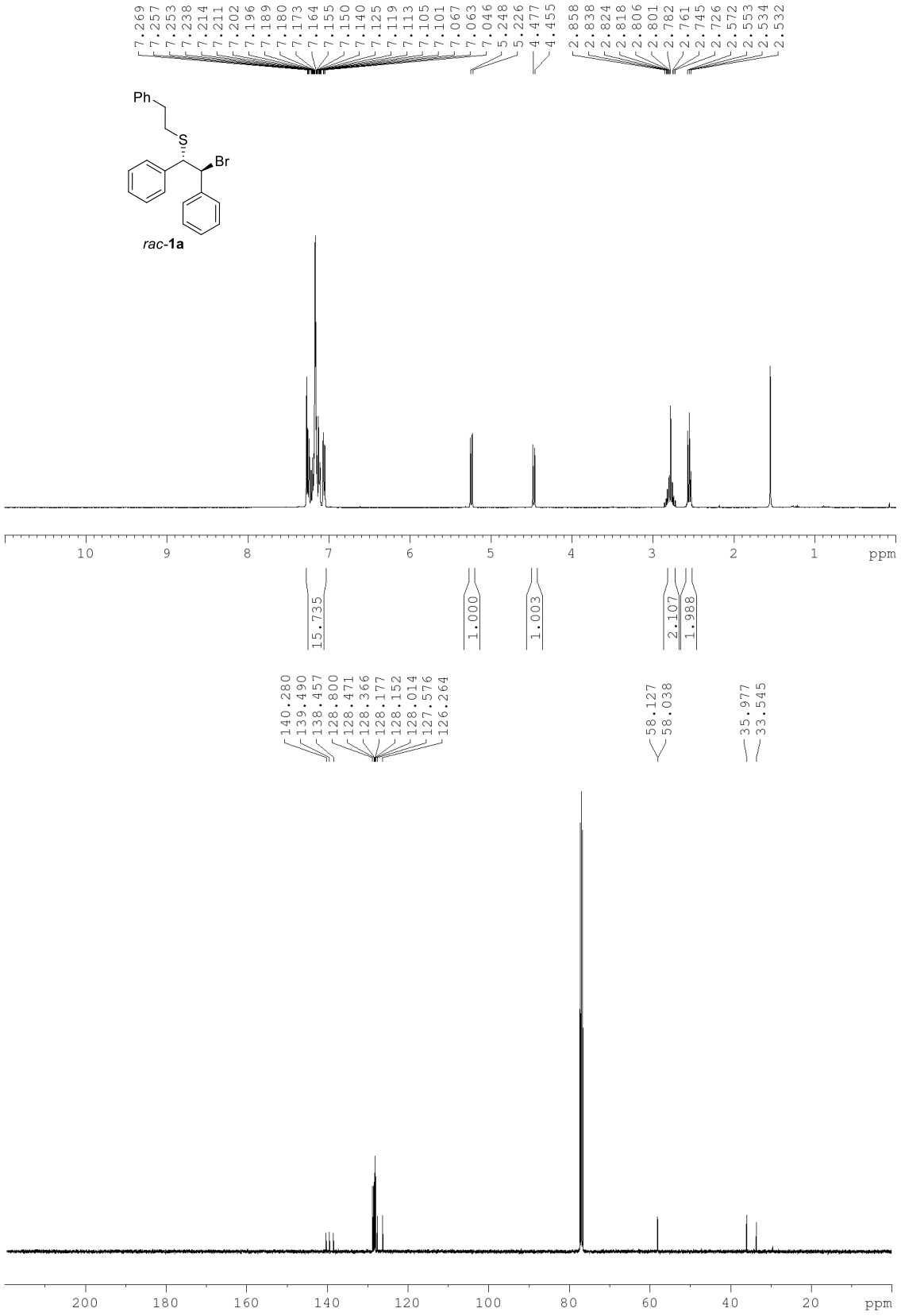


7.29
7.29
7.27
7.26
7.23
7.22
7.21
7.20
7.20
7.19
7.18
7.17
7.17
7.16
7.15
7.14
7.14
7.13
7.12
7.08
7.07
5.20
5.18
4.40
4.38
2.84
2.83
2.83
2.82
2.81
2.80
2.80
2.78
2.77
2.61
2.59
2.58

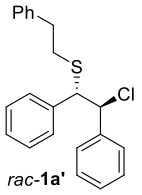
Ph
S
Cl

rac-**1a'**

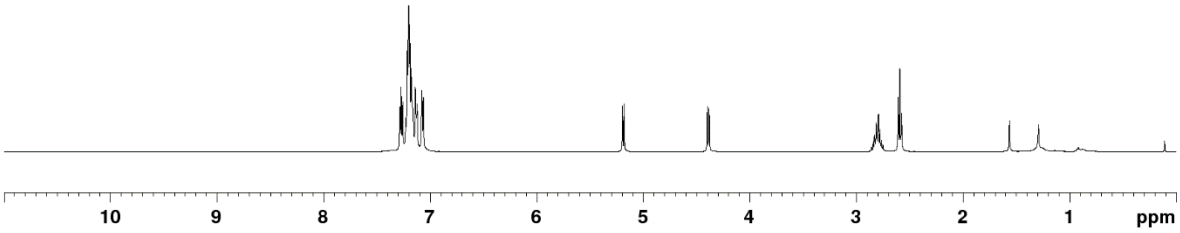
10
9
8
7
6
5
4
3
2
1
ppm


140.36
139.02
138.41
129.02
128.53
128.44
128.25
128.21
128.02
127.86
127.68
126.34
66.83
58.53
36.08
33.45

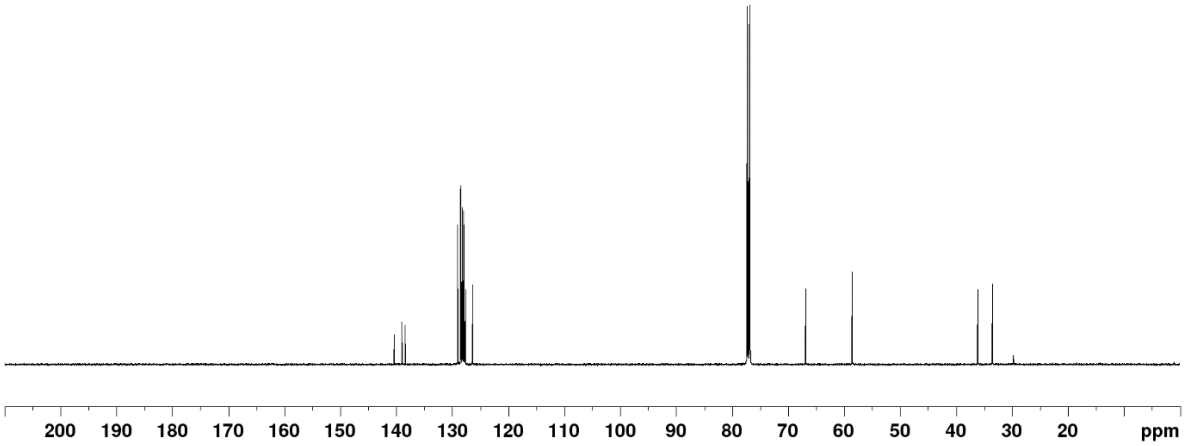
200
190
180
170
160
150
140
130
120
110
100
90
80
70
60
50
40
30
20
ppm


8.37
7.28
7.26
7.26
7.25
7.23
7.22
7.22
7.22
7.21
7.20
7.19
7.19
7.18
7.17
7.16
7.16
7.15
7.14
7.09
7.08
6.14
6.12
4.34
4.32
2.82
2.82
2.81
2.79
2.71
2.70
2.69
2.68
2.68
2.67

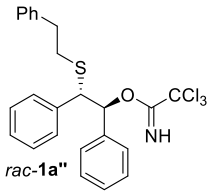
Ph
S
O
CCl3
NH

rac-**1a''**

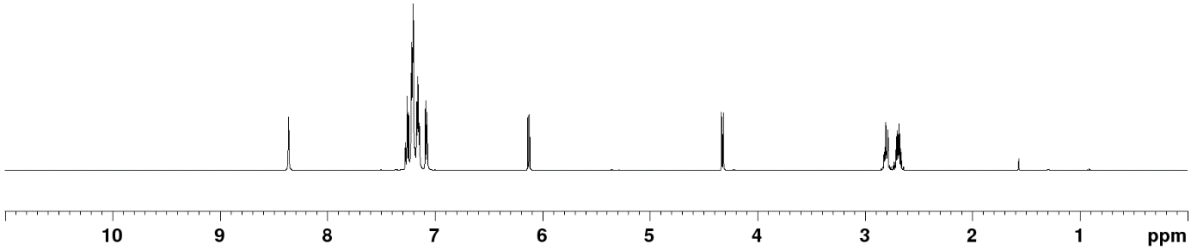
10
9
8
7
6
5
4
3
2
1
ppm


163.38
142.74
140.26
139.50
131.47
130.84
130.67
130.41
130.38
130.08
129.83
129.42
128.54
93.75
85.68
57.83
38.45
35.58

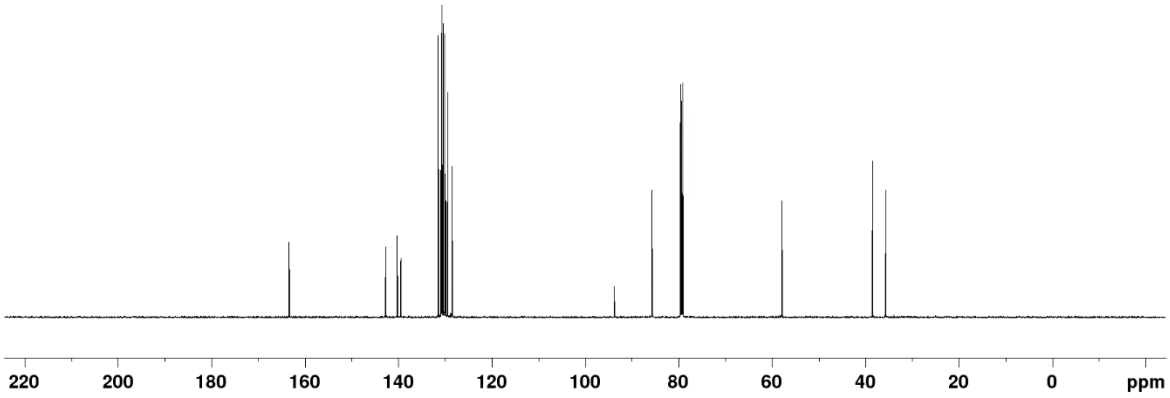
220
200
180
160
140
120
100
80
60
40
20
0
ppm

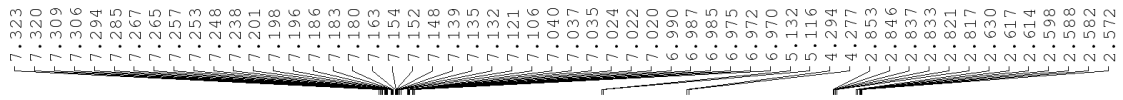
7.323
7.320
7.309
7.306
7.294
7.285
7.267
7.265
7.257
7.253
7.248
7.238
7.201
7.198
7.196
7.186
7.183
7.180
7.163
7.154
7.152
7.148
7.139
7.135
7.132
7.121
7.106
7.040
7.037
7.035
7.024
7.022
7.020
6.990
6.987
6.985
6.975
6.972
6.970
5.132
5.116
4.294
4.277
2.853
2.846
2.837
2.833
2.821
2.817
2.630
2.617
2.614
2.598
2.588
2.582
2.572

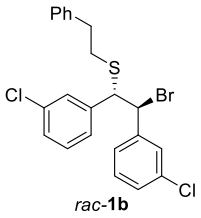
Ph
S
Cl
Br
Cl

rac-**1b**

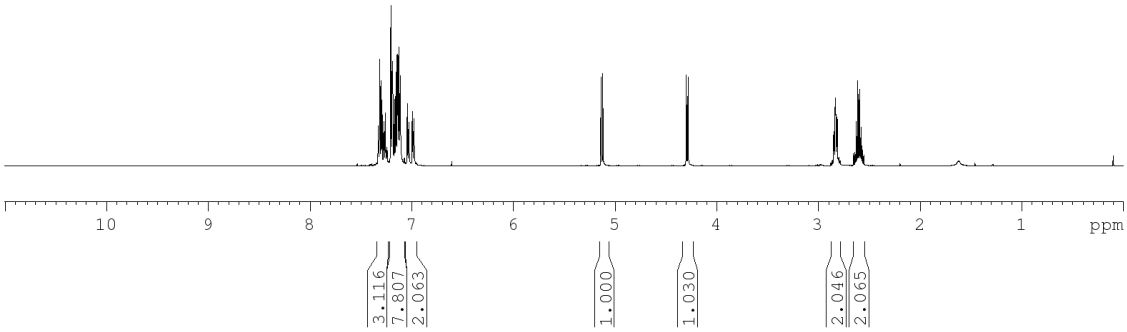
10
9
8
7
6
5
4
3
2
1
ppm
3.116
7.807
2.063
1.000
1.030
2.046
2.065

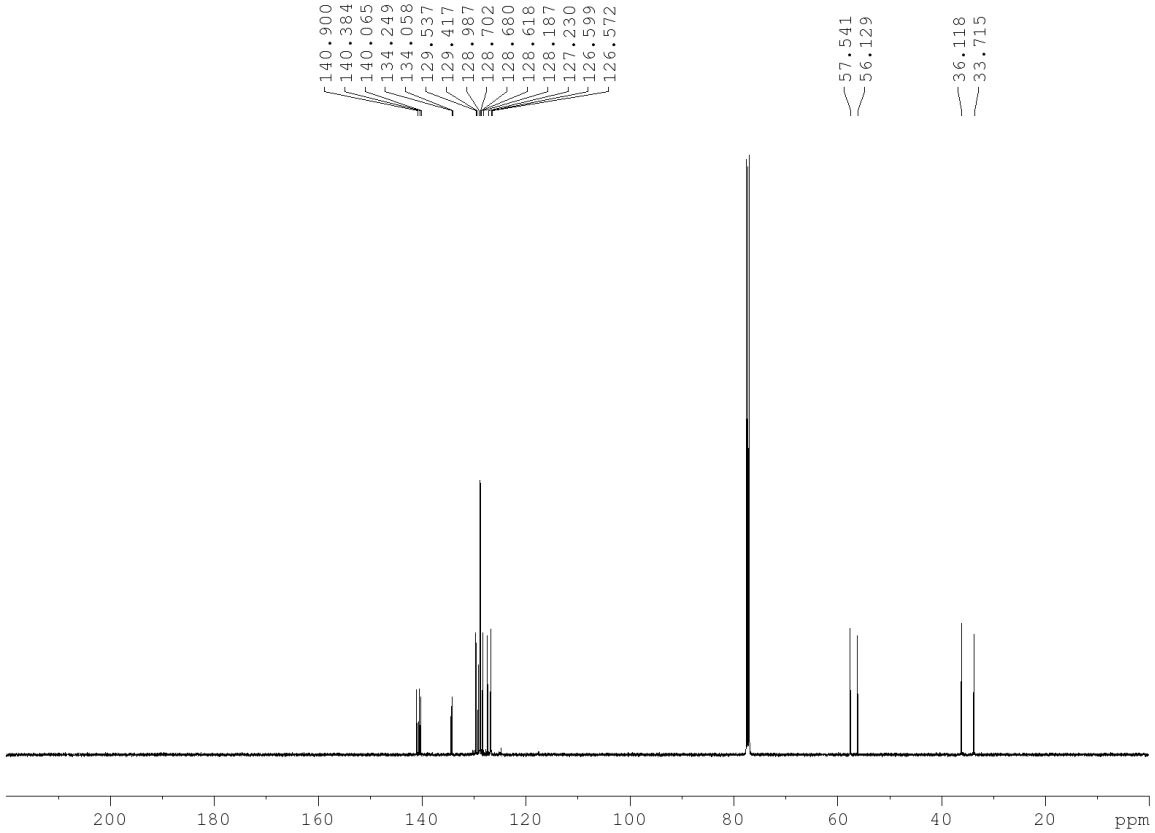
140.900
140.384
140.065
134.249
134.058
129.537
129.417
128.987
128.702
128.680
128.618
128.187
127.230
126.599
126.572
57.541
56.129
36.118
33.715
200
180
160
140
120
100
80
60
40
20
ppm

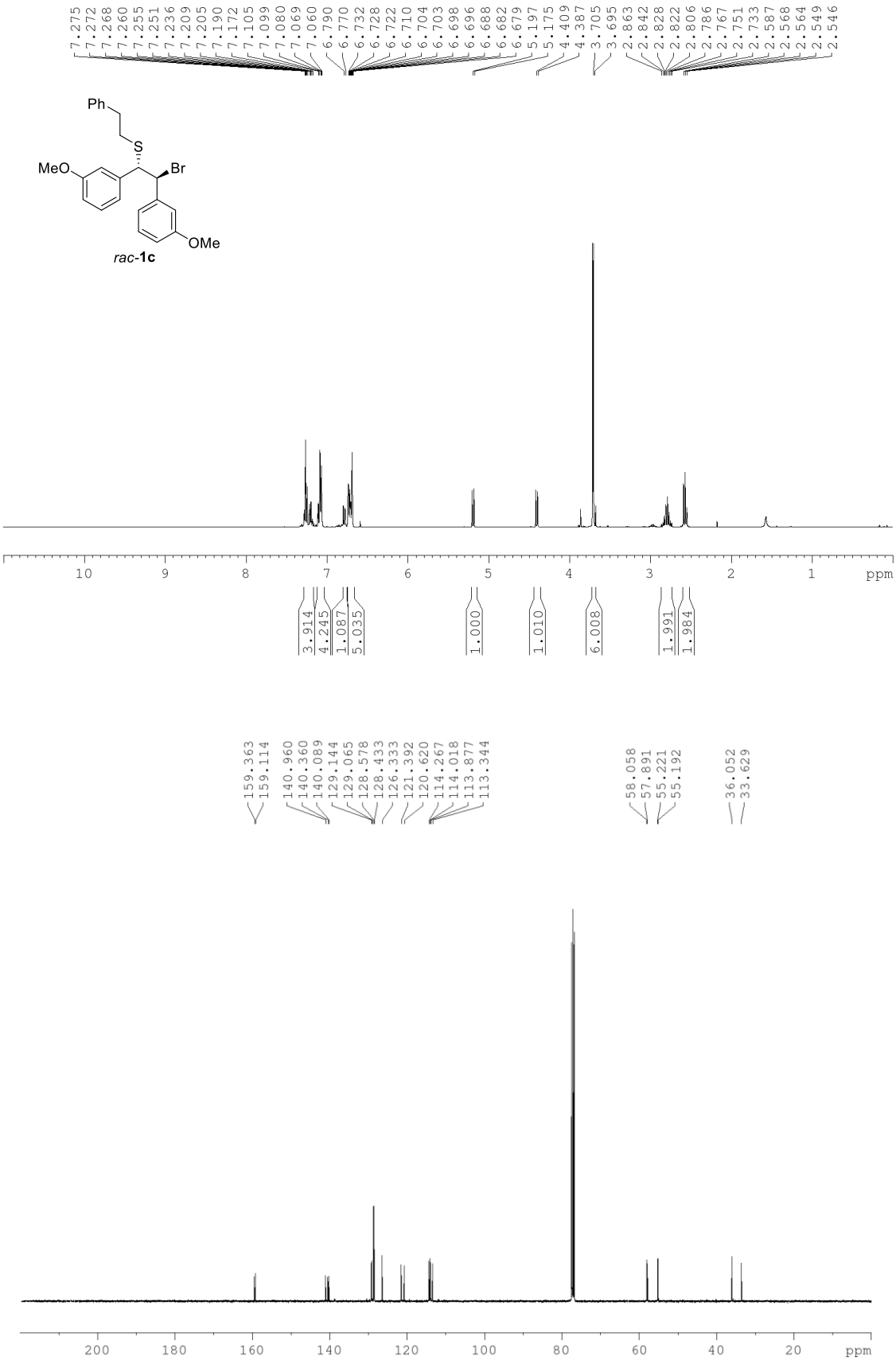
7.275
7.272
7.268
7.260
7.255
7.251
7.236
7.209
7.205
7.190
7.172
7.105
7.099
7.080
7.069
7.060
6.790
6.770
6.732
6.728
6.722
6.710
6.704
6.703
6.698
6.696
6.688
6.682
6.679
5.197
5.175
4.409
4.387
3.705
3.695
2.863
2.842
2.828
2.822
2.806
2.786
2.767
2.751
2.733
2.587
2.568
2.564
2.549
2.546
Ph
S
MeO
Br
OMe
rac-1c
10
9
8
7
6
5
4
3
2
1
ppm
3.914
4.245
1.087
5.035
1.000
1.010
6.008
1.991
1.984
159.363
159.114
140.960
140.360
140.089
129.144
129.065
128.578
128.433
126.333
121.392
120.620
114.267
114.018
113.877
113.344
58.058
57.891
55.221
55.192
36.052
33.629
200
180
160
140
120
100
80
60
40
20
ppm

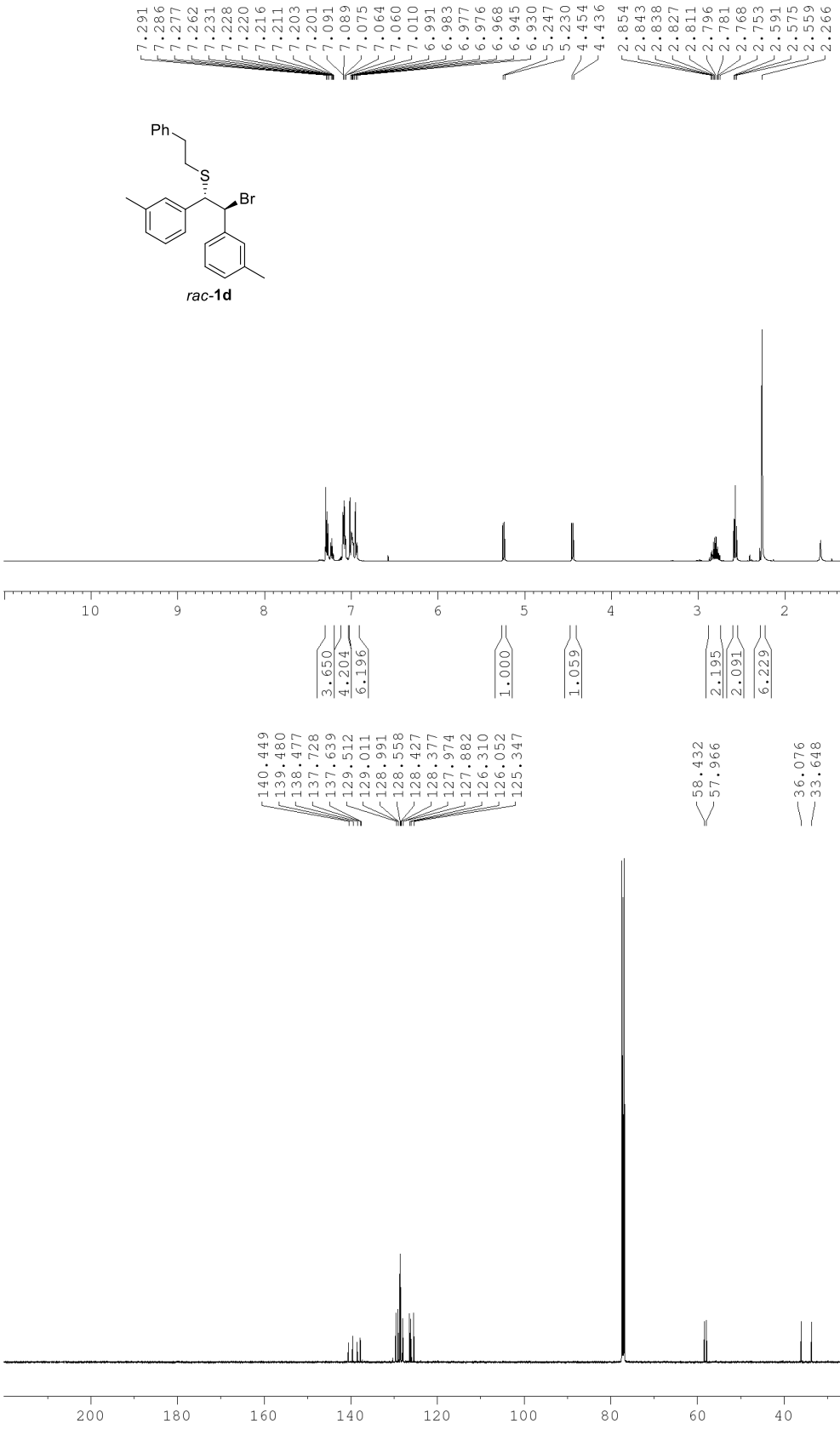
7.291
7.286
7.277
7.262
7.231
7.228
7.220
7.216
7.211
7.203
7.201
7.091
7.089
7.075
7.064
7.060
7.010
6.991
6.983
6.977
6.976
6.968
6.945
6.930
5.247
5.230
4.454
4.436
2.854
2.843
2.838
2.827
2.811
2.796
2.781
2.768
2.753
2.591
2.575
2.559
2.266
Ph
S
Br
rac-1d
10
9
8
7
6
5
4
3
2
1
ppm
3.650
4.204
6.196
1.000
1.059
2.195
2.091
6.229
140.449
139.480
138.477
137.728
137.639
129.512
129.011
128.991
128.558
128.427
128.377
127.974
127.882
126.310
126.052
125.347
58.432
57.966
36.076
33.648
21.342
21.289
200
180
160
140
120
100
80
60
40
20
ppm

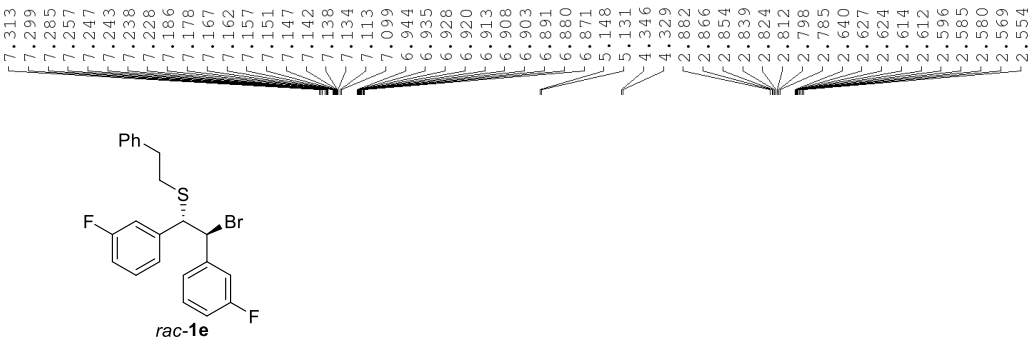
7.313
7.299
7.285
7.257
7.247
7.243
7.238
7.228
7.186
7.178
7.167
7.162
7.157
7.151
7.147
7.142
7.138
7.134
7.113
7.099
6.944
6.935
6.928
6.920
6.913
6.908
6.903
6.891
6.880
6.871
5.148
5.131
4.346
4.329
2.882
2.866
2.854
2.839
2.824
2.812
2.798
2.785
2.640
2.627
2.624
2.614
2.612
2.596
2.585
2.580
2.569
2.554

Ph
S
F
Br
F

rac-**1e**

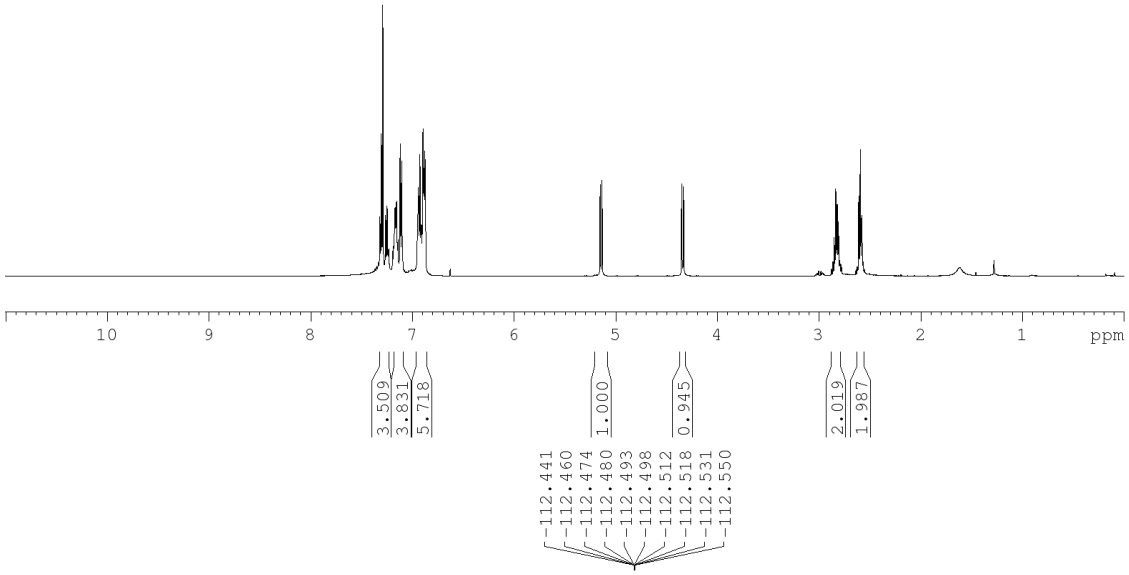
10
9
8
7
6
5
4
3
2
1
ppm
3.509
3.831
5.718
1.000
0.945
2.019
1.987
-112.441
-112.460
-112.474
-112.480
-112.493
-112.498
-112.512
-112.518
-112.531
-112.550

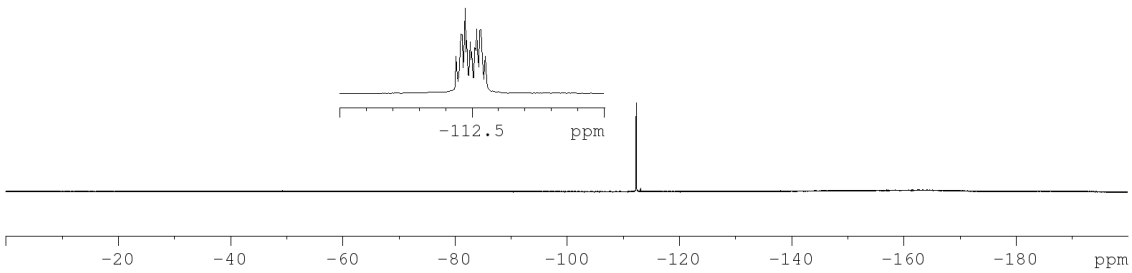
-112.5
ppm
-20
-40
-60
-80
-100
-120
-140
-160
-180
ppm

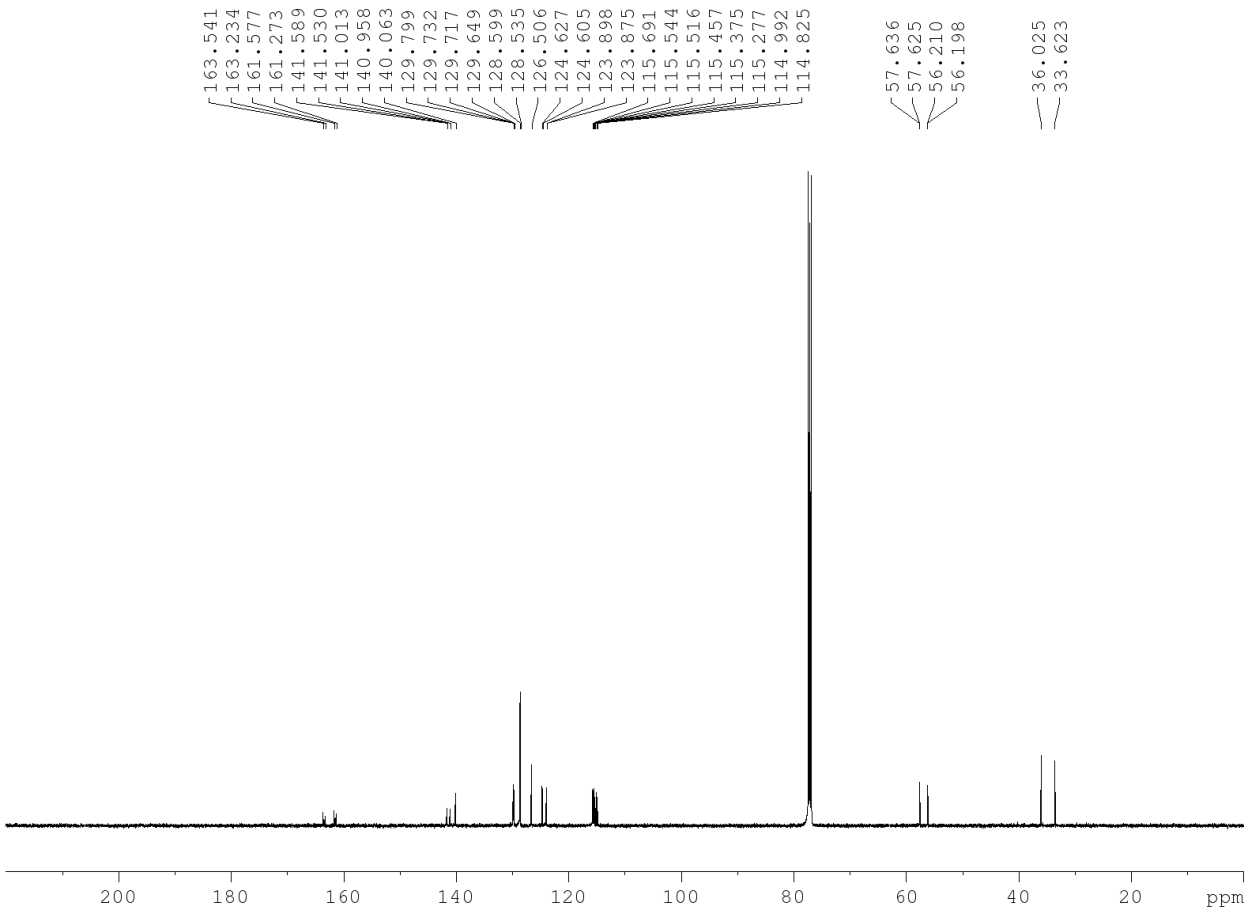
163.541
163.234
161.577
161.273
141.589
141.530
141.013
140.958
140.063
129.799
129.732
129.717
129.649
128.599
128.535
126.506
124.627
124.605
123.898
123.875
115.691
115.544
115.516
115.457
115.375
115.277
114.992
114.825
57.636
57.625
56.210
56.198
36.025
33.623
200
180
160
140
120
100
80
60
40
20
ppm

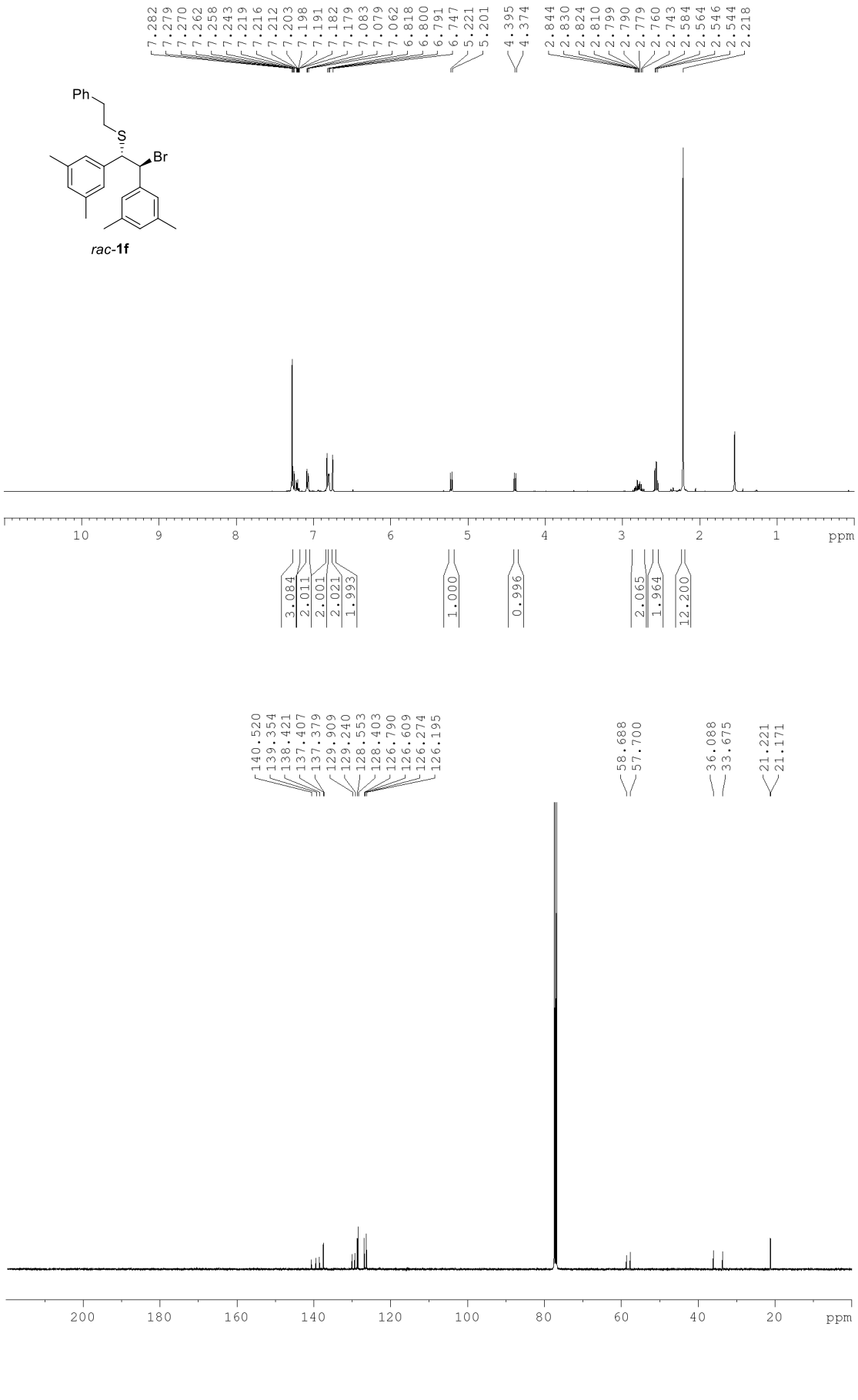
7.282
7.279
7.270
7.262
7.258
7.243
7.219
7.216
7.212
7.203
7.198
7.191
7.182
7.179
7.083
7.079
7.062
6.818
6.800
6.791
6.747
5.221
5.201
4.395
4.374
2.844
2.830
2.824
2.810
2.799
2.790
2.779
2.760
2.743
2.584
2.564
2.546
2.544
2.218
Ph
S
Br
rac-1f
10
9
8
7
6
5
4
3
2
1
ppm
3.084
2.011
2.001
2.021
1.993
1.000
0.996
2.065
1.964
12.200
140.520
139.354
138.421
137.407
137.379
129.909
129.240
128.553
128.403
126.790
126.609
126.274
126.195
58.688
57.700
36.088
33.675
21.221
21.171
200
180
160
140
120
100
80
60
40
20
ppm

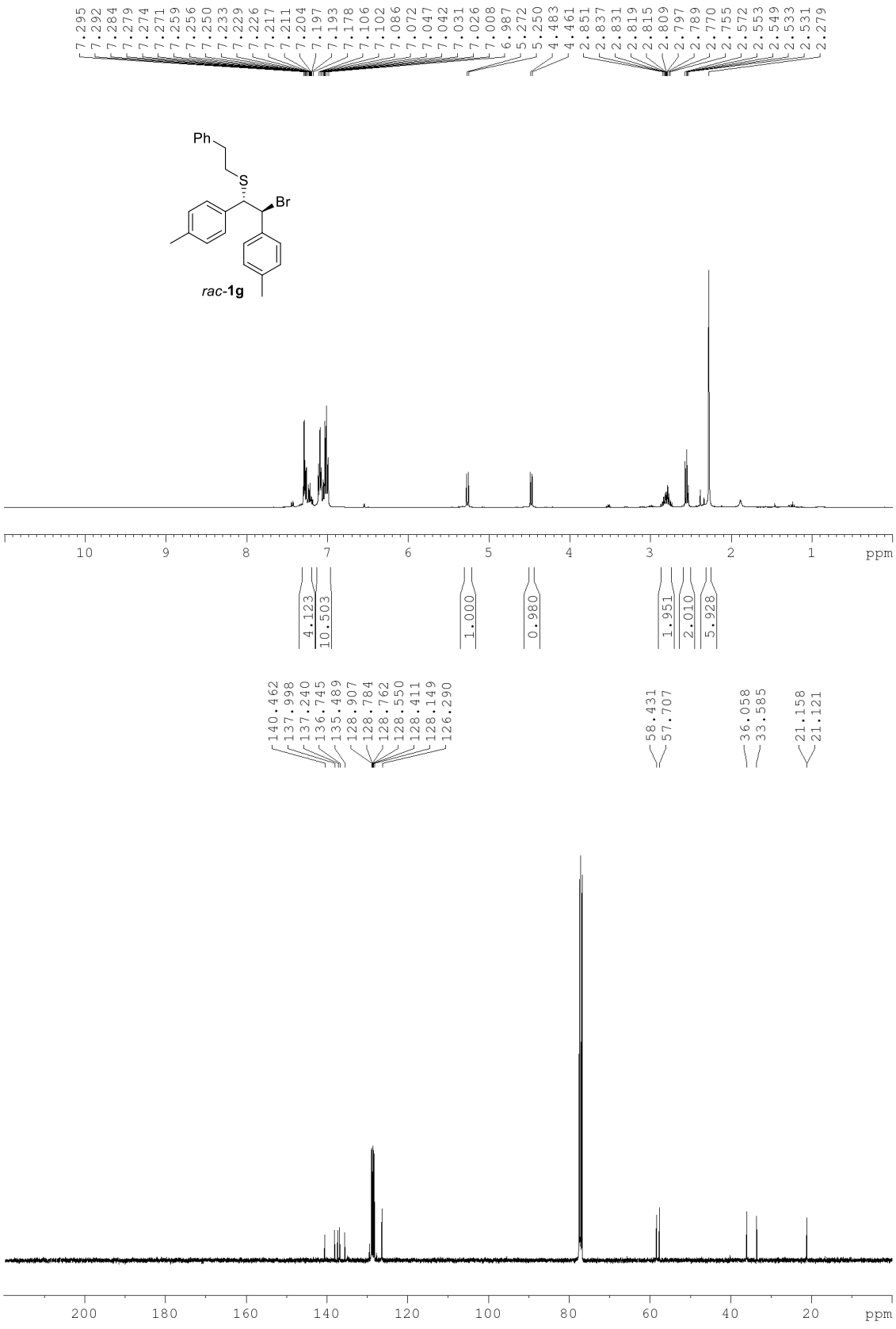
7.295
7.292
7.284
7.279
7.274
7.271
7.259
7.256
7.250
7.233
7.229
7.226
7.217
7.211
7.204
7.197
7.193
7.178
7.106
7.102
7.086
7.072
7.047
7.042
7.031
7.026
7.008
6.987
5.272
5.250
4.483
4.461
2.851
2.837
2.831
2.819
2.815
2.809
2.797
2.789
2.770
2.755
2.572
2.553
2.549
2.533
2.531
2.279
Ph
S
Br
rac-1g
10
9
8
7
6
5
4
3
2
1
ppm
4.123
10.503
1.000
0.980
1.951
2.010
5.928
140.462
137.998
137.240
136.745
135.489
128.907
128.784
128.762
128.550
128.411
128.149
126.290
58.431
57.707
36.058
33.585
21.158
21.121
200
180
160
140
120
100
80
60
40
20
ppm

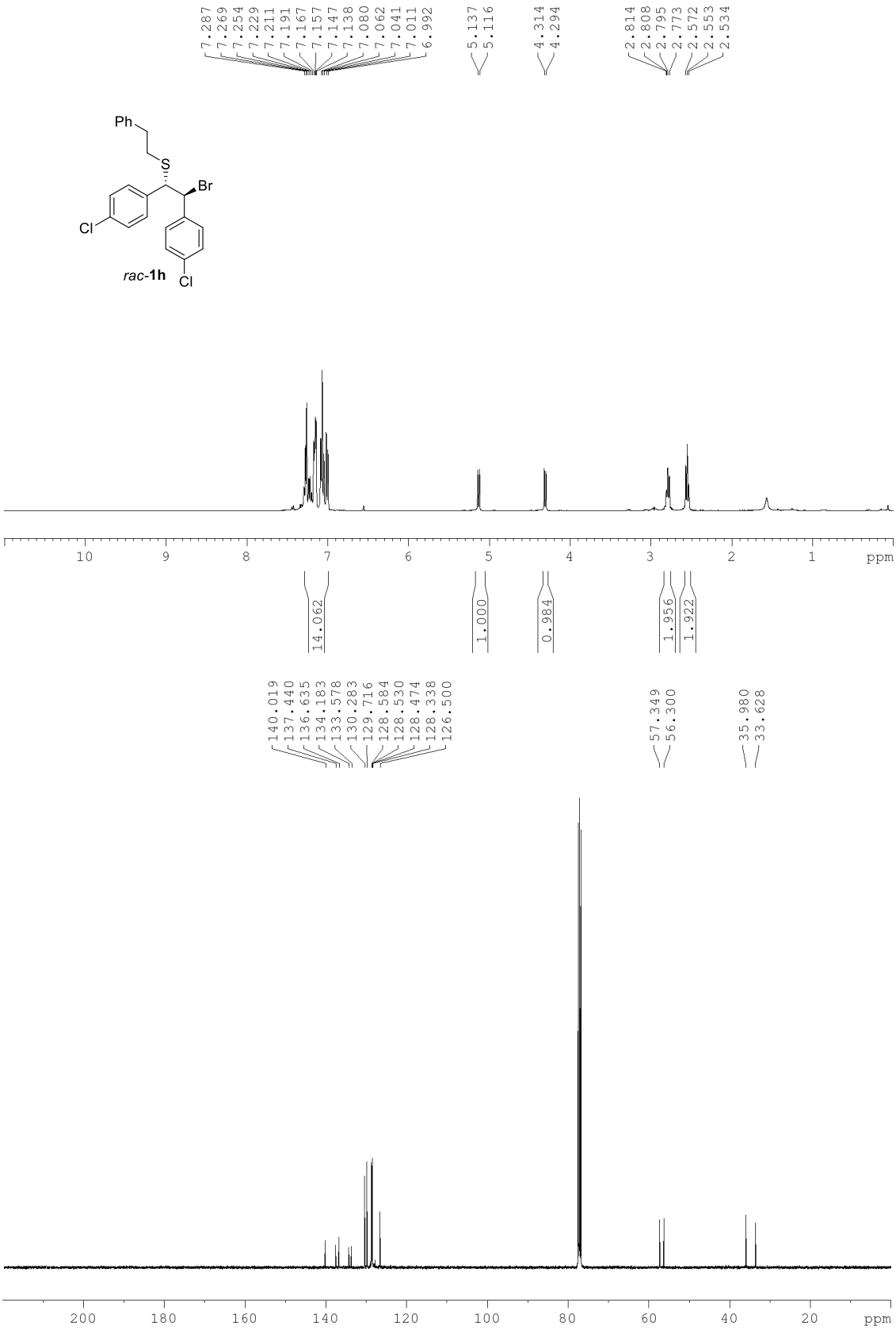
7.287
7.269
7.254
7.229
7.211
7.191
7.167
7.157
7.147
7.138
7.080
7.062
7.041
7.011
6.992
5.137
5.116
4.314
4.294
2.814
2.808
2.795
2.773
2.572
2.553
2.534
Ph
S
Br
Cl
Cl
rac-1h
10
9
8
7
6
5
4
3
2
1
ppm
14.062
1.000
0.984
1.956
1.922
140.019
137.440
136.635
134.183
133.578
130.283
129.716
128.584
128.530
128.474
128.338
126.500
57.349
56.300
35.980
33.628
200
180
160
140
120
100
80
60
40
20
ppm

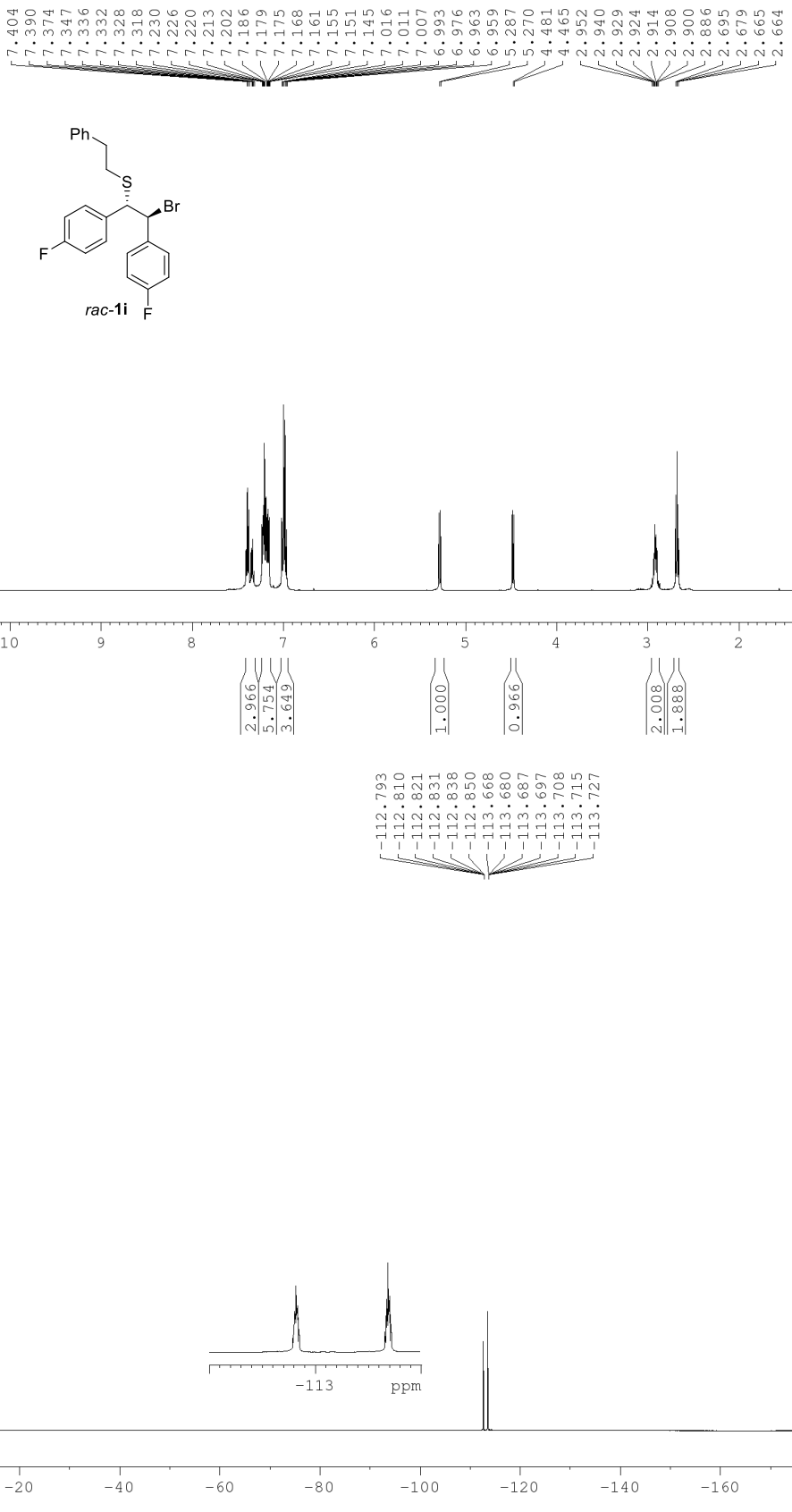
7.404
7.390
7.374
7.347
7.336
7.332
7.328
7.318
7.230
7.226
7.220
7.213
7.202
7.186
7.179
7.175
7.168
7.161
7.155
7.151
7.145
7.016
7.011
7.007
6.993
6.976
6.963
6.959
5.287
5.270
4.481
4.465
2.952
2.940
2.929
2.924
2.914
2.908
2.900
2.886
2.695
2.679
2.665
2.664
Ph
S
Br
F
F
rac-1i
10
9
8
7
6
5
4
3
2
1
ppm
2.966
5.754
3.649
1.000
0.966
2.008
1.888
-112.793
-112.810
-112.821
-112.831
-112.838
-112.850
-113.668
-113.680
-113.687
-113.697
-113.708
-113.715
-113.727
-113
ppm
-20
-40
-60
-80
-100
-120
-140
-160
-180
ppm

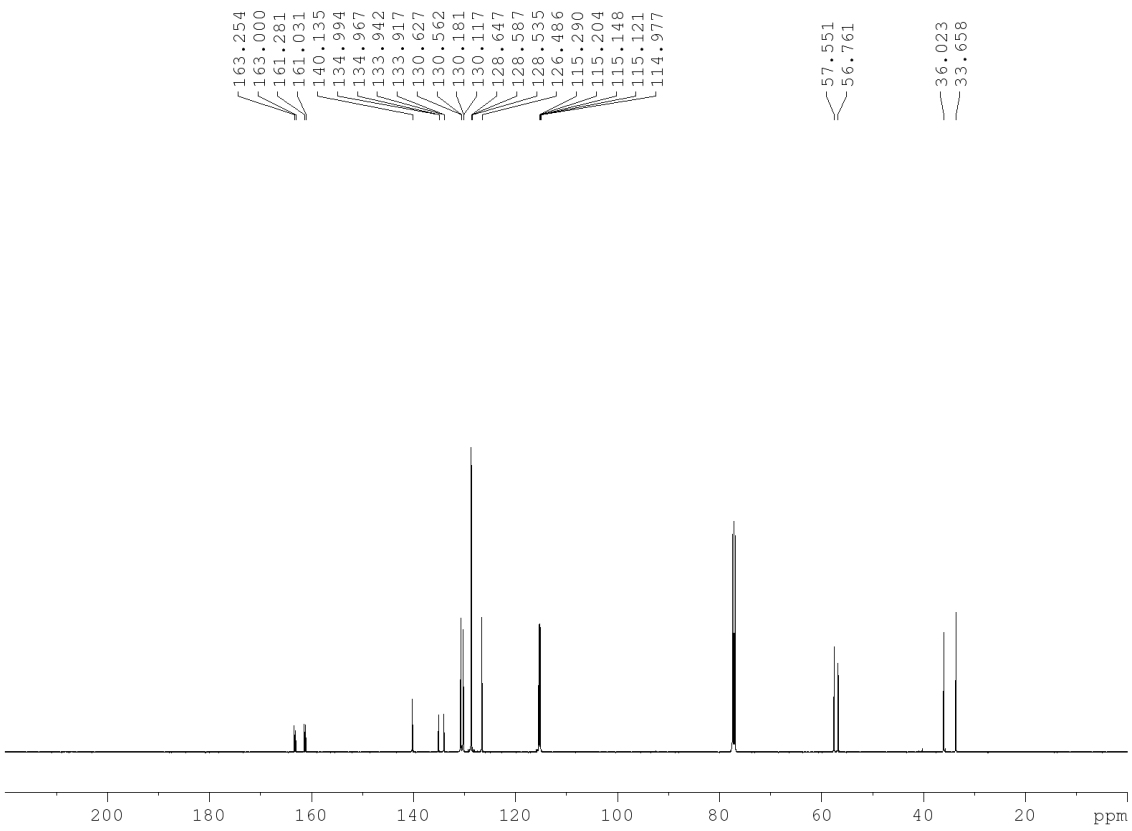
163.254
163.000
161.281
161.031
140.135
134.994
134.967
133.942
133.917
130.627
130.562
130.181
130.117
128.647
128.587
128.535
126.486
115.290
115.204
115.148
115.121
114.977
57.551
56.761
36.023
33.658
200
180
160
140
120
100
80
60
40
20
ppm

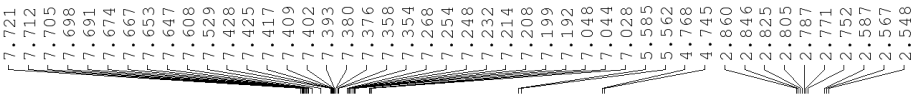
7.721
7.712
7.705
7.698
7.691
7.674
7.667
7.653
7.647
7.608
7.529
7.428
7.425
7.417
7.409
7.402
7.393
7.380
7.376
7.358
7.354
7.268
7.254
7.248
7.232
7.214
7.208
7.199
7.192
7.048
7.044
7.028
5.585
5.562
4.768
4.745
2.860
2.846
2.825
2.805
2.787
2.771
2.752
2.587
2.567
2.548

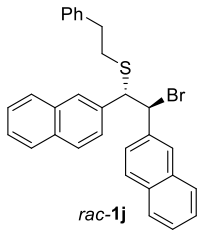
Ph
S
Br

rac-**1j**

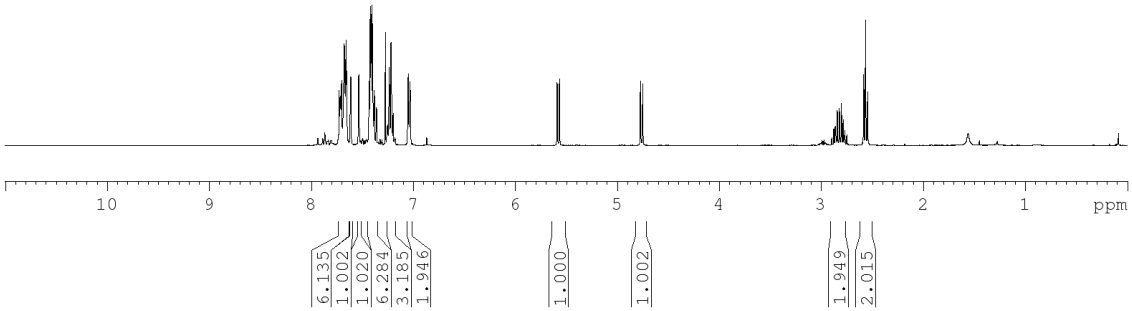
10
9
8
7
6
5
4
3
2
1
ppm
6.135
1.002
1.020
6.284
3.185
1.946
1.000
1.002
1.949
2.015

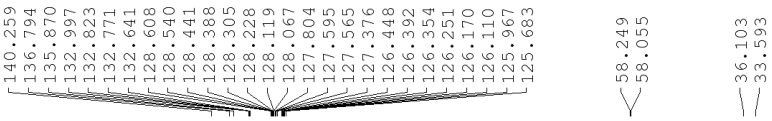
140.259
136.794
135.870
132.997
132.823
132.771
132.641
128.608
128.540
128.441
128.388
128.305
128.228
128.119
128.067
127.804
127.595
127.565
127.376
126.448
126.392
126.354
126.251
126.170
126.110
125.967
125.683
58.249
58.055
36.103
33.593

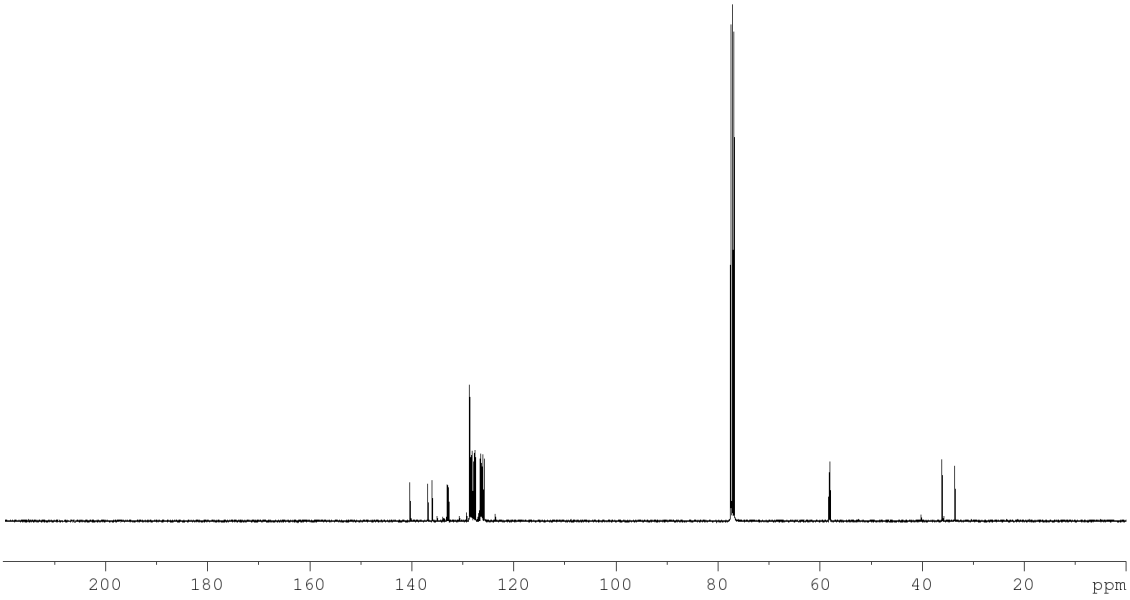
200
180
160
140
120
100
80
60
40
20
ppm

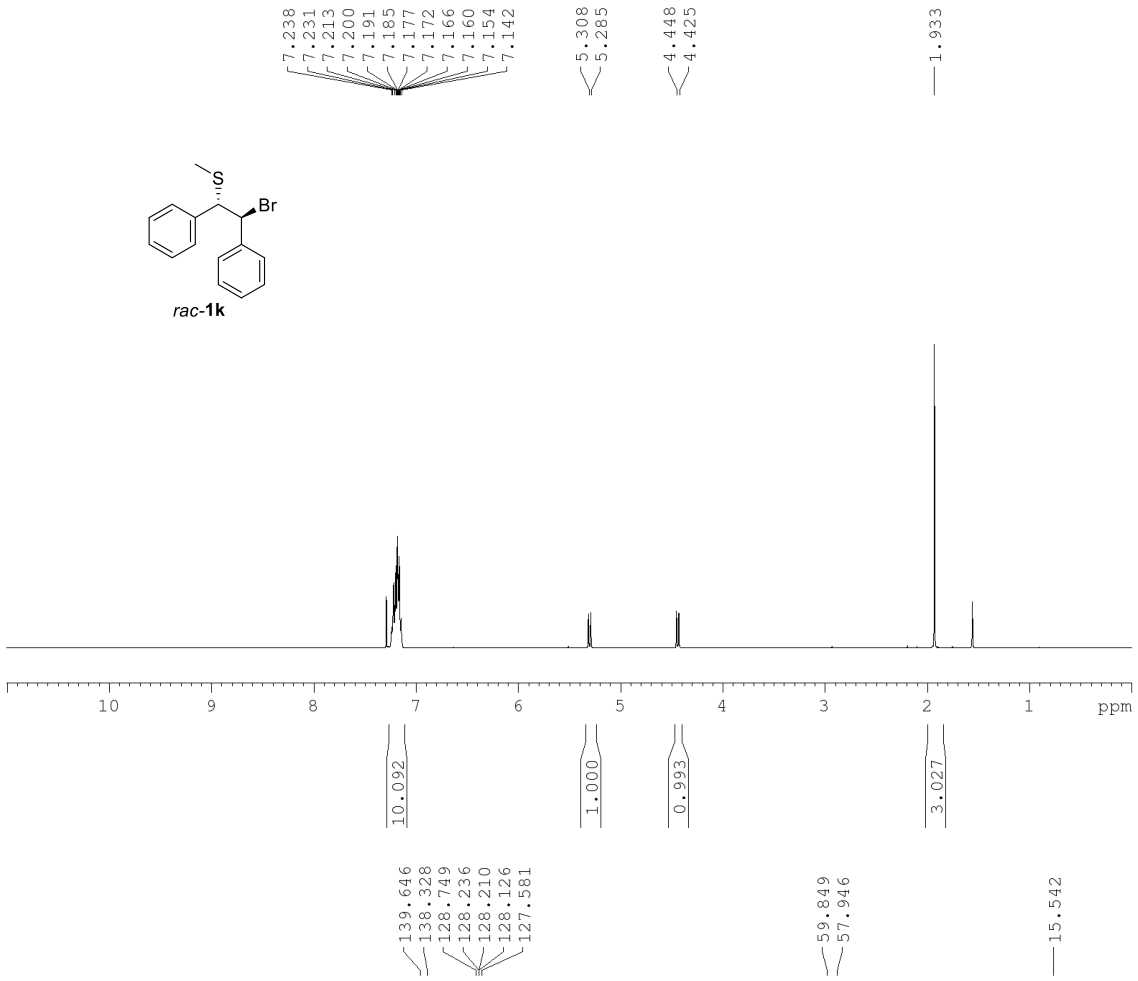
7.238
7.231
7.213
7.200
7.191
7.185
7.177
7.172
7.166
7.160
7.154
7.142
5.308
5.285
4.448
4.425
1.933
S
Br
rac-1k
10.092
1.000
0.993
3.027
ppm

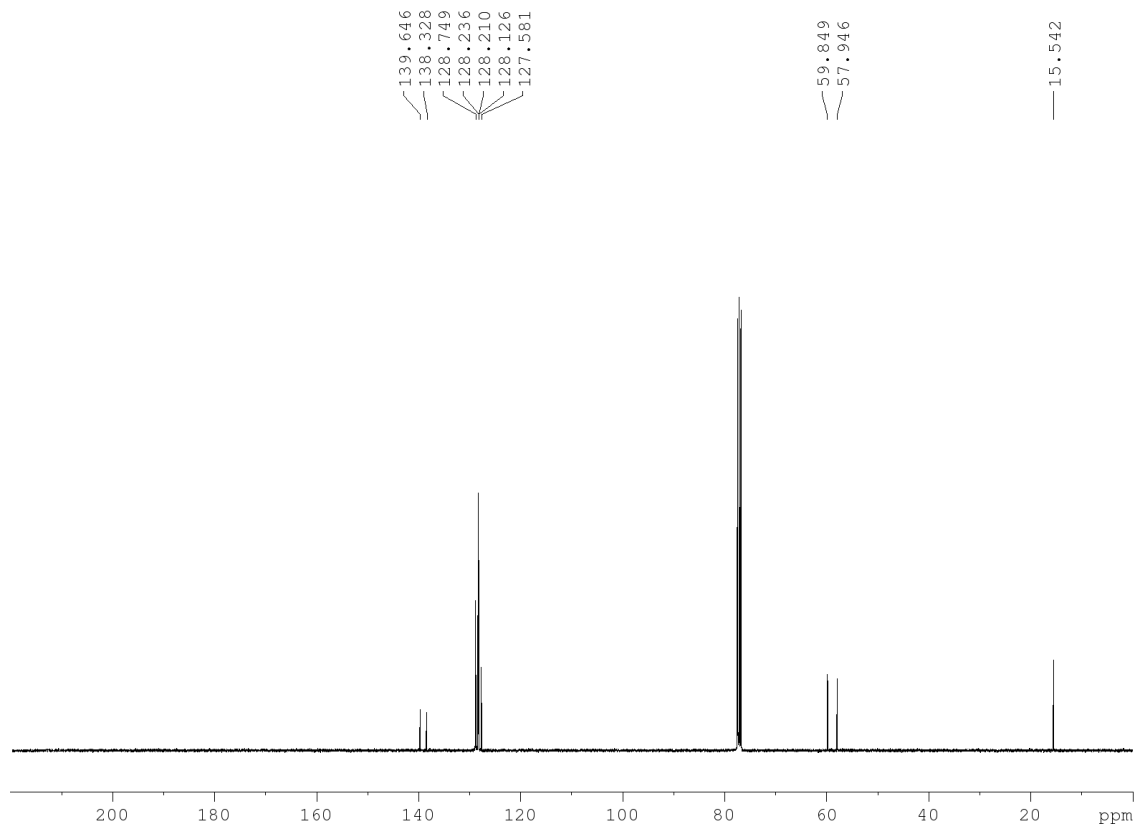
139.646
138.328
128.749
128.236
128.210
128.126
127.581
59.849
57.946
15.542
ppm

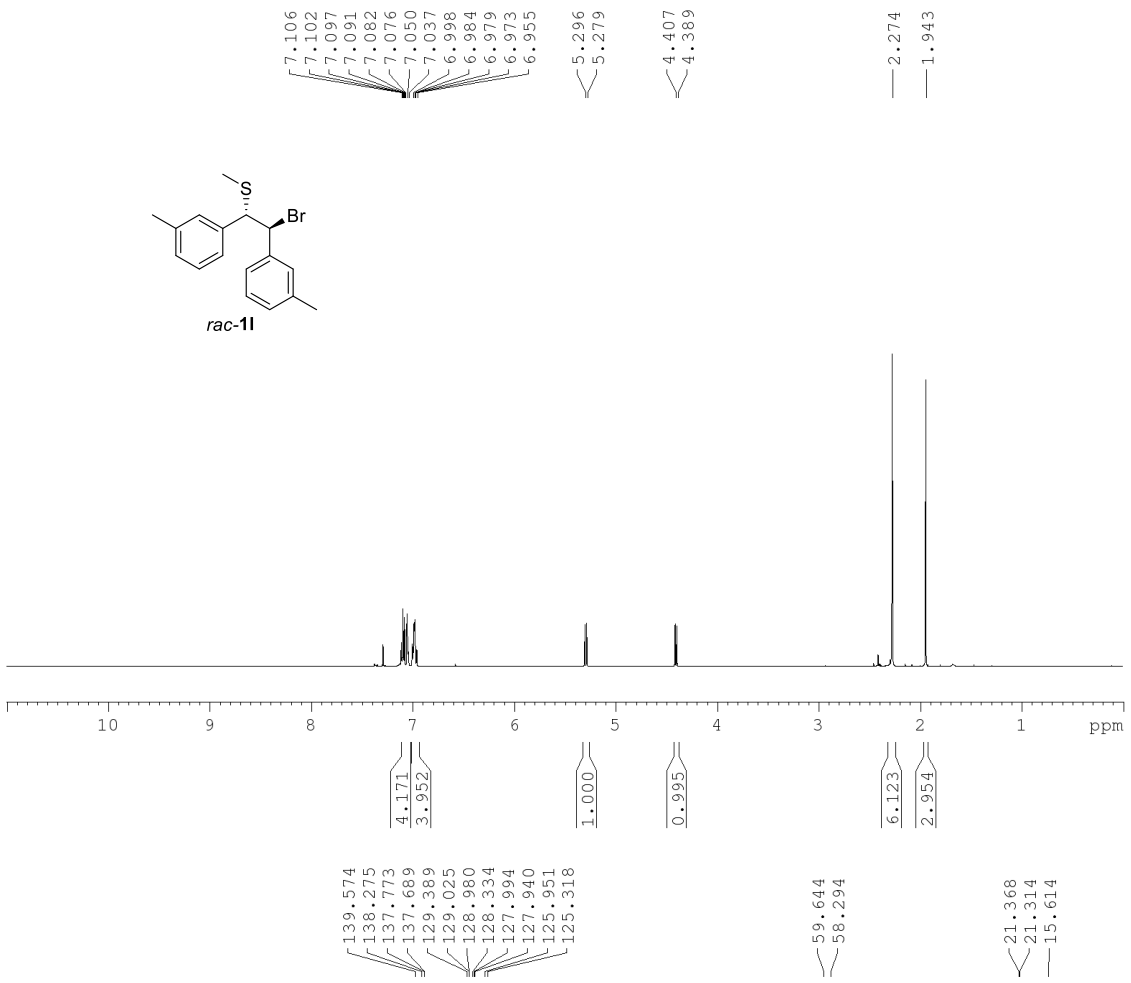
7.106
7.102
7.097
7.091
7.082
7.076
7.050
7.037
6.998
6.984
6.979
6.973
6.955
5.296
5.279
4.407
4.389
2.274
1.943
S
Br
rac-1l
10
9
8
7
6
5
4
3
2
1
ppm
4.171
3.952
1.000
0.995
6.123
2.954

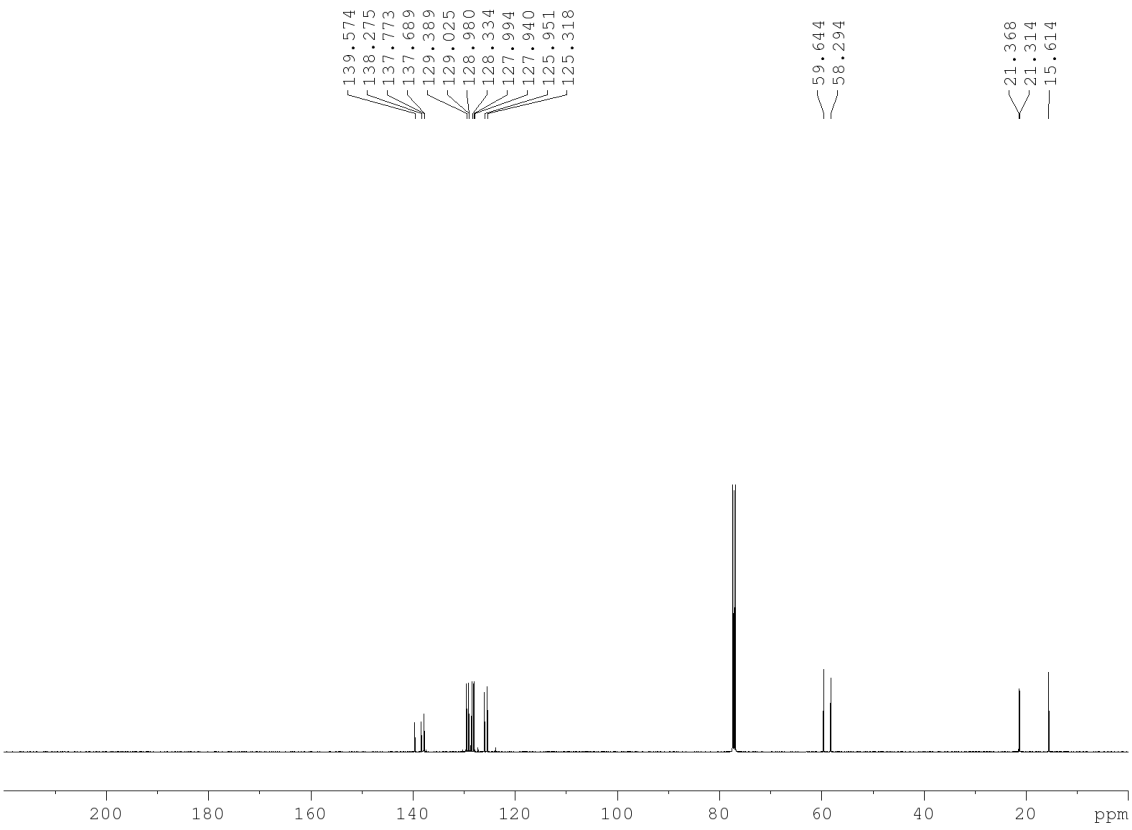
139.574
138.275
137.773
137.689
129.389
129.025
128.980
128.334
127.994
127.940
125.951
125.318
59.644
58.294
21.368
21.314
15.614
200
180
160
140
120
100
80
60
40
20
ppm

Products

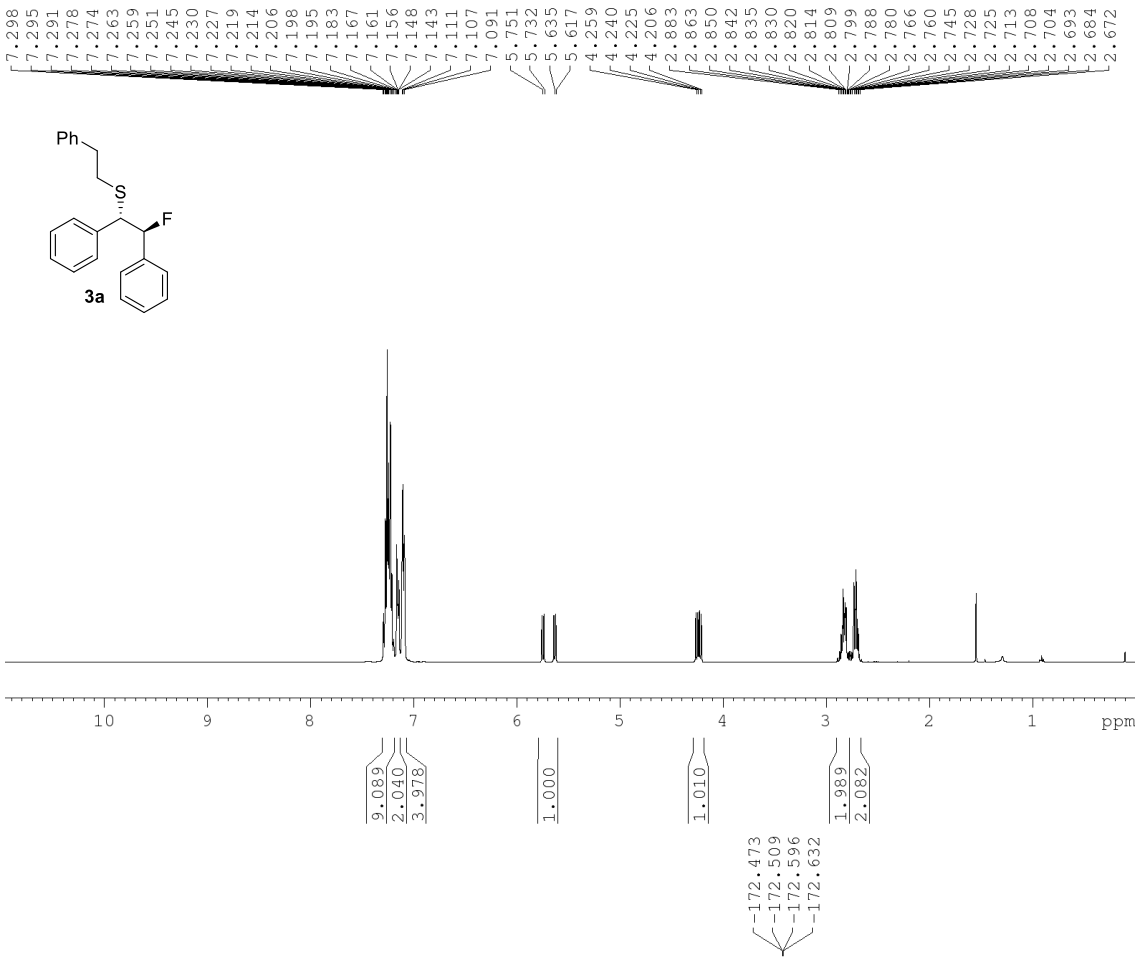
7.298
7.295
7.291
7.278
7.274
7.263
7.259
7.251
7.245
7.230
7.227
7.219
7.214
7.206
7.198
7.195
7.183
7.167
7.161
7.156
7.148
7.143
7.111
7.107
7.091
5.751
5.732
5.635
5.617
4.259
4.240
4.225
4.206
2.883
2.863
2.850
2.842
2.835
2.830
2.820
2.814
2.809
2.799
2.788
2.780
2.766
2.760
2.745
2.728
2.725
2.713
2.708
2.704
2.693
2.684
2.672
Ph
S
F
3a
10
9
8
7
6
5
4
3
2
1
ppm
9.089
2.040
3.978
1.000
1.010
1.989
2.082
-172.473
-172.509
-172.596
-172.632

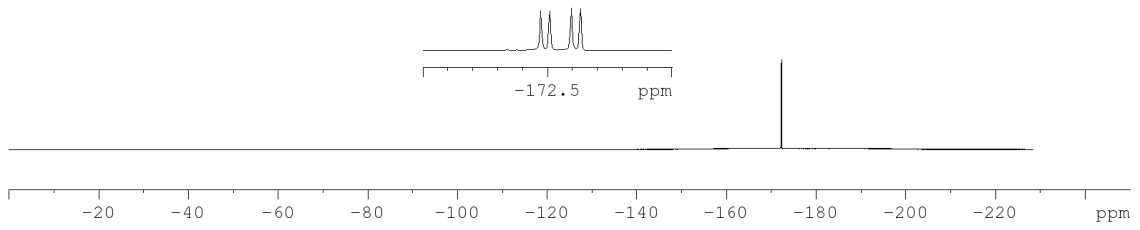
-172.5
ppm
-20
-40
-60
-80
-100
-120
-140
-160
-180
-200
-220
ppm

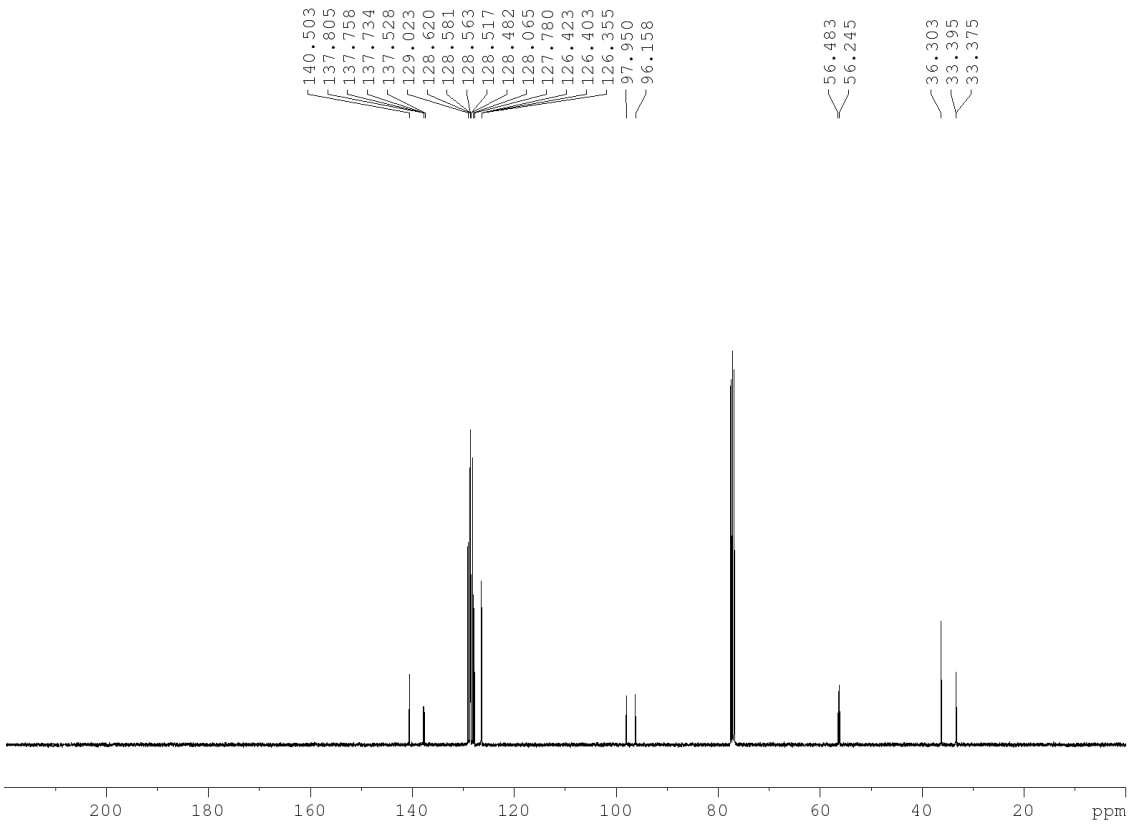
140.503
137.805
137.758
137.734
137.528
129.023
128.620
128.581
128.563
128.517
128.482
128.065
127.780
126.423
126.403
126.355
97.950
96.158
56.483
56.245
36.303
33.395
33.375
200
180
160
140
120
100
80
60
40
20
ppm

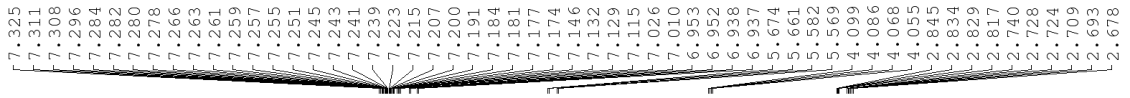
7.325
7.311
7.308
7.296
7.284
7.282
7.280
7.278
7.266
7.263
7.261
7.259
7.257
7.255
7.251
7.245
7.243
7.241
7.239
7.223
7.215
7.207
7.200
7.191
7.184
7.181
7.177
7.174
7.146
7.132
7.129
7.115
7.026
7.010
6.953
6.952
6.938
6.937
5.674
5.661
5.582
5.569
4.099
4.086
4.068
4.055
2.845
2.834
2.829
2.817
2.740
2.728
2.724
2.709
2.693
2.678

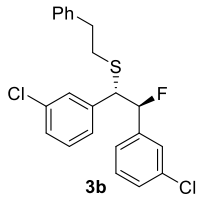
Ph
S
Cl
F
Cl

3b

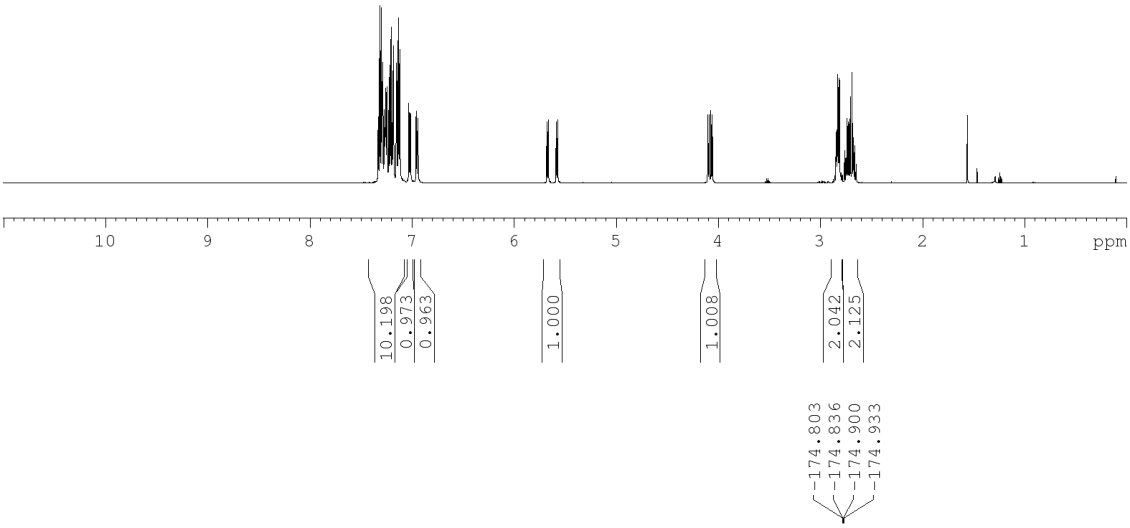
10
9
8
7
6
5
4
3
2
1
ppm
10.198
0.973
0.963
1.000
1.008
2.042
2.125
-174.803
-174.836
-174.900
-174.933

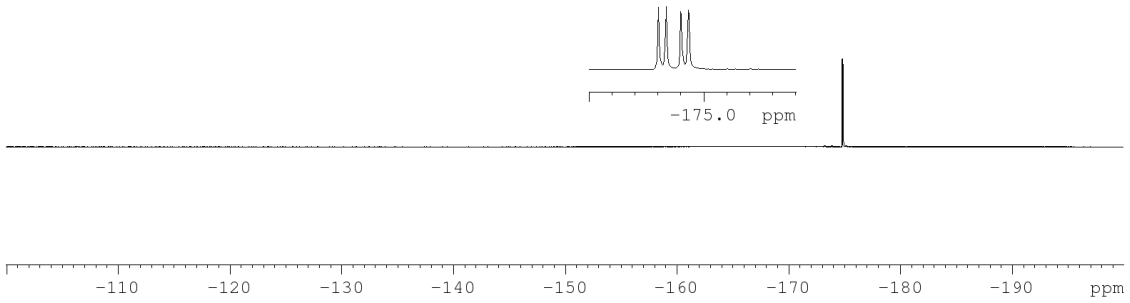
-175.0
ppm
-110
-120
-130
-140
-150
-160
-170
-180
-190
ppm

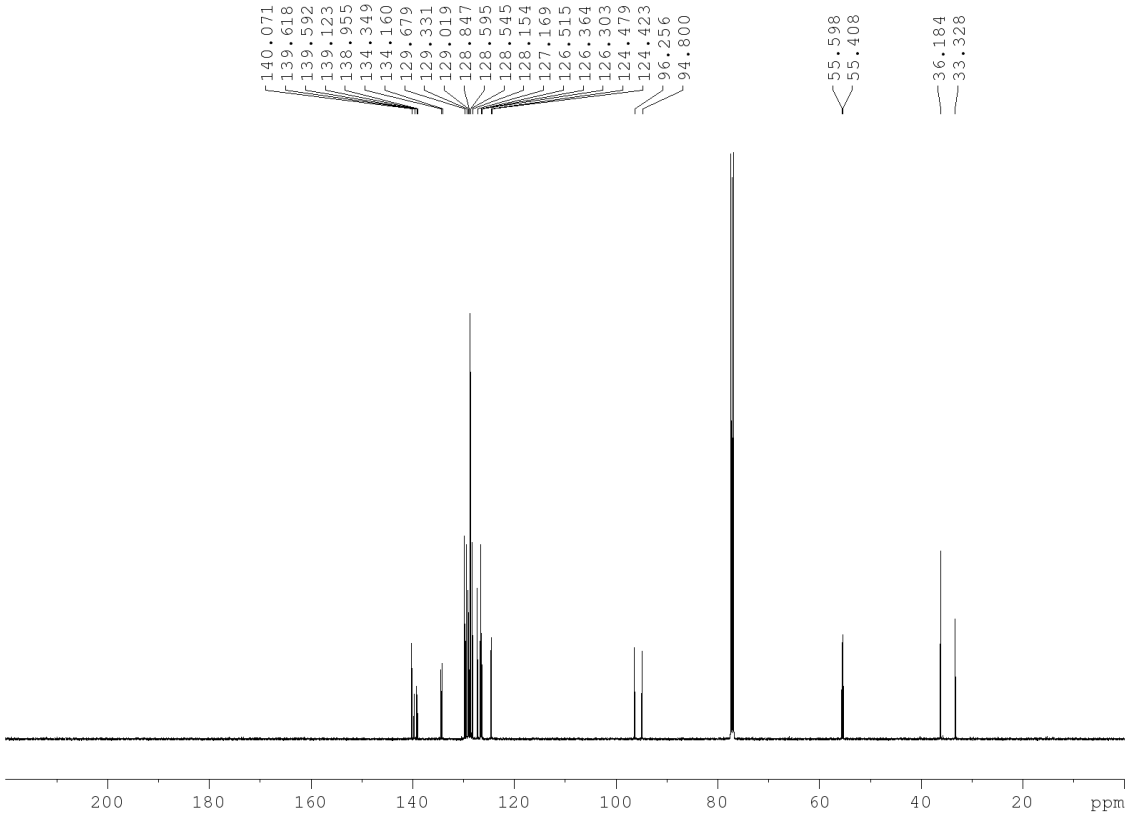
140.071
139.618
139.592
139.123
138.955
134.349
134.160
129.679
129.331
129.019
128.847
128.595
128.545
128.154
127.169
126.515
126.364
126.303
124.479
124.423
96.256
94.800
55.598
55.408
36.184
33.328
200
180
160
140
120
100
80
60
40
20
ppm

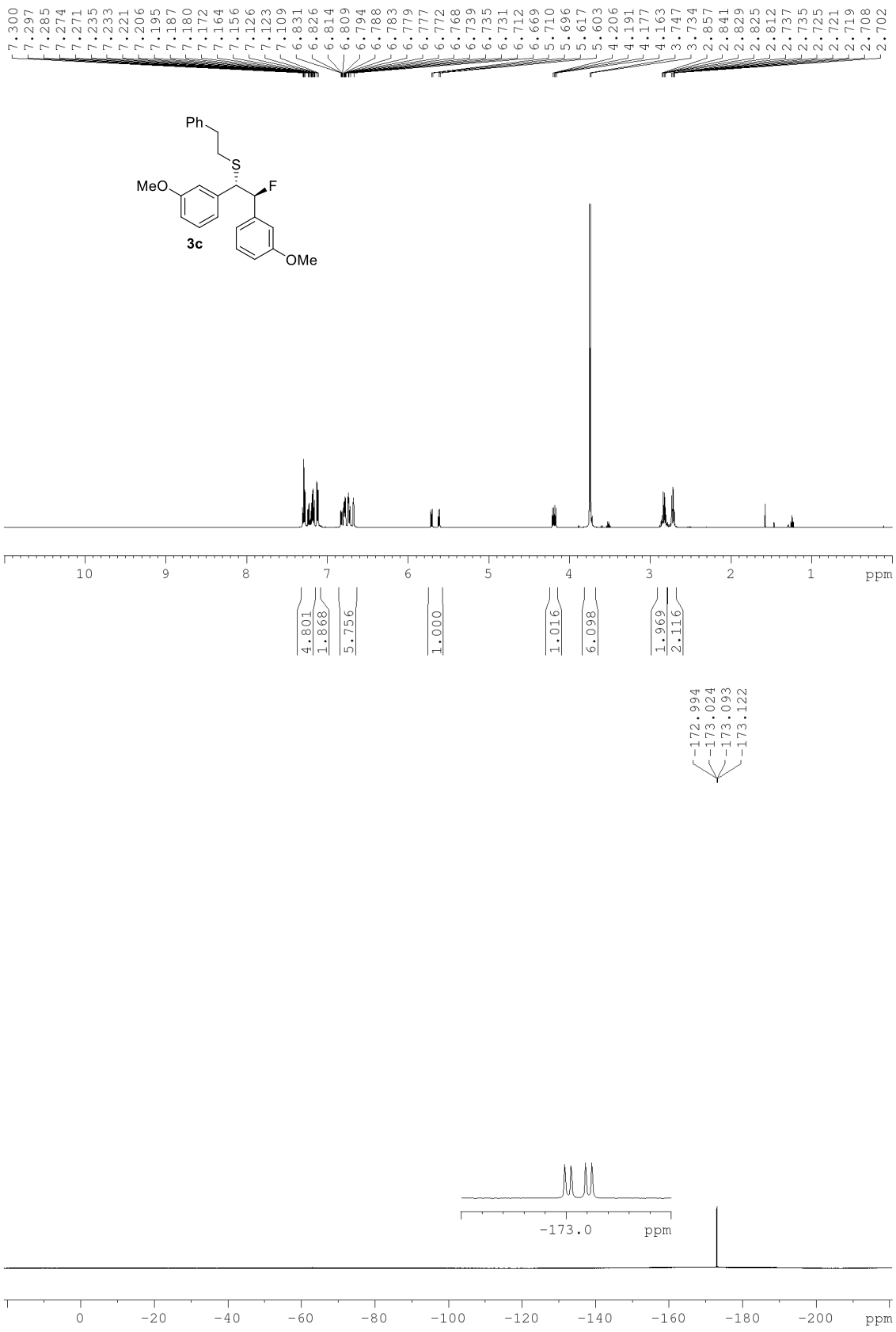
7.300
7.297
7.285
7.274
7.271
7.235
7.233
7.221
7.206
7.195
7.187
7.180
7.172
7.164
7.156
7.126
7.123
7.109
6.831
6.826
6.814
6.809
6.794
6.788
6.783
6.779
6.777
6.772
6.768
6.739
6.735
6.731
6.712
6.669
5.710
5.696
5.617
5.603
4.206
4.191
4.177
4.163
3.747
3.734
2.857
2.841
2.829
2.825
2.812
2.737
2.735
2.725
2.721
2.719
2.708
2.702
Ph
S
MeO
F
OMe
3c
10
9
8
7
6
5
4
3
2
1
ppm
4.801
1.868
5.756
1.000
1.016
6.098
1.969
2.116
-172.994
-173.024
-173.093
-173.122
-173.0
ppm
0
-20
-40
-60
-80
-100
-120
-140
-160
-180
-200
ppm

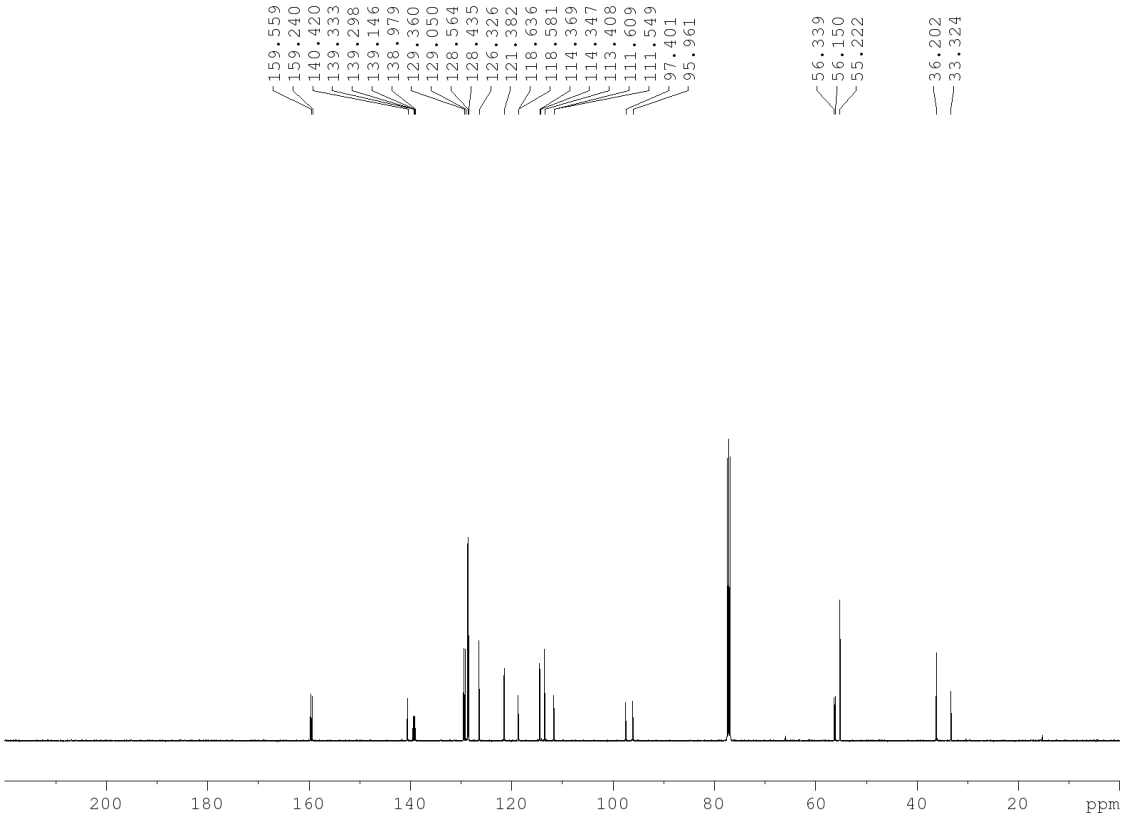
159.559
159.240
140.420
139.333
139.298
139.146
138.979
129.360
129.050
128.564
128.435
126.326
121.382
118.636
118.581
114.369
114.347
113.408
111.609
111.549
97.401
95.961
56.339
56.150
55.222
36.202
33.324
200
180
160
140
120
100
80
60
40
20
ppm

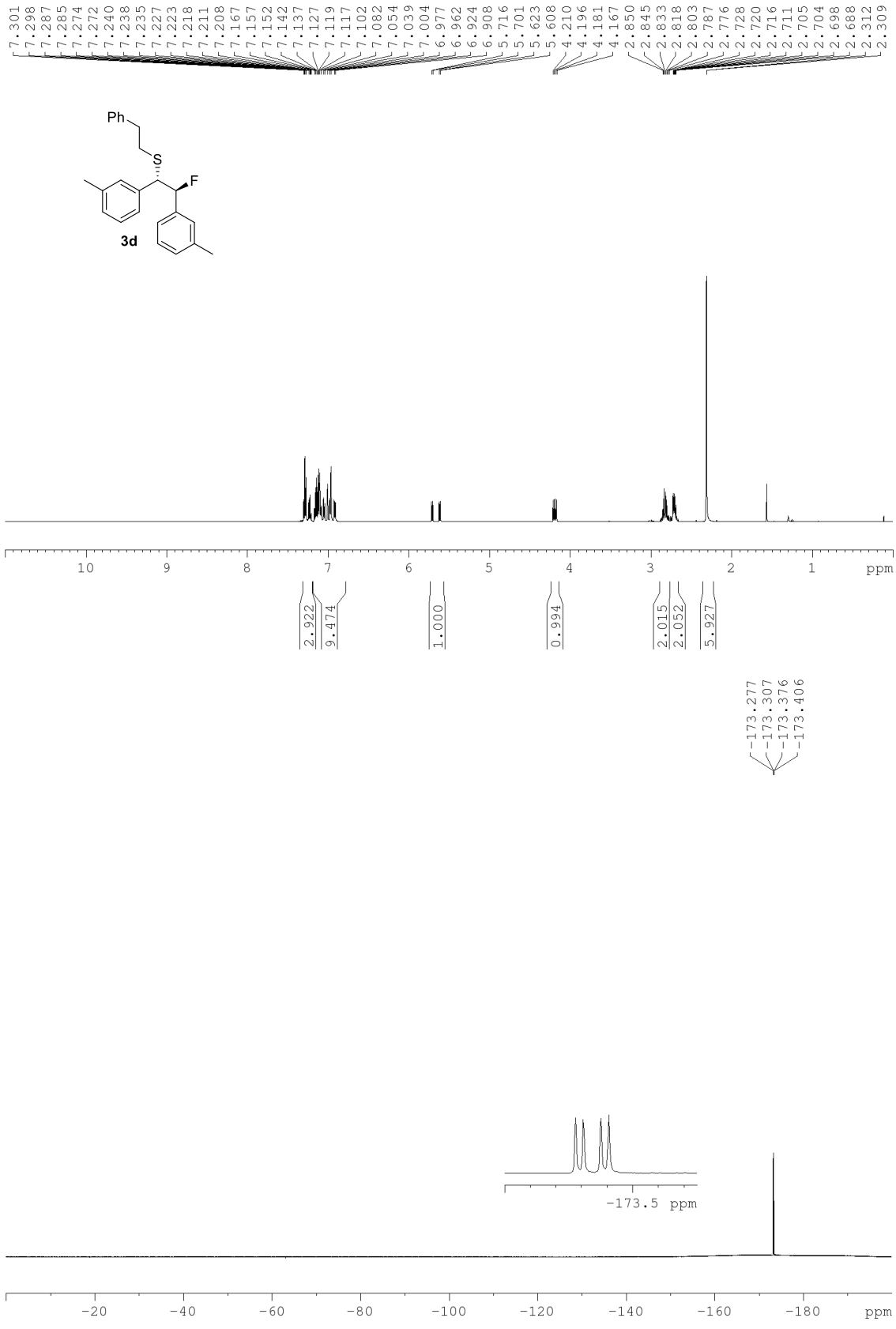
7.301
7.298
7.287
7.285
7.274
7.272
7.240
7.238
7.235
7.227
7.223
7.218
7.211
7.208
7.167
7.157
7.152
7.142
7.137
7.127
7.119
7.117
7.102
7.082
7.054
7.039
7.004
6.977
6.962
6.924
6.908
5.716
5.701
5.623
5.608
4.210
4.196
4.181
4.167
2.850
2.845
2.833
2.818
2.803
2.787
2.776
2.728
2.720
2.716
2.711
2.705
2.704
2.698
2.688
2.312
2.309
Ph
S
F
3d
10
9
8
7
6
5
4
3
2
1
ppm
2.922
9.474
1.000
0.994
2.015
2.052
5.927
-173.277
-173.307
-173.376
-173.406
-173.5 ppm
-20
-40
-60
-80
-100
-120
-140
-160
-180
ppm

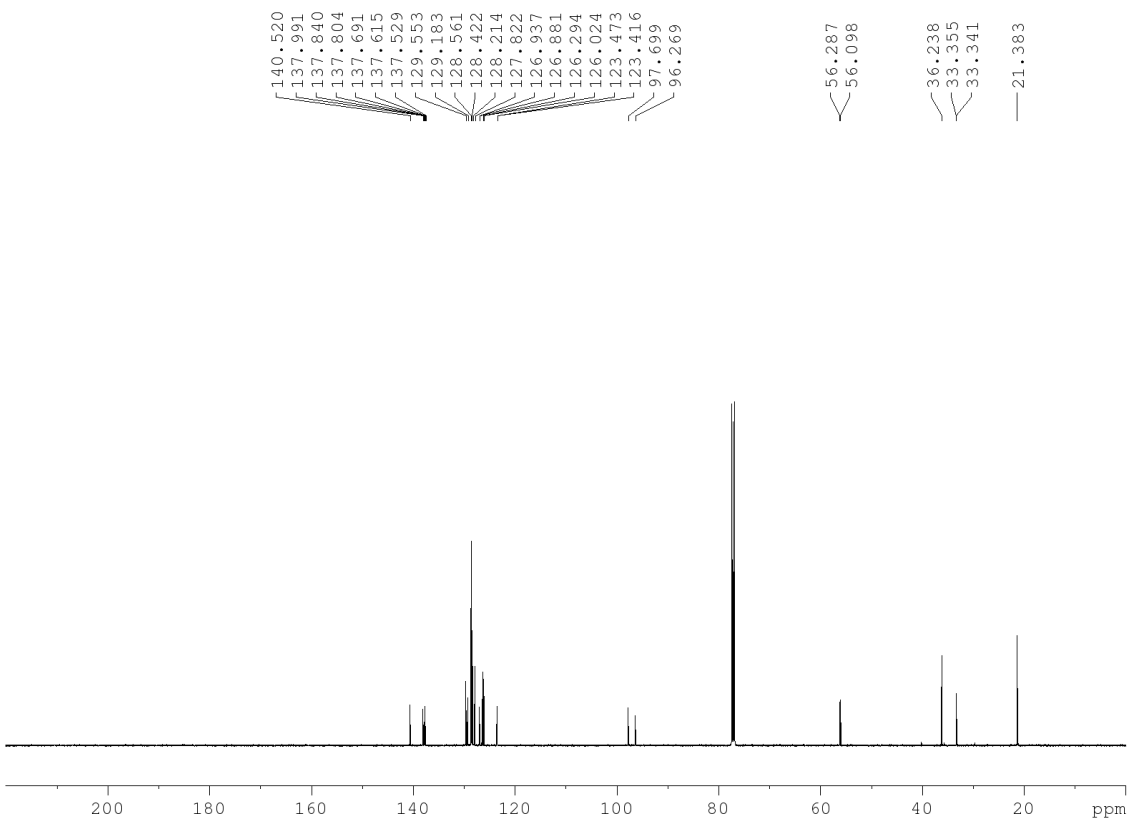
140.520
137.991
137.840
137.804
137.691
137.615
137.529
129.553
129.183
128.561
128.422
128.214
127.822
126.937
126.881
126.294
126.024
123.473
123.416
97.699
96.269
56.287
56.098
36.238
33.355
33.341
21.383
200
180
160
140
120
100
80
60
40
20
ppm

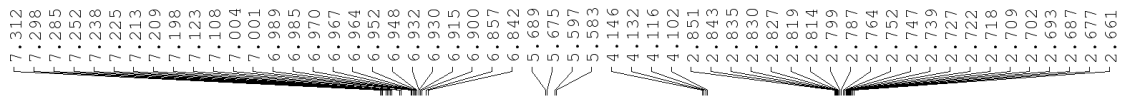
7.312
7.298
7.285
7.252
7.238
7.225
7.213
7.209
7.198
7.123
7.108
7.004
7.001
6.989
6.985
6.970
6.967
6.964
6.952
6.948
6.932
6.930
6.915
6.900
6.857
6.842
5.689
5.675
5.597
5.583
4.146
4.132
4.116
4.102
2.851
2.843
2.835
2.830
2.827
2.819
2.814
2.799
2.787
2.764
2.752
2.747
2.739
2.727
2.722
2.718
2.709
2.702
2.693
2.687
2.677
2.661

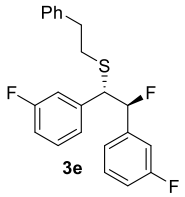
Ph
S
F
F
F

3e

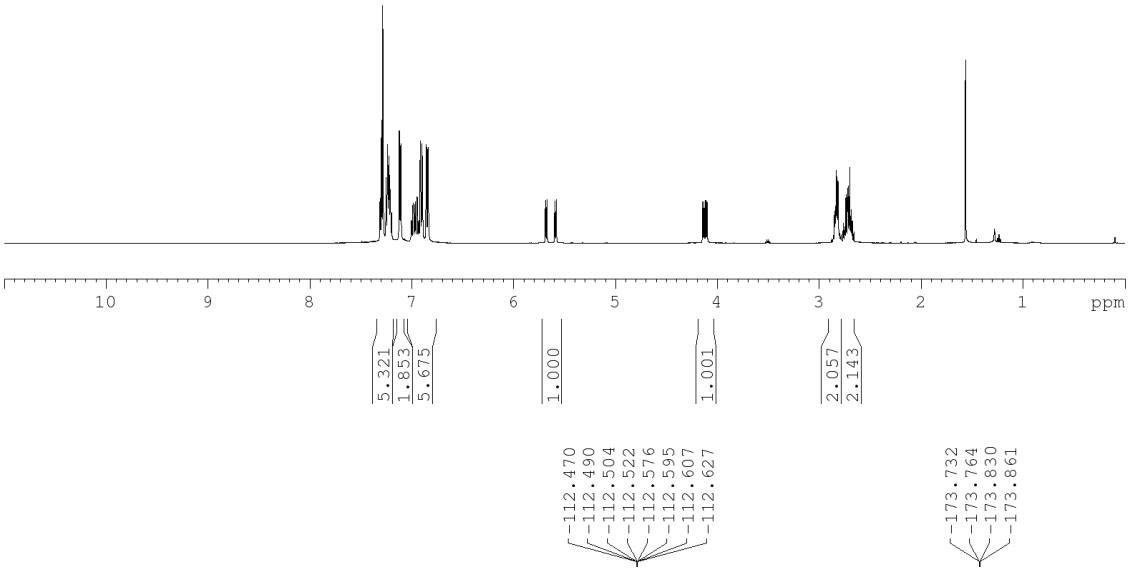
10
9
8
7
6
5
4
3
2
1
ppm
5.321
1.853
5.675
1.000
1.001
2.057
2.143

-112.470
-112.490
-112.504
-112.522
-112.576
-112.595
-112.607
-112.627

-173.732
-173.764
-173.830
-173.861

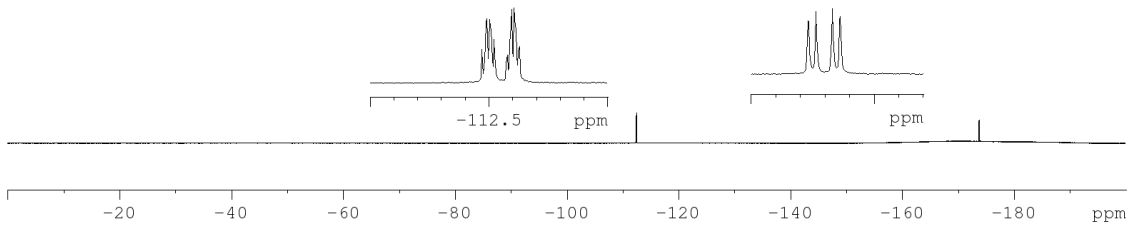
-112.5
ppm
ppm
-20
-40
-60
-80
-100
-120
-140
-160
-180
ppm

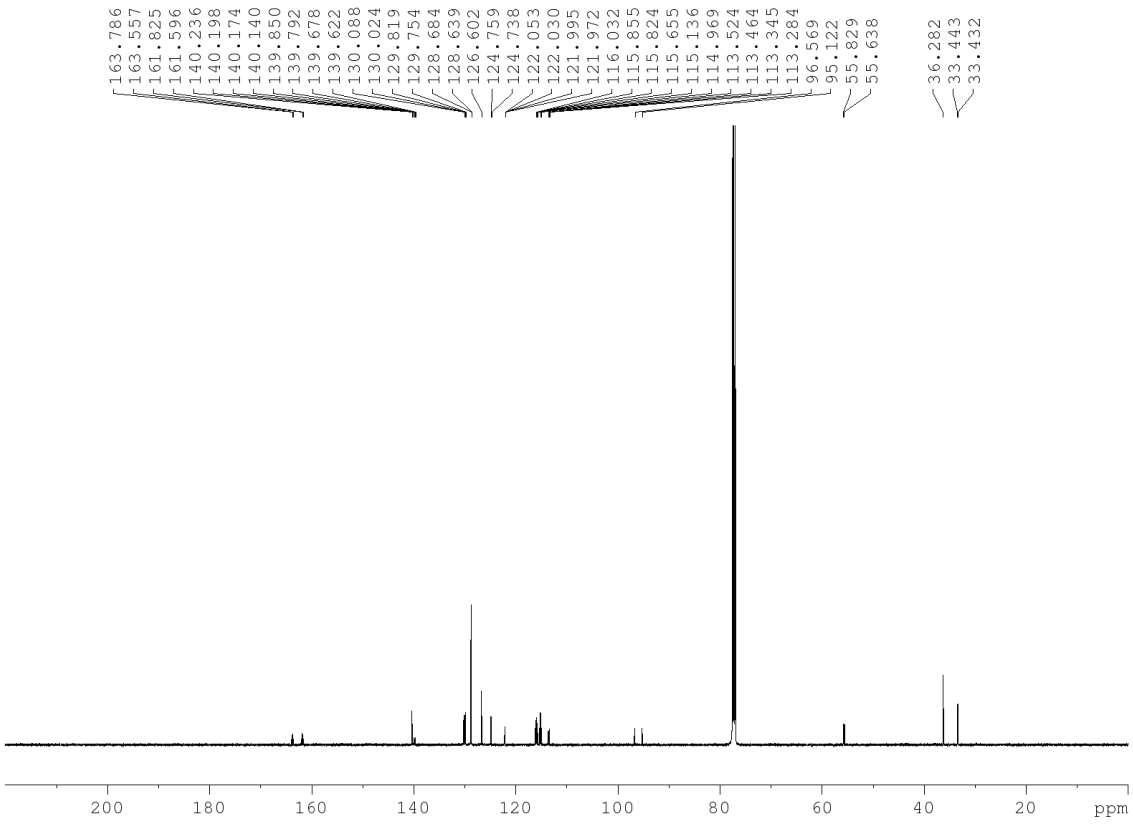
163.786
163.557
161.825
161.596
140.236
140.198
140.174
140.140
139.850
139.792
139.678
139.622
130.088
130.024
129.819
129.754
128.684
128.639
126.602
124.759
124.738
122.053
122.030
121.995
121.972
116.032
115.855
115.824
115.655
115.136
114.969
113.524
113.464
113.345
113.284
96.569
95.122
55.829
55.638
36.282
33.443
33.432
200
180
160
140
120
100
80
60
40
20
ppm

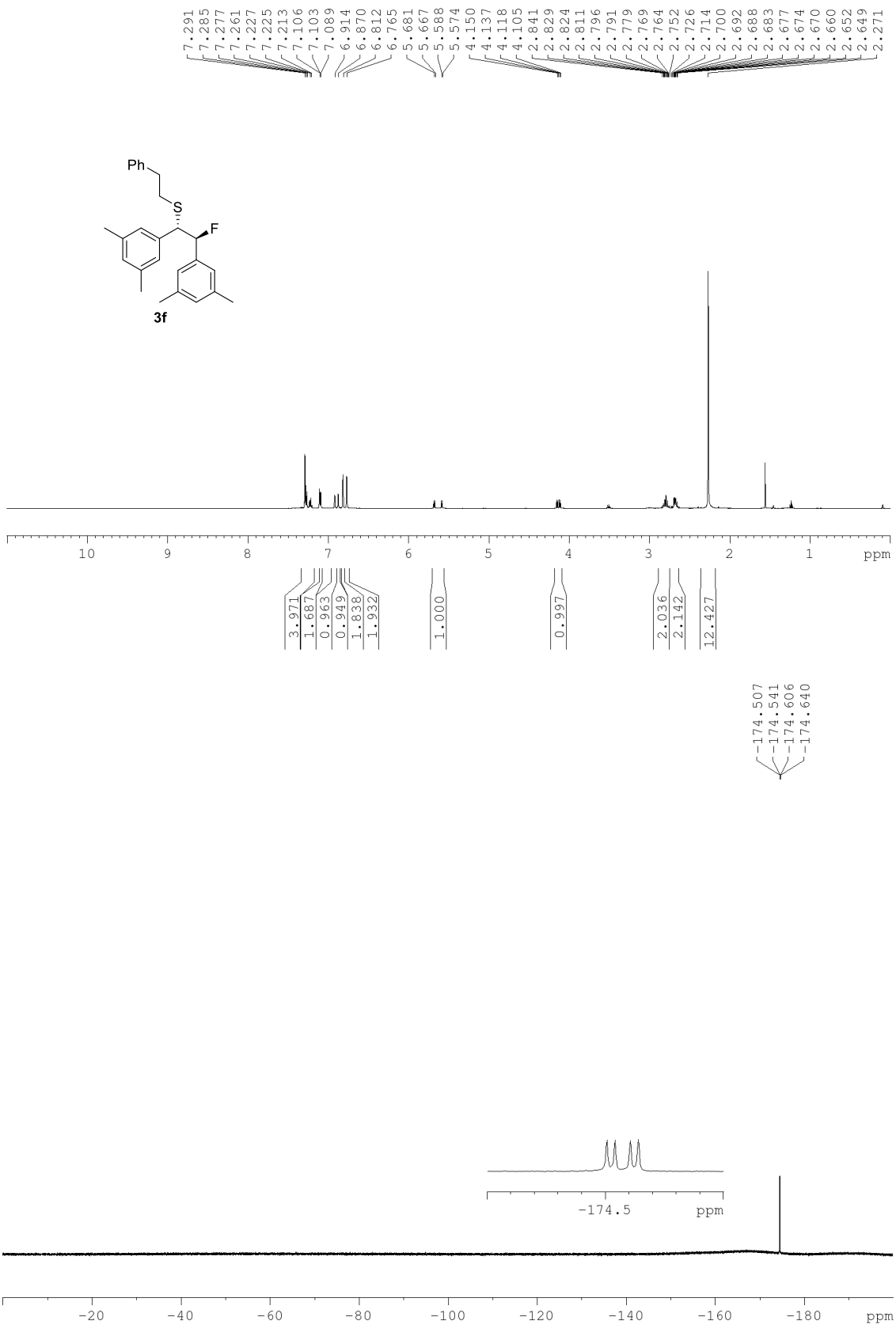
7.291
7.285
7.277
7.261
7.227
7.225
7.213
7.106
7.103
7.089
6.914
6.870
6.812
6.765
5.681
5.667
5.588
5.574
4.150
4.137
4.118
4.105
2.841
2.829
2.824
2.811
2.796
2.791
2.779
2.769
2.764
2.752
2.726
2.714
2.700
2.692
2.688
2.683
2.677
2.674
2.670
2.660
2.652
2.649
2.271
Ph
S
F
3f
10
9
8
7
6
5
4
3
2
1
ppm
3.971
1.687
0.963
0.949
1.838
1.932
1.000
0.997
2.036
2.142
12.427
-174.507
-174.541
-174.606
-174.640
-174.5
ppm
-20
-40
-60
-80
-100
-120
-140
-160
-180
ppm

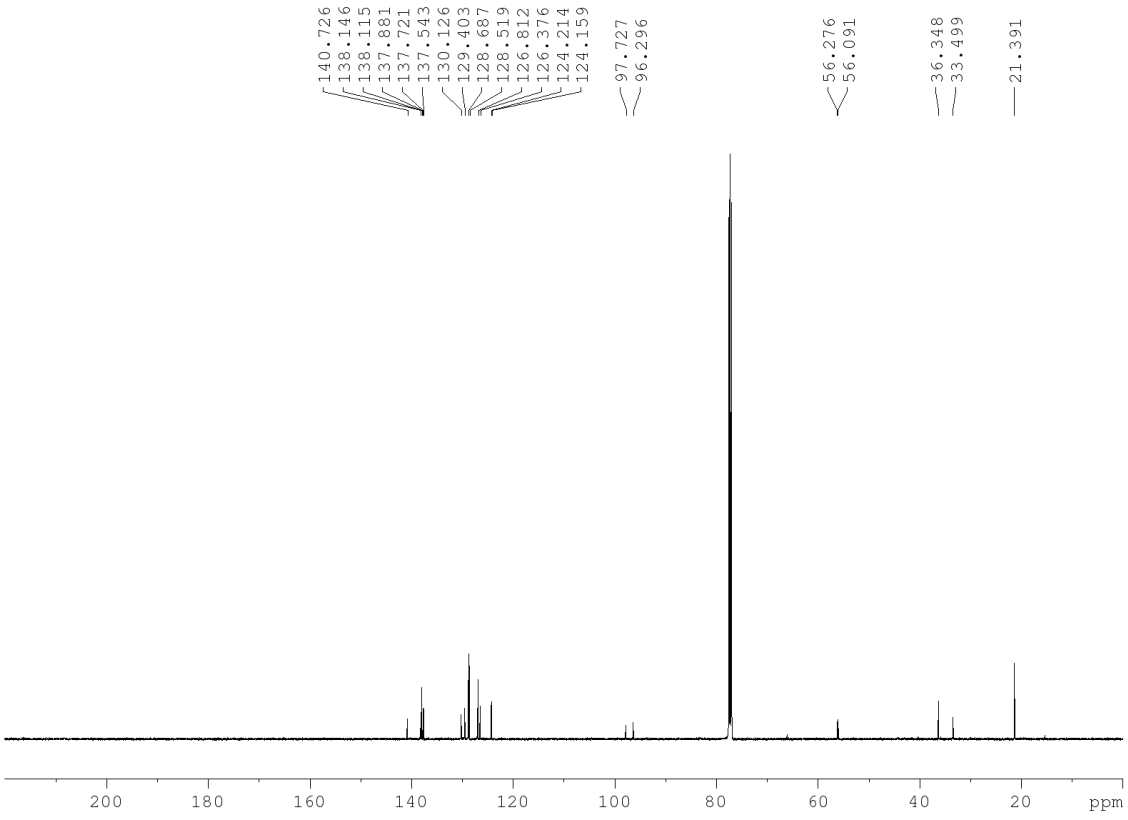
140.726
138.146
138.115
137.881
137.721
137.543
130.126
129.403
128.687
128.519
126.812
126.376
124.214
124.159
97.727
96.296
56.276
56.091
36.348
33.999
21.391
200
180
160
140
120
100
80
60
40
20
ppm

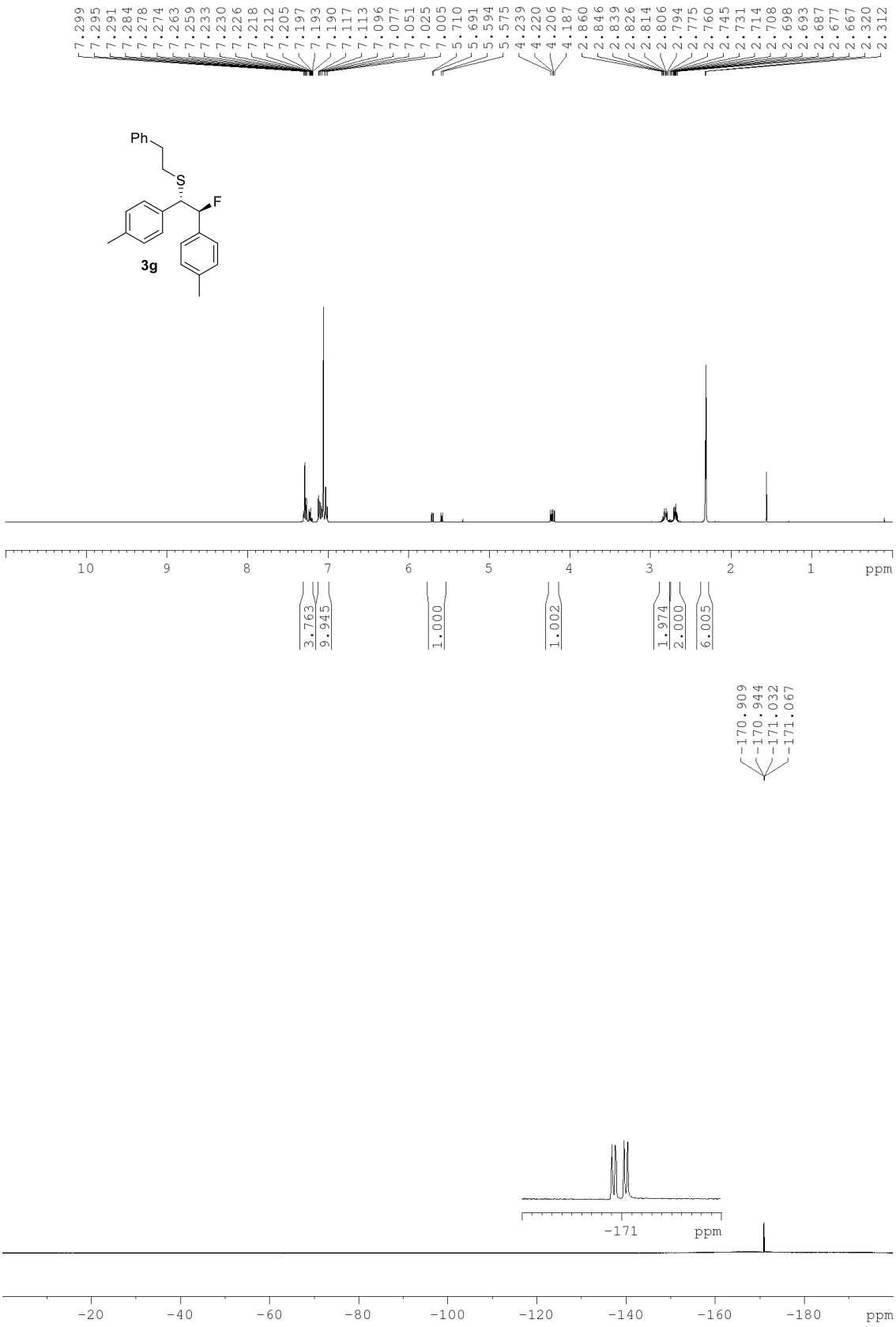
7.299
7.295
7.291
7.284
7.278
7.274
7.263
7.259
7.233
7.230
7.226
7.218
7.212
7.205
7.197
7.193
7.190
7.117
7.113
7.096
7.077
7.051
7.025
7.005
5.710
5.691
5.594
5.575
4.239
4.220
4.206
4.187
2.860
2.846
2.839
2.826
2.814
2.806
2.794
2.775
2.760
2.745
2.731
2.714
2.708
2.698
2.693
2.687
2.677
2.667
2.320
2.312
Ph
S
F
3g
10
9
8
7
6
5
4
3
2
1
ppm
3.763
9.945
1.000
1.002
1.974
2.000
6.005
-170.909
-170.944
-171.032
-171.067
-171
ppm
-20
-40
-60
-80
-100
-120
-140
-160
-180
ppm

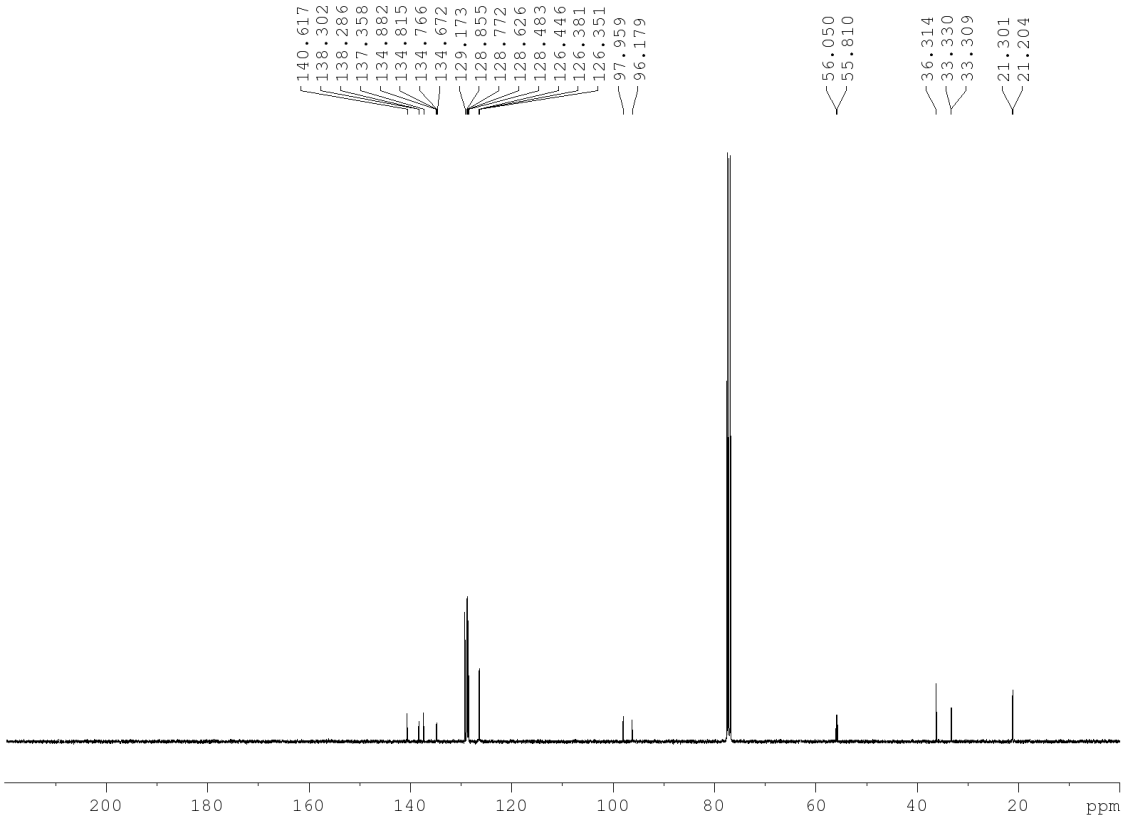
140.617
138.302
138.286
137.358
134.882
134.815
134.766
134.672
129.173
128.855
128.772
128.626
128.483
126.446
126.381
126.351
97.959
96.179
56.050
55.810
36.314
33.330
33.309
21.301
21.204
200
180
160
140
120
100
80
60
40
20
ppm

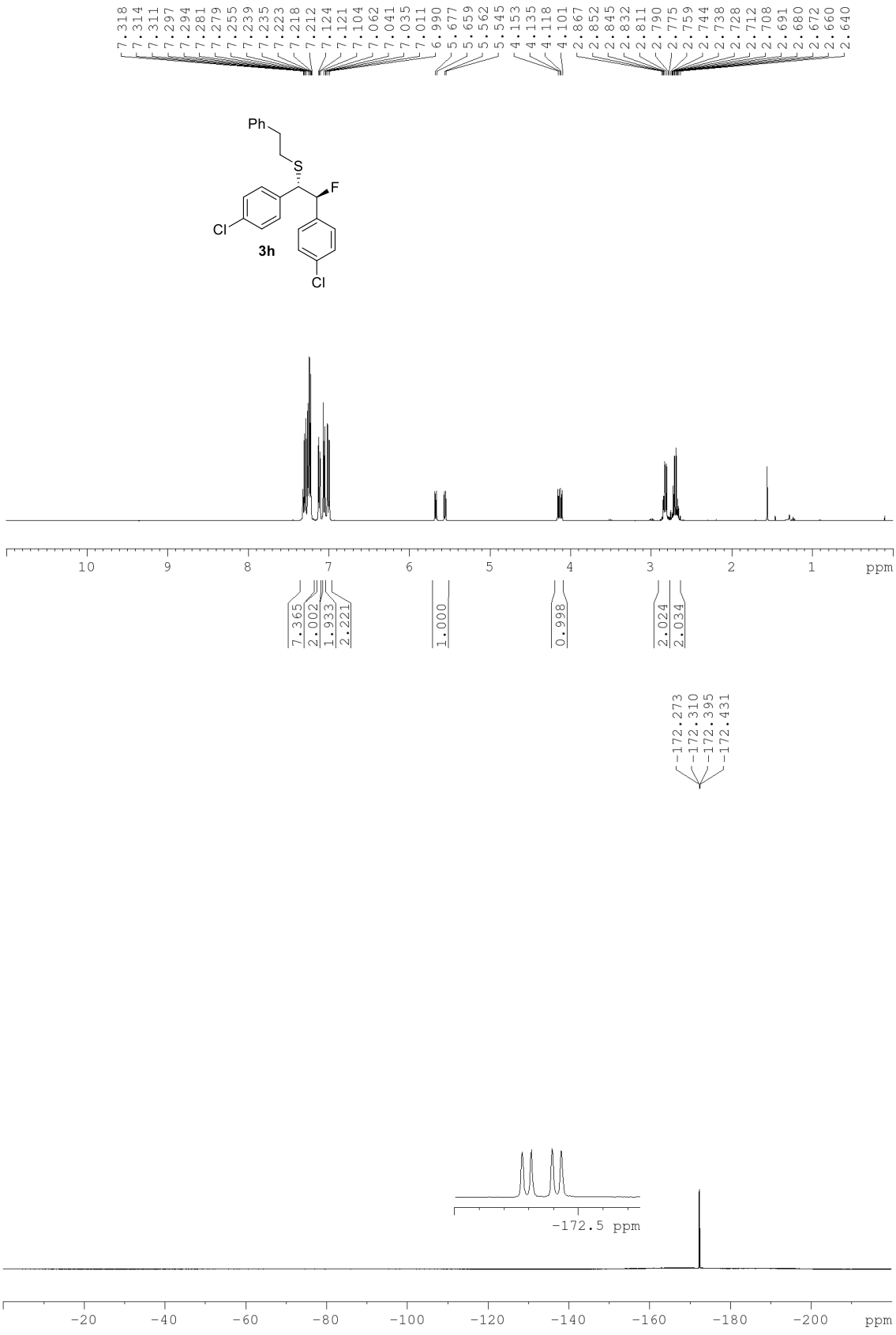
7.318
7.314
7.311
7.297
7.294
7.281
7.279
7.255
7.239
7.235
7.223
7.218
7.212
7.124
7.121
7.104
7.062
7.041
7.035
7.011
6.990
5.677
5.659
5.562
5.545
4.153
4.135
4.118
4.101
2.867
2.852
2.845
2.832
2.811
2.790
2.775
2.759
2.744
2.738
2.728
2.712
2.708
2.691
2.680
2.672
2.660
2.640
Ph
S
F
Cl
3h
Cl
10
9
8
7
6
5
4
3
2
1
ppm
7.365
2.002
1.933
2.221
1.000
0.998
2.024
2.034
-172.273
-172.310
-172.395
-172.431
-172.5 ppm
-20
-40
-60
-80
-100
-120
-140
-160
-180
-200
ppm

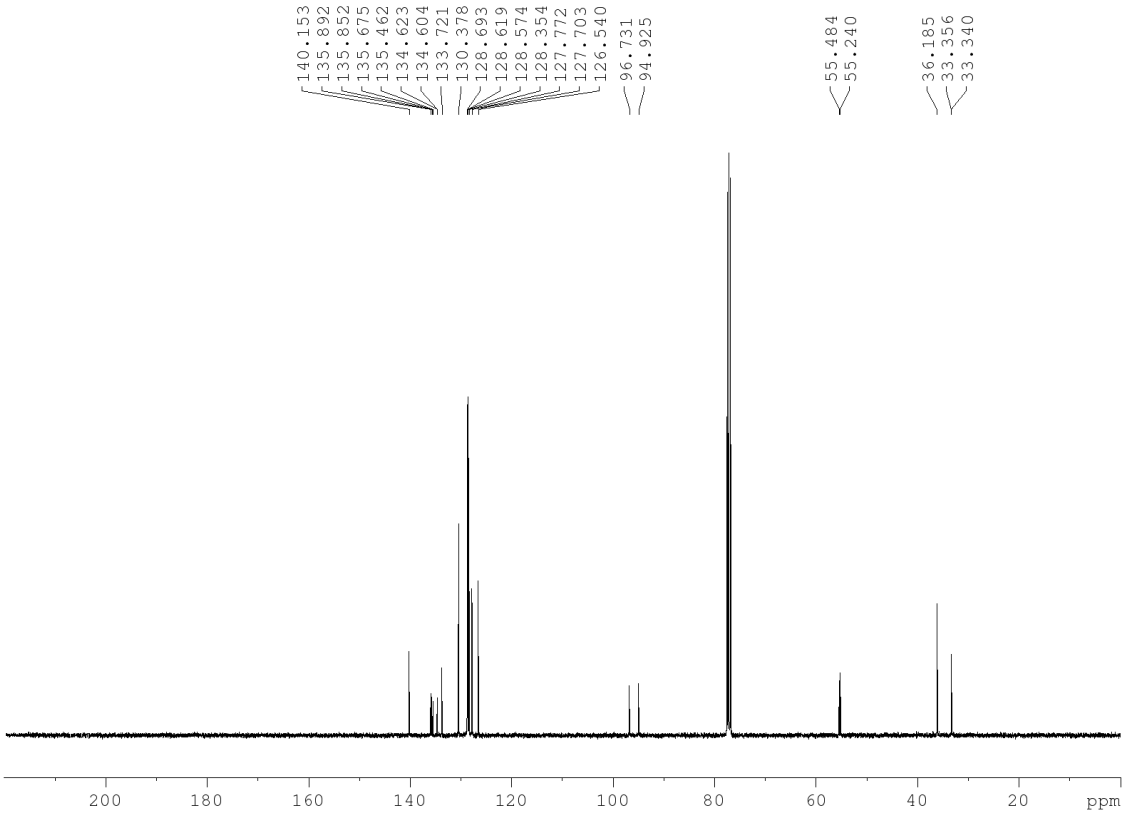
140.153
135.892
135.852
135.675
135.462
134.623
134.604
133.721
130.378
128.693
128.619
128.574
128.354
127.772
127.703
126.540
96.731
94.925
55.484
55.240
36.185
33.356
33.340
200
180
160
140
120
100
80
60
40
20
ppm

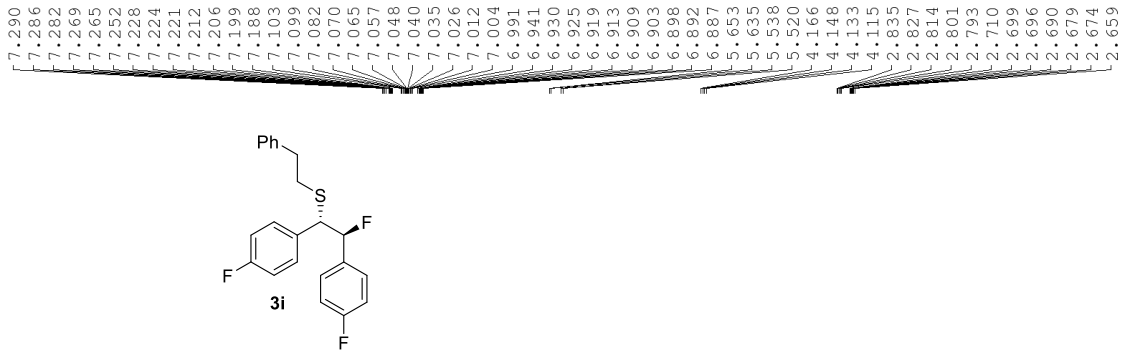
7.290
7.286
7.282
7.269
7.265
7.252
7.228
7.224
7.221
7.212
7.206
7.199
7.188
7.103
7.099
7.082
7.070
7.065
7.057
7.048
7.040
7.035
7.026
7.012
7.004
6.991
6.941
6.930
6.925
6.919
6.913
6.909
6.903
6.898
6.892
6.887
5.653
5.635
5.538
5.520
4.166
4.148
4.133
4.115
2.835
2.827
2.814
2.801
2.793
2.710
2.699
2.696
2.690
2.679
2.674
2.659

Ph
S
F
F
F
3i

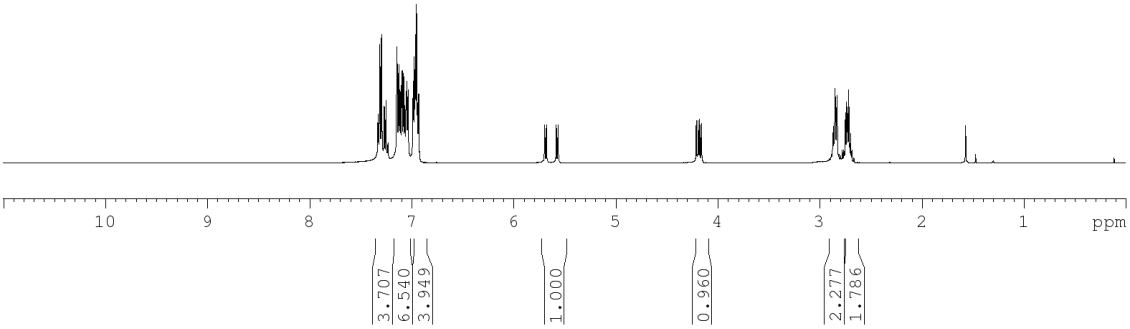
10
9
8
7
6
5
4
3
2
1
ppm
3.707
6.540
3.949
1.000
0.960
2.277
1.786

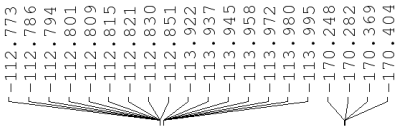
-112.773
-112.786
-112.794
-112.801
-112.809
-112.815
-112.821
-112.830
-112.851
-113.922
-113.937
-113.945
-113.958
-113.972
-113.980
-113.995
-170.248
-170.282
-170.369
-170.404

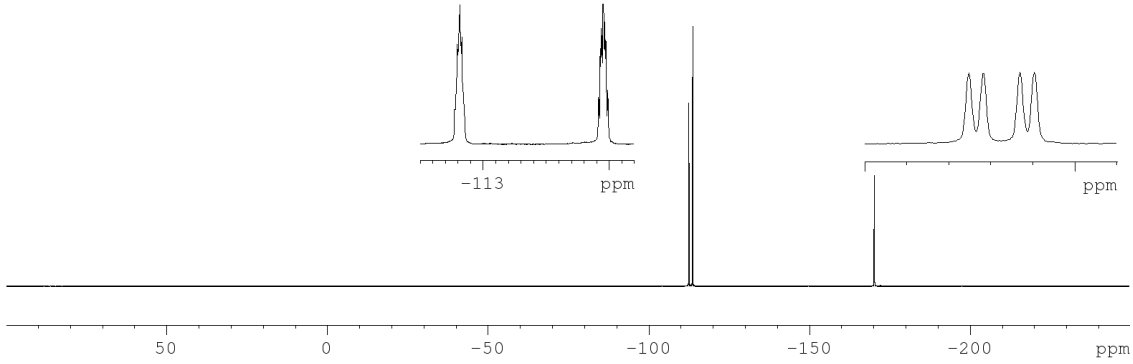
-113
ppm
ppm
50
0
-50
-100
-150
-200
ppm

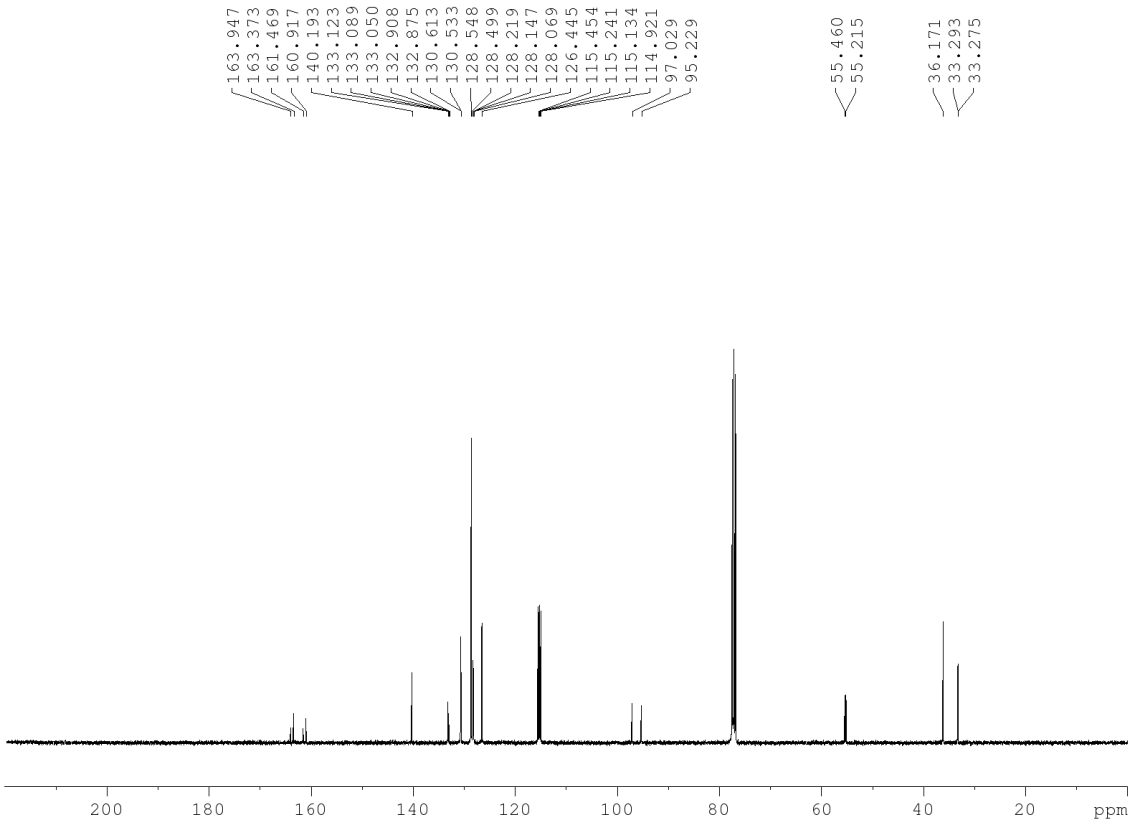
163.947
163.373
161.469
160.917
140.193
133.123
133.089
133.050
132.908
132.875
130.613
130.533
128.548
128.499
128.219
128.147
128.069
126.445
115.454
115.241
115.134
114.921
97.029
95.229
55.460
55.215
36.171
33.293
33.275
200
180
160
140
120
100
80
60
40
20
ppm

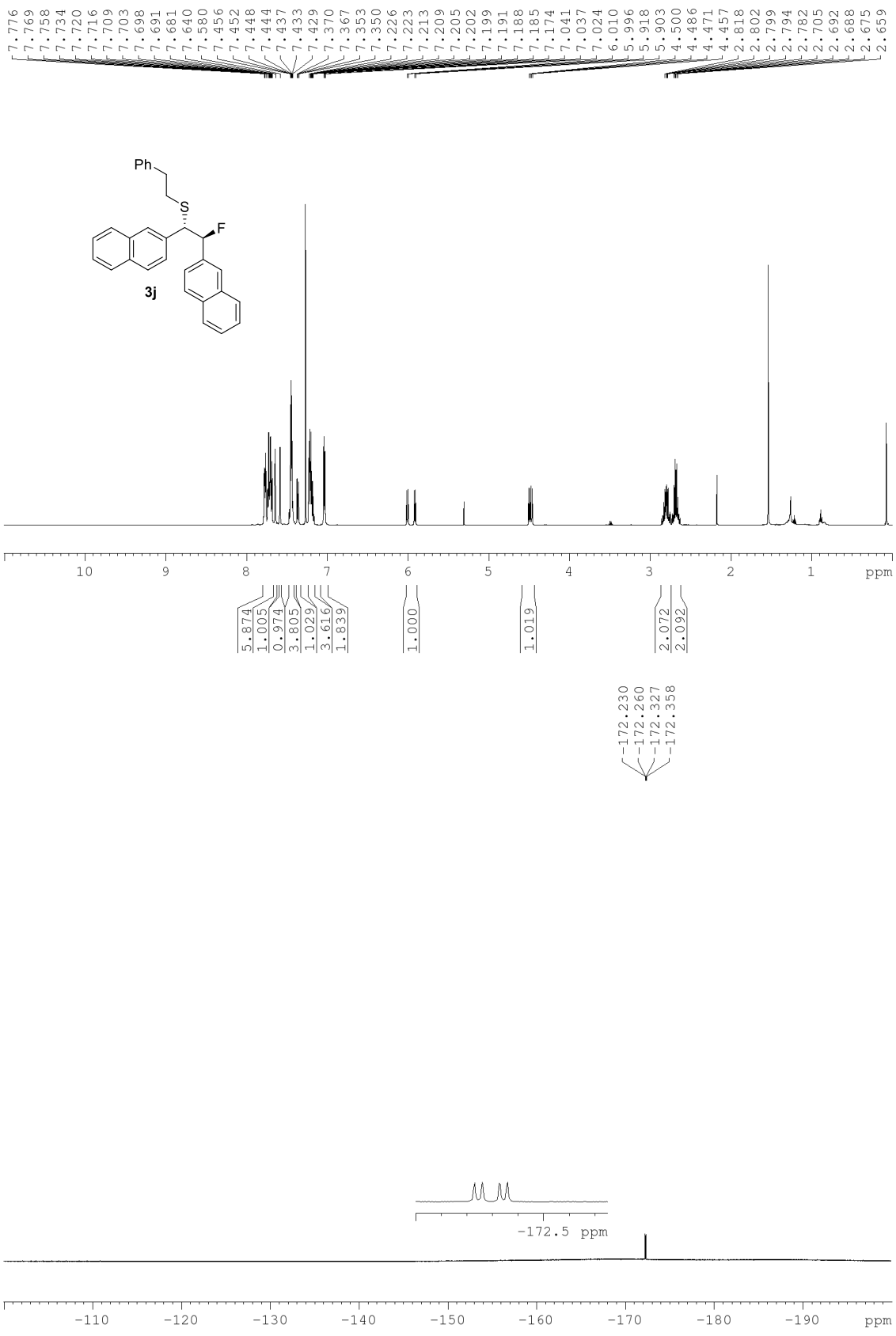
7.776
7.769
7.758
7.734
7.720
7.716
7.709
7.703
7.698
7.691
7.681
7.640
7.580
7.456
7.452
7.448
7.444
7.437
7.433
7.429
7.370
7.367
7.353
7.350
7.226
7.223
7.213
7.209
7.205
7.202
7.199
7.191
7.188
7.185
7.174
7.041
7.037
7.024
6.010
5.996
5.918
5.903
4.500
4.486
4.471
4.457
2.818
2.802
2.799
2.794
2.782
2.705
2.692
2.688
2.675
2.659
Ph
S
F
3j
10
9
8
7
6
5
4
3
2
1
ppm
5.874
1.005
0.974
3.805
1.029
3.616
1.839
1.000
1.019
2.072
2.092
-172.230
-172.260
-172.327
-172.358
-172.5 ppm
-110
-120
-130
-140
-150
-160
-170
-180
-190
ppm

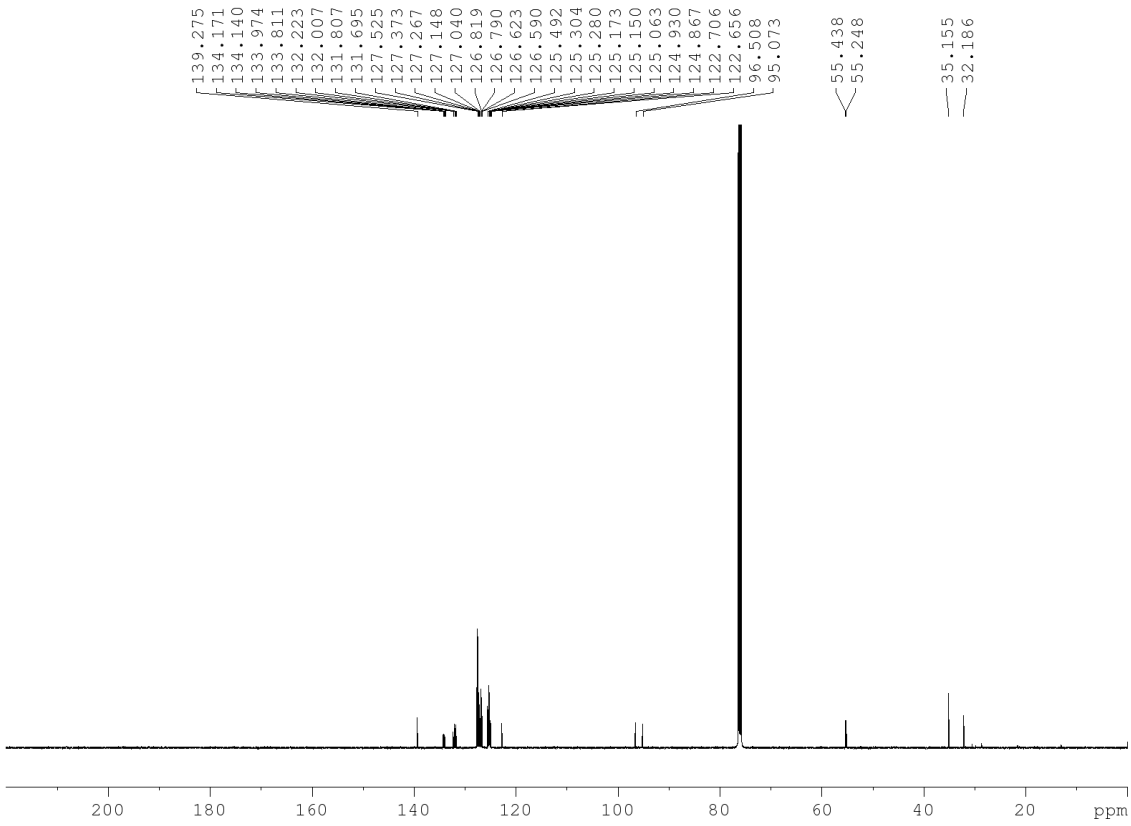
139.275
134.171
134.140
133.974
133.811
132.223
132.007
131.807
131.695
127.525
127.373
127.267
127.148
127.040
126.819
126.790
126.623
126.590
125.492
125.304
125.280
125.173
125.150
125.063
124.930
124.867
122.706
122.656
96.508
95.073
55.438
55.248
35.155
32.186
200
180
160
140
120
100
80
60
40
20
ppm

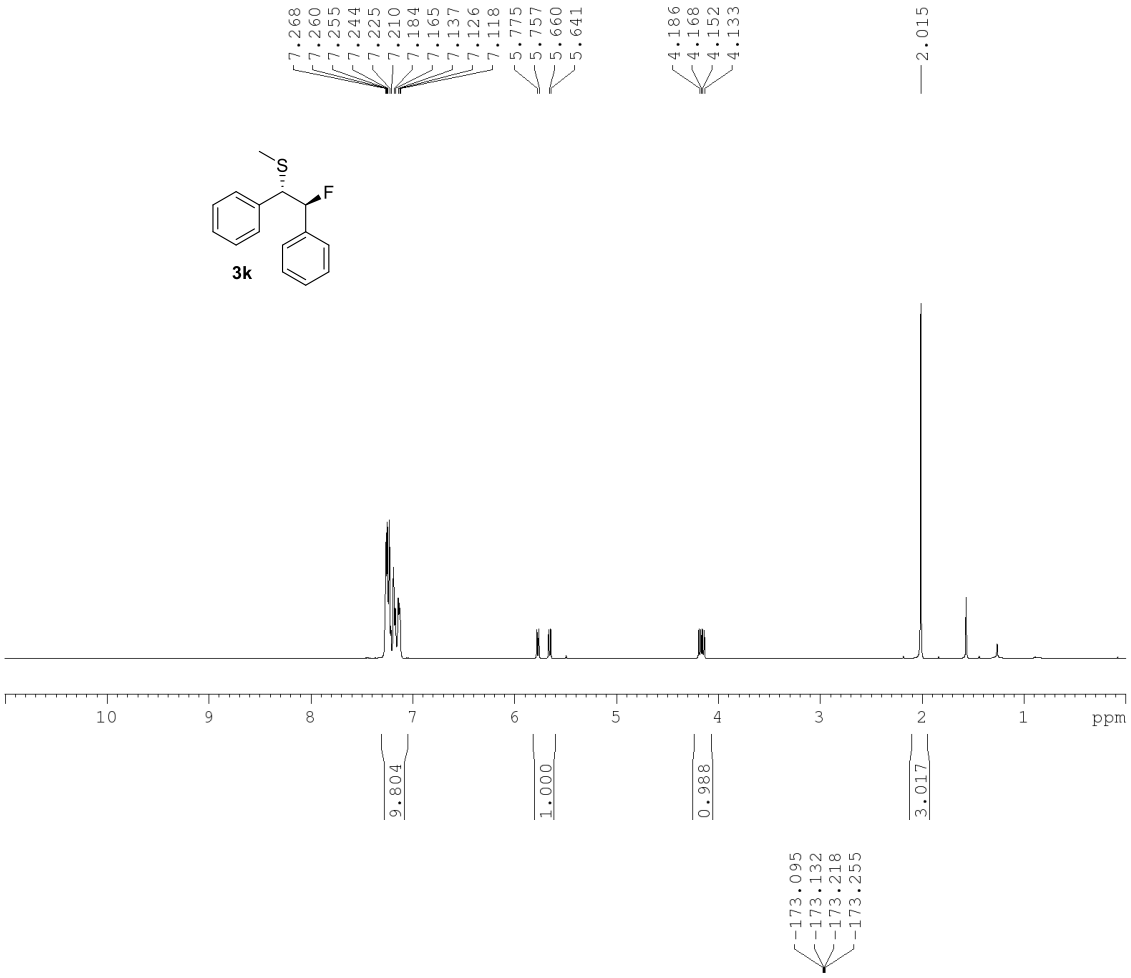
7.268
7.260
7.255
7.244
7.225
7.210
7.184
7.165
7.137
7.126
7.118
5.775
5.757
5.660
5.641
4.186
4.168
4.152
4.133
2.015
S
F
3k
10
9
8
7
6
5
4
3
2
1
ppm
9.804
1.000
0.988
3.017

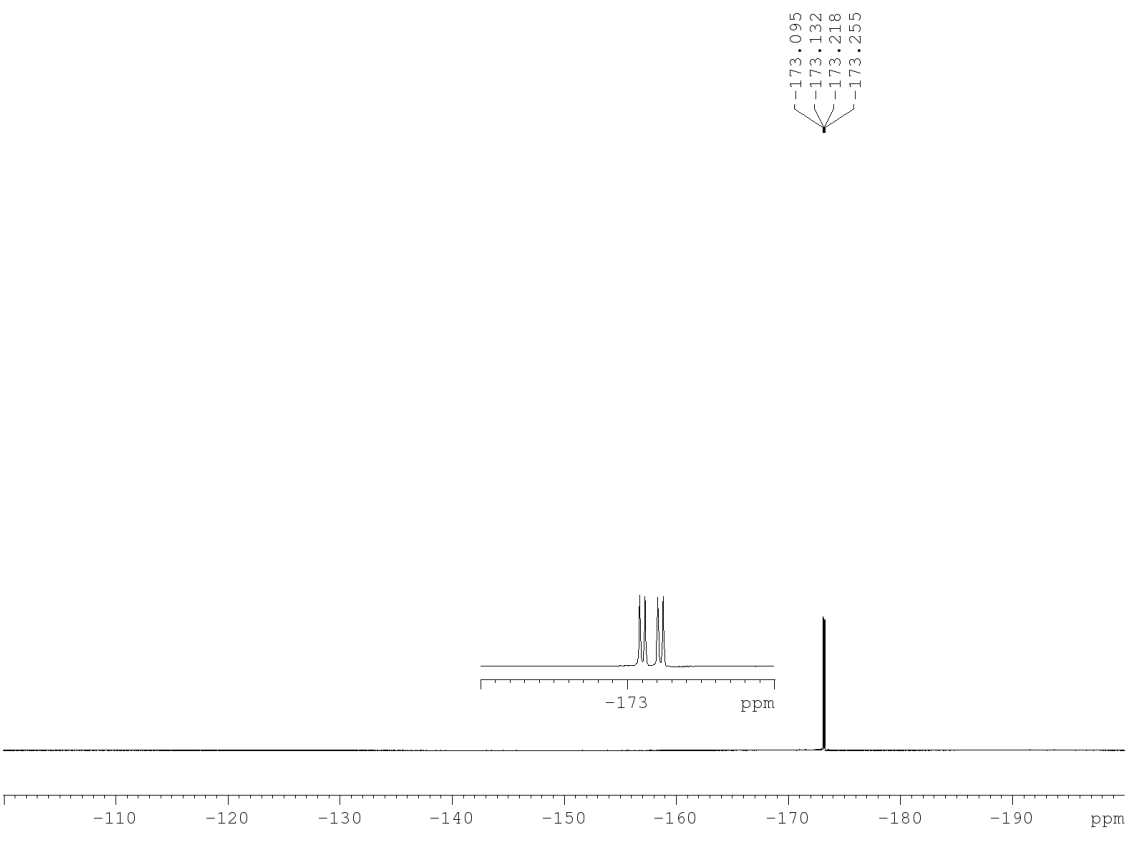
-173.095
-173.132
-173.218
-173.255
-173
ppm
-110
-120
-130
-140
-150
-160
-170
-180
-190
ppm

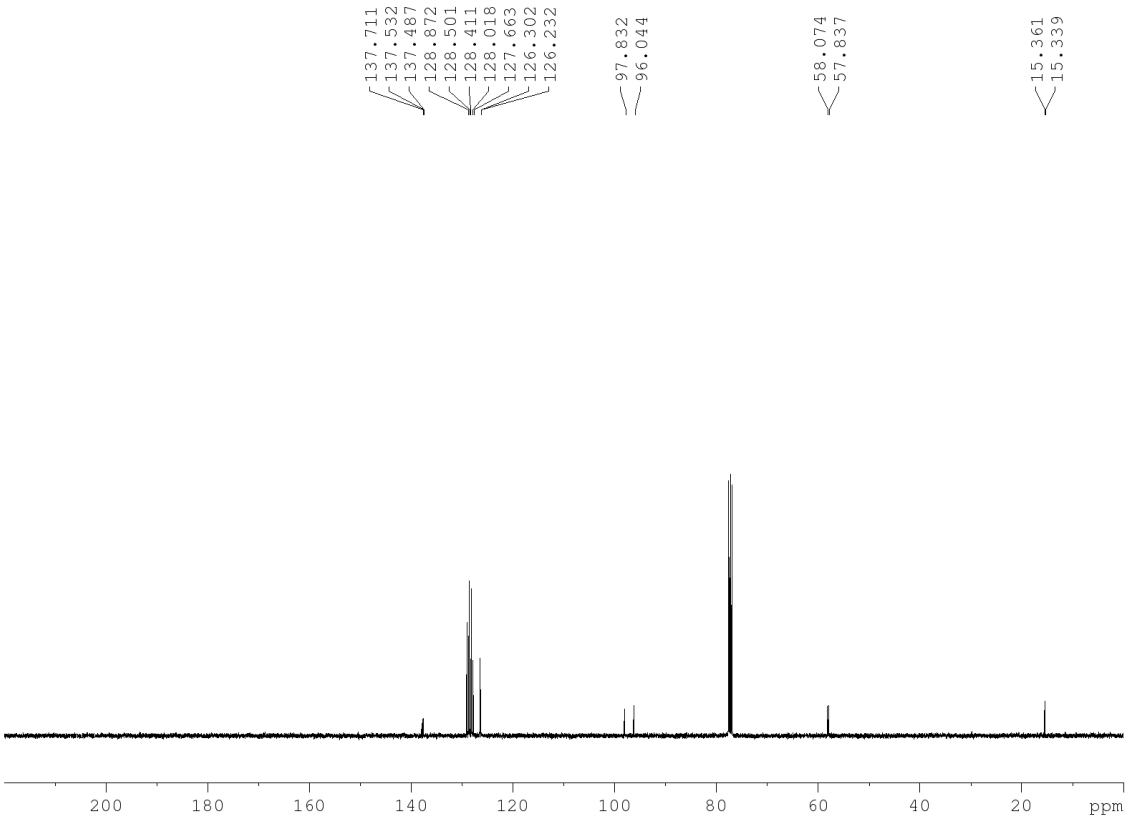
137.711
137.532
137.487
128.872
128.501
128.411
128.018
127.663
126.302
126.232
97.832
96.044
58.074
57.837
15.361
15.339
200
180
160
140
120
100
80
60
40
20
ppm

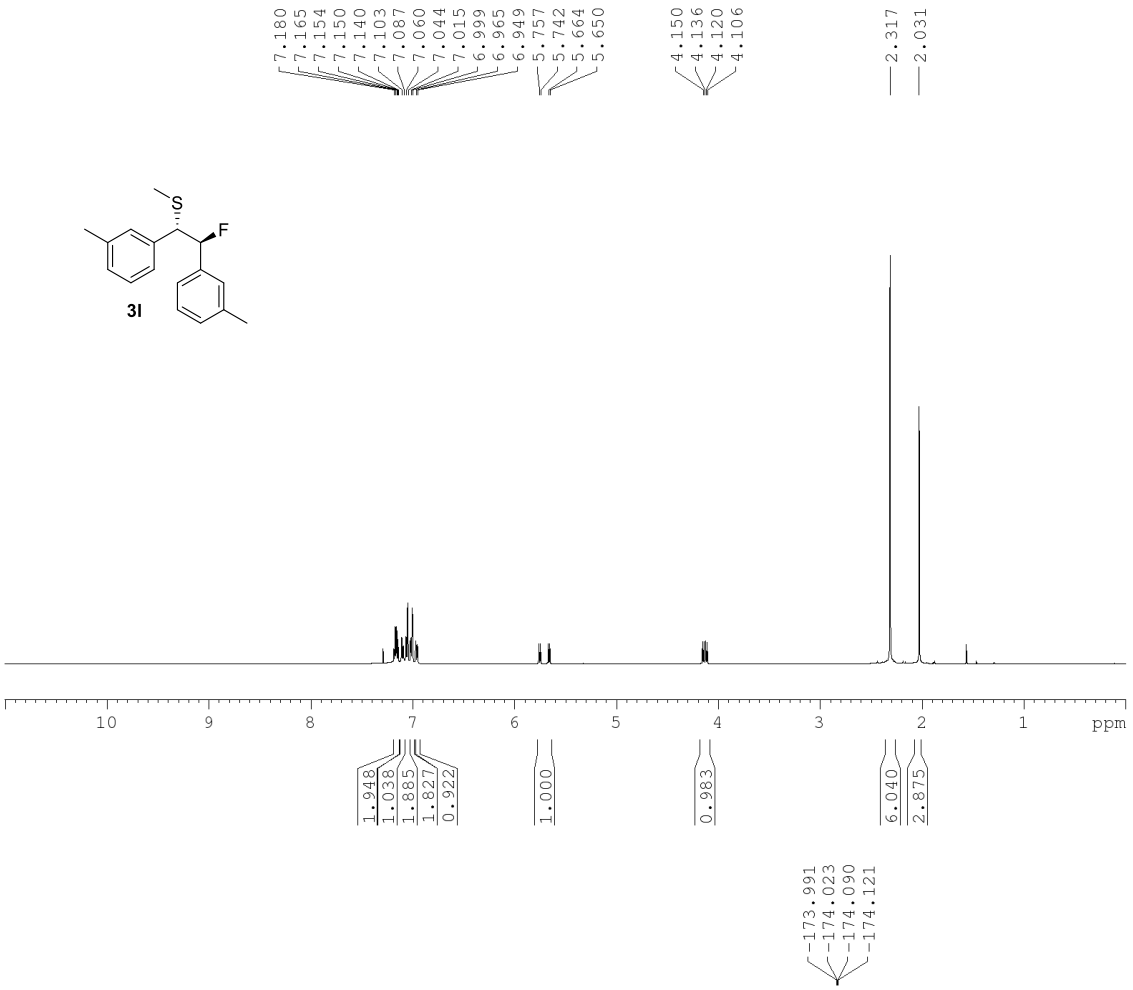
7.180
7.165
7.154
7.150
7.140
7.103
7.087
7.060
7.044
7.015
6.999
6.965
6.949
5.757
5.742
5.664
5.650
4.150
4.136
4.120
4.106
2.317
2.031
S
F
3l
10
9
8
7
6
5
4
3
2
1
ppm
1.948
1.038
1.885
1.827
0.922
1.000
0.983
6.040
2.875

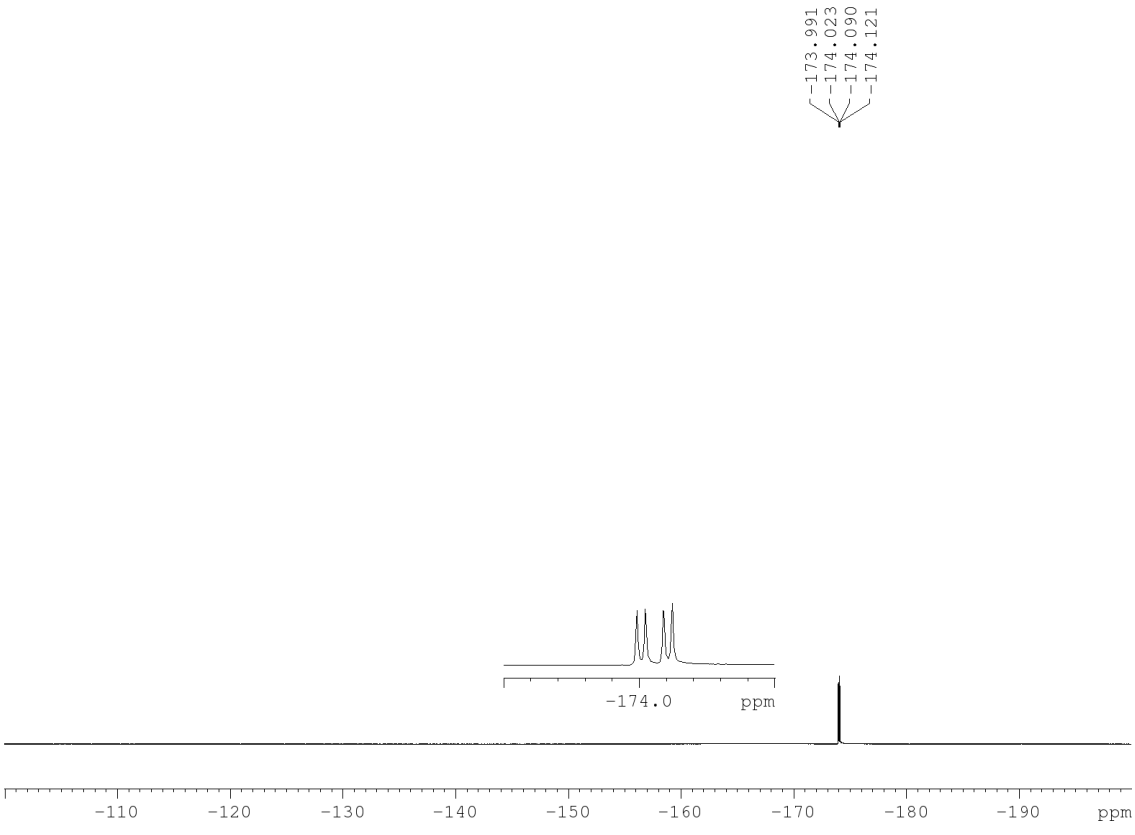
-173.991
-174.023
-174.090
-174.121
-174.0
ppm
-110
-120
-130
-140
-150
-160
-170
-180
-190
ppm

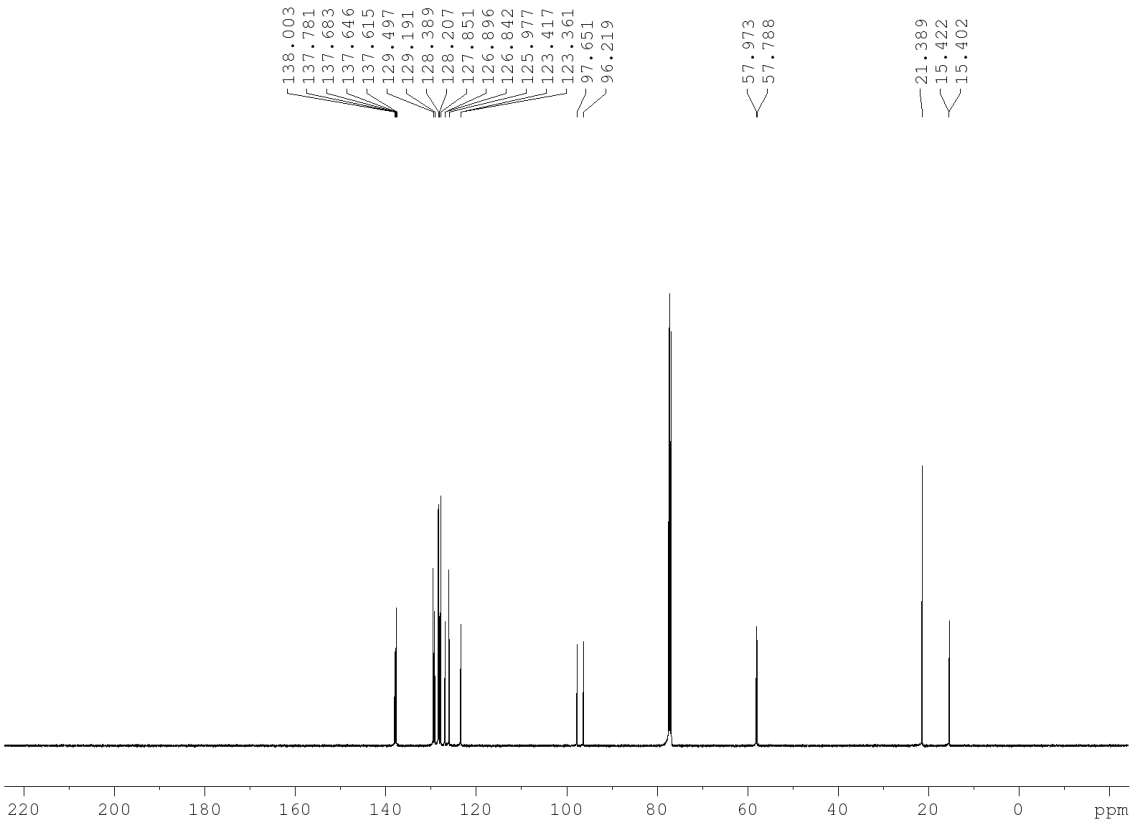
138.003
137.781
137.683
137.646
137.615
129.497
129.191
128.389
128.207
127.851
126.896
126.842
125.977
123.417
123.361
97.651
96.219
57.973
57.788
21.389
15.422
15.402
220
200
180
160
140
120
100
80
60
40
20
0
ppm

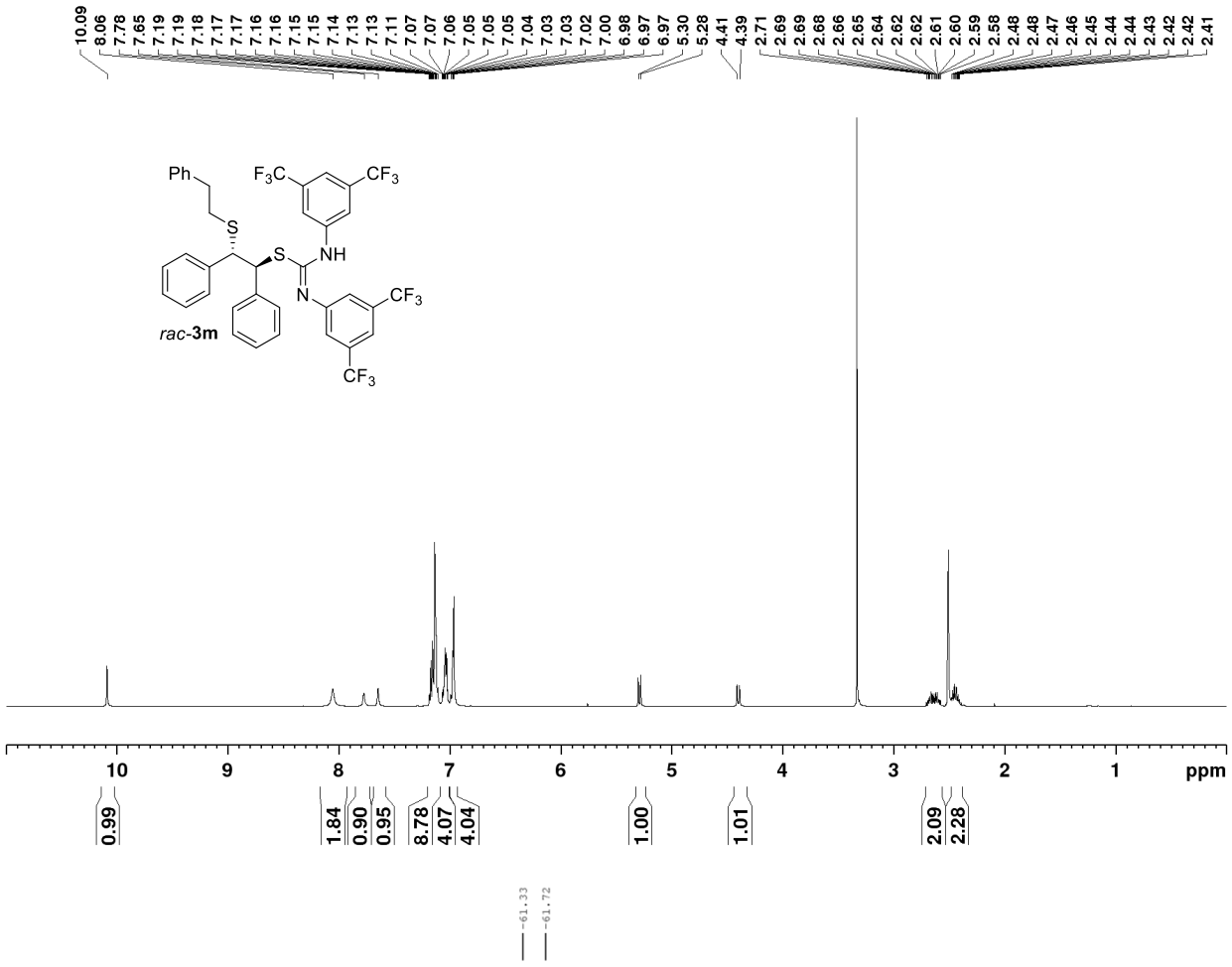
10.09 8.06 7.78 7.65 7.19 7.19 7.18 7.17 7.17 7.16 7.16 7.15 7.15 7.14 7.13 7.13 7.11 7.07 7.07 7.06 7.05 7.05 7.05 7.04 7.03 7.03 7.02 7.00 6.98 6.97 6.97 5.30 5.28 4.41 4.39 2.71 2.69 2.69 2.68 2.66 2.65 2.64 2.62 2.62 2.61 2.60 2.59 2.58 2.48 2.48 2.47 2.46 2.45 2.44 2.44 2.43 2.42 2.42 2.41
Ph
S
S
NH
N
F3C
CF3
CF3
CF3
rac-3m
10 9 8 7 6 5 4 3 2 1 ppm
0.99 1.84 0.90 0.95 8.78 4.07 4.04 1.00 1.01 2.09 2.28

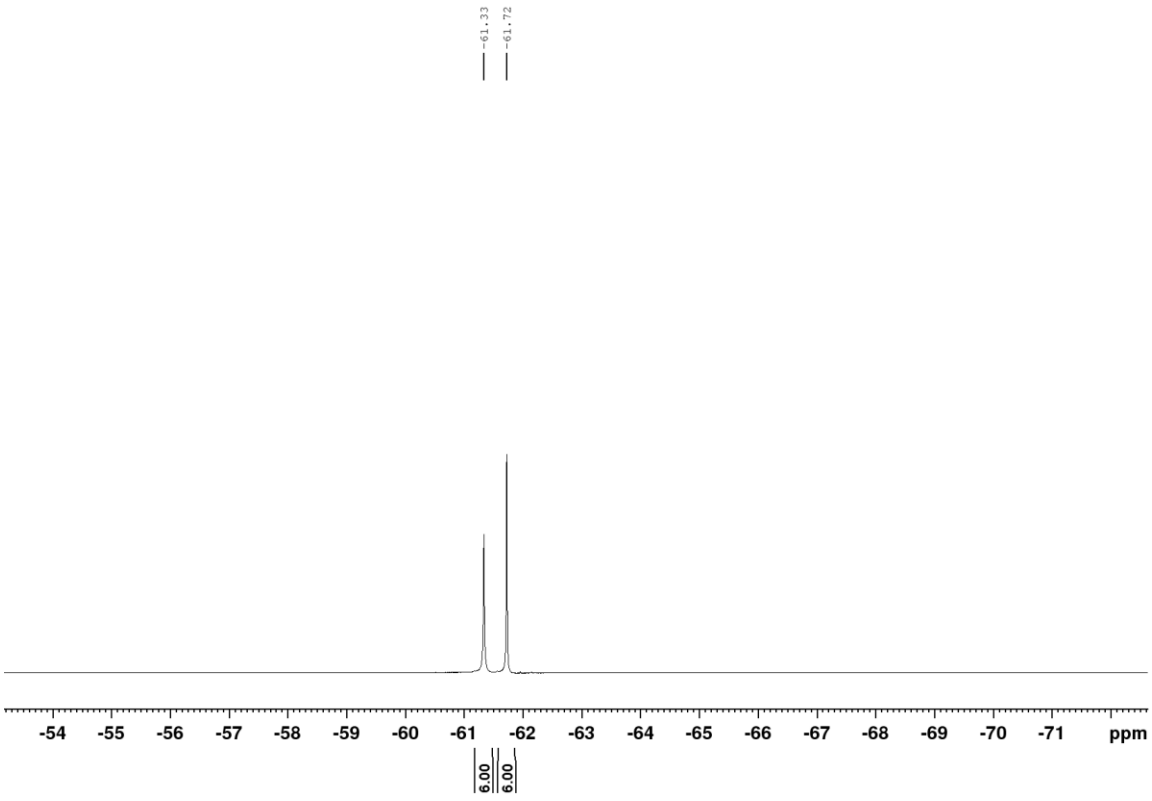
-61.33
-61.72
-54 -55 -56 -57 -58 -59 -60 -61 -62 -63 -64 -65 -66 -67 -68 -69 -70 -71 ppm
6.00 6.00

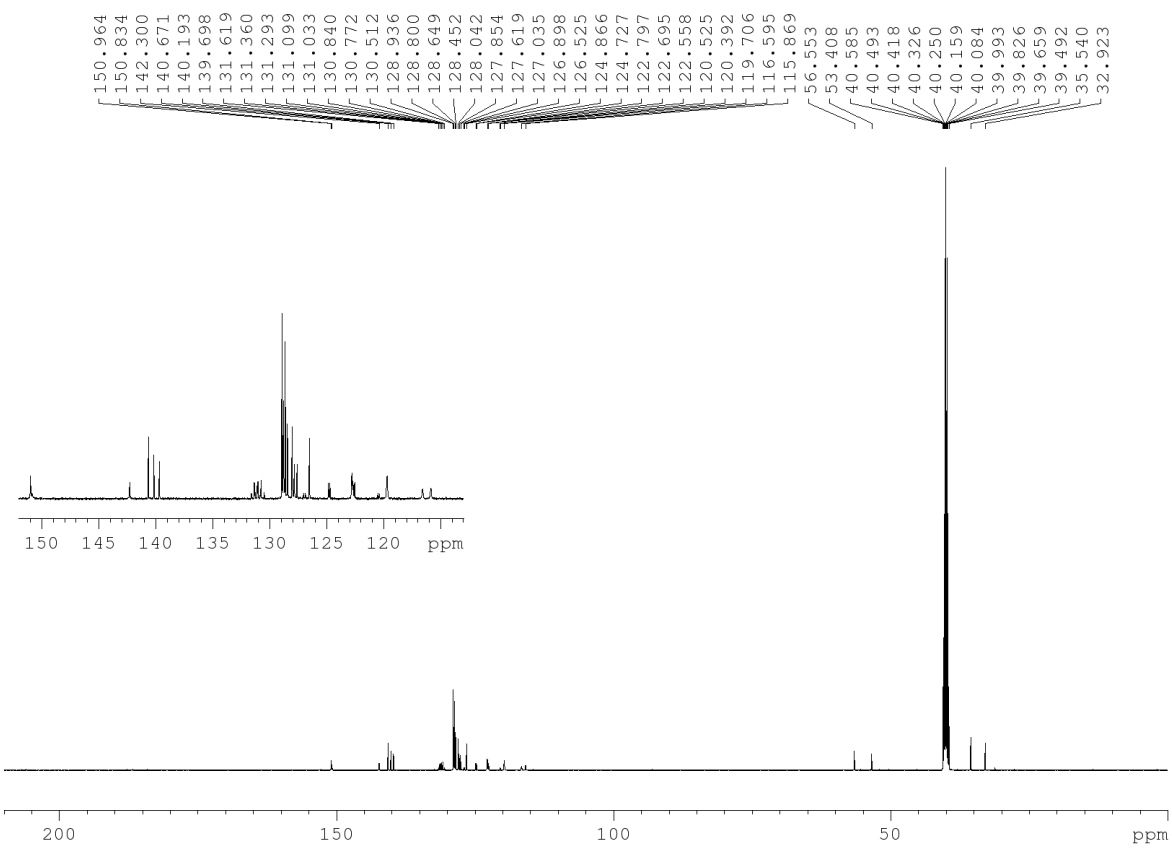
150.964
150.834
142.300
140.671
140.193
139.698
131.619
131.360
131.293
131.099
131.033
130.840
130.772
130.512
128.936
128.800
128.649
128.452
128.042
127.854
127.619
127.035
126.898
126.525
124.866
124.727
122.797
122.695
122.558
120.525
120.392
119.706
116.595
115.869
56.553
53.408
40.585
40.493
40.418
40.326
40.250
40.159
40.084
39.993
39.826
39.659
39.492
35.540
32.923
150 145 140 135 130 125 120 ppm
200 150 100 50 ppm

Copies of HPLC traces

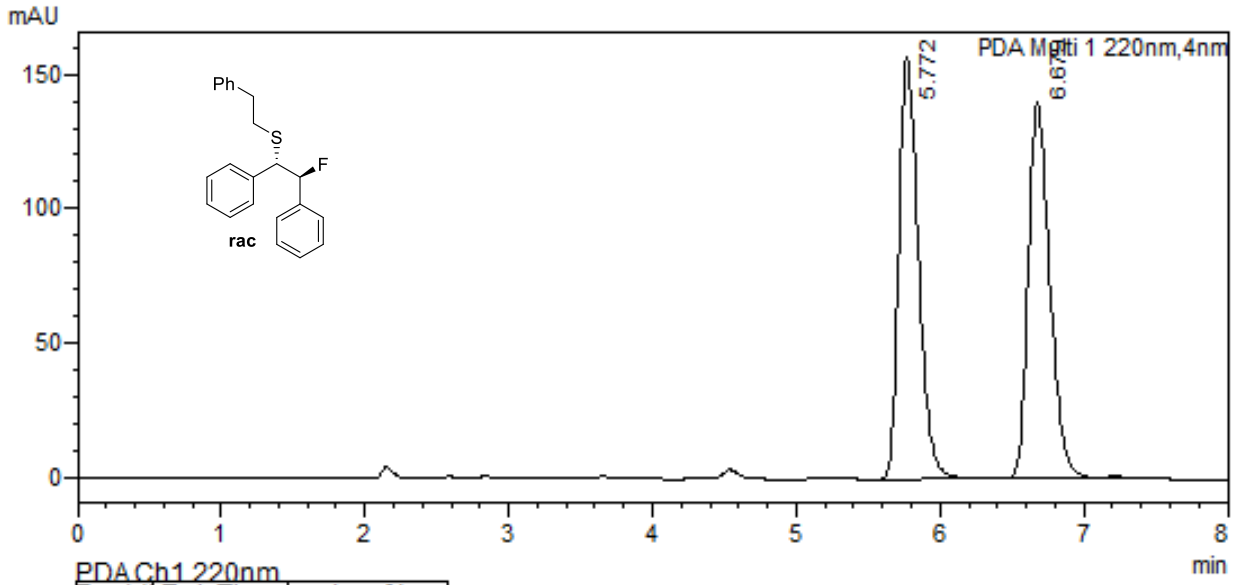

PDA Ch1 220nm

Peak#	Ret. Time	Area%
1	5.772	49.986
2	6.679	50.014

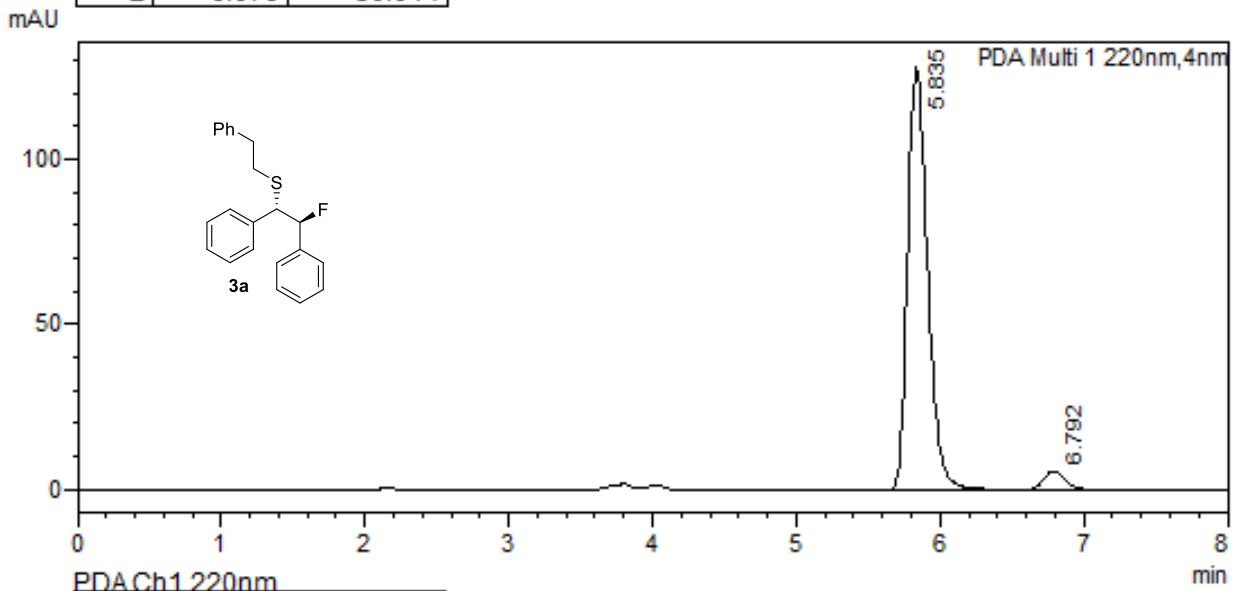

PDA Ch1 220nm

Peak#	Ret. Time	Area%
1	5.835	95.556
2	6.792	4.444

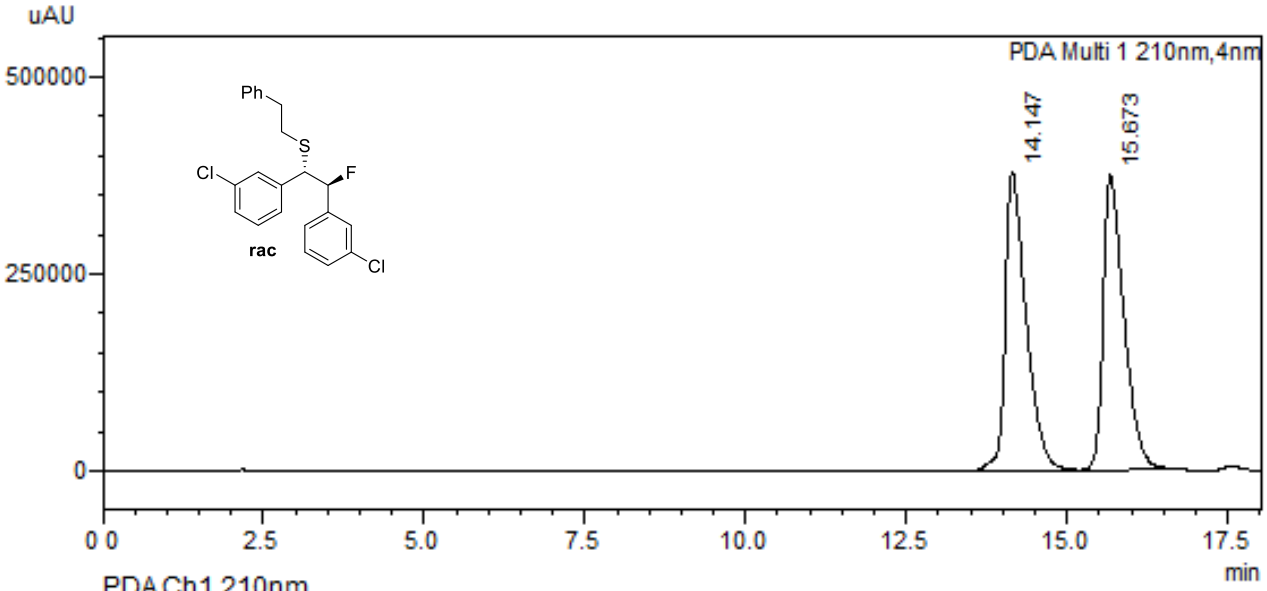

PDA Ch1 210nm

Peak#	Ret. Time	Area%
1	14.147	50.658
2	15.673	49.342

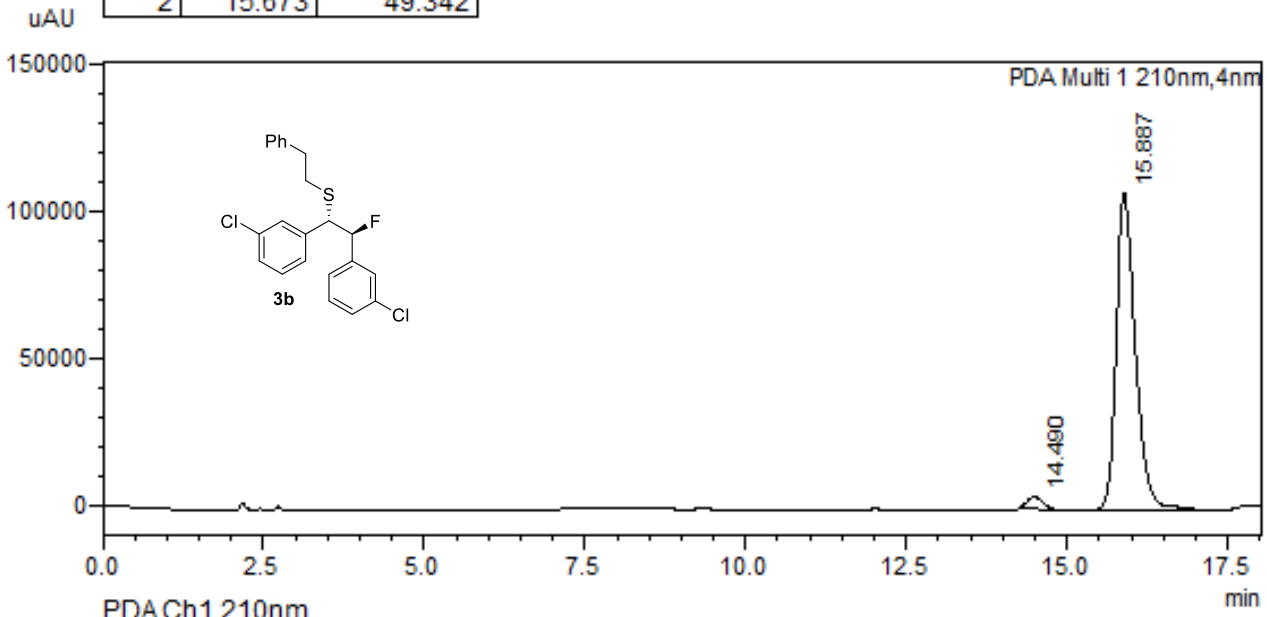

PDA Ch1 210nm

Peak#	Ret. Time	Area%
1	14.490	3.065
2	15.887	96.935

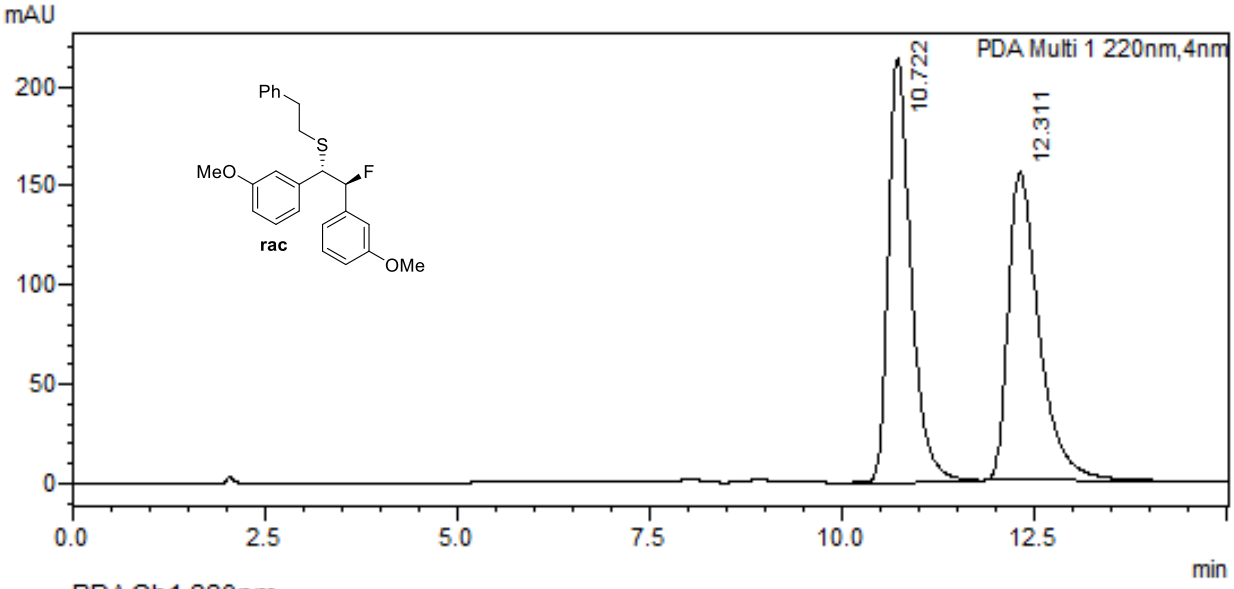

PDA Ch1 220nm

Peak#	Ret. Time	Area%
1	10.722	50.227
2	12.311	49.773

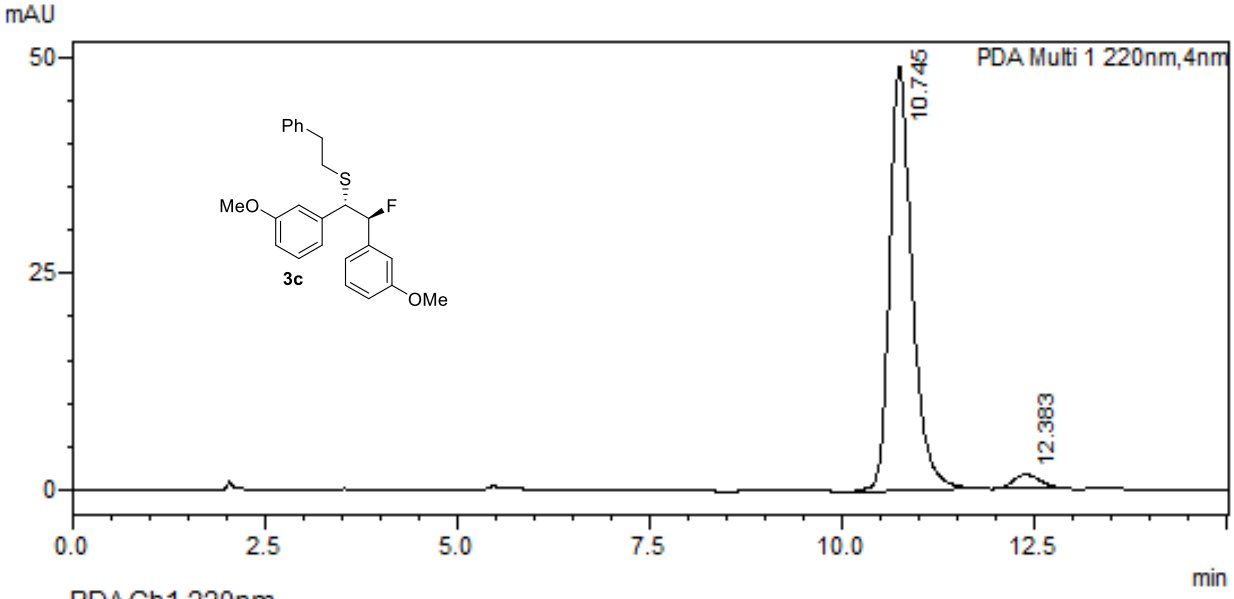

PDA Ch1 220nm

Peak#	Ret. Time	Area%
1	10.745	96.092
2	12.383	3.908

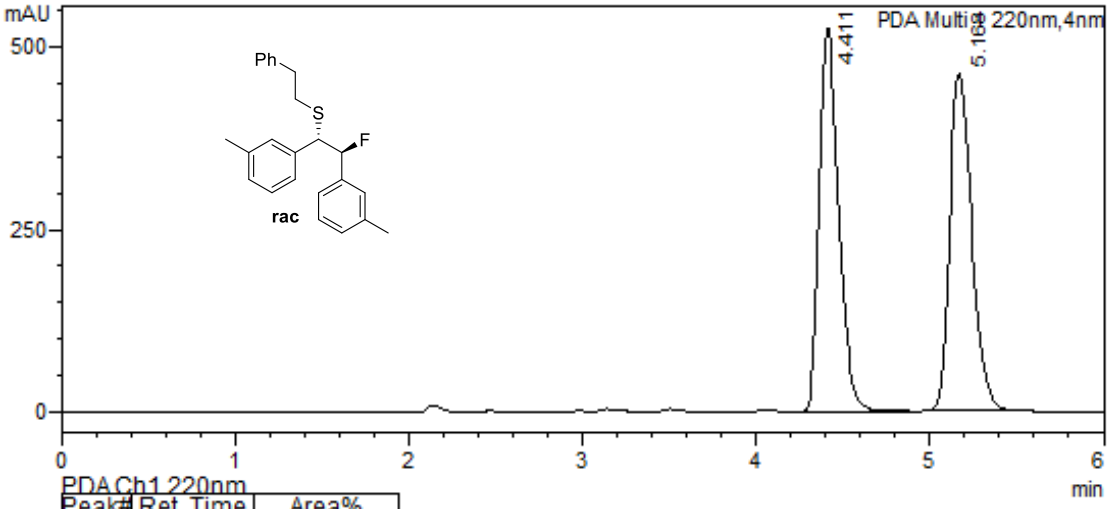

PDA Ch1 220nm

Peak#	Ret. Time	Area%
1	4.411	50.113
2	5.168	49.887

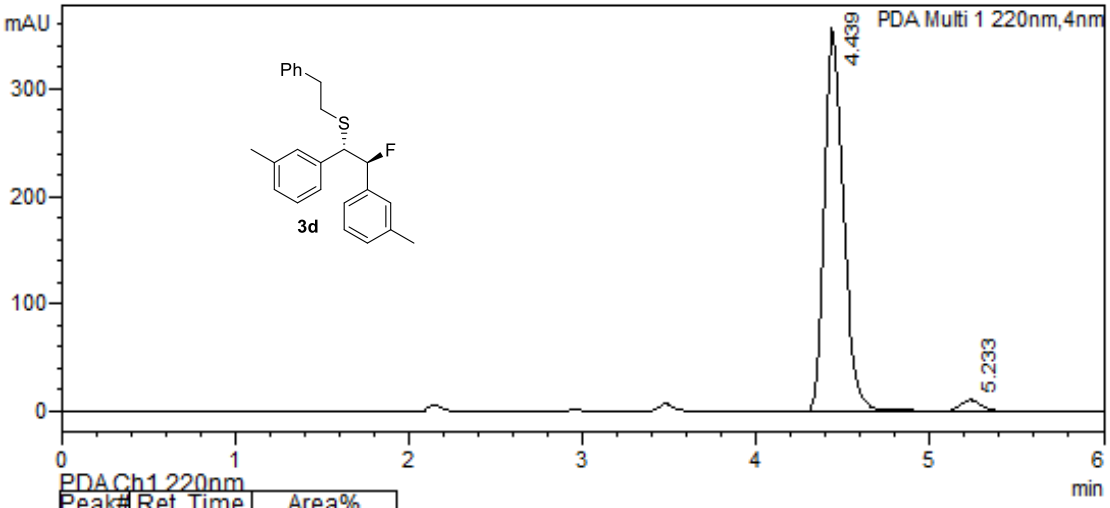

PDA Ch1 220nm

Peak#	Ret. Time	Area%
1	4.439	97.099
2	5.233	2.901

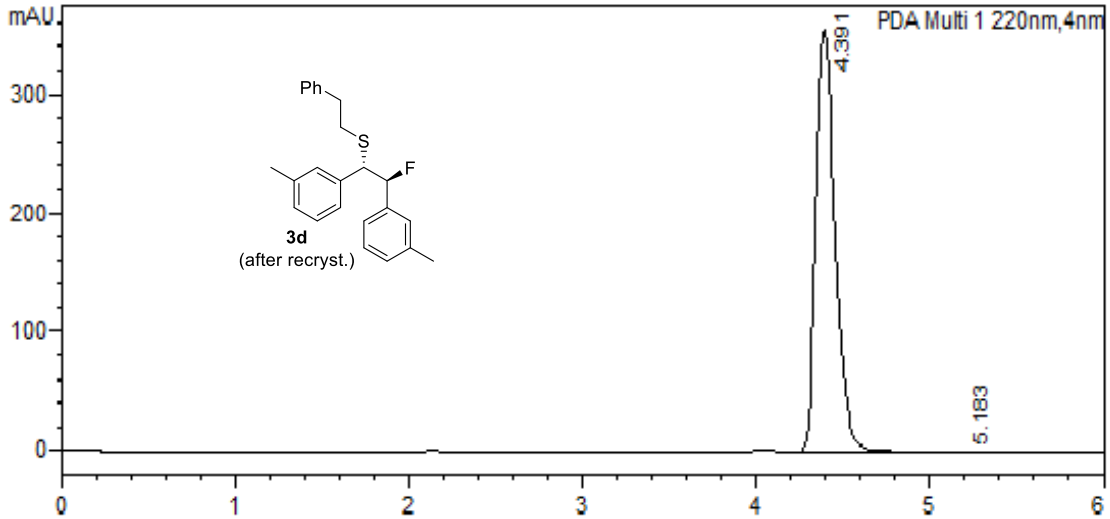

PDA Ch1 220nm

Peak#	Ret. Time	Area%
1	4.391	99.936
2	5.183	0.064

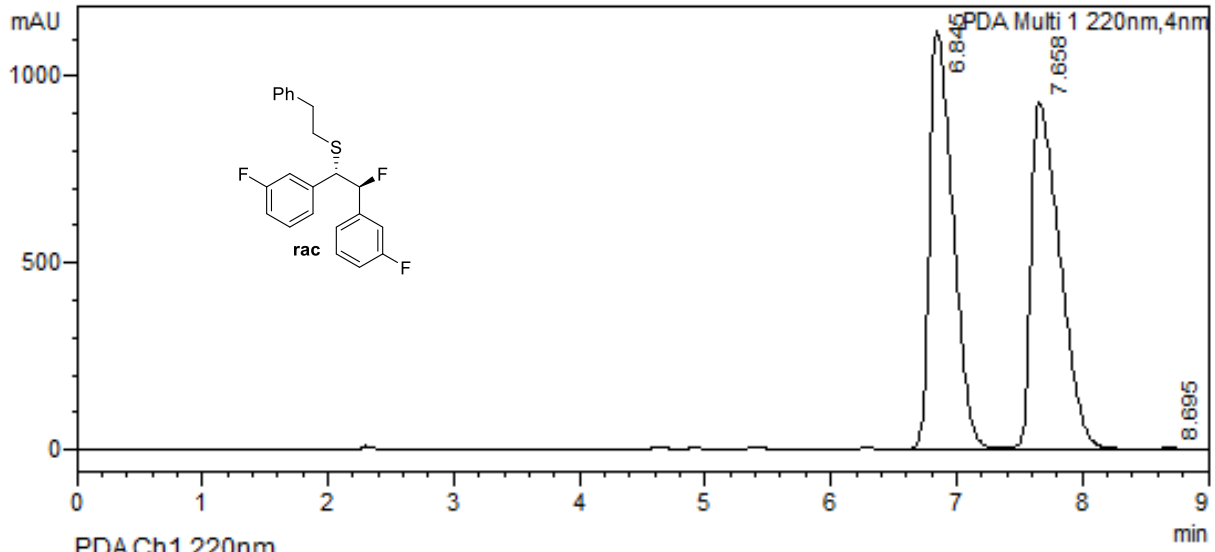

PDA Ch1 220nm

Peak#	Ret. Time	Area%
1	6.845	49.336
2	7.658	50.601

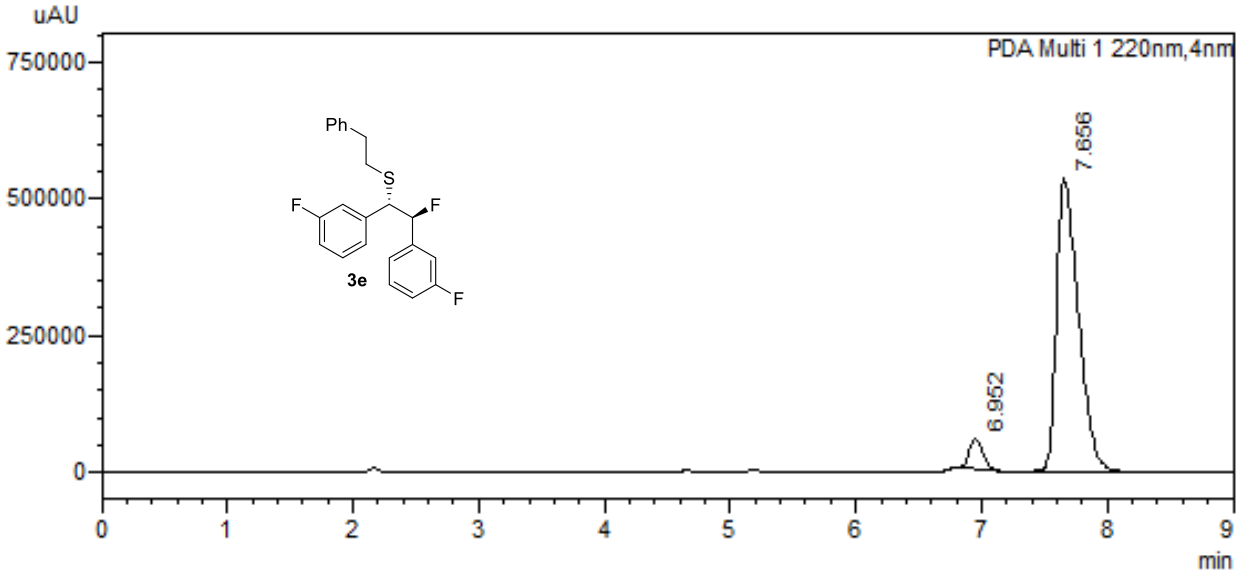

PDA Ch1 220nm

Peak#	Ret. Time	Area%
1	6.952	5.947
2	7.656	94.053

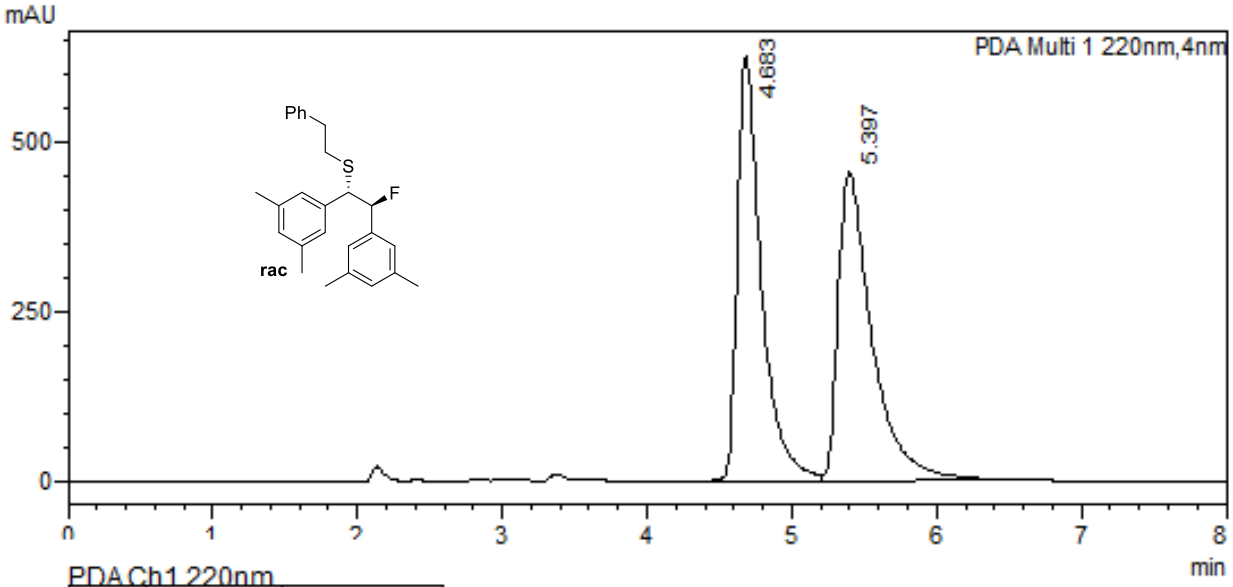

PDA Ch1 220nm

Peak#	Ret. Time	Area%
1	4.683	49.759
2	5.397	50.241

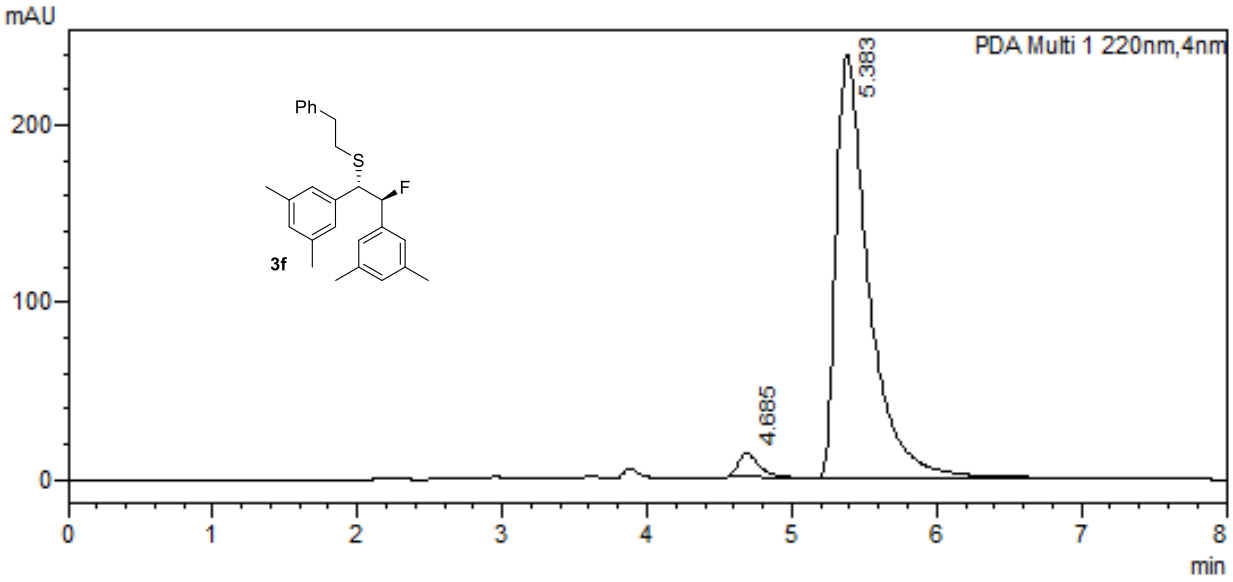

PDA Ch1 220nm

Peak#	Ret. Time	Area%
1	4.685	3.452
2	5.383	96.548

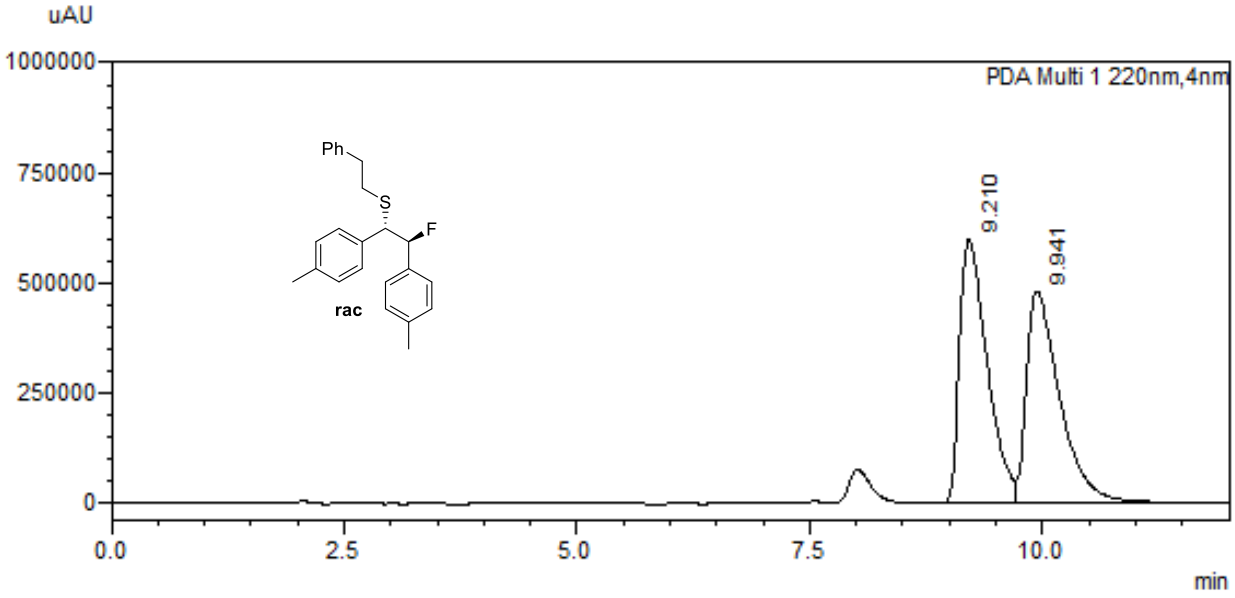

PDA Ch1 220nm

Peak#	Ret. Time	Area%
1	9.210	50.641
2	9.941	49.359

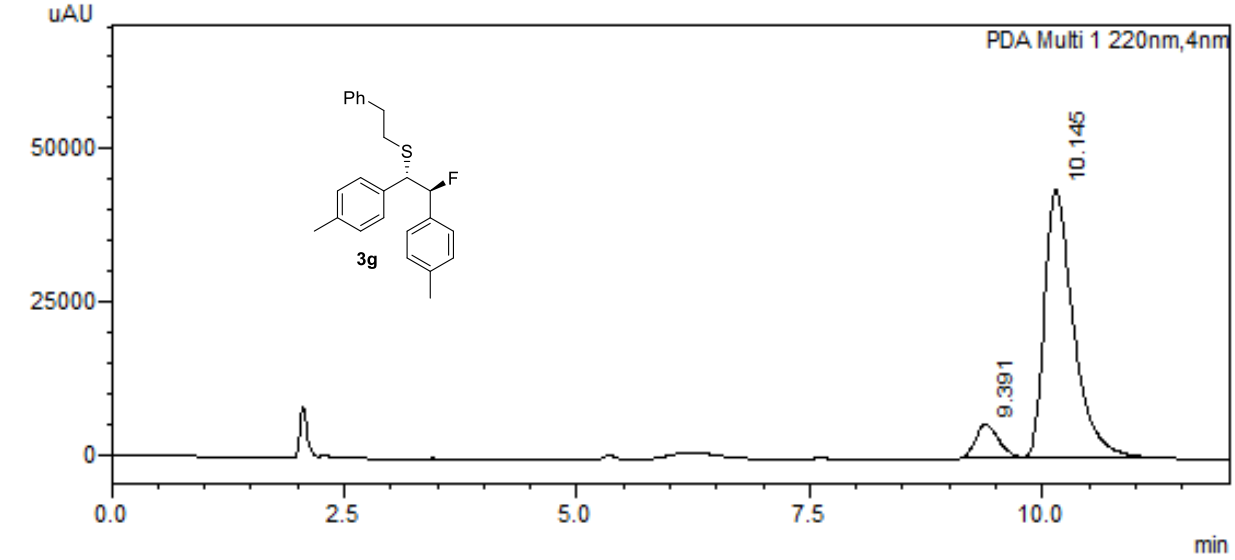

PDA Ch1 220nm

Peak#	Ret. Time	Area%
1	9.391	8.937
2	10.145	91.063

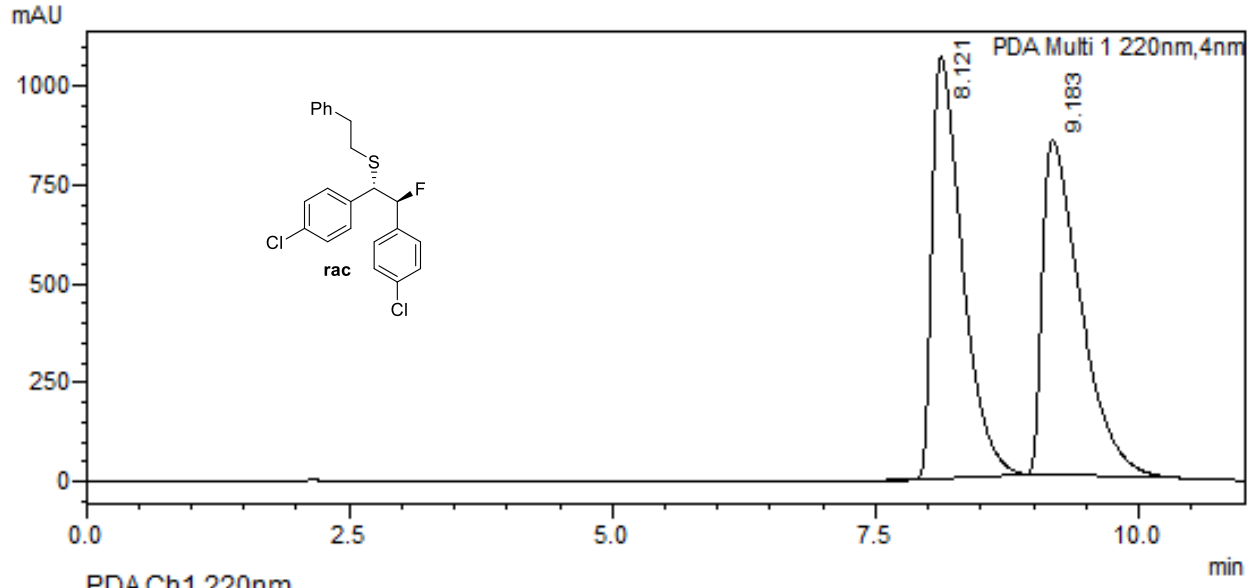

PDA Ch1 220nm

Peak#	Ret. Time	Area%
1	8.121	50.185
2	9.183	49.815

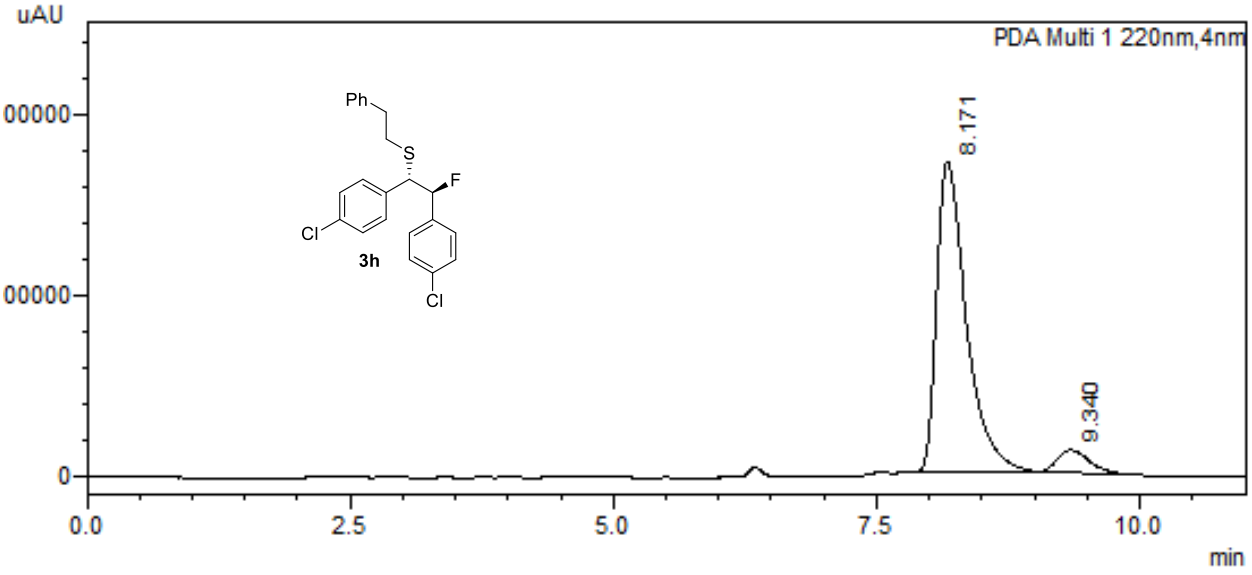

PDA Ch1 220nm

Peak#	Ret. Time	Area%
1	8.171	93.009
2	9.340	6.991

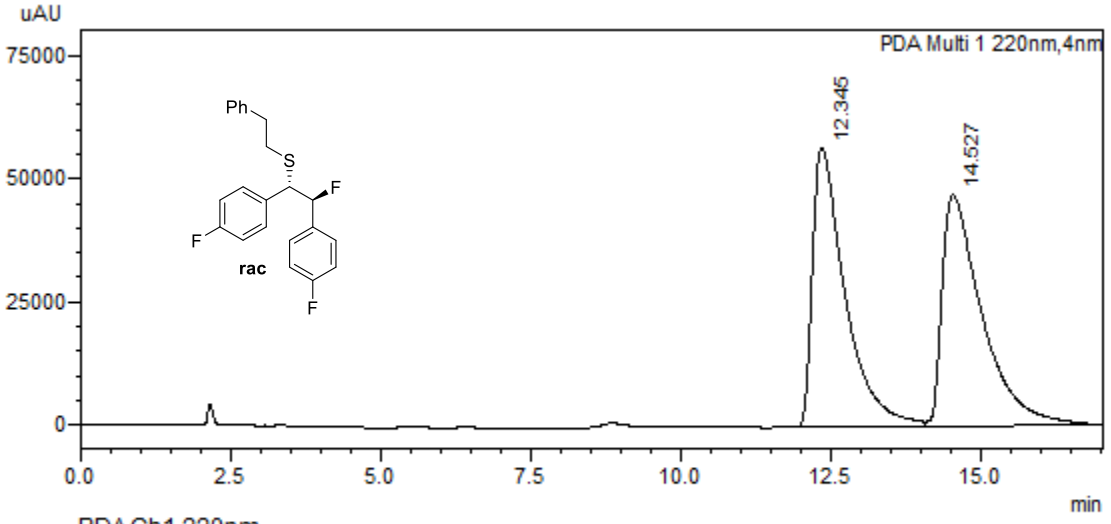

PDA Ch1 220nm

Peak#	Ret. Time	Area%
1	12.345	49.809
2	14.527	50.191

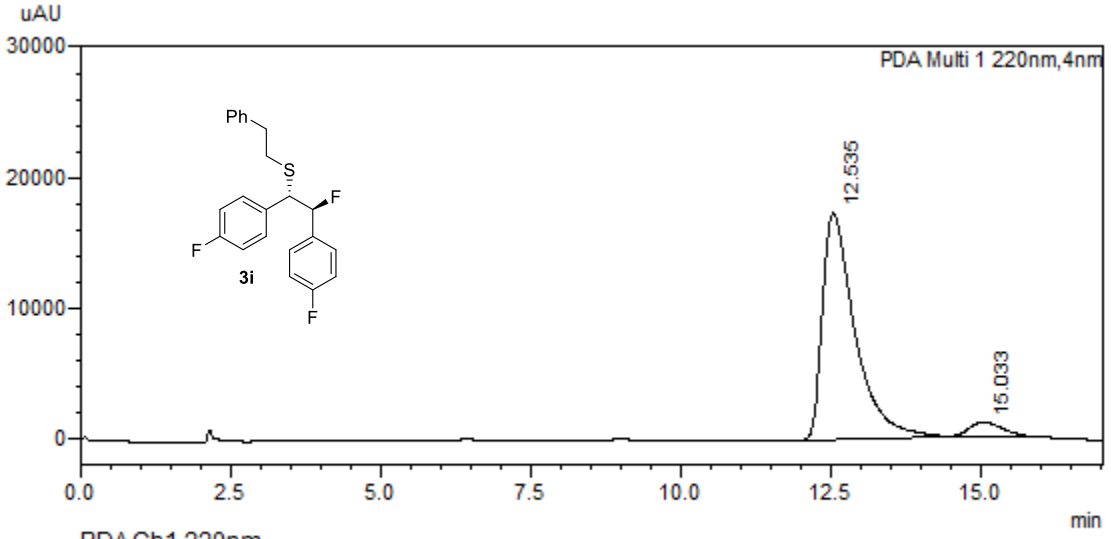

PDA Ch1 220nm

Peak#	Ret. Time	Area%
1	12.535	93.895
2	15.033	6.105

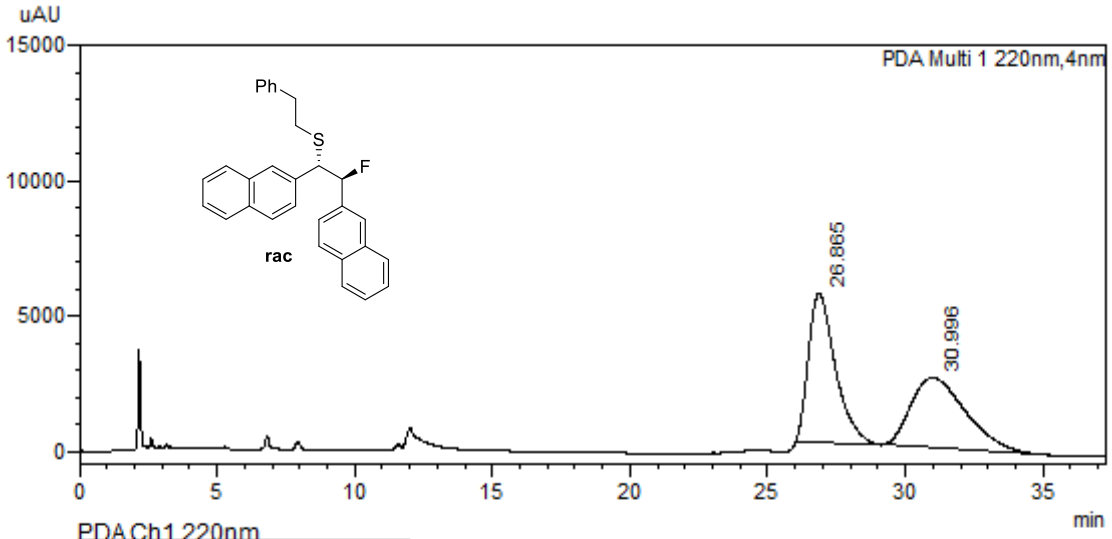

PDA Ch1 220nm

Peak#	Ret. Time	Area%
1	26.865	50.882
2	30.996	49.118

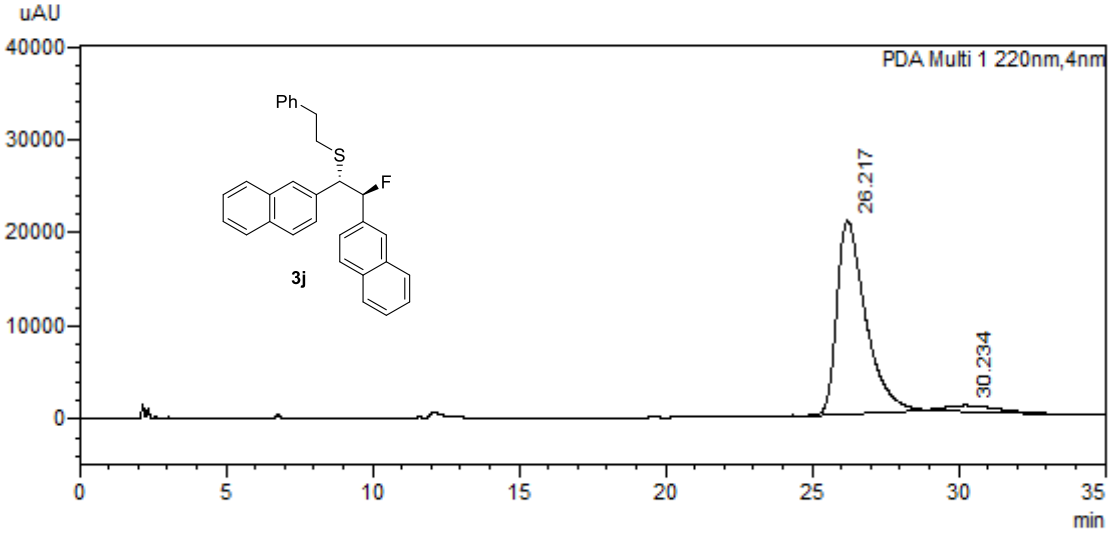

PDA Ch1 220nm

Peak#	Ret. Time	Area%
1	26.217	95.529
2	30.234	4.471

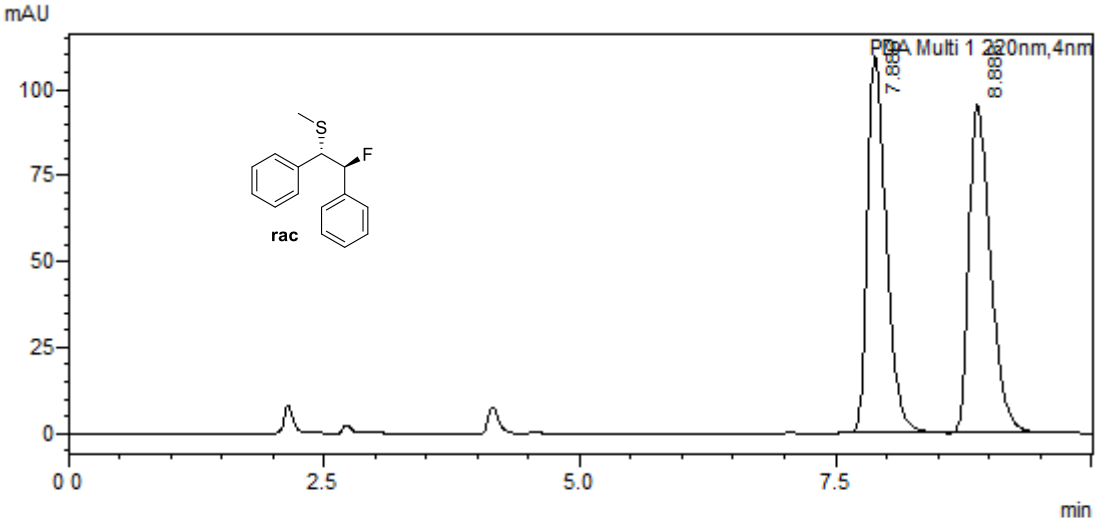

PDA Ch1 220nm

Peak#	Ret. Time	Area%
1	7.886	50.177
2	8.888	49.823

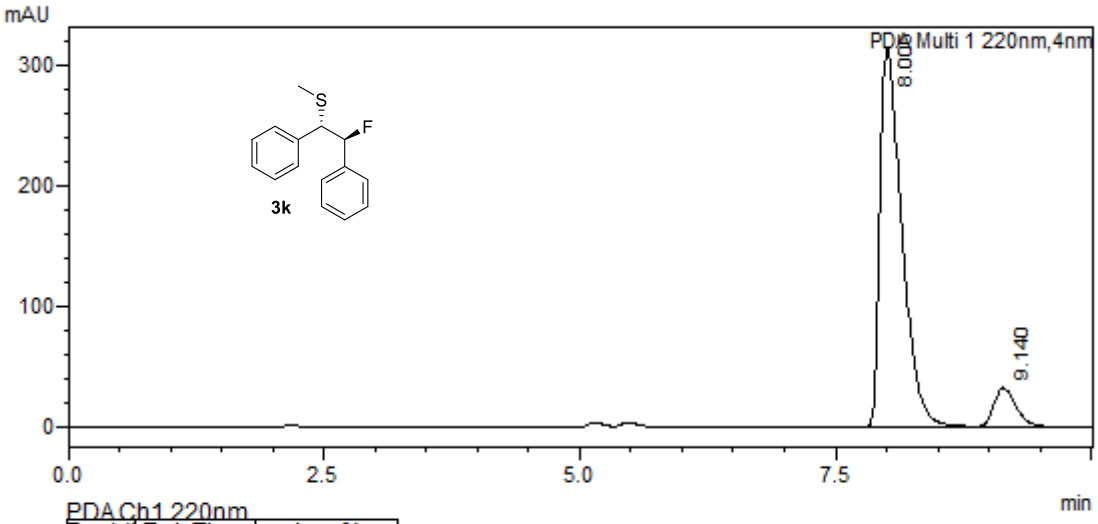

PDA Ch1 220nm

Peak#	Ret. Time	Area%
1	8.005	90.988
2	9.140	9.012

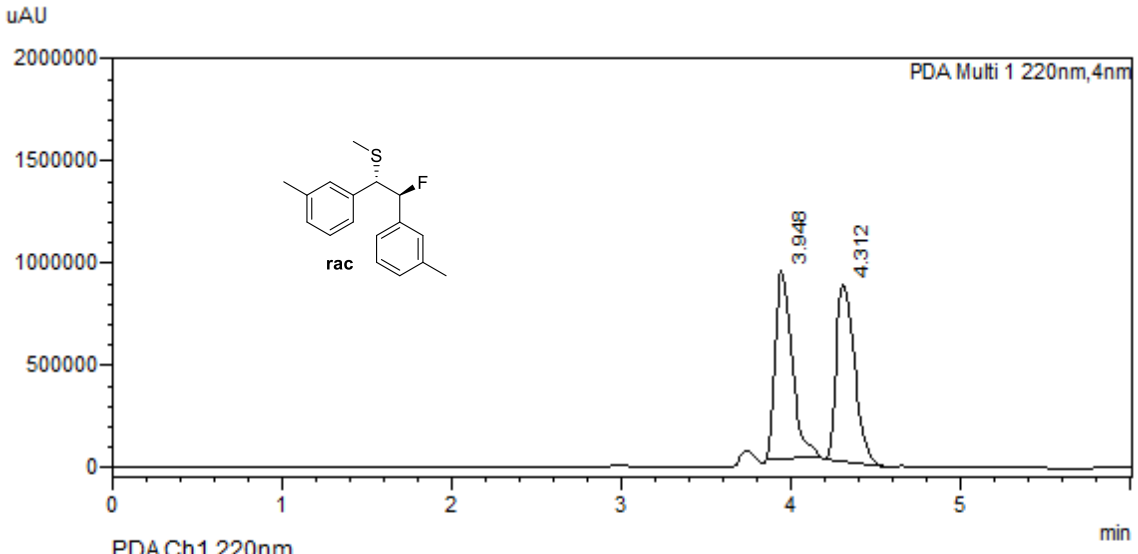

PDA Ch1 220nm

Peak#	Ret. Time	Area%
1	3.948	49.713
2	4.312	50.287

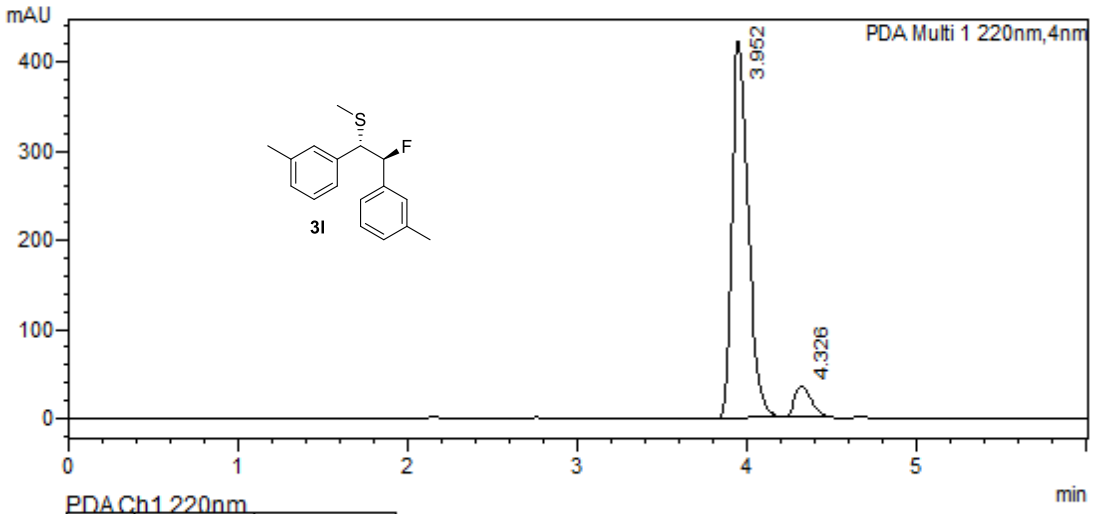

PDA Ch1 220nm

Peak#	Ret. Time	Area%
1	3.952	92.443
2	4.326	7.557

X-ray Analysis

Data were reduced using CrysAlisPro, solved using SuperFlip (98) and refined using CRYSTALS (*99, 100*). The Flack x parameter (*101, 102*) was refined in each case. Bayesian analysis of the Bijvoet pairs was also carried out using all the data used in the refinement (*103*). This gave the Hooft y parameter, the P2 probability (the likely-hood that the hand is correct given the crystal was enantiopure), and the P3 probability (the likely-hood that the hand is correct given the crystal was enantiopure or racemic).

Crystallographic Data for TBAF-4h complex

Table S29. Crystal data and structure refinement for TBAF·**4h** complex.

Empirical formula	C57 H64 F13 N5 O2	
Formula weight	1098.14	
Temperature	150 K	
Wavelength	1.54184 Å	
Crystal system	Orthorhombic	
Space group	P 21 21 21	
Unit cell dimensions	a = 10.22990(10) Å	α= 90°
	b = 21.55920(10) Å	β= 90°
	c = 25.00480(10) Å	γ = 90°
Volume	5514.77(6) $Å^3$	
Z	4	
Density (calculated)	1.323 Mg/m^3	
Absorption coefficient	0.951 mm^{-1}	
F(000)	2296	
Crystal size	0.28 x 0.25 x 0.21 mm^3	
Theta range for data collection	4.088 to 76.391°.	
Index ranges	-12<=h<=12, -27<=k<=27, -31<=l<=31	
Reflections collected	164650	
Independent reflections	11531 [R(int) = 0.046]	
Completeness to theta = 76.391°	99.9 %	
Absorption correction	Semi-empirical from equivalents	
Max. and min. transmission	0.82 and 0.70	

Refinement method	Full-matrix least-squares on F^2
Data / restraints / parameters	11531 / 456 / 751
Goodness-of-fit on F^2	1.0039
Final R indices [I>2sigma(I)]	R1 = 0.0504, wR2 = 0.1438
R indices (all data)	R1 = 0.0511, wR2 = 0.1451
Absolute structure parameter	0.000(16)
Largest diff. peak and hole	0.63 and -0.49 e.Å^{-3}

Table S30. Hydrogen bonds for TBAF·**4h** complex [Å and °].

D-H...A	d(D-H)	d(H...A)	d(D...A)	<(DHA)
C(46)-H(461)...O(3)	0.94	2.18	2.795(4)	122
C(81)-H(812)...O(33)#1	0.99	2.34	3.225(4)	148
C(87)-H(871)...O(33)#1	0.96	2.41	3.313(4)	157

Symmetry transformations used to generate equivalent atoms: #1 -x,y-1/2,-z+1/2

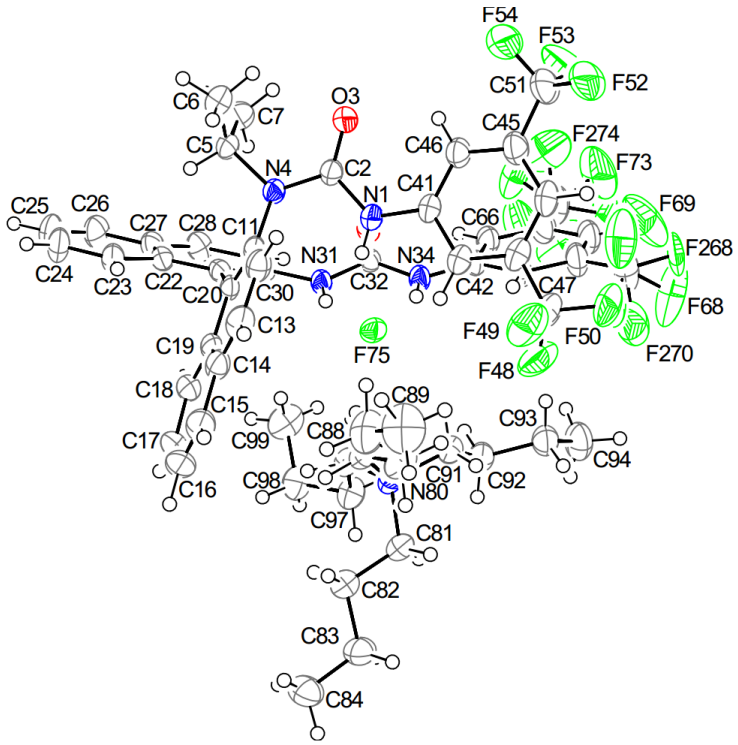

Figure S32. Crystal structure of TBAF·**4h** complex.

Crystallographic Data for 3d

Table S31.Crystal data and structure refinement for **3d**.

Empirical formula	C24 H25 F S	
Formula weight	364.53	
Temperature	150 K	
Wavelength	1.54184 Å	
Crystal system	Monoclinic	
Space group	P 21	
Unit cell dimensions	a = 11.4021(3) Å	α= 90°.
	b = 7.21710(10) Å	β= 108.519(3)°.
	c = 12.6576(3) Å	γ = 90°.
Volume	987.66(4) $Å^3$	
Z	2	
Density (calculated)	1.226 Mg/m^3	
Absorption coefficient	1.547 mm^{-1}	
F(000)	388	
Crystal size	0.28 x 0.22 x 0.15 mm^3	
Theta range for data collection	3.683 to 76.429°.	
Index ranges	-14<=h<=14, -9<=k<=9, -15<=l<=15	
Reflections collected	22206	
Independent reflections	4088 [R(int) = 0.033]	
Completeness to theta = 76.429°	99.6 %	
Absorption correction	Semi-empirical from equivalents	
Max. and min. transmission	0.79 and 0.66	
Refinement method	Full-matrix least-squares on F^2	
Data / restraints / parameters	4088 / 1 / 236	
Goodness-of-fit on F^2	1.0056	
Final R indices [I>2sigma(I)]	R1 = 0.0317, wR2 = 0.0839	
R indices (all data)	R1 = 0.0318, wR2 = 0.0841	
Absolute structure parameter	0.007(3)	
Largest diff. peak and hole	0.35 and -0.20 e.$Å^{-3}$	

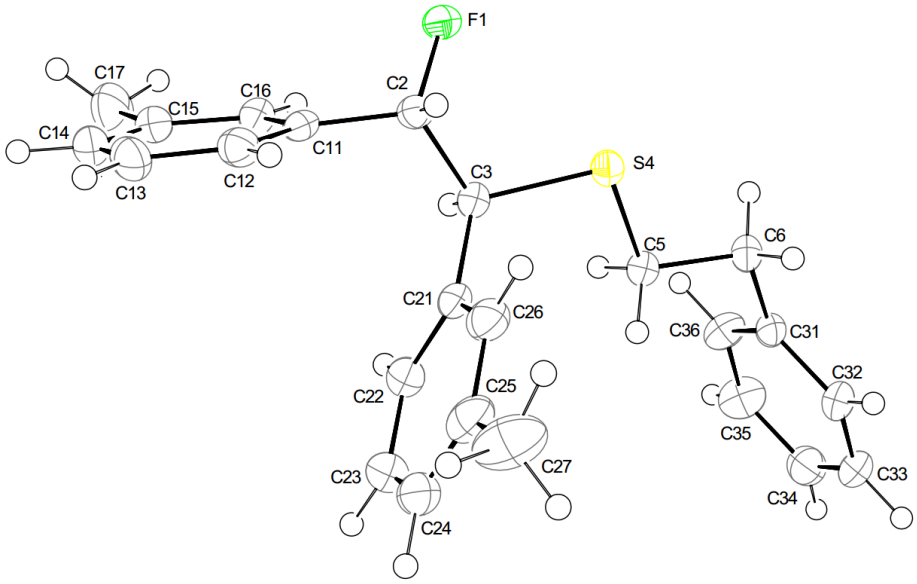

Figure S33. Crystal Structure of **3d**.

References

1. K. Maruoka, Ed., *Asymmetric Phase Transfer Catalysis* (Wiley-VCH, Weinheim, Germany, 2008).
2. T. Ooi, K. Maruoka, Recent advances in asymmetric phase-transfer catalysis. *Angew. Chem. Int. Ed.* **46**, 4222–4226 (2007).
3. V. Rauniyar, A. D. Lackner, G. L. Hamilton, F. D. Toste, Asymmetric electrophilic fluorination using an anionic chiral phase-transfer catalyst. *Science* **334**, 1681–1684 (2011).
4. K. Müller, C. Faeh, F. Diederich, Fluorine in pharmaceuticals: looking beyond intuition. *Science* **317**, 1881–1886 (2007).
5. S. Purser, P. R. Moore, S. Swallow, V. Gouverneur, Fluorine in medicinal chemistry. *Chem. Soc. Rev.* **37**, 320–330 (2008).
6. I. Ojima, Ed., *Fluorine in Medicinal Chemistry and Chemical Biology* (Wiley-Blackwell, Chichester, UK, 2009).
7. X. Yang, T. Wu, R. J. Phipps, F. D. Toste, Advances in catalytic enantioselective fluorination, mono-, di-, and trifluoromethylation, and trifluoromethylthiolation reactions. *Chem. Rev.* **115**, 826–870 (2015).
8. J. A. Kalow, A. G. Doyle, Enantioselective ring opening of epoxides by fluoride anion promoted by a cooperative dual-catalyst system. *J. Am. Chem. Soc*. **132**, 3268–3269 (2010).
9. M. H. Katcher, A. G. Doyle, Palladium-catalyzed asymmetric synthesis of allylic fluorides. *J. Am. Chem. Soc*. **132**, 17402–17404 (2010).
10. J. A. Kalow, A. G. Doyle, Mechanistic investigations of cooperative catalysis in the enantioselective fluorination of epoxides. *J. Am. Chem. Soc.* **133**, 16001–16012 (2011).
11. M. H. Katcher, A. Sha, A. G. Doyle, Palladium-catalyzed regio- and enantioselective fluorination of acyclic allylic halides. *J. Am. Chem. Soc.* **133**, 15902–15905 (2011).
12. S. Suzuki, T. Kamo, K. Fukushi, T. Hiramatsu, E. Tokunaga, T. Dohi, Y. Kita, N. Shibata, Iodoarene-catalyzed fluorination and aminofluorination by an Ar–I/HF·pyridine/mCPBA system. *Chem. Sci.* **5**, 2754–2760 (2014).
13. X. Wang, Q. lan, S. Shirakawa, K. Maruoka, Chiral bifunctional phase transfer catalysts for asymmetric fluorination of β-keto esters. *Chem. Commun*. **46**, 321–323 (2010).
14. C. L. Liotta, H. P. Harris, Chemistry of naked anions. I. Reactions of the 18-crown-6 complex of potassium fluoride with organic substrates in aprotic organic solvents. *J. Am. Chem. Soc.* **96**, 2250–2252 (1974).
15. V. H. Jadhav, H. J. Jeong, W. Choi, D. W. Kim, Crown ether metal complex fluoride salt as a facile and low hygroscopic fluoride source for nucleophilic fluorination. *Chem. Eng. J.*, **270**, 36–40 (2015).

16. J. A. Birrell, J. N. Desrosiers, E. N. Jacobsen, Enantioselective acylation of silyl ketene acetals through fluoride anion-binding batalysis. *J. Am. Chem. Soc.* **133**, 13872–13875 (2011).
17. A. G. Doyle, E. N. Jacobsen, Small-molecule H-bond donors in asymmetric catalysis. *Chem. Rev.* **107**, 5713–5743 (2007).
18. K. Brak, E. N. Jacobsen, Asymmetric ion-pairing catalysis. *Angew. Chem. Int. Ed.* **52**, 534–561 (2013).
19. S. M. Banik, A. Levina, A. M. Hyde, E. N. Jacobsen, Lewis acid enhancement by hydrogen-bond donors for asymmetric catalysis. *Science* **358**, 761–764 (2017).
20. R. J. Phipps, G. L. Hamilton, F. D. Toste, The progression of chiral anions from concepts to applications in asymmetric catalysis. *Nat. Chem.* **4**, 603–614 (2012).
21. S. Lin, E. N. Jacobsen, Thiourea-catalysed ring opening of episulfonium ions with indole derivatives by means of stabilizing non-covalent interactions. *Nat Chem.* **4**, 817–824 (2012).
22. J. **–**W. Lee, M. T. Oliveira, H. B. Jang, S. Lee, D. Y. Chi, D. W. Kim, C. E. Song, Hydrogen-bond promoted nucleophilic fluorination: concept, mechanism and applications in positron emission tomography. *Chem. Soc. Rev.* **45**, 4638–4650 (2016).
23. S. Liang, G. B. Hammond, B. Xu, Hydrogen bonding: regulator for nucleophilic fluorination. *Chem. Eur. J.* **23**, 17850–17861 (2017).
24. K. M. Engle, L. Pfeifer, G. W. Pidgeon, G. T. Giuffredi, A. L. Thompson, R. S. Paton, J. M. Brown, V. Gouverneur, Coordination diversity in hydrogen-bonded homoleptic fluoride–alcohol complexes modulates reactivity. *Chem. Sci.* **6**, 5293–5302 (2015).
25. L. Pfeifer, K. M. Engle, G. W. Pidgeon, H. A. Sparkes, A. L. Thompson, J. M. Brown, V. Gouverneur, Hydrogen-bonded homoleptic fluoride–diarylurea complexes: structure, reactivity, and coordinating power. *J. Am. Chem. Soc.* **138**, 13314–13325 (2016).
26. D. O'Hagan, C. Schaffrath, S. L. Cobb, J. T. G. Hamilton, C. D. Murphy, Biosynthesis of an organofluorine molecule. *Nature* **416**, 279 (2002).
27. C. Dong, F. Huang, H. Deng, C. Schaffrath, J. B. Spencer, D. O'Hagan, J. H. Naismith, Crystal structure and mechanism of a bacterial fluorinating enzyme. *Nature* **427**, 561–565 (2004).
28. X. Zhu, D. A. Robinson, A. R. McEwan, D. O'Hagan, J. H. Naismith, Mechanism of enzymatic fluorination in *Streptomyces cattleya*. *J. Am. Chem. Soc.* **129**, 14597–14604 (2007).
29. D. O'Hagan, H. Deng, Enzymatic fluorination and biotechnological developments of the fluorinase. *Chem. Rev.* **115**, 634–649 (2015).
30. C. Thiehoff, M.C. Holland, C. Daniliuc, K. N. Houk, R. Gilmour, Can acyclic conformational control be achieved via a sulfur–fluorine *gauche* effect?. *Chem. Sci.* **6**, 3565–3571 (2015).
31. P. R. Schreiner, Metal-free organocatalysis through explicit hydrogen bonding interactions. *Chem. Soc. Rev.* **32**, 289–296 (2003).

32. E. M. Fleming, T. McCabe, S. J. Connon, Novel axially chiral bis-arylthiourea-based organocatalysts for asymmetric Friedel–Crafts type reactions. *Tetrahedron Lett.* **47**, 7037–7042 (2006).
33. Z. Yuan, H. –Y. Wang, X. Mu, P. Chen, Y. –L. Guo, G. Liu, Highly selective Pd-catalyzed intermolecular fluorosulfonylation of styrenes. *J. Am. Chem. Soc.* **137**, 2468–2471 (2015).
34. H. Y. Kim, K. Oh, Highly Diastereo- and enantioselective aldol reaction of methyl α-isocyanoacetate: a cooperative catalysis approach. *Org. Lett.* **13**, 1306–1309 (2011).
35. C. B. Tripathi, S. Mukherjee, Lewis base catalysis by thiourea: *N*-bromosuccinimide-mediated oxidation of alcohols. *J. Org. Chem.* **77**, 1592–1598 (2012).
36. S. –H. Lee, H. Matsushita, B. Clapham, K. D. Janda, The direct conversion of carbamates to ureas using aluminum amides. *Tetrahedron* **60**, 3439–3443 (2004).
37. G. Jakab, A. Hosseini, H. Hausmann, P. R. Schreiner, Mild and selective organocatalytic iodination of activated aromatic compounds. *Synthesis* **45**, 1635–1640 (2013).
38. M. Shi, X. –G. Liu, Asymmetric Morita-Baylis-Hillman reaction of arylaldehydes with 2-cyclohexen-1-one catalyzed by chiral bis(thio)urea and DABCO. *Org. Lett.* **10**, 1043–1046 (2008).
39. R. Holakovský, M. März, R. Cibulka, Urea derivatives based on a 1,1′-binaphthalene skeleton as chiral solvating agents for sulfoxides. *Tetrahedron: Asymmetry* **26**, 1328–1334 (2015).
40. M. C. Mimmi, M. Gullotti, L. Santagostini, R. Pagliarin, L. De Gioia, E. Monzani, L. Casella, synthesis and conformational studies of a chiral octadentate ligand derived from (*R*)-1,1′-binaphthyl-2,2′-diamine and its dinuclear zinc(II) and nickel(II) complexes. *Eur. J. Inorg. Chem.* **2003**, 3934–3944 (2003).
41. K. H. Kim, D. –W. Lee, Y. –S. Lee, D. –H. Ko, D. –C. Ha, Enantioselective oxidative coupling of methyl 3-hydroxy-2-naphthoate using mono-*N*-alkylated octahydrobinaphthyl-2,2′-diamine ligand. *Tetrahedron* **60**, 9037–9042 (2004).
42. A. Crespo–Peña, D. Monge, E. Martín-Zamora, E. Álvarez, R. Fernández, J. M. Lassaletta, Asymmetric formal carbonyl-ene reactions of formaldehyde *tert*-butyl hydrazone with α-keto esters: dual activation by bis-urea catalysts. *J. Am. Chem. Soc.* **134**, 12912–12915 (2012).
43. X. Pu, X. Qi, J. M. Ready, Allenes in asymmetric catalysis: asymmetric ring opening of *meso*-epoxides catalyzed by allene-containing phosphine oxides. *J. Am. Chem. Soc.* **131**, 10364–10365 (2009).
44. N. Ajvazi, S. Stavber, Direct halogenation of alcohols with halosilanes under catalyst- and organic solvent-free reaction conditions. *Tetrahedron Lett.* **57**, 2430–2433 (2016).
45. G. K. Helmkam, D. J. Pettitt, Mechanism of the desulfurization of episulfides with methyl iodide. *J. Org. Chem.* **29**, 3258–3262 (1964).
46. S. E. Denmark, T. Vogler, Synthesis and reactivity of enantiomerically enriched thiiranium ions. *Chem. Eur. J.* **15**, *15*, 11737–11745 (2009).

47. P. Sokkalingam, C. –H. Lee, Highly sensitive fluorescence “turn-on” indicator for fluoride anion with remarkable selectivity in organic and aqueous media. *J. Org. Chem.* **76**, 3820–3828 (2011)

48. P. Kuzmič, Program DYNAFIT for the analysis of enzyme kinetic data: application to HIV proteinase. *Anal. Biochem.* **237**, 260–273 (1996).

49. M. J. Frisch, G. W. Trucks, H. B. Schlegel, G. E. Scuseria, M. A. Robb, J. R. Cheeseman, G. Scalmani, V. Barone, G. A. Petersson, H. Nakatsuji, X. Li, M. Caricato, A. Marenich, J. Bloino, B. G. Janesko, R. Gomperts, B. Mennucci, H. P. Hratchian, J. V. Ortiz, A. F. Izmaylov, J. L. Sonnenberg, D. Williams-Young, F. Ding, F. Lipparini, F. Egidi, J. Goings, B. Peng, A. Petrone, T. Henderson, D. Ranasinghe, V. G. Zakrzewski, J. Gao, N. Rega, G. Zheng, W. Liang, M. Hada, M. Ehara, K. Toyota, R. Fukuda, J. Hasegawa, M. Ishida, T. Nakajima, Y. Honda, O. Kitao, H. Nakai, T. Vreven, K. Throssell, J. A. Montgomery Jr., J. E. Peralta, F. Ogliaro, M. Bearpark, J. J. Heyd, E. Brothers, K. N. Kudin, V. N. Staroverov, T. Keith, R. Kobayashi, J. Normand, K. Raghavachari, A. Rendell, J. C. Burant, S. S. Iyengar, J. Tomasi, M. Cossi, J. M. Millam, M. Klene, C. Adamo, R. Cammi, J. W. Ochterski, R. L. Martin, K. Morokuma, O. Farkas, J. B. Foresman, and D. J. Fox, Gaussian 09, Revision D.01, Gaussian, Inc., Wallingford CT, (2016).

50. Y. Zhao, D. G. Truhlar, The M06 suite of density functionals for main group thermochemistry, thermochemical kinetics, noncovalent interactions, excited states, and transition elements: two new functionals and systematic testing of four M06-class functionals and 12 other functionals. *Theor. Chem. Acc.* **120**, 215–241 (2008).

51. F. Weigend, R. Ahlrichs, Balanced basis sets of split valence, triple zeta valence and quadruple zeta valence quality for H to Rn: design and assessment of accuracy. *Phys. Chem. Chem. Phys.* **7**, 3297–3305 (2005).

52. A. Hellweg, D. Rappoport, Development of new auxiliary basis functions of the Karlsruhe segmented contracted basis sets including diffuse basis functions (def2-SVPD, def2-TZVPPD, and def2-QVPPD) for RI-MP2 and RI-CC calculations. *Phys. Chem. Chem. Phys.* **17**, 1010–1017 (2015).

53. D. Rappoport, F. Furche, Property-optimized Gaussian basis sets for molecular response calculations. *J. Chem. Phys.* **133**, 134105 (2010).

54. T. Leininger, A. Nicklass, W. Küchle, H. Stoll, M. Dolg, A. Bergner, The accuracy of the pseudopotential approximation: non-frozen-core effects for spectroscopic constants of alkali fluorides XF (X = K, Rb, Cs). *Chem. Phys. Lett.* **255**, 274–280 (1996).

55. V. Barone, M. Cossi, Quantum calculation of molecular energies and energy gradients in solution by a conductor solvent model. *J. Phys. Chem. A.* **102**, 1995–2001 (1998).

56. M. Cossi, N. Rega, G. Scalmani, V. Barone, Energies, structures, and electronic properties of molecules in solution with the C-PCM solvation model. *J. Comput. Chem.* **24**, 669–681 (2003).

57. Y. Takano, K. N. Houk, Benchmarking the conductor-like polarizable continuum model (CPCM) for aqueous solvation free energies of neutral and ionic organic molecules. *J. Chem. Theory Comput.* **1**, 70–77 (2005).
58. R. S. Paton, I. Funes-Ardois, GoodVibes.py, doi:10.5281/zenodo.60811.
59. S. Grimme, Supramolecular binding thermodynamics by dispersion-corrected density functional theory. *Chem. Eur. J.* **18**, 9955–9964 (2012).
60. J. Contreras-García, E. R. Johnson, S. Keinan, R. Chaudret, J. –P. Piquemal, D. N. Beratan, W. Yang, NCIPLOT: A program for plotting noncovalent interaction regions. *J. Chem. Theory Comput.* **7**, 625–632 (2011).
61. E. R. Johnson, S. Keinan, P. Mori Sánchez, J. Contreras–García, A. J. Cohen, W. Yang, Revealing noncovalent interactions. *J. Am. Chem. Soc.* **132**, 6498–6506 (2010).
62. F. Neese, The ORCA program system. *Wiley Interdiscip. Rev. Comput. Mol. Sci.* **2**, 73–78 (2012).
63. J. –D. Chai, M. Head-Gordon, Long-range corrected hybrid density functionals with damped atom–atom dispersion corrections. *Phys. Chem. Chem. Phys.* **10**, 6615–6620 (2008).
64. Y. –S. Lin, G. –D. Li, S. –P. Mao, J. –D. Chai, Long-range corrected hybrid density functionals with improved dispersion corrections. *J. Chem. Theory Comput.* **9**, 263–272 (2013).
65. S. Grimme, J. Antony, S. Ehrlich, H. Krieg, A consistent and accurate *ab initio* parametrization of density functional dispersion correction (DFT-D) for the 94 elements H-Pu. *J. Chem. Phys.* **132**, 154104 (2010).
66. J. Zheng, X. Xu, D. G. Truhlar, Minimally augmented Karlsruhe basis sets. *Theor. Chem. Acc.* **128**, 295–305 (2011).
67. A. Klamt, G. Schüürmann, COSMO: a new approach to dielectric screening in solvents with explicit expressions for the screening energy and its gradient. *J. Chem. Soc., Perkin Trans. 2*, 799–805 (1993).
68. K. Raghavachari, G. W. Trucks, J. A. Pople, M. Head-Gordon, A fifth-order perturbation comparison of electron correlation theories. *Chem. Phys. Lett.* **157**, 479–483 (1989).
69. Spartan ’16., Wavefunction, Inc., Irvine, CA, (2016).
70. T. A. Halgren, Merck molecular force field. I. Basis, form, scope, parameterization, and performance of MMFF94. *J. Comput. Chem.* **17**, 490–519 (1996).
71. C. Møller, M. S. Plesset, Note on an approximation treatment for many-electron systems. *Phys. Rev.* **46**, 618–622 (1934).
72. H. J. C. Berendsen, D. van der Spoel, R. van Drunen, GROMACS: A message-passing parallel molecular dynamics implementation. *Comput. Phys. Commun.* **91**, 43–56 (1995).
73. E. Lindahl, B. Hess, D. van der Spoel, GROMACS 3.0: a package for molecular simulation and trajectory analysis. *J. Mol. Model.* **7**, 306–317 (2001).

74. D. Van Der Spoel, E. Lindahl, B. Hess, G. Groenhof, A. E. Mark, H. J. C. Berendsen, GROMACS: Fast, flexible, and free. *J. Comput. Chem.* **26**, 1701–1718 (2005).
75. B. Hess, C. Kutzner, D. Van Der Spoel, E. Lindahl, GROMACS 4: Algorithms for highly efficient, load-balanced, and scalable molecular simulation. *J. Chem. Theory Comput.* **4**, 435–447 (2008).
76. S. Pronk, S. Páll, R. Schulz, P. Larsson, P. Bjelkmar, R. Apostolov, M. R. Shirts, J. C. Smith, P. M. Kasson, D. van der Spoel, B. Hess, E. Lindahl, GROMACS 4.5: a high-throughput and highly parallel open source molecular simulation toolkit. *Bioinformatics* **29**, 845–854 (2013).
77. M. J. Abraham, T. Murtola, R. Schulz, S. Páll, J. C. Smith, B. Hess, E. Lindah, GROMACS: High performance molecular simulations through multi-level parallelism from laptops to supercomputers. *SoftwareX*. **1**–**2**, 19–25 (2015).
78. W. L. Jorgensen, J. Tirado-Rives, The OPLS [optimized potentials for liquid simulations] potential functions for proteins, energy minimizations for crystals of cyclic peptides and crambin. *J. Am. Chem. Soc.* **110**, 1657–1666 (1988).
79. W. L. Jorgensen, D. S. Maxwell, J. Tirado-Rives, Development and testing of the OPLS all-atom force field on conformational energetics and properties of organic liquids. *J. Am. Chem. Soc.* **118**, 11225–11236 (1996).
80. Schrödinger Release 2017-2, Schrödinger, LLC, New York, NY, (2017).
81. C. I. Bayly, P. Cieplak, W. D. Cornell, P. A. Kollman, A well-behaved electrostatic potential based method using charge restraints for deriving atomic charges: the RESP model. *J. Phys. Chem.* **97**, 10269–10280 (1993).
82. W. D. Cornell, P. Cieplak, C. I. Bayly, P. A. Kollman, Application of RESP charges to calculate conformational energies, hydrogen bond energies, and free energies of solvation. *J. Am. Chem. Soc.* **115**, 9620–9631 (1993).
83. F. Duarte, R. S. Paton, Molecular recognition in asymmetric counteranion catalysis: Understanding chiral phosphate-mediated desymmetrization. *J. Am. Chem. Soc.* **139**, 8886–8896 (2017).
84. D. A. Case, D. S. Cerutti, T. E. Cheatham III, T. A. Darden, R. E. Duke, T. J. Giese, H. Gohlke, A. W. Goetz, D. Greene, N. Homeyer, S. Izadi, A. Kovalenko, T. S. Lee, S. LeGrand, P. Li, C. Lin, J. Liu, T. Luchko, R. Luo, D. Mermelstein, K. M. Merz, G. Monard, H. Nguyen, I. Omelyan, A. Onufriev, F. Pan, R. Qi, D. R. Roe, A. Roitberg, C. Sagui, C. L. Simmerling, W. M. Botello-Smith, J. Swails, R. C. Walker, J. Wang, R. M. Wolf, X. Wu, L. Xiao, D. M. York and P. A. Kollman, AMBER 2017, University of California, San Francisco (2017).
85. D. Van Der Spoel, P. J. van Maaren, C. Caleman, GROMACS molecule & liquid database. *Bioinformatics*. **28**, 752–753 (2012).
86. S. Chen, S. Yi, W. Gao, C. Zuo, Z. Hu, Force field development for organic molecules: modifying dihedral and 1–n pair interaction parameters. *J. Comput. Chem.* **36**, 376–384 (2015).

87. U. Essmann, L. Perera, M. L. Berkowitz, T. Darden, H. Lee, L. G. Pedersen, A smooth particle mesh Ewald method. *J. Chem. Phys.* **103**, 8577–8593 (1995).

88. B. Hess, H. Bekker, H. J. C. Berendsen, J. G. E. M. Fraaije, LINCS: A linear constraint solver for molecular simulations. *J. Comput. Chem.* **18**, 1463–1472 (1997).

89. G. Bussi, D. Donadio, M. Parrinello, Canonical sampling through velocity rescaling. *J. Chem. Phys.* **126**, 014101 (2007).

90. M. Parrinello, A. Rahman, Crystal structure and pair potentials: a molecular-dynamics study. *Phys. Rev. Lett.* **45**, 1196–1199 (1980).

91. M. Parrinello, A. Rahman, Polymorphic transitions in single crystals: a new molecular dynamics method. *J. Appl. Phys.* **52**, 7182–7190 (1981).

92. X. Daura, K. Gademann, B. Jaun, D. Seebach, W. F. van Gunsteren, A. E. Mark, Peptide folding: when simulation meets experiment. *Angew. Chem. Int. Ed.* **38**, 236–240 (1999).

93. J. R. Pliego Jr., J. M. Riveros, New insights on reaction pathway selectivity promoted by crown ether phase-transfer catalysis: Model *ab initio* calculations of nucleophilic fluorination. *J. Mol. Catal. A Chem.* **363**–**364**, 489–494 (2012).

94. N. F. Carvalho, J. R. Pliego Jr., Theoretical design and calculation of a crown ether phase-transfer-catalyst scaffold for nucleophilic fluorination merging two catalytic concepts. *J. Org. Chem.* **81**, 8455–8463 (2016).

95. W. M. Haynes, D. R. Lide, T. J. Bruno, *CRC Handbook of chemistry and physics* (Taylor & Francis Inc., Boca Raton, 97th ed., 2017).

96. Y. Marcus, A. Loewenschuss, Chapter 4. Standard entropies of hydration of ions. *Annu. Reports Sect. "C" (Physical Chem.)* **81**, 81–135 (1984).

97. D. O'Hagan, Recent developments on the fluorinase from *Streptomyces cattleya*, *J. Fluor. Chem*, **127**, 1479–1483 (2006).

98. L. Palatinus, G. Chapuis, SUPERFLIP – A computer program for the solution of crystal structures by charge flipping in arbitrary dimensions. *J. Appl. Cryst.* **40**, 786–790 (2007).

99. P. W. Betteridge, J. R. Carruthers, R. I. Cooper, K. Prout, D. J. Watkin, CRYSTALS version 12: software for guided crystal structure analysis. *J. Appl. Cryst.* **36**, 1487 (2003).

100. R. I. Cooper, A. L. Thompson, D. J. Watkin, CRYSTALS enhancements: dealing with hydrogen atoms in refinement. *J. Appl. Cryst.* **43**, 1100–1107 (2010).

101. H. D. Flack, On enantiomorph-polarity estimation. *Acta Cryst.* **A39**, 876–881 (1983).

102. H. D. Flack, G. Bernardinelli, Reporting and evaluating absolute-structure and absolute-configuration determinations. *J. Appl. Cryst.* **33**, 1143–1148 (2000).

103. R. W. W. Hooft, L. H. Straver, A. L. Spek, Determination of absolute structure using Bayesian statistics on Bijvoet differences. *J. Appl. Cryst.* **41**, 96–103 (2008).